

**ANALYSIS AND MITIGATION OF NONLINEAR FIBER
IMPAIRMENTS IN HIGH BIT RATE ALL-OPTICAL
ORTHOGONAL FREQUENCY DIVISION
MULTIPLEXING SYSTEM**

JASSIM KADIM HMOOD

**THESIS SUBMITTED IN FULFILLMENT OF THE
REQUIREMENTS FOR THE DEGREE OF DOCTOR OF
PHILOSOPHY/ELECTRICAL ENGINEERING**

**FACULTY OF ENGINEERING
UNIVERSITY OF MALAYA
KUALA LUMPUR**

2016

UNIVERSITI MALAYA
ORIGINAL LITERARY WORK DECLARATION

Name of Candidate: **JASSIM KADIM HMOOD**
Registration/Matric No: **KHA130056**
Name of Degree: **DOCTOR OF PHILOSOPHY (Ph. D.)**

Title of Project Paper/Research Report/Dissertation/Thesis (“this Work”):
**ANALYSIS AND MITIGATION OF NONLINEAR FIBER IMPAIRMENTS IN
HIGH BIT RATE ALL-OPTICAL ORTHOGONAL FREQUENCY DIVISION
MULTIPLEXING SYSTEM**

Field of Study: **PHOTONICS & OPTICAL COMMUNICATIONS**

I do solemnly and sincerely declare that:

- (1) I am the sole author/writer of this Work;
- (2) This Work is original;
- (3) Any use of any work in which copyright exists was done by way of fair dealing and for permitted purposes and any excerpt or extract from, or reference to or reproduction of any copyright work has been disclosed expressly and sufficiently and the title of the Work and its authorship have been acknowledged in this Work;
- (4) I do not have any actual knowledge nor do I ought reasonably to know that the making of this work constitutes an infringement of any copyright work;
- (5) I hereby assign all and every rights in the copyright to this Work to the University of Malaya (“UM”), who henceforth shall be owner of the copyright in this Work and that any reproduction or use in any form or by any means whatsoever is prohibited without the written consent of UM having been first had and obtained;
- (6) I am fully aware that if in the course of making this Work I have infringed any copyright whether intentionally or otherwise, I may be subject to legal action or any other action as may be determined by UM.

Candidate’s Signature

Date

Subscribed and solemnly declared before,

Witness’s Signature

Date

Name:

Designation:

ABSTRACT

All-optical orthogonal frequency division multiplexing (AO-OFDM) techniques have been recently considered for optical transmission systems applications. The all-optical solution has obtained an immense interest since it could work beyond the state-of-art electronics speed. However, AO-OFDM systems suffer highly from phase noise that induced by fiber nonlinearities, such as self-phase modulation (SPM), cross-phase modulation (XPM), and four-wave mixing (FWM). This thesis aims to analyze the effects of fiber nonlinearity and proposes new techniques to mitigate their impairments in AO-OFDM systems. At first, an analytical model that evaluates linear and nonlinear phase noises induced by the interaction of amplified spontaneous emission (ASE) noise with SPM, XPM, and FWM phenomena in m-array quadrature-amplitude modulation (mQAM) AO-OFDM transmission systems is developed. This analytical model is able to quantitatively compare the nonlinear phase noise variation due to variations in power of subcarrier, number of subcarriers, transmission distance and subcarrier index. Our results reveal that, in contrast to wavelength division multiplexing (WDM) transmission systems, the nonlinear phase noise induced by FWM dominates over other factors in AO-OFDM systems. Furthermore, it is shown that optical OFDM systems are immune to chromatic dispersion (CD) where the total phase noise decreases with CD effects at high subcarrier power. Four approaches are proposed in this thesis to mitigate the nonlinear fiber impairments in AO-OFDM systems; reducing the power of signal inside fiber, minimizing the interaction time between the subcarriers, reducing peak-to-average power ratio (PAPR), or using phase-conjugated twin waves (PCTWs) technique. In first approach, the power of the signal is reduced by shaping envelope of QAM subcarriers using return-to-zero (RZ) coder to mitigate the nonlinear fiber impairments. In second approach, the interaction time between subcarriers is minimized by shaping the envelopes of QAM subcarriers using RZ coding and making a delay time between even

and odd subcarriers. Due to the subcarriers are alternately delayed (AD), the AD RZ-QAM AO-OFDM signal is produced after combining all subcarriers. The results reveal that the nonlinear phase noise is significantly mitigated when the time delay is equal to half symbol period. In the third approach, the reduction of peak-to-average power ratio (PAPR) is proposed based on constellation rotation to reduce the nonlinear fiber impairments. The odd subcarriers are modulated with rotated mQAM constellation, while the even subcarriers are modulated with standard mQAM constellation. The results reveal that PAPR is minimized when the angle of rotation is equal to $\pi/4$ for the 4QAM AO-OFDM system. Finally, in the fourth approach, a new technique to suppress nonlinear phase noise in spatially multiplexed AO-OFDM systems based on PCTWs technique is demonstrated. In this technique, AO-OFDM signal and its phase-conjugated copy are directly transmitted through two identical fiber links. At the receiver, the two signals are coherently superimposed to cancel the phase noise and to enhance signal-to-noise ratio (SNR). The results reveal that the performance of the proposed system is substantially improved as compared with original system.

ABSTRAK

Teknik-teknik pemultipleksan pembahagian frekuensi ortogonal (AO-OFDM) telah baru-baru ini dipertimbangkan untuk aplikasi sistem penghantaran optik. Penyelesaian optik keseluruhan telah mendapat tarikan yang hebat kerana ia boleh berfungsi melebihi kelajuan elektronik terkini. Walau bagaimanapun, sistem AO-OFDM terjejas oleh hingar fasa yang disebabkan oleh parameter tidak lurus fiber, seperti modulasi fasa sendiri (SPM), modulasi merentas fasa (XPM), dan pencampuran empat gelombang (FWM). Tesis ini bertujuan untuk menganalisis kesan ketaklurusan gentian dan mencadangkan teknik-teknik baru untuk mengalihkan kekurangan mereka dalam sistem AO-OFDM. Pada mulanya, model analisis yang menilai hingar fasa lurus dan tidak lurus yang disebabkan oleh interaksi hingar pelepasan spontan yang dikuatkan (ASE) dengan fenomena SPM, XPM, dan FWM dalam sistem penghantaran modulasi amplitud kuadratur m-tatasusunan (mQAM) AO-OFDM yang dibangunkan. Analisis model ini mampu untuk membandingkan secara kuantitatif variasi hingar fasa tidak lurus yang disebabkan oleh perubahan kuasa subpembawa, bilangan subpembawa, jarak penghantaran dan indeks subpembawa. Keputusan kami menunjukkan bahawa, berbeza dengan sistem penghantaran pemultipleksan pembahagian panjang gelombang (WDM), hingar fasa tidak lurus disebabkan oleh FWM lebih mendominasi faktor-faktor lain dalam sistem AO-OFDM. Tambahan pula, ia menunjukkan bahawa sistem OFDM optik adalah kebal terhadap penyebaran kromatik (CD) di mana jumlah hingar fasa berkurangan dengan kesan CD pada kuasa subpembawa yang tinggi. Empat pendekatan adalah dicadangkan dalam tesis ini untuk mengurangkan penjejasan gentian tidak lurus dalam sistem AO-OFDM; mengurangkan kuasa isyarat dalam gentian, mengurangkan masa interaksi antara subpembawa, mengurangkan nisbah kuasa puncak-ke-purata (PAPR), atau menggunakan teknik gelombang kembar terkonjugat fasa (PCTWs). Dalam pendekatan

pertama, kuasa isyarat dikurangkan dengan membentuk sampul subpembawa QAM menggunakan pengukur kembali ke sifar (RZ) untuk mengurangkan penjejasan fiber tidak lurus. Dalam pendekatan kedua, masa interaksi antara subpembawa dikurangkan dengan membentuk sampul subpembawa QAM menggunakan pengekodan RZ dan membuat lengah masa antara subpembawa genap dan ganjil. Oleh kerana subpembawa ditangguhkan secara berselang-seli (AD), isyarat AD RZ-QAM AO-OFDM dihasilkan selepas menyikat semua subpembawa. Keputusan menunjukkan bahawa hingar fasa tidak lurus dapat dikurangkan dengan ketara apabila lengah masa adalah sama dengan tempoh separuh simbol. Dalam pendekatan ketiga, pengurangan nisbah kuasa puncak-ke-purata (PAPR) dicadangkan berdasarkan giliran kekisi untuk mengurangkan penjejasan gentian tidak lurus. Subpembawa yang ganjil dimodulatkan dengan kekisi mQAM yang diputar, manakala subpembawa genap dimodulatkan dengan kekisi mQAM piawai. Keputusan menunjukkan bahawa PAPR dikurangkan apabila sudut putaran adalah sama dengan $\pi/4$ untuk sistem 4 QAM AO-OFDM. Akhir sekali, dalam pendekatan keempat, teknik baru untuk menyekat hingar fasa tidak lurus dalam sistem AO-OFDM termultipleks ruang berdasarkan teknik PCTWs telah ditunjukkan. Dalam teknik ini, isyarat AO-OFDM dan salinan fasa terkonjugat dipancarkan secara langsung melalui dua pautan gentian yang serupa. Pada penerima, kedua-dua isyarat telah ditindakan secara koheren untuk membatalkan hingar fasa dan untuk meningkatkan nisbah isyarat-kepada-hingar (SNR). Keputusan menunjukkan bahawa prestasi sistem yang dicadangkan itu dengan bertambah baik dengan ketara berbanding dengan sistem asal.

ACKNOWLEDGEMENTS

Firstly, thanks to Allah almighty that enables me to do the research and to write this thesis.

I would like to express my deep sense of gratitude to my supervisor Prof. Dr. Sulaiman Wadi Bin Harun for his sincere guidance and the continuous support for my Ph.D study and related research. I would like to thank him for his patience, motivation, and guidance that helped me in all the time of research and writing of this thesis. I would like to express my gratefulness to my supervisor Associate Prof. Dr. Kamarul Ariffin Bin Noordin for his support, encouragement, and keen interest that help me in my research.

My sincere thanks and appreciations also go to Prof. Dr. Hossam M. H. Shalaby and Dr. Siamak D. Emami for their insightful comments, suggestions, and constructive criticism, which contributed to grow my ideas on the research.

I am thankful to University of Technology - Ministry of Higher Education and Scientific Research - Iraq for providing PhD scholarship funding.

I would like to express my gratefulness and my full-hearted thank for my family members namely my parents, my wife, my sister Iman and My brother Asst. Prof. Dr. Haider for all of their sacrifices that have made on my behalf.

Finally, I dedicate this thesis to my family.

LIST OF CONTENTS

ORIGINAL LITERARY WORK DECLARATION	ii
ABSTRACT	iii
ABSTRAK.....	v
ACKNOWLEDGEMENTS	vii
LIST OF CONTENTS	viii
LIST OF FIGURES.....	xii
LIST OF TABLES.....	xviii
LIST OF SYMBOLS AND ABBREVIATIONS.....	xix
CHAPTER 1: INTRODUCTION.....	1
1.1 Background of orthogonal frequency division multiplexing systems	1
1.1.1 Conventional optical OFDM systems	2
1.1.2 AO-OFDM systems	3
1.1.3 Advanced modulation formats in optical OFDM systems	4
1.2 Problem statement	5
1.3 Objectives of the study	6
1.4 Scope of the study.....	7
1.5 Original contributions	7
1.6 Thesis structure	8
CHAPTER 2: LITERATURE REVIEW.....	11
2.1 Introduction.....	11
2.2 Optical OFDM systems	12

2.3 Conventional optical OFDM system	13
2.4 AO-OFDM systems	16
2.4.1 AO-OFDM transmitters using OIFT	17
2.4.2 AO-OFDM transmitter using optical multicarrier source	23
2.4.3 AO-OFDM receiver.....	27
2.5 Impairments in the AO-OFDM systems.....	29
2.5.1 Peak-to-average power ratio.....	30
2.5.2 Optical fiber impairments.....	32
2.5.3 ASE noise	40
2.6 All-optical phase noise mitigation in optical OFDM systems.....	41
2.6.1 Reduction of PAPR	42
2.6.2 Coherent superposition in spatially multiplexing optical signals.....	44
2.6.3 Phase-conjugated twin waves technique	48
CHAPTER 3: PERFORMANCE ANALYSIS OF AN ALL-OPTICAL OFDM SYSTEM IN PRESENCE OF NONLINEAR PHASE NOISE	53
3.1 Introduction.....	53
3.2 All-optical OFDM system architecture	55
3.3 Analytical modeling of an AO-OFDM system.....	58
3.3.1 SPM and XPM phase noise in AO-OFDM systems.....	59
3.3.2 FWM phase noise	62
3.4 Results and discussions	64
3.4.1 Analytical results	64
3.4.2 Comparison of simulation and analytical results.....	77

3.5 Summary.....	82
CHAPTER 4: MITIGATION OF NONLINEAR FIBER IMPAIRMENTS	
IN AO-OFDM SYSTEM USING RZ-mQAM MODULATION FORMAT	84
4.1 Introduction.....	84
4.2 Performance improvement of AO-OFDM systems based on combining RZ coding with mQAM formats.....	85
4.2.1 Effect of employing RZ-mQAM format on phase noise.....	87
4.2.2 Effect of RZ-mQAM on power of FWM	91
4.2.3 AO-OFDM system setup.....	93
4.2.4 Results and discussion.....	96
4.3 Mitigation of phase noise in AO-OFDM systems based on minimizing interaction time between subcarriers	109
4.3.1 Analytical model of the proposed system.....	110
4.3.2 XPM phase noise	112
4.3.3 FWM phase noise	114
4.3.4 AO-OFDM system setup.....	117
4.3.5 Results and discussion.....	120
4.4 Summary.....	126
CHAPTER 5: REDUCTION OF PEAK-TO-AVERAGE POWER RATIO	
IN AO-OFDM SYSTEM USING ROTATED CONSTELLATION	
APPROACH.....	128
5.1 Introduction.....	128
5.2 PAPR reduction principle	130

5.3 Effect of rotated constellation method on fiber nonlinearity	134
5.3.1 XPM Phase Noise	135
5.3.2 FWM phase noise	136
5.4 All-optical OFDM system setup	136
5.5 Results and discussion	139
5.5.1 Transmitter side	139
5.5.2 Receiver side.....	142
5.6 Summary.....	146
CHAPTER 6: EFFECTIVENESS OF PHASE-CONJUGATED TWIN WAVES ON FIBER NONLINEARITY IN SPATIALLY MULTIPLEXED AO-OFDM SYSTEM.....	147
6.1 Introduction.....	147
6.2 Basic principle of PCTWs technique.....	149
6.3 Spatially multiplexed AO-OFDM system setup.....	153
6.4 Results and discussions	156
6.5 Summary.....	163
CHAPTER 7: CONCLUSIONS AND FUTURE WORKS	164
7.1 Conclusions	164
7.2 Future works	168
REFERENCES	170
LIST OF PUBLICATIONS	184

LIST OF FIGURES

Figure 2.1: Block diagram of conventional OFDM System	14
Figure 2.2: Optical IQ Modulator (Kikuchi, 2011).....	16
Figure 2.3: Optical IFT using bank of laser sources (X. Liu et al., 2011c)	17
Figure 2.4: Scheme of AO-OFDM system that utilizes OIDFT/ODFT (Lee et al., 2008).	19
Figure 2.5: Scheme of 4-order OFDT based on PLC technology (W. Li et al., 2010)	20
Figure 2.6: AO-OFDM transmitter utilizes the AWGs to implement OIFT (A. J. Lowery & Du, 2011).	21
Figure 2.7: All-optical Fourier transform using the time lens (Wei Li et al., 2009).	22
Figure 2.8: Block diagram of AO-OFDM system based on time lens (Y. Li et al., 2011).	23
Figure 2.9: Output spectra of the mode-lock fiber laser (Xuesong Liu et al., 2012).	25
Figure 2.10: Optical spectra of the 15-line OFCG that utilizes two cascaded intensity modulators (Shang et al., 2014).	25
Figure 2.11: AO-OFDM transmitter using OFCG (Sano et al., 2009)	26
Figure 2.12: 4-order OFFT circuit for symbol period T ; (a) traditional implementation; (b) combining the SPC with OFFT; (c), simplified combination of SPC with OFFT by using two identical MZIs; (d) low-complexity scheme with combined SPC and OFFT (Hillerkuss et al., 2010a), block with “0” is zero phase shifter.	28
Figure 2.13: AO-OFDM receiver utilizes the OFFT, which comprises of cascaded MZIs, demultiplexers and EAM gates. The received	

signal of each subcarrier is detected by optical QAM receivers (Hillerkuss et al., 2011)	29
Figure 2.14: High peak appearance in OFDM systems (Jayapalasingam & Alias, 2012).....	31
Figure 2.15: Measured attenuation spectrum of a standard single-mode fiber.....	34
Figure 2.16: Additional frequencies generated through FWM	40
Figure 2.17: Schematic diagram of a 4×4 OIDFT (Liang et al., 2009).	43
Figure 2.18: Architecture of coherent superposition of spatially multiplexed waves over multi-span multi-fiber link. M: number of fibers; PS: optical splitter; PC: optical combiner; PM: power meter (Shahi & Kumar, 2012).	45
Figure 2.19: Schematic of the experimental setup. TMC: tapered multi-core coupler; OLO: optical local oscillator (Xiang Liu et al., 2012a).....	46
Figure 2.20: Improvement of quality factor vs. number of superimposed signals. Insets: typical recovered constellations (Xiang Liu et al., 2012a).	46
Figure 2.21: Experimentally measured signal quality versus signal launch power (Xiang Liu et al., 2012b).....	47
Figure 2.22: Scheme of the experimental setup for superchannel transmission with employing PCTWs technique to cancel nonlinear distortion (X. Liu et al., 2013).....	49
Figure 2.23: Quality factor of received signal versus launch power after 8,000 km TWRS fiber transmission, inset: recovered constellations (X. Liu et al., 2013).....	50

Figure 2.24: Block diagram of 112 Gbps PDM coherent OFDM transmissions with PCP technique. I/Q: I/Q modulator, PBS: polarization beam splitter (Le et al., 2015).....	52
Figure 2.25: Quality factor as a function of the launch power in the system with and without PCPs for nonlinear fiber mitigation (Le et al., 2015).	52
Figure 3.1: Transmitter configuration of an AO-OFDM transmission system.....	56
Figure 3.2: Receiver components of an AO-OFDM transmission system with OFFT scheme.....	57
Figure 3.3: Phase noise variance versus subcarrier peak power for an AO-OFDM system employing 4QAM modulation format: (a) total phase noise variance; (b) phase noise variances due to SPM, XPM, FWM (at $D = 0$ ps/nm/km), and FWM (at $D = 16$ ps/nm/km) ; the inset is a logarithmic scale figure.	66
Figure 3.4: Phase noise variance versus sub-carrier peak power for an all-optical OFDM system employing 16QAM modulation format: (a) total phase noise variance; (b) phase noise variances due to SPM, XPM, and FWM; the inset is a logarithmic scale figure.	68
Figure 3.5: Phase noise variance due to SPM, XPM, and FWM versus the number of subcarriers: (a) 4QAM AO-OFDM system; the inset is a logarithmic scale figure. (b) 16QAM AO-OFDM system; the inset is a logarithmic scale figure.	70
Figure 3.6: Phase noise variance due to SPM, XPM, and FWM versus transmission distance: (a) 4QAM AO-OFDM system; the inset is a logarithmic scale figure. (b) 16QAM AO-OFDM system; the inset is a logarithmic scale figure. (c) 4QAM AO-OFDM system	

for span lengths 55km and 80km. d) 16QAM AO-OFDM system for span lengths 55km and 80km.	72
Figure 3.7: Total phase noise variance versus symbol rate: (a) 4QAM AO- OFDM system. (b) 16QAM AO-OFDM system.	74
Figure 3.8: Total phase noise variance versus subcarrier index: (a) 4QAM AO- OFDM system, (b) 16QAM AO-OFDM system.	76
Figure 3.9: EVM versus subcarrier power: (a) 4QAM AO-OFDM system, (b) 16QAM AO-OFDM system.	79
Figure 3.10: EVM versus subcarrier power: (a) 4QAM AO-OFDM system. (b) 16QAM AO-OFDM system.	81
Figure 4.1: Optical fields of four subcarriers that modulated by RZ-QAM	88
Figure 4.2: The setup of proposed system.	94
Figure 4.3: Conversion of RZ-4QAM signal to 4QAM signal by employing an MZI with delay time of $T_s / 2$	96
Figure 4.4: Influence of employing RZ-4QAM format on the phase noise reduction, a) details of phase noise, b) total phase noise variance.	98
Figure 4.5: Influence of employing RZ-16QAM format on the phase noise reduction, a) details of phase noise, b) total phase noise variance.	99
Figure 4.6: Effect of combination RZ with mQAM in AO-OFDM systems on the EVM, a) RZ-4QAM and 4QAM, b) RZ-16QAM and 16QAM.	101
Figure 4.7: EVM versus transmission distance, a) RZ-4QAM and 4QAM b) RZ-16QAM and 16QAM.	103
Figure 4.8: The constellation diagrams of (a) 4QAM, (b) RZ-4QAM, c) 16QAM, d) RZ-16QAM.	104

Figure 4.9: Bit rate error versus transmission distance at symbol rate of 25GSymbol/s, a) 4QAM and RZ-4QAM, b) 16QAM and RZ- 16QAM.	106
Figure 4.10: Performance comparison of AO-OFDM that employ: a) RZ- 4QAM and 4QAM, b) RZ-16QAM and 16QAM.....	108
Figure 4.11: Illustration of proposed odd and even subcarriers. δ is the delay time and T_s is the symbol period.....	111
Figure 4.12: Schematic of an AD RZ-QAM OFDM transmitter.....	118
Figure 4.13: Schematic of an AD RZ-QAM OFDM receiver.	119
Figure 4.14: The dependence of the nonlinear phase noise variance on the delay time δ	121
Figure 4.15: Influence of AD RZ-4QAM OFDM format on the phase noise reduction, a) details of phase noise, b) total phase noise variance.	123
Figure 4.16: BER versus transmission distance for both AD RZ-4QAM OFDM and 4QAM OFDM systems.....	124
Figure 4.17: Eye diagram of in-phase component (I) of received signal at 550 km and 1100 km: (a) and (b) 4QAM AO-OFDM system, (c) and (d) AD RZ-4QAM AO-OFDM system.	125
Figure 4.18: BER performances of proposed and conventional systems.....	126
Figure 5.1: Rotated 4QAM constellation.....	131
Figure 5.2: All-optical OFDM system setup.....	138
Figure 5.3: The impact of rotation angle on the PAPR, a) complementary cumulative distribution function (CCDF) versus PAPR, b) the PAPR for various rotation angles.	140
Figure 5.4: Effect of rotation angle on the optical waveforms of AO-OFDM signals.	142

Figure 5.5: Influence of rotated constellation on the fiber nonlinearities impairments	143
Figure 5.6: Influence of the angle of rotation on the BER performance of the AO- OFDM system.....	145
Figure 6.1: Illustration of the spatially multiplexed transmission link based on PCTWs technique.	151
Figure 6.2: Schematic of a spatially multiplexed AO-OFDM system based on PCTW technique.....	155
Figure 6.3: EVM versus power of subcarrier in AO-OFDM system with and without PCTW, a) 4QAM AO-OFDM system, b) 16QAM AO- OFDM system.....	157
Figure 6.4: SNR versus power of subcarrier in AO-OFDM system with and without PCTW, a) 4QAM AO-OFDM system, b) 16QAM AO- OFDM system.....	158
Figure 6.5: Bit rate error versus transmission distance in AO-OFDM system with and without PCTW, a) 4QAM AO-OFDM system, b) 16QAM AO-OFDM system.	159
Figure 6.6: Constellation diagrams of the AO-OFDM signal with and without PCTWs technique for 4QAM and 16QAM formats.....	161
Figure 6.7: BER performance for spatially multiplexed AO-OFDM, a) 4QAM, b) 16QAM.....	162

LIST OF TABLES

Table 4.1: Probability of interaction between the subcarriers

115

University of Malaya

LIST OF SYMBOLS AND ABBREVIATIONS

AD	Alternately delayed
ADC	Analog-to-digital converter
AO-OFDM	All-optical orthogonal frequency division multiplexing
ASE	Amplified spontaneous emission
AWG	Arrayed waveguide gratings
AWGN	Additive white Gaussian noise
BER	Bit error rate
CCDF	Complementary cumulative density function
CD	Chromatic dispersion
CDF	Cumulative distribution function
D	Dispersion coefficient
DAB/DVB	Digital audio/video broadcasting
DAC	Digital -to- analog converter
DBP	Digital-back-propagation
DCF	Dispersion compensating optical fiber
DCS	Digital coherent superposition
DFT	Discrete Fourier transform
DG	Degenerated
DOF	Degrees of freedom
EAMs	Electro-absorption modulators
EDFA	Erbium doped fiber amplifier
ESP	Electrical signal processor
EVM	Error vector magnitude
FFT	Fast Fourier transform

FWM	Four-wave mixing
ICI	Inter-carrier interference
IFFT	Inverse fast Fourier transform
IM	Intensity modulator
IM-DD	Intensity modulation- direct detection
IQ	In-phase and quadrature phase
ISI	Inter-symbol interference
LANs	Local area networks
LW	Linewidth
MCF	Multi-core fiber
MCM	Multicarrier multiplexing
MLLs	Mode-lock lasers
mPSK	m-array phase shift keying
mQAM	m-array quadrature amplitude modulation
MZIs	Mach Zehnder interferometers
MZM	Mach Zehnder modulator
NDG	Non-degenerated
NF	Noise figure
NRZ	Non-return to zero
ODFT	All-optical discrete Fourier transformation
OFCG	Optical frequency comb generator
OFDM	Orthogonal frequency division multiplexing
OIDFT	All-optical inverse discrete Fourier transformation
OIFT/OFT	All-optical inverse Fourier transform / Fourier transform
OOK	On-off keying
OPC	Optical phase conjugation

OSNR	Optical signal-to-noise ratio
PAPR	Peak-to-average power ratio
PCPs	Phase-conjugated pilots
PCTWs	Phase-Conjugate twin waves
PDM	Polarization division multiplexing
PLC	Planar lightwave circuit
PMD	Polarization-mode dispersion
PRBS	Pseudo-random binary sequence
PRT	Phase rotate term
PSC	Parallel -to- serial converter
QAM	Quadrature-amplitude modulation
Q-factor	Quality factor
QPSK	Quadrature phase shift keying
RF	Radio frequency
RZ	Return-to-zero
RZ-DBPSK	Return to zero differential binary phase shift keying
RZ-DQPSK	Return to zero differential quadrature phase shift keying
SCS	Scrambling coherent superposition
SLM	Selected mapping
SNR	Signal to noise ratio
SPC	Serial-to-parallel converter
SPM	Self-phase modulation
SSMF	Standard single mode optical fiber
TDM	Time division multiplexing
TWRS	TrueWave reduced slope
WDM	Wavelength division multiplexing

XPM	Cross-phase modulation
XPolM	Cross-polarization modulation
dB	Decibel
dBm	Decibel per mill watt
Gbps	Giga bit per second
GHz	Giga Hertz
Gsymbol/s	Giga symbol/second
km	Kilometer
m	Meter
nm	Nanometer
ps	Picosecond
rad	Radian
Tbps	Tera bit per second
W	Watt
μm	Micrometer

CHAPTER 1

INTRODUCTION

1.1 Background of orthogonal frequency division multiplexing systems

Nowadays, communication systems are incredibly developed to meet the demands of users everywhere due to advancement in smart mobile phone, multimedia devices, computers, and industrial monitoring. This advancement is rapidly increased more and more, requiring high data transmission technologies. The optical communication systems can gain this demand due to ability to transmit the required data rate, specifically with evolving the multichannel optical transmission systems such as wavelength division multiplexing (WDM), time division multiplexing (TDM), and orthogonal frequency division multiplexing (OFDM) systems. The optical OFDM systems have a higher interest among multichannel system due to high spectral efficiency and ability of transmitting a high bit rate over long-haul optical fiber link. Furthermore, the optical OFDM systems are much more resilient to dispersion (Armstrong, 2009; Hillerkuss et al., 2011), high flexibility in the generation of the OFDM signal and channel estimation in a time-varying environment.

One of the major strengths of the OFDM techniques is more adapted to a wide range of applications. In radio frequency (RF) domain, the OFDM systems are utilized in broad range communication such as digital audio/video broadcasting (DAB/DVB) and wireless local area networks (LANs). In optical domain, the optical OFDM systems have been recently considered for optical transmission applications (Dixon et al., 2001; Kim et al., 2004). The OFDM techniques have been employed for transmitting a high

bite rate signals in long-haul transmission systems. Furthermore, the OFDM modulation scheme has considerable advantages, making many optical networks employ OFDM scheme in physical layer. However, optical OFDM systems suffer from nonlinearity that occurred in transmitter, channel and receiver. In transmitter site, there are two intrinsic disadvantages: a laser phase noise, and a high PAPR. The fiber nonlinearity effects can have significant impairments on the OFDM signal due to phase noise that produced by interacting the nonlinear fiber impairments with the signal. Therefore, performance analysis of the optical OFDM system is essential to understand the origin of the impairments and to propose approaches to overcome or to reduce these effects.

Up to date, two types of existing optical OFDM systems was implemented. First type called conventional optical OFDM systems, and second type called all-optical OFDM systems (AO-OFDM).

1.1.1 Conventional optical OFDM systems

In late of 1996, OFDM technique was presented in the optical domain (Pan & Green, 1996). Although, the proposed OFDM system has been operated on the optical domain, it was implemented based on same idea that used in the RF OFDM system (A. J. Lowery & Armstrong, 2005). We call this system by conventional optical OFDM system. The most parts of the transmitter and receiver have been realized with similar parts of the RF OFDM system. For example fast Fourier transform (FFT) processing, analog-to-digital converter (ADC), digital-to-analog converter (DAC), serial-to-parallel converter (SPC) and parallel-to-serial converter (PSC) have been utilized to generate OFDM signal (Kumar, 2011). Moreover, many techniques to reduce the peak-to-average power ratio (PAPR), inter-symbol interference (ISI), and inter-carrier

interference (ICI) are implemented in same manner that has been used in the RF OFDM system (Y. Chen et al., 2012; Le Khoa et al., 2012; W_ Shieh et al., 2008).

In conventional optical OFDM system, the electrical OFDM signal is modulated by either direct modulation (Pan & Green, 1996) or by using external modulators to generate the optical OFDM signal (Djordjevic & Vasic, 2006; W Shieh et al., 2007). The electrical OFDM signal is typically generated by utilizing inverse fast Fourier transform (IFFT) processors SPC, PSC and DAC in electrical domain. Because of optical OFDM signal is produced by aiding electrical processors, the bit rate and capacity of the conventional optical OFDM system is limited. However, the conventional optical OFDM systems are able to transmit a high data rate in long-haul link as compared with WDM or TDM systems due to employing a high number of subcarriers.

1.1.2 AO-OFDM systems

In conventional optical OFDM systems, both FFT and IFFT are typically performed in the electronic domain, and they therefore limit the transmission bit rate. Until now, real-time electronic IFFT and FFT signal processing for optical OFDM signals up to 101.5 Gbps has been demonstrated (Schmogrow et al., 2011). This limitation seems to be too far-fetched to reach desirable values for the generation or reception of Tera bit per second (Tbps) OFDM signals. All-optical solution that could work beyond the state-of-art electronics speed would therefore be of immense interest. Recently, the critics argued against optical OFDM techniques because of system capacity and nonlinearity of modulators are solved by proposing the AO-OFDM systems. With developing optical components, such as optical frequency comb

generator (OFCG), selective optical switches and arrayed waveguide gratings (AWGs), the implementation of AO-OFDM system has been realized (Hillerkuss et al., 2010a; Z. Wang et al., 2011). With advancements made in optical components and invention of AO-OFDM techniques, the system capacity limitation is no longer an impediment anymore because the huge bandwidth of optical fiber and high signal processing speed obtainable by the optical components. In the AO-OFDM systems, the OFDM subcarriers are optically generated and IFFT/FFT processing is optically implemented by utilizing optical components. Each subcarrier is modulated by using external modulator and it carries a high data information rate as compared with conventional OFDM subcarriers. Therefore, large transmission capacity and higher bit rate can be accomplished by AO-OFDM systems. The real-time generation of AO-OFDM signals by real-time optical FFT processing of 10.8 Tbps and 26 Tbps has been experimentally demonstrated (Hillerkuss et al., 2011).

1.1.3 Advanced modulation formats in optical OFDM systems

In optical OFDM systems, on-off keying (OOK) and advanced modulation formats such as m-array phase shift keying (mPSK) and m-array quadrature-amplitude modulation (mQAM) formats are mostly used as modulation formats (I Kang et al., 2011; A. Lowery & Armstrong, 2006; William Shieh et al., 2008; W. Wang et al., 2014). It is believed that mQAM format is more power efficient than OOK format because mQAM format can transmit $\log_2(m)$ bits with only one symbol. Therefore, the functionality enhancement and increase of the spectral efficiency are the main advantages of employing the multilevel modulation formats in optical OFDM systems as compared with OOK formats (Ho, 2005; Nakazawa et al., 2013; Nakazawa et al., 2010). The multilevel modulation formats can also have mitigated the phase noise and

increased tolerance towards fiber nonlinearity due to the more optimum allocation of symbols on the complex plane. Moreover, continuous envelope with different phases of the transmitted signal decreases influence of the dispersion on the transmitted signal. In addition, the full advantage of employing multilevel modulation format can be obtained with using coherent detection and digital signal processing (DSP) in the receiver (Ellis & Gunning, 2005; Nakazawa et al., 2013; Omiya et al., 2013).

The polarization division multiplexing (PDM) technique has been cited to enhance the transmission capacity of the optical communication systems (X. Liu et al., 2011a; Dirk van den Borne et al., 2007; Wree et al., 2003). Indeed, the PDM technique allows the optical OFDM system to carry information over two orthogonal states of polarization (Hayee et al., 2001). By employing the PDM technique in multi-carrier optical communication systems, the optical carriers can be significantly expanded in two dimensions: wavelength and polarization (Kikuchi, 2011). However, the PDM technique suffers from polarization-mode dispersion (PMD) effect, which is caused by the differential group delay between orthogonal states of polarization. The PMD can break up the orthogonality between the polarization states, degrading performance of optical communication system (Bhandare et al., 2005; Hayee et al., 2001; H. Liu et al., 2006).

1.2 Problem statement

Among all the multiplexing systems, the AO-OFDM system is able to transmit huge data information with bit rate of Tera bit per second (Tbps) over one fiber, because its subcarriers can carry a high rate data. By aiding the optical components, the online processing can be executed for transmitting and receiving the optical OFDM signal.

Unfortunately, it was identified early that the transmission performance of AO-OFDM system in terms of bit error rate (BER), optical signal-to-noise ratio (OSNR) and achievable transition distance, was limited by phase noise. The phase noise is a big problem facing the researchers in long-haul optical OFDM systems, which is caused by the fiber nonlinearity as well as the amplified spontaneous emission (ASE) noise and its interaction with fiber nonlinearity. These phase noises significantly degrade the system performance and limit its capacity. This thesis intends to develop an analytical model to understand the factors that govern the nonlinear impairments and then propose approaches to improve the transmission performance of AO-OFDM system by solving the phase noise problem.

1.3 Objectives of the study

This thesis primarily aims to propose, analyze and simulate various AO-OFDM schemes for mitigating the fiber nonlinearity impairments so that the transmission performance of the system can be improved. This study focuses on the following objectives:

- a) To develop an analytical model that estimates the effect of fiber nonlinear impairments and their interaction with ASE noise;
- b) To investigate a combination of mQAM modulation format with return-to-zero (RZ) coding format for mitigating the nonlinear phase noise;
- c) To mitigate the fiber nonlinear effects and to reduce the phase noise by minimizing the interaction time between the subcarriers;

- d) To proposed a new approach for reducing PAPR based on modulating half subcarriers in AO-OFDM systems with rotated QAM constellation.
- e) To investigate the effectiveness of phase-conjugated twin waves (PCTWs) technique on mitigation of fiber nonlinear impairments in spatially multiplexed AO-OFDM systems.

1.4 Scope of the study

This thesis provides a comprehensive analysis of AO-OFDM performance in presence of nonlinear phase noises. Furthermore, four techniques to reduce the phase noise and to increase the maximum reach of AO-OFDM are proposed. These techniques are analytically modeled and numerically demonstrated. The investigation of these techniques is carried out for both 4QAM and 16QAM modulation formats. For the various schemes, our investigations are focused on demonstrating and comparing the results that obtain from analytical model and that achieved by VPItransmissionMaker software to evaluate the effect of parameters such as power of subcarrier, transmission distance, number of subcarriers and fiber dispersion on the nonlinear phase noise and BER performance of AO-OFDM systems.

1.5 Original contributions

The following original contributions to the field of optical fiber communication have been made in the course of this research work, giving rise to the following publications:

- Development of analytical model that evaluates linear and nonlinear phase noises that induced by SPM, XPM, and FWM phenomena and their interaction with ASE noise in both 4QAM and 16QAM AO-OFDM transmission systems (J. K. Hmood et al., 2015b)(Chapter 3).
- Development and demonstration of a new technique to improve the performance of AO-OFDM systems based on combining RZ coding with mQAM formats (J. Hmood et al., 2015)(Section 4.2).
- Mitigation of phase noise in AO-OFDM systems based on minimizing interaction time between subcarrier, which is enabled by employing RZ-mQAM modulation format and making a time delay between the odd and even subcarriers (J. K. Hmood et al., 2015d)(Section 4.3).
- A new approach for reducing PAPR based on modulated half subcarriers in AO-OFDM systems with rotated QAM constellation is presented (J. K. Hmood et al., 2015c)(Chapter 5).
- The effectiveness of PCTWs technique is investigated for mitigating fiber nonlinear impairments in spatially multiplexed AO-OFDM system (Hmood et al., 2016).

1.6 Thesis structure

This thesis is organized into seven chapters where Chapter 1 introduces AO-OFDM and describes the problem statement, objectives and the scope of this study.

Chapter 2 provides an overview of optical OFDM systems, covering conventional and all-optical OFDM technologies, principle, and recent progress. Furthermore, the theory of the optical channel is detailed by characterizing the linear

fiber impairments such as attenuation, and chromatic dispersion (CD) as well as fiber nonlinearity impairments, such as SPM, XPM and FWM.

Chapter 3 analyzes the performance of mQAM AO-OFDM system by developing an analytical model. The developed model is able to estimate the linear and nonlinear phase noises that induced by the fiber nonlinearity effects and their interaction with ASE noise. The accuracy of the analytical model is verified by comparing the obtained results from analytical model with the simulation results that obtained by using VPItransmissionMaker[®] commercial software.

Chapter 4 deals with two new approaches to mitigate fiber nonlinearity and reduce the effect of nonlinear phase noise on the performance of AO-OFDM system that employ QAM format. Section 4.2 proposes a new combination between RZ coding format and 4QAM and 16QAM modulation formats in AO-OFDM system for improving the system performance. At transmitter side, the conversion from mQAM to RZ-mQAM formats is optically realized by using a single Mach-Zehnder modulator (MZM) after mQAM modulator for each subcarrier. The effectiveness of RZ-4QAM and RZ-16QAM in AO-OFDM systems is numerically demonstrated. The impacts of subcarrier peak power and fiber length on error vector magnitude (EVM) are also studied.

A new approach to mitigate the phase noise and improve the performance of AO-OFDM systems based on minimizing the interaction time between subcarriers is presented in Section 4.3. The interaction time between subcarriers is minimized by shaping the envelopes of QAM subcarriers and making a delay time between even and odd subcarriers. RZ coding is adopted for shaping the envelopes of subcarriers. In addition, the subcarriers are alternately delayed (AD) by optical time delayers. The performance of an AO-OFDM system that implements the proposed technique is

analytically modeled and numerically demonstrated. The total phase noise variance, achievable transmission distance and OSNR are investigated and compared to AO-OFDM systems that adopt traditional mQAM modulation formats.

A simple technique to reduce PAPR based on rotated constellation in coherent AO-OFDM system is described in Chapter 5. In this approach, the subcarriers are divided into odd and even subsets. Then the constellation of odd subcarriers is rotated counter clockwise while the constellation of even subcarriers is remained without rotation. The impact of the rotation angle on the PAPR is mathematically modeled. Then, the effect of resulting PAPR reduction on the total phase noise in AO-OFDM systems is mathematically modeled and numerically investigated. The nonlinear phase noise variance and BER performance are explored and compared to AO-OFDM systems that adopt traditional mQAM modulation formats.

Chapter 6 investigates the effectiveness of PCTWs technique on mitigation of fiber nonlinearity impairments in spatially multiplexed AO-OFDM systems. In this technique, AO-OFDM signal and its phase-conjugated copy is directly transmitted through two fiber links. At receiver, two signals are coherently superimposed to cancel the phase noise and to enhance signal-to-noise ratio (SNR). To show the effectiveness of proposed technique, a spatially multiplexed AO-OFDM system is demonstrated by numerical simulation.

The finding of this study is concluded in Chapter 7.

CHAPTER 2

LITERATURE REVIEW

2.1 Introduction

Orthogonal frequency division multiplexing (OFDM) system is a special class of multicarrier multiplexing (MCM) systems where OFDM subcarriers are orthogonal to each other (William Shieh & Djordjevic, 2009). The optical OFDM systems have a broader band as compare with the other MCM systems, because the data is transported over many close-spaced subcarriers. The optical OFDM systems have been got a higher interest among multichannel system due to high spectral efficiency and ability of transmitting a high bit rate over long-haul optical fiber link. Moreover, all optical circuits such as all-optical inverse fast Fourier transform / fast Fourier transform (OIFFT/ OFFT) circuits have been proposed to increase both processing speed and transmission rate optical OFDM systems, substantially. Indeed, all-optical OFDM (AO-OFDM) systems, which employ OIFFT/OFFT, could not only eliminate electronic speed limitations, but also achieve real-time transmission (Hillerkuss et al., 2011; Y. Li et al., 2011). Therefore, the demand of data rate in near future can be provided by using such system.

This chapter starts with explaining the conventional optical OFDM system as well as AO-OFDM system. The basic principles of both systems are discussed. Moreover, in order to explore the effects that impair the transmission performance of optical OFDM

system, the theory of peak-to-average power ratio (PAPR), optical fiber impairments and optical amplifier noise are briefly explained. After explaining linear effects such as attenuation and chromatic dispersion (CD), the nonlinear impairments such as self-phase modulation (SPM), cross-phase modulation (XPM), and four-wave mixing (FWM), which are caused by the Kerr effects, are discussed too. Finally, the optical mitigation techniques, which have been reported in previous works, are presented.

2.2 Optical OFDM systems

The theory of the OFDM technique was developed in the Bell Lab in the year 1966 by developing the frequency division multiplexing (FDM) technique (Chang, 1966). The earlier versions of the OFDM system were using a bank of analogue modulators. In order to reduce the implementation complexity of the OFDM communication system, the OFDM communication system that employed the discrete Fourier transform (DFT) has been proposed (Weinstein & Ebert, 1971). In latter, with developing the digital techniques, the OFDM system was developed to use the inverse fast Fourier transform (IFFT) and fast Fourier transform (FFT) to preserve the orthogonality of subcarriers. In late of 1996, OFDM technique was presented in the optical domain (Pan & Green, 1996). Although, the proposed OFDM system has been operated on the optical domain, it was implemented based on same idea that used in the radio frequency (RF) OFDM system (A. J. Lowery & Armstrong, 2005). The most parts of the transmitter and receiver have been realized with similar parts of the RF OFDM system, for example IFFT, FFT, ADC, DAC, serial-to-parallel converter (SPC) and parallel-to-serial converter (PSC) (Kumar, 2011). Moreover, many techniques to reduce PAPR, inter-symbol interference (ISI) and inter-carrier interference (ICI) have been implemented in same manner that have been used in the RF OFDM system (Y. Chen et

al., 2012; Le Khoa et al., 2012; W_ Shieh et al., 2008). With developing optical components, such as optical frequency comb generator, selective optical switches and arrayed waveguide gratings (AWGs), OIFFT/OFFT circuits have been implemented to provide the necessary processing speed. The implementation of OIFFT/OFFT enables the high bit rate AO-OFDM system (Hillerkuss et al., 2010a; Z. Wang et al., 2011). In following sections, both the conventional optical OFDM and AO-OFDM systems are introduced.

2.3 Conventional optical OFDM system

Figure 2.1 depicts the block diagram of the conventional optical OFDM system. In the transmitter, the signal processing is performed by employing electronic and optical parts. The electronic part comprises of SPC, IFFT, PSC, and digital-to-analog converter (DAC) modules while the laser source and external optical modulator are the main elements in the optical part. Electrical OFDM signal is generated by electronic modules and converted to optical domain by optical part. Similarly, in receiver side, the optical part includes the optical detectors that convert the optical signal to electrical signal while the electronic parts consist of ADC, SPC, FFT, and PSC modules that restore a data.

Generally, at the transmitter, the incoming data is converted to parallel by SPC and mapped according to the modulation technique. After that, subcarriers are modulated in the digital domain by using IFFT module (Armstrong, 2009). The output of the IFFT represents a superposition of all modulated subcarriers. The output of the IFFT module is converted to serial by PSC and then to analogue by DAC. After that, the electrical OFDM signal (output of DAC) drives the optical modulator. In case of the

OFDM subcarriers are modulated by high-order modulation format such as m-array quadrature-amplitude modulation (mQAM) format, the in-phase (I) component of the signal is obtained by converting the real part of the serial signal to analogue signal by DAC. Similarly, the quadrature phase (Q) component is generated by converting the imaginary part of serial signal to the analogue signal by another DAC. Both I and Q components are fed to external optical modulator for producing optical OFDM signal.

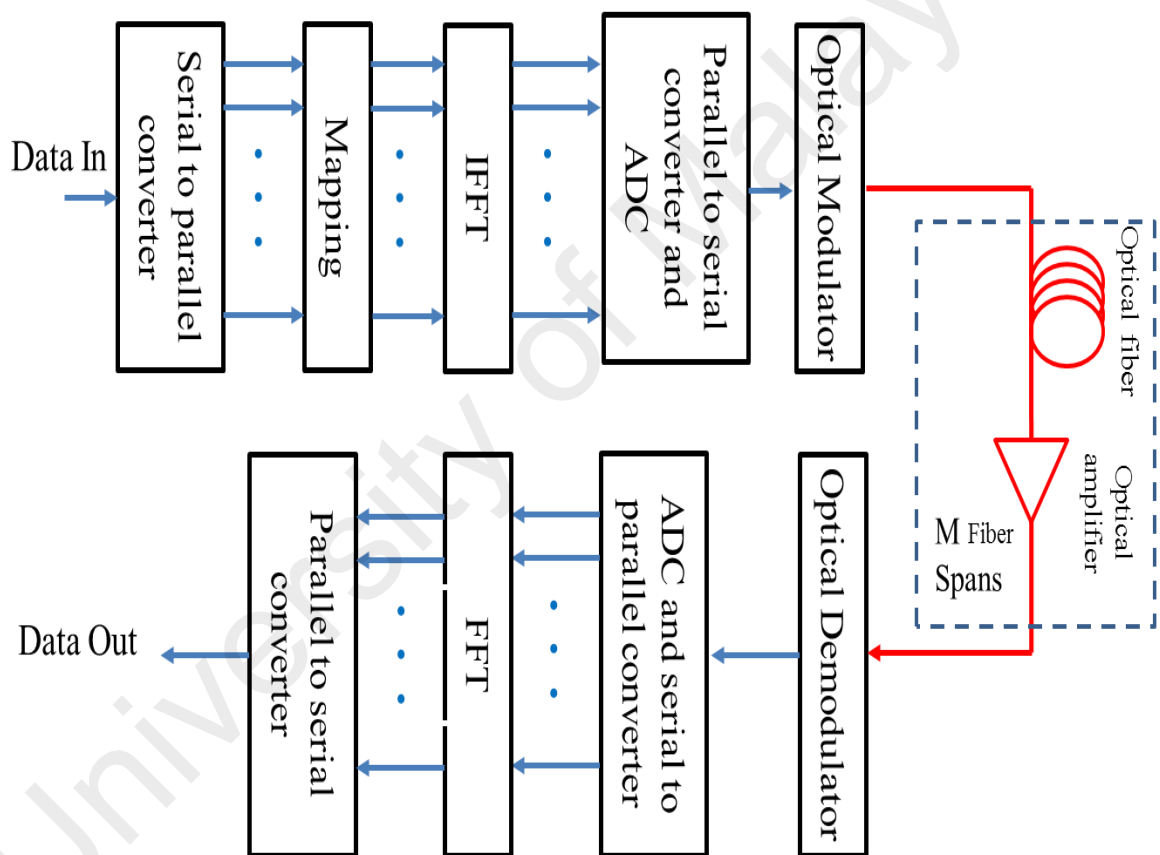


Figure 2.1: Block diagram of conventional OFDM System

In order to transmit the OFDM signal optically, the combination of the laser source and external optical modulator are used to convert the OFDM signal from electrical domain to the optical domain. Mach Zehnder Modulator (MZM) is commonly used in optical fiber communication systems as an external optical modulator. In optical OFDM systems that employ high-order modulation format, both the real and imaginary components of the OFDM signal in electrical domain modulate the amplitude and phase of the laser source signal. Therefore, the OFDM signal derives a complex optical modulator called in-phase - quadrature phase (IQ) modulator, which is able to modulate the in-phase and quadrature phase envelopes. Figure 2.2 shows the structure of optical IQ modulator. The optical IQ modulator composes of two arms where the upper arm consists of one MZM, while lower arm contains one MZM and $\pi/2$ phase shifter. Two MZMs in the lower and upper arms are simultaneously driven by the in-phase and quadrature components of the complex envelope, respectively. (Hayee et al., 2001; Kikuchi, 2011).

The generated optical OFDM signal is transmitted through a multi-spans optical fiber link. Each span composes from standard single mode optical fiber (SSMF) and optical amplifier for compensating losses of optical fiber. At end of transmission line, the optical receiver processes the modulated signal for restoring the transmitted data. At optical OFDM receiver, the received signal is converted from optical domain to electrical domain by optical demodulator. Then, the signal is arranged in parallel to form the FFT inputs after converting it to digital signal by ADC. Each FFT input is corresponded to a subcarrier. All subcarriers are demodulated by an FFT operation and converted to the serial data by a PSC.

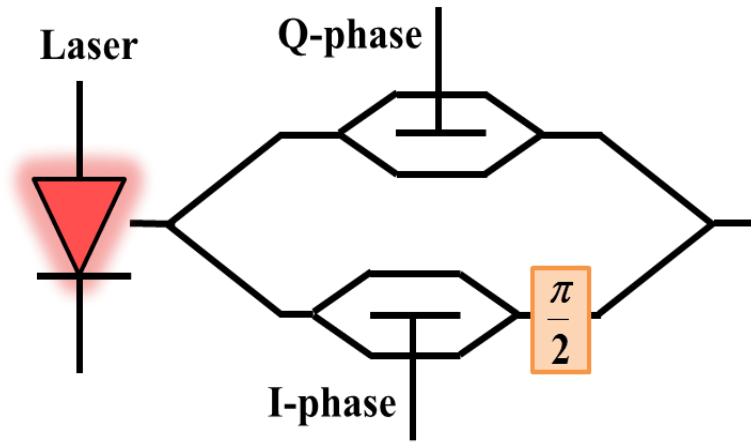


Figure 2.2: Optical IQ Modulator (Kikuchi, 2011)

2.4 AO-OFDM systems

The advancement of the optical component fabrication enables the implementation of all-optical inverse Fourier transforms (OIFT)/ Fourier transform (OFT). Various AO-OFDM schemes have been proposed based on real-time processing by using OIFT/OFT. Generally, the AO-OFDM transmitters, which have been reported in previous works, can be divided into two categories. In first category, the transmitters utilize an OIFT, in which the modulated optical pulse train is transformed to the OFDM symbol (Hillerkuss et al., 2010a; Lee et al., 2008). In the second category, an optical multicarrier source such as a bank of laser sources or an optical frequency comb generator (OFCG) is employed to provide OFDM subcarriers optically as shown in Figure 2.3 (X. Liu et al., 2011c). These subcarriers are individually modulated before combining to form OFDM signal. In this section, the two categories of AO-OFDM transmitter are briefly described. Furthermore, the schemes of AO-OFDM receiver are presented.

2.4.1 AO-OFDM transmitters using OIFT

In the AO-OFDM transmitter, the main function of OIFT is to transform the input optical pulses into OFDM symbol. In other words, the optical pulses train that provided by pulse generator, such as a mode-locked laser, is split into N copies. Each copy of the pulses train is individually modulated with a modulation format. Then all modulated pulse trains are combined by the OIFT circuit to form OFDM signal (Guan et al., 2014; Hillerkuss et al., 2010a).

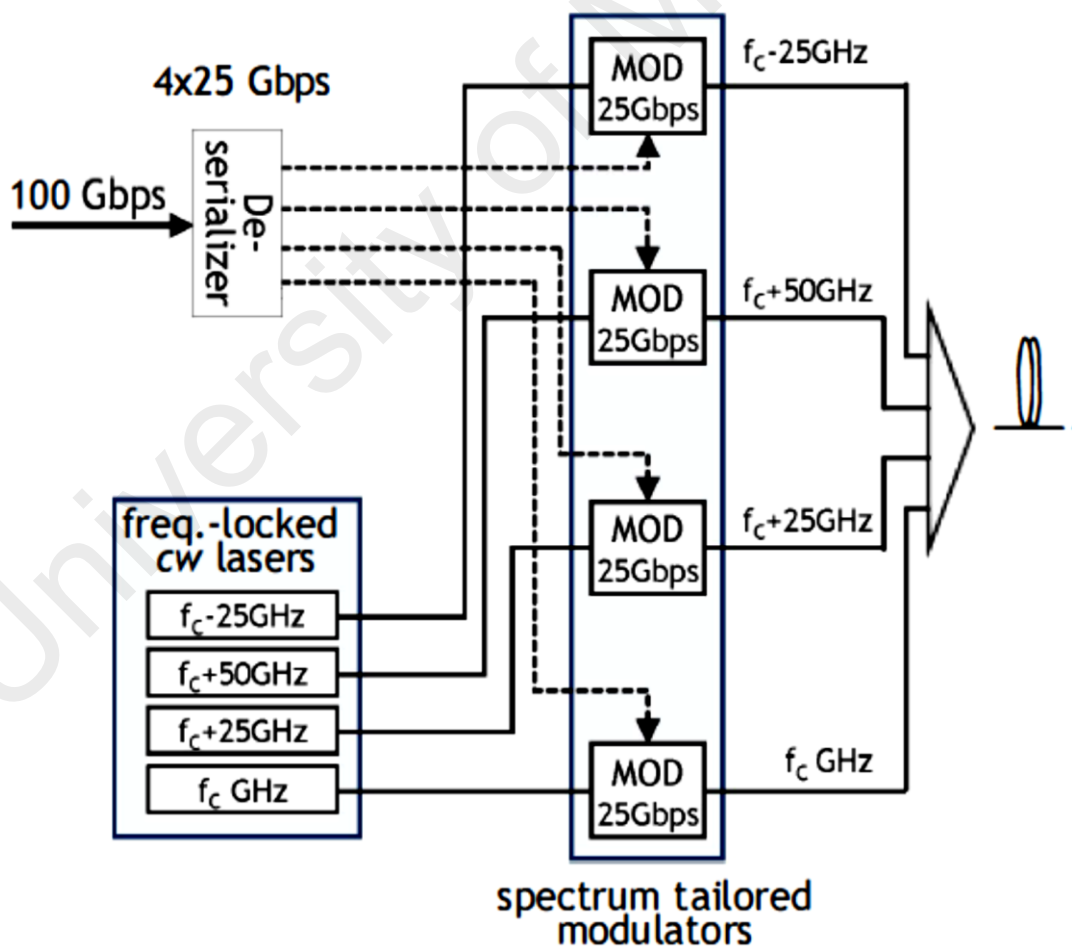


Figure 2.3: Optical IFT using bank of laser sources (X. Liu et al., 2011c)

Up to date, two kinds of the OIFT have been proposed in the AO-OFDM transmitter. Several AO-OFDM transmitters utilizes an all-optical inverse discrete Fourier transformation (OIDFT) circuit, in which optical phase shifters, time delayers and couplers were employed to generate optical OFDM signal (Lee et al., 2008). The other AO-OFDM transmitter schemes use a continuous OIFT system based on time lens (Kumar & Yang, 2008; Y. Li et al., 2010).

Many techniques have been reported for designing the OIDFT/ODFT circuit by combining optical time delayers and phase shifters for producing and recovering the optical OFDM signal. The OIDFT/ODFT circuit, which is constructed by combining the optical couplers, time delayers and phase shifters, has been introduced for 4×25 Gbps AO-OFDM systems as shown in Figure 2.4 (Lee et al., 2008). In this system, the bandwidth requirements for electronics devices are reduced to 25 Gbps due to employing OIDFT/ODFT. However, because of using many time delayers and phase shifters, the system was complex and expensive, particularly at high number of subcarriers. To reduce the cost and complexity of the system, a silicon planar lightwave circuit (PLC) has been utilized to implement OIDFT/ODFT for AO-OFDM systems. The phase shifters, optical delayers, and optical couplers were fabricated and integrated in one silicon PLC. Figure 2.5 depicts the scheme of 4×4 OFDT based on silicon PLC technology, which has been implemented in 160 Gbps AO-OFDM system (W. Li et al., 2010).

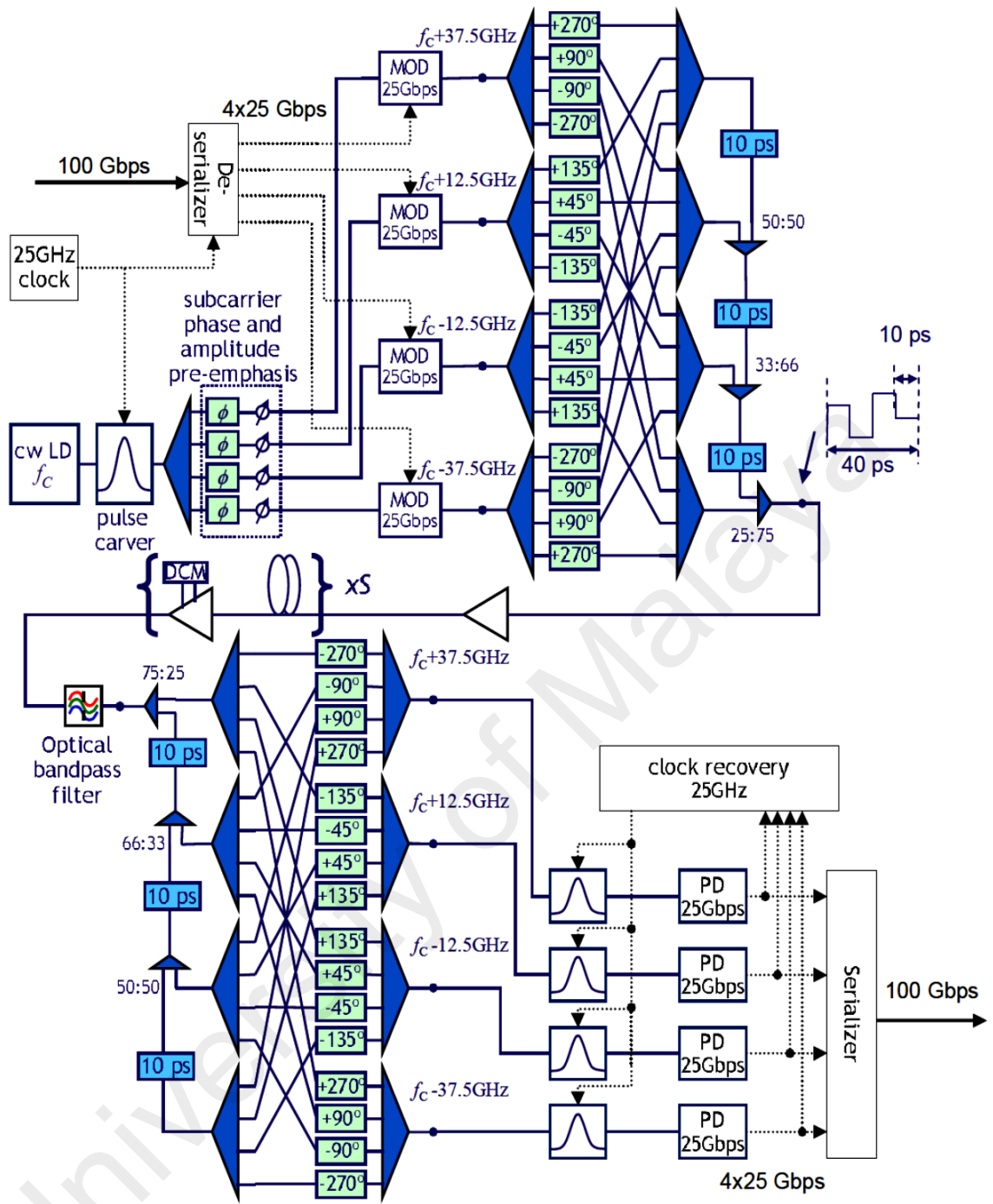


Figure 2.4: Scheme of AO-OFDM system that utilizes OI DFT/ODFT (Lee et al., 2008).

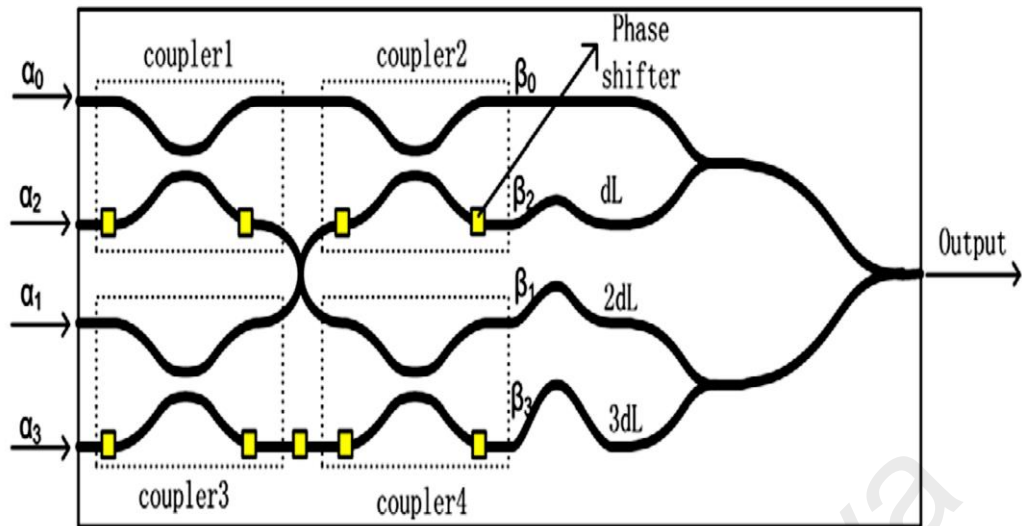


Figure 2.5: Scheme of 4-order OFDT based on PLC technology (W. Li et al., 2010)

Furthermore, the OIIFT/OIFT have been realized by an AWGs (Z. Wang et al., 2011). The AWGs are commonly used in wavelength division multiplexing (WDM) systems for multiplexing the channels at transmitter and de-multiplexing them at receiver. The main advantage of the OIIFT/OIFT based on AWGs is less complexity, specifically for large number of OFDM subcarriers. Moreover, the AWGs are passive integrated devices and they not require electronic drive circuits. The required phase shift and time delay can be achieved by precise design of AWGs multiplexer. The construction of OIIFT/OIFT by AWGs is shown in Figure 2.6 (A. J. Lowery & Du, 2011). The AO-OFDM systems that realized by using AWGs have been demonstrated for high data rate (Lim & Rhee, 2011; Shimizu et al., 2012; Z. Wang et al., 2011).

The continuous OIIFT/OIFT based on time lenses has been proposed to realize the AO-OFDM system (Kumar & Yang, 2008, 2009). The time lens utilizes a cascade of dispersive element (such as optical fiber or fiber grating), quadratic phase modulator and a dispersive element as shown in Figure 2.7 (Wei Li et al., 2009). The quadratic

phase modulator can be implemented by driving the phase modulator by quadratic wave (t^2) (Yang & Kumar, 2009). The quadratic phase modulator plays significant role in the operation of continuous OIFT/OFT. However, it is difficult to realize the quadratic phase modulator at high frequency. Therefore, the quadratic phase modulator has been driven by arbitrary wave generator (Yang & Kumar, 2009) or by electric clock that generated by the system (Y. Li et al., 2011).

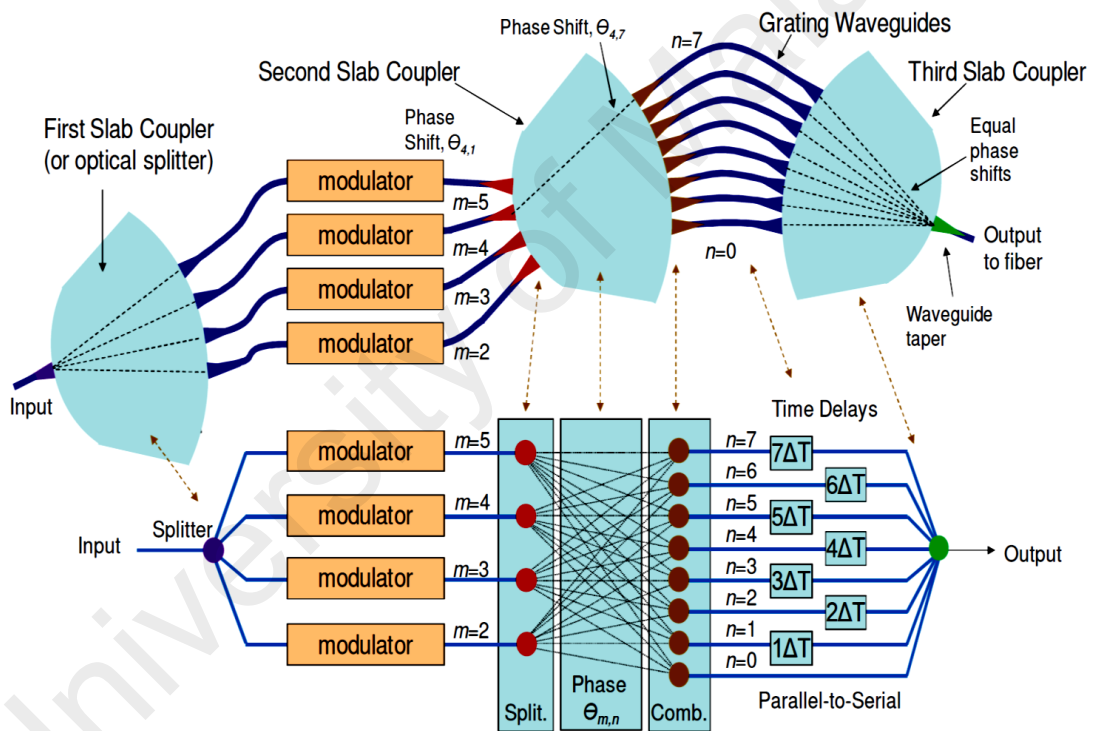


Figure 2.6: AO-OFDM transmitter utilizes the AWGs to implement OIFT (A. J. Lowery & Du, 2011).

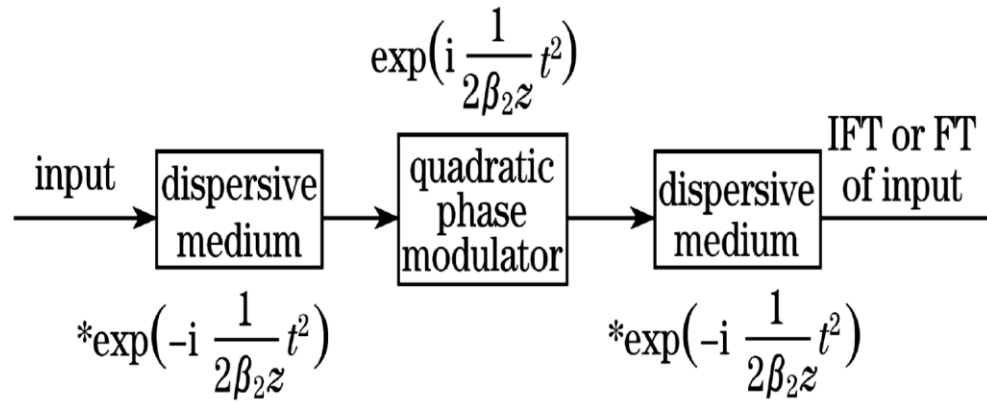


Figure 2.7: All-optical Fourier transform using the time lens (Wei Li et al., 2009).

A real time 8×2.5 Gbps AO-OFDM system based on two time lenses has been experimentally demonstrated as shown in Figure 2.8 (Y. Li et al., 2011). At the transmitter, a continuous OIFT, which contains a quadratic phase modulator and two high dispersive elements, transforms the modulated optical pulses into AO-OFDM symbols. At the receiver, another continuous OFT that has similar components, converts the AO-OFDM symbols to original modulated optical pulses. The quadratic phase modulators were driven by a sinusoidal wave instead of quadric wave (t^2). To drive the phase modulator at the receiver, the sinusoidal wave has been generated in the transmitter with certain phase shift. Experiment results reveal that the OFDM signal has been successfully transmitted over 200 km non-zero dispersion shifted fiber (G.655 fiber) without any dispersion compensation. However, the phase modulator has been driven by sinusoidal wave, causing a very narrow time window for Fourier transformation operation.

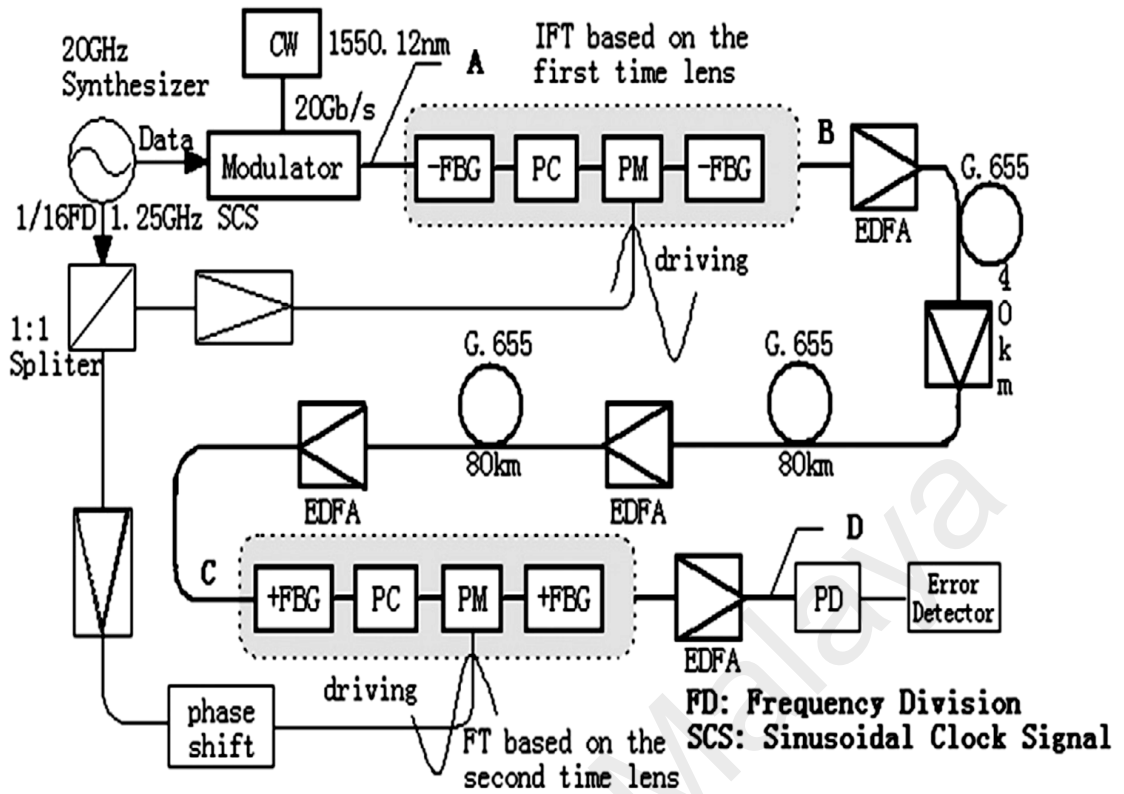


Figure 2.8: Block diagram of AO-OFDM system based on time lens (Y. Li et al., 2011).

2.4.2 AO-OFDM transmitter using optical multicarrier source

The AO-OFDM transmitters using OIFT requires complex optical components and phase sensitive operation conditions. Therefore, the OIFT circuit can be replaced by a simple circuit, which consists of an optical multicarrier source, optical modulators and multiplexer, as shown in Figure 2.3. If accurate optical frequency control is provided for optical carriers (X. Liu et al., 2011c), the orthogonality can be preserved. On other words, the frequency spacing between two adjacent optical carriers is adjusted to be equal to the symbol rate for satisfying the orthogonality condition. Furthermore, a phase correlation, which is known as coherence, is required between all of the optical

subcarriers to mitigate crosstalk between optical subcarriers. For realizing these conditions, the OFCG is employed in AO-OFDM systems. The OFCG can produce a set of frequency carriers with fixed frequency spacing and phase. Single laser source is employed to generate comb frequency lines (Dou et al., 2012), making all subcarriers have an inherent phase correlation or coherence.

Optical frequency comb generation has significant role in the different fields of technologies including optical communication systems. The OFCG has three important features, which distinguish it from the other optical multicarrier sources, namely the constant frequency spacing between frequency comb lines (orthogonality), strong phase coherence across the spectral bandwidth (stability) and the possibility to tune oscillation frequency (flexibility). However, the number of generated comb lines, the flatness of spectral comb lines, complexity, and cost are the main limitations of using OFCG in optical communication system. For example, the mode-lock lasers (MLLs) are able to generate high number of comb lines, but the stability and flatness of spectral comb lines are low as shown Figure 2.9. Another example of OFCG that utilizes optical modulation components, such as phase and intensity modulators and phase shifters, can provide a stable frequency comb lines with precise channel spacing and fixed phase as shown in

Figure 2.10 (Shang et al., 2014). Moreover, the oscillation frequency can be flexibly tuned. However, the limited number of generated comb lines and using high power of external RF signal to drive the modulators are main limitations of this technique.

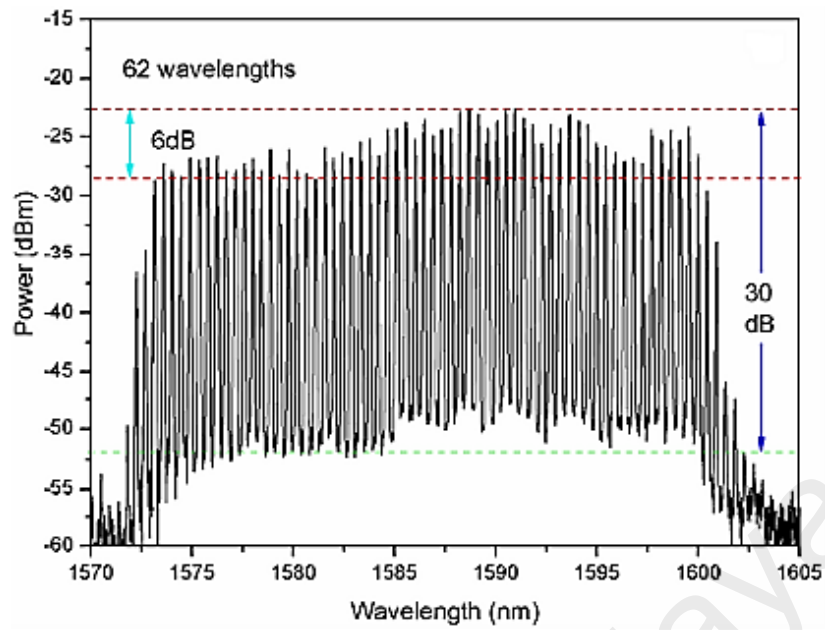


Figure 2.9: Output spectra of the mode-lock fiber laser (Xuesong Liu et al., 2012).

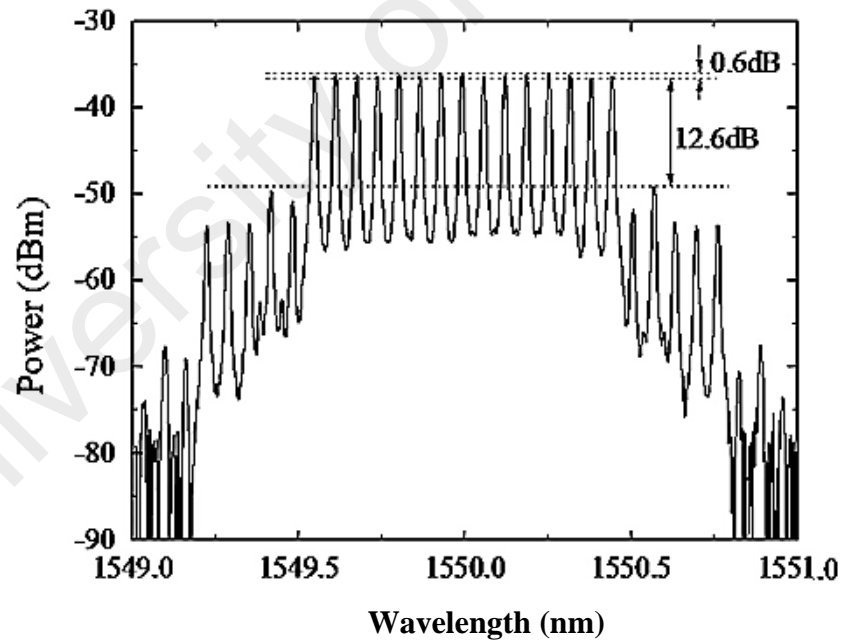


Figure 2.10: Optical spectra of the 15-line OFCG that utilizes two cascaded intensity modulators (Shang et al., 2014).

The AO-OFDM transmitter that employs OFCG has been reported to simplify the transmitter circuit, especially, with higher number of subcarriers (Chandrasekhar et al., 2009; Hillerkuss et al., 2011; Sano et al., 2009). Indeed, the OIFFT can be implemented by employing some optical components such as OFCG, optical multiplexer/demultiplexer, and optical modulators. The block diagram of the all-optical OFDM transmitter using OFCG is shown in Figure 2.11 (Sano et al., 2009). The subcarriers, which are generated by OFCG, are split by optical demultiplexed and simultaneously applied to external optical modulators. Each subcarrier is individually modulated. After that, the modulated OFDM subcarriers are combined by an optical multiplexer to form the optical OFDM signal (Sano et al., 2007; Yonenaga et al., 2008).

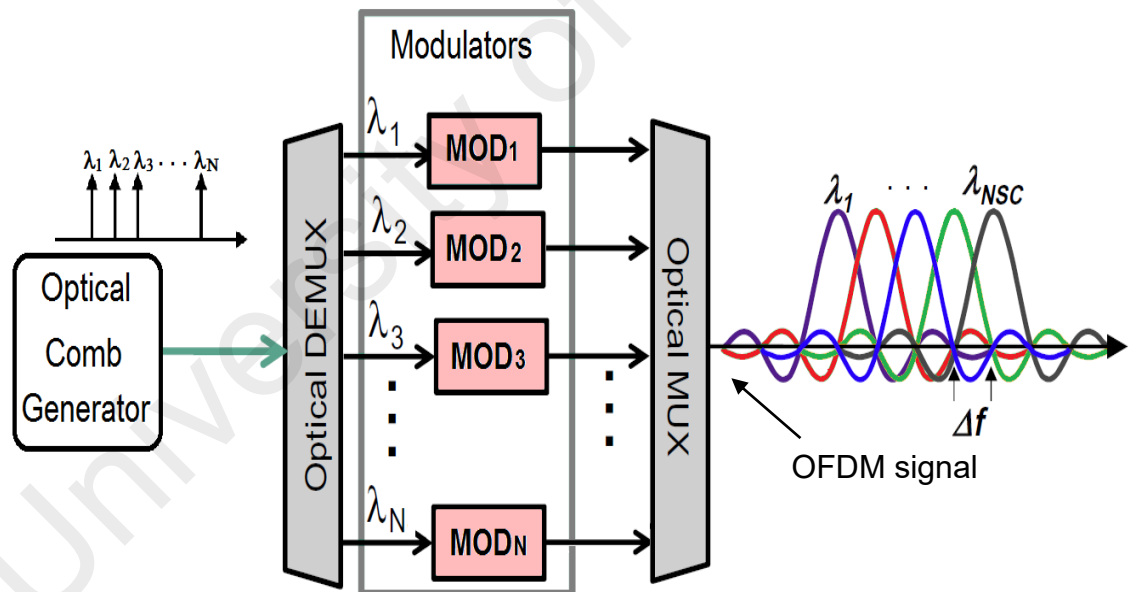


Figure 2.11: AO-OFDM transmitter using OFCG (Sano et al., 2009)

2.4.3 AO-OFDM receiver

The adjacent OFDM subcarriers are closely spaced where the frequency spacing between neighboring subcarriers is equal to the symbol rate, making their spectra overlap. Actually, any two adjacent subcarriers are orthogonal to each other if only if the frequency spacing between them makes the integration over symbol period equal to zero. Accordingly, the frequency spacing should be equal to the symbol rate. Therefore, the using optical filters are not appropriate for extracting the subcarriers optically. Consequently, proper receivers that use FFT can detect them. In conventional optical OFDM systems, the FFT is performed in the electronic domain by digital signal processing. Currently, the speed of digital processor limits transmission rate of optical OFDM systems that use electronic implementation of FFT.

In AO-OFDM system, the real-time OFFT signal processing is realized at speed far beyond the limits of electronic digital processing (Hillerkuss et al., 2010a). Similar to implementation of OIFFT, the OFFT is implemented by optical couplers, phase shifters, time delayers, and optical sampling gates (Hillerkuss et al., 2010b; Lee et al., 2008). The OFFT processing has been simplified to reduce the number of used optical components, especially at high number of subcarriers (Hillerkuss et al., 2010b). The simplifying steps are illustrated in Figure 2.12, where the redundancy in optical components is eliminated by relocating the optical sampling gate at end of the OFFT and then rearranging and replacing some time delayers. Actually, after simplifying the OFFT circuit composes of many Mach Zehnder interferometers (MZIs), where two couplers, one phase shifter and one time delayer are connected to form one MZI. Low-complexity 4-order OFFT circuit has been designed with three MZIs and four optical sampling gates as shown in Figure 2.12 (d) (Hillerkuss et al., 2010a).

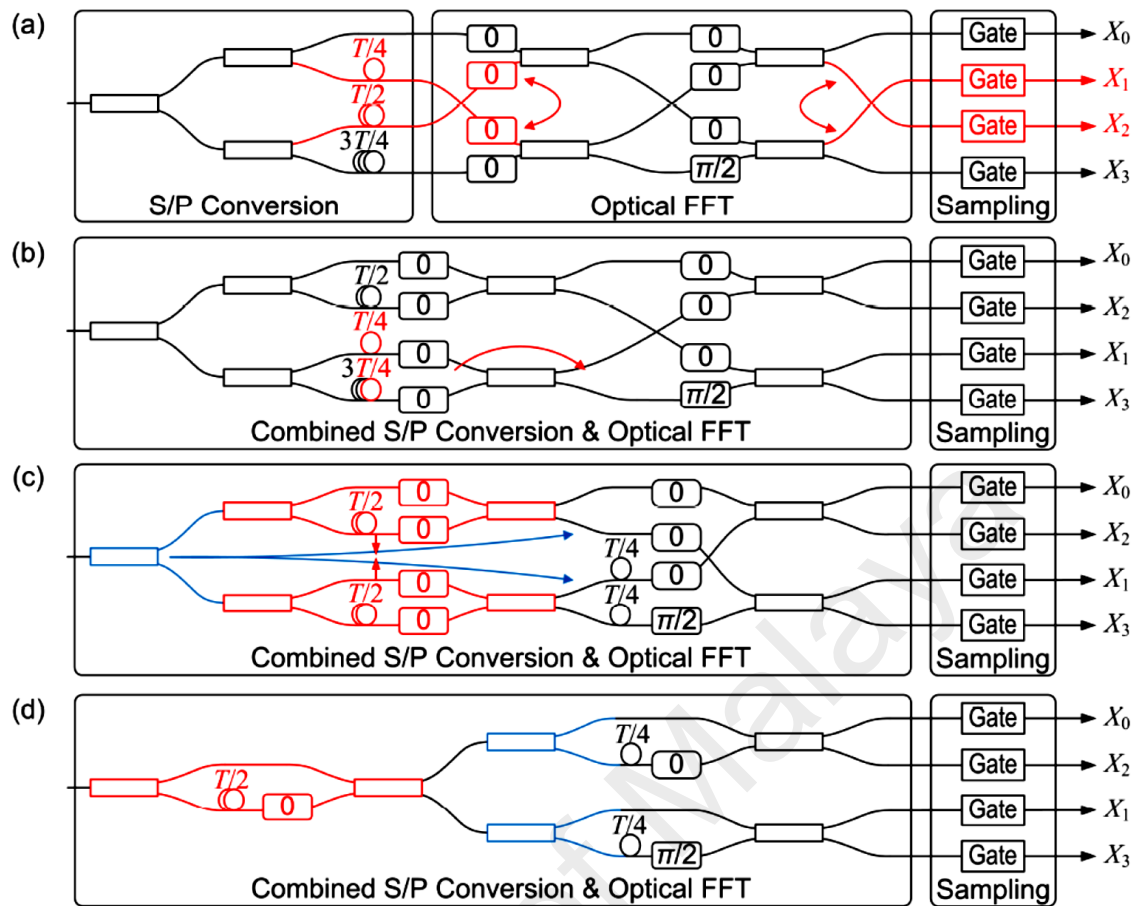


Figure 2.12: 4-order OFFT circuit for symbol period T ; (a) traditional implementation; (b) combining the SPC with OFFT; (c), simplified combination of SPC with OFFT by using two identical MZIs; (d) low-complexity scheme with combined SPC and OFFT (Hillerkuss et al., 2010a), block with “0” is zero phase shifter.

The AO-OFDM receiver has also been demonstrated using real-time OFFT processing for 10.8 and 26 Tbps line-rate OFDM signals (Hillerkuss et al., 2011). The received OFDM signal has been processed using a low-complexity OFFT circuit based on cascaded MZIs and sampling gates. The AO-OFDM receiver sequentially extracts the subcarriers by using 8-order OFFT, as shown in Figure 2.13, where seven MZIs, eight optical demultiplexers, and optical sampling gates were required. The first MZI time delay was adjusted to 20 ps, while the time delay of two other subsequent parallel

MZIs was set to 10 ps. The time delay of last four MZIs was regulated to 5 ps. After being processed by the OFFT, the resulting signals were sampled by electro-absorption modulators (EAMs). Afterwards, the output from each EAM is fed to an optical filter and detected by using optical QAM demodulator.

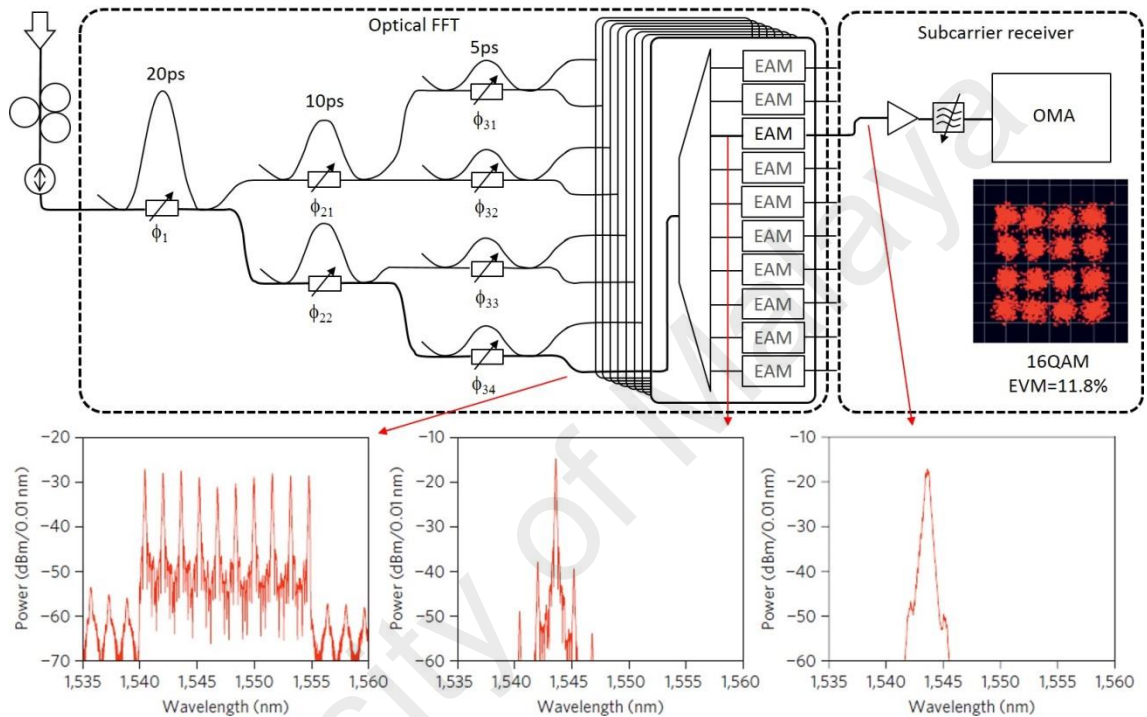


Figure 2.13: AO-OFDM receiver utilizes the OFFT, which comprises of cascaded MZIs, demultiplexers and EAM gates. The received signal of each subcarrier is detected by optical QAM receivers (Hillerkuss et al., 2011) .

2.5 Impairments in the AO-OFDM systems

AO-OFDM system suffers from many types of impairments. Some of them are originated in the transmitter such as laser phase noise and PAPR. Other impairments are induced by optical fiber link such as fiber nonlinearity and amplified spontaneous emission (ASE) noise. Moreover, the shot noise, and thermal noise of the receiver are

impaired the AO-OFDM system. This section discusses the most significant impairments in AO-OFDM systems such as PAPR, fiber impairments and ASE noise. These phenomena can cause a high distortion, specifically; they influence each other when the OFDM signal travels along optical fiber. The interaction between these phenomena may lead to deterministic as well as stochastic impairments (Nakazawa et al., 2010). These impairments are briefly explained in the following subsections:

2.5.1 Peak-to-average power ratio

Due to nature of generation the OFDM signal, the high peaks of power can occur when most subcarriers are coherently added. The high power peaks can exacerbate the nonlinear fiber impairments in OFDM communication systems; therefore, peak-to-average power ratio (PAPR) has been intensively studied. Due to its effect on the transmission performance of optical OFDM systems, high PAPR has been considered as one of the major drawbacks of optical OFDM modulation format (Kumar, 2011; Xiao et al., 2015). It has been cited that optical OFDM systems experience excessive nonlinear distortion due to high PAPR (X. Chen et al., 2013).

The PAPR of the OFDM signal, $u(t)$, is defined as the ratio of the peak of instantaneous power to the average power, and it is given as (B. Liu et al., 2012):

$$PAPR = \frac{\max(|u(t)|^2)}{E[(u(t))^2]}, \quad (2.1)$$

where $E[\bullet]$ is the expectation operator. The highest possible of PAPR can be obtain when N subcarriers are coherently superimposed (Jayapalasingam & Alias, 2012) as shown in Figure 2.14 and it can be given in decibel (dB) as:

$$PAPR_{dB} = 10\log_{10}(N). \quad (2.2)$$

From Eq. (2.2), the maximum occurrence of the PAPR is determined by number of subcarriers. Another common technique to calculate the probability of the PAPR exceeds a certain value (x) is called the complementary cumulative density function (CCDF). The CCDF is defined as:

$$CCDF = P(PAPR > x). \quad (2.3)$$

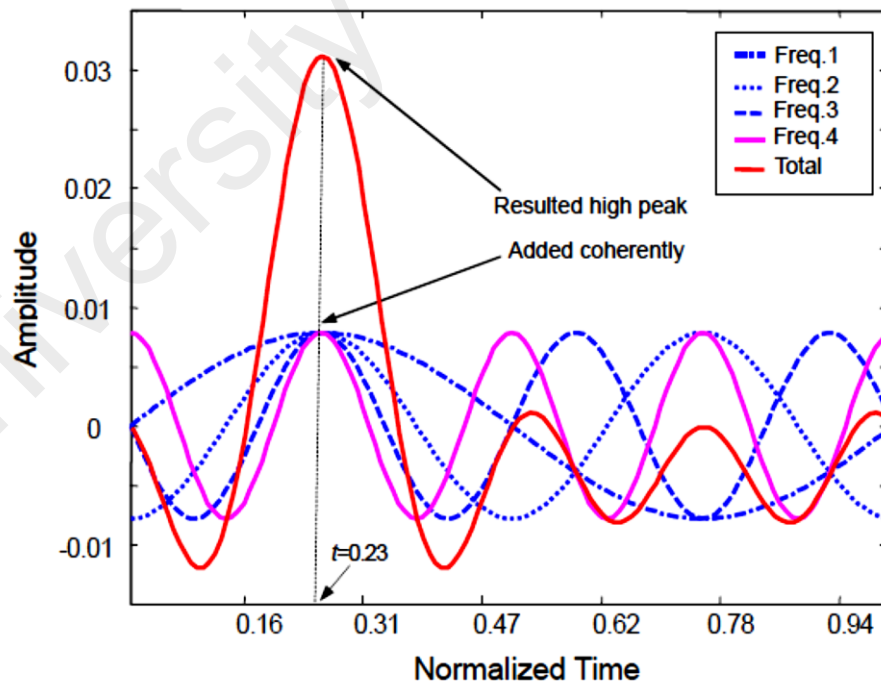


Figure 2.14: High peak appearance in OFDM systems (Jayapalasingam & Alias, 2012).

2.5.2 Optical fiber impairments

Once the optical signal propagates inside multi-span optical fiber link, it suffers from linear and nonlinear fiber impairments and optical amplifier noise. These phenomena are interacted inside the optical fiber link as well as inside the optical amplifier, producing a phase noise. Fiber attenuation and CD are the main sources of linear impairments, which cause a linear phase noise. Whilst the nonlinear fiber impairments that induced by SPM, XPM and FWM, add a nonlinear phase noise to received signal. ASE noise, which is generated by the Erbium doped fiber amplifier (EDFA), interacts with SPM, XPM and FWM and causes random nonlinear phase noise (Nakazawa et al., 2010). The interaction between nonlinear fiber impairments and random noise of optical amplifier may lead to deterministic as well as stochastic impairments. It is hard to compensate random nonlinear phase noise due to its random nature.

A particular attention has been paid to the optical fiber impairments in optical communication systems because the phase of received signal can be distorted by the phase noise (X. Li et al., 2007; Xie, 2009). The multichannel optical communication systems are degraded by fiber impairments. In particular, the optical OFDM systems highly suffer from phase noise, which can create a phase rotate term (PRT) on each subcarrier, and result in interference due to the destruction of the orthogonality of subcarriers (Hoxha & Cincotti, 2013; Lin et al., 2011; Wei & Chen, 2010). The phase noise can limit achievable transmission distance, specifically the optical OFDM systems that employ high-order modulation formats (Demir, 2007; Nazarathy et al., 2008; Yao et al., 2013). In the following subsections, both linear and nonlinear impairments are briefly discussed.

2.5.2.1 Linear fiber impairments

Both fiber attenuation and CD have been considered as main sources of linear fiber impairments in optical communication systems. The fiber attenuation can be compensated by using optical amplifier while the CD can be compensated either by inserting dispersion compensating optical fiber (DCF) in fiber link or by linear equalizer at the receiver.

Fiber attenuation

Due to the fiber attenuation, the power of optical signal is reduced when the optical signal propagates along optical fiber. The fiber attenuation is caused by several factors. The main two factors are material absorption and Rayleigh scattering. It is well known that the single mode optical fiber is made from silica glass. The material of silica glass totally absorbs the light in both ultraviolet region due to the electron resonance and the far-infrared region beyond 2 μm due to vibrational resonances (Wei Li et al., 2009; Yonenaga et al., 2008). Fortunately, it absorbs a little light in the wavelength region extending from 0.5 to 2 μm (Agrawal, 2007). Figure 2.15 shows the measured attenuation spectrum of SSMF. It can be observed that a small amount of impurities, such as Hydrogen Oxide (OH) ions, inside structure of optical fiber can significantly increase the absorption in that wavelength range.

Another source of attenuation is Rayleigh scattering loss. The main reason to appear the Rayleigh scattering loss is the density fluctuation that produced by the fabrication process (Agrawal, 2013). As result of the density fluctuation, the refractive index is fluctuated too, making light scatters in all directions. However, the influence of

the Rayleigh scattering loss is dominant at low-wavelength range (William Shieh & Djordjevic, 2009). The power of optical signal, at the end of fiber, can be calculated by:

$$P_r = P \exp(-\alpha L), \quad (2.4)$$

where P is the power of optical signal that lunched to optical fiber, α is called attenuation coefficient and L is the optical fiber length. From Figure 2.15, the measured attenuation spectrum reveals that the lower absorption is occurred at wavelength of 1550 nm region (C-band) with a fiber attenuation coefficient of ~ 0.2 dB/km.

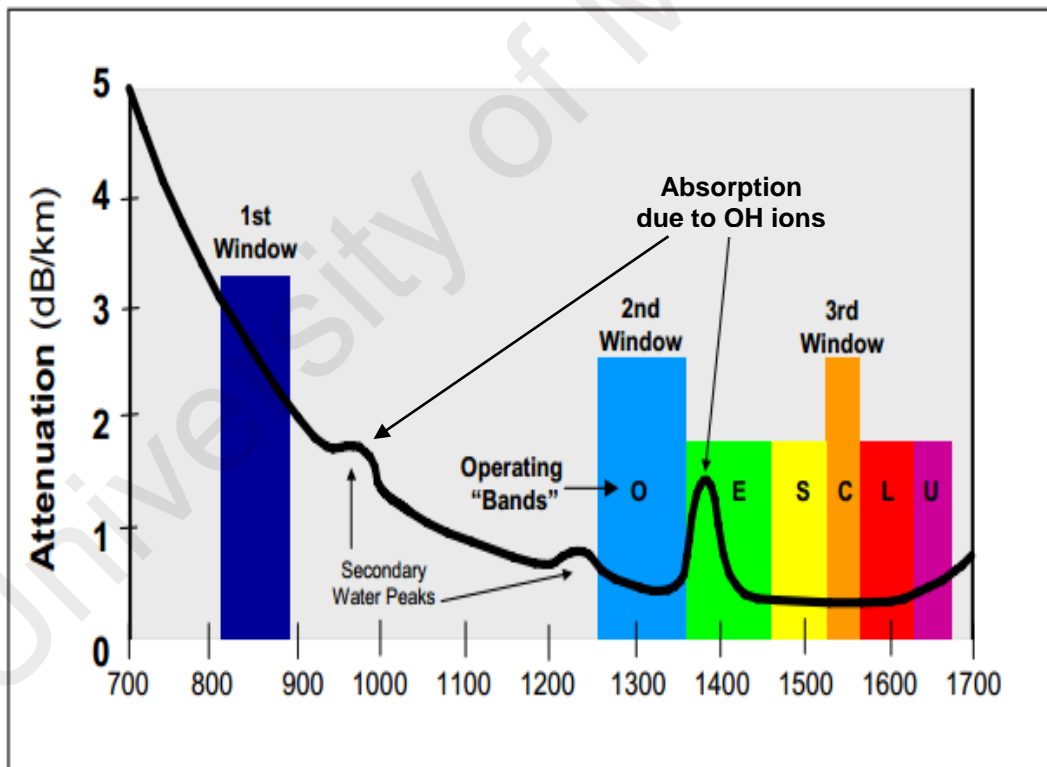


Figure 2.15: Measured attenuation spectrum of a standard single-mode fiber.

Chromatic dispersion

The chromatic dispersion (CD) in optical fiber is occurred when the different components of emitted light travel with different frequencies and velocities (Agrawal, 2007). The CD has a critical role in optical communication because it broadens the propagated optical pulse. Therefore, CD can cause an ISI, which degrades the quality of received signal and reduces the achievable transmission distance. To explore the CD mathematically, the dependence of velocity on the wavelength can be described by the mode-propagation constant β . It can be expanded the mode-propagation constant by utilizing Taylor series and it can be given as:

$$\beta(\omega) = \beta_0 + \beta_1(\omega - \omega_0) + \frac{1}{2}\beta_2(\omega - \omega_0)^2 + \dots, \quad (2.5)$$

where ω_0 is the center frequency and $\beta_m = \left[\frac{d^m \beta}{d\omega^m} \right]_{\omega=\omega_0}$, ($m=0,1,2,\dots$). Physically, it can be said that the envelope of an optical pulse moves at the group velocity, $v_g = 1/\beta_1$, while the parameter β_2 represents dispersion of the group velocity, causing pulse broadening (Agrawal, 2013). Moreover, the dispersion coefficient, D is normally used to refer to the CD. The chromatic dispersion coefficient, D , as a function of parameters β_1 and β_2 can be written as:

$$D = \frac{d\beta_1}{d\lambda} = -\frac{2\pi c}{\lambda^2} \beta_2. \quad (2.6)$$

2.5.2.2 Nonlinear fiber impairments

The nonlinear behavior in optical fiber is resulted from changing the refractive index with the optical intensity. This behavior is occurred due to Kerr effects. Therefore, the influence of fiber nonlinearity in optical communication systems is directly proportional to the optical power. The higher optical power leads to degrade the performance of optical communication system due to the impact of the fiber nonlinearity. On other hand, the launch power should be increased to maintain reasonable signal-to-noise ratio (SNR) at receiver circuit. The nonlinear fiber impairments can be divided into three classes: SPM, XPM and FWM. Each of SPM, XPM and FWM plays important role in optical OFDM systems, specifically that employ multilevel modulation formats and transmitted high bitrate data along multi-spans optical fiber.

Self- and cross-phase modulation

The first consequence of the Kerr effect is SPM, where the optical field experiences a nonlinear phase delay, which results from its own intensity. On the other hand, XPM refers to the nonlinear phase shift of an optical field induced by another field with different wavelength, direction, or state of polarization (Agrawal, 2013). That is the nonlinearity in optical fibers produces an intensity modulation. Furthermore, the phase of propagated signal is distorted by its own intensity or other optical signals in the same fiber. The SPM and XPM have significant influence on the multichannels optical communication systems like WDM and OFDM systems. The nonlinear crosstalk or ICI due to SPM and XPM phenomena have been extensively studied in WDM and optical OFDM systems (Arthur J Lowery et al., 2007; Wu & Way, 2004; Zhu & Kumar, 2010).

Due to intensity dependence of the refractive index, the phases of optical carriers are shifted, depending on their optical intensities. Furthermore, each carrier in the multi-carrier communication system modulates the phase of other carriers and the magnitude of the phase shift depends on the power of all carriers. To explore mathematical meaning of SPM and XPM, we assume that two optical fields at different frequencies and single polarization are simultaneously launched to the optical fiber. At transmission distance of z , the optical field can be expressed as (Agrawal, 2013):

$$u(z,t) = \frac{1}{2}x [u_1 \exp(-j\omega_1 t) + u_2 \exp(-j\omega_2 t) + \text{c.c.}], \quad (2.7)$$

where; $u(z,t)$ is the resultant optical field, x denotes to polarized state along the x -axis, and ω_1 and ω_2 are the frequencies of two optical carriers. The nonlinear phase shift is generated due to interaction of one optical field with itself or with another optical field and it can be expressed as:

$$\phi_{NL} = \frac{2\pi L n_2}{\lambda} [|u_1(z,t)| + 2|u_2(z,t)|], \quad (2.8)$$

where n_2 is the nonlinear-index coefficient and λ is the wavelength. The first term of Eq. (2.8) represents the phase shift due to the SPM while the phase shift due to XPM is expressed by second term. It can be noted that XPM able to induce higher nonlinear phase noise than the SPM because more than one optical field are contributed.

Four-wave mixing

FWM phenomenon has important role in multi-carrier optical communication. The FWM is occurred when four optical waves interact nonlinearly inside an optical fiber. This process can only occur efficiently when a phase-matching condition is satisfied. According to FWM phenomenon, the interaction between two or three waves can produce new waves, which have different frequencies (Agrawal, 2013; Okamoto, 2010). In other words, if three waves at frequencies ω_h, ω_i and ω_k propagate through optical fiber, the FWM process can create new wave at frequency of $\omega_j = \omega_h + \omega_i - \omega_k$. The phase mismatch governs the FWM process where the FWM is vanished only if phase matching nearly vanishes (Agrawal, 2012; Ahmed et al., 2013). To reduce effect of FWM in optical communication systems, the phase matching between the waves that travel through the fiber should be minimized.

In multicarrier optical fiber communication systems, the occurrence of FWM can be minimized by reducing the phase matching between optical carriers. The efficiency of FWM can be reduced by moderate levels of fiber chromatic dispersion (Al-Mamun & Islam, 2011; Seimetz, 2009). In other words, the chromatic dispersion makes the phase matching condition for FWM process more difficult to occur due to different group velocity of waves inside optical fiber. Therefore, the nonlinear phase noise that induced by FWM can be diminished when the transmitted signal propagates through optical fiber with adequate chromatic dispersion (Kumar, 2011; Zhu & Kumar, 2010).

In a multicarrier optical fiber communication system such as WDM and OFDM systems, the FWM process can originate a high number of new products. Many of new products can fall into signal band and can interfere with the original carriers, causing degradation performance of optical communication system. The new generated waves

are divided to degenerated (DG) when $\omega_h = \omega_i$ and non-degenerated (NDG) FWM products when $\omega_h \neq \omega_i$. In optical OFDM system, the number of DG and NDG FWM products that falling on given subcarrier can be calculated by (Goebel et al., 2008; S. T. Le et al., 2014):

$$DG(k) = \begin{cases} \frac{N-2}{2}, & N \text{ even} \\ \frac{N-2-(-1)^k}{2}, & N \text{ odd} \end{cases} \quad (2.9)$$

$$NDG(k) = \begin{cases} \frac{N^2/2 - 3N + kN - k^2 + k + 2}{2}, & N \text{ even} \\ \frac{N^2/2 - 3N + kN - k^2 + k + 2 + (-1)^k / 2}{2}, & N \text{ odd} \end{cases} \quad (2.10)$$

respectively, where N is the number of subcarriers and $k \in \{1, 2, \dots, N\}$ is given subcarrier. To explain the FWM process in optical OFDM systems, Figure 2.16 shows twelve new waves would be generated due to FWM, when three carriers with different frequencies and equal frequency spacing interact inside optical fiber. Only four of them fall into the optical signal.

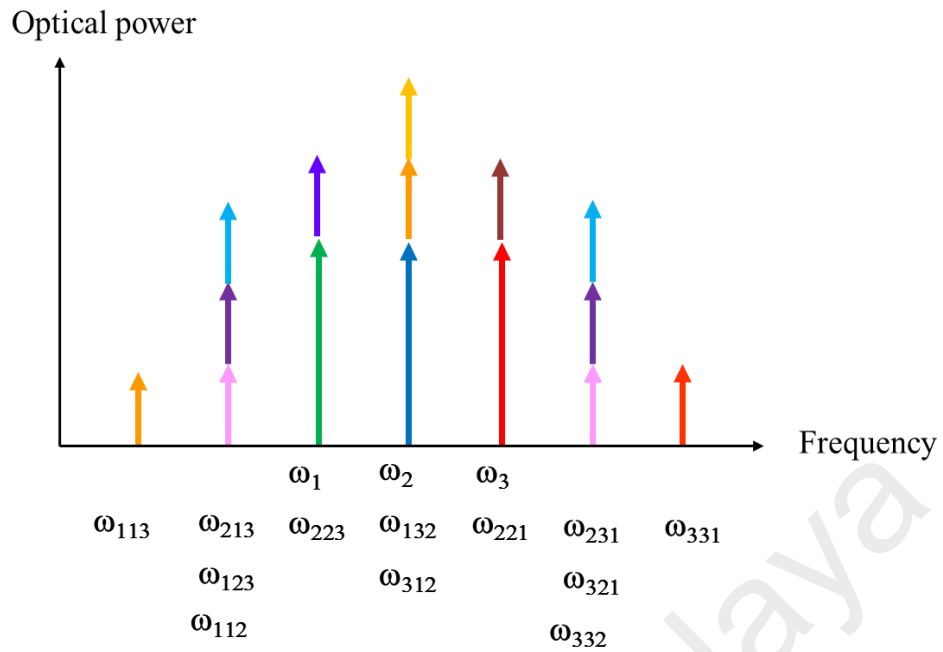


Figure 2.16: Additional frequencies generated through FWM

2.5.3 ASE noise

Once the optical carrier is transmitted through the optical fiber link, its power is attenuated due to the fiber attenuation as discussed before. In order to keep the power of the optical carriers at acceptable level, the optical amplifiers are used to this purpose. The optical amplifier such as EDFA can optically restore the average power of signal without converting it to electrical domain. However, the main disadvantage of the using the EDFA is a noise that added to the amplified signal. This noise is called amplified spontaneous emission (ASE) noise. The origin of the ASE noise is the spontaneous emission of photons in the EDFA amplifiers. Since the ASE noise is naturally occurred, it can be modeled as an additive white Gaussian noise (AWGN) where the noise spectral density per one state of polarization is given as (Jacobsen et al., 1998):

$$\rho_{ASE} = hfn_{sp}(G - 1), \quad (2.11)$$

where G is the amplifier gain, h is Planck constant, f is carrier frequency, and n_{sp} is spontaneous noise factor. During the amplification process, the ASE noise degrades the quality of the amplified signal and decreases the SNR. The ratio between SNRs of input and output of amplifier characterizes an optical amplifier and it is defined as noise figure (NF) of amplifier, which is given as:

$$NF = \frac{SNR_{in}}{SNR_{out}}. \quad (2.12)$$

2.6 All-optical phase noise mitigation in optical OFDM systems

Various techniques have been reported to mitigate nonlinear fiber impairments in optical OFDM system. For instance, digital-back-propagation (DBP) technique was proposed to eliminate nonlinear distortion by inverting the distorted signal at the receiver digitally (Ip & Kahn, 2008; Rafique & Ellis, 2011). The DBP technique uses a digital signal processing for solving the inverse nonlinear Schrödinger equation. However, the DBP technique requires computationally expensive, leading to limit the transmission rate of the optical communication systems. To enhance the processing time, optical-based compensation techniques have been proposed. The optical-based compensation techniques have been reported in optical OFDM systems to mitigate the nonlinear impairments (Iida et al., 2012; Koga et al., 2013; Xiang Liu et al., 2012a). This section discusses all-optical techniques that have been employed in previous research to mitigate the nonlinear impairments in optical OFDM systems.

2.6.1 Reduction of PAPR

High PAPR is a result of summing many subcarriers during generating OFDM signal. In optical OFDM systems, the high power peaks of transmitted signal exacerbate nonlinear fiber impairments and thus degrade the performance of optical OFDM system. Therefore, various methods have been proposed to reduce the PAPR. In conventional optical OFDM systems, many schemes such as clipping and filtering (Hao et al., 2012; B. Liu et al., 2012) partial transmit sequence (PTS) (Weilin Li et al., 2009), coding (Abdalla et al., 2014), selected mapping (SLM) (Xiao et al., 2015), have been reported to reduce PAPR. All these schemes are implemented in electrical domain by digital signal processing. However, these schemes increase complexity and cost of the system, limiting speed and capacity of transmission. In addition, they may be unfeasible in AO-OFDM systems.

Similar to conventional optical OFDM systems, high PAPR is one major drawback of the AO-OFDM systems, deteriorating nonlinear fiber impairments. To improve the performance of AO-OFDM systems, phase pre-emphases scheme has been proposed to reduce the PAPR in optical domain (Liang et al., 2009; Shao et al., 2010). Phase pre-emphasis means that optimized phase values are pre-chirped to optical pulses on different subcarriers before OIFD in OFDM systems. Figure 2.17 shows a proposed scheme for PAPR reduction using a PLC-based OIFD with 4 subcarriers in intensity modulation-direct detection (IM-DD) AO-OFDM systems (Liang et al., 2009). The proposed scheme consists of 4-order OIFD and two additional phase shifters. The 4-order OIFD is implemented by four couplers, nine phase shifters (in yellow) and three delay lines. Two additional phase shifter (in red) are inserted in path of two subcarriers to implement phase pre-emphasis. In Figure 2.17, four input lights with amplitude of α_0 , α_1 , α_2 , α_3 are transformed by OIFD. The outputs of OIFD β_0 , β_1 , β_2 , β_3 are delayed by

delay lines (dL , $2dL$, $3dL$) before combined together. The PAPR reduction process is based on adjusting four phase shifters that located at the left side to obtain minimum PAPR. The simulation results reveal that the PAPR has been reduced by 3.74 dB. In addition, the performance of 160 Gbps IM-DD AO-OFDM system has been improved where the maximal transmitted powers increase by 39% at bit error rate (BER) of 1×10^{-9} . That means, the propose scheme significantly mitigates the nonlinear impairment and enhances the transmission performance contributes.

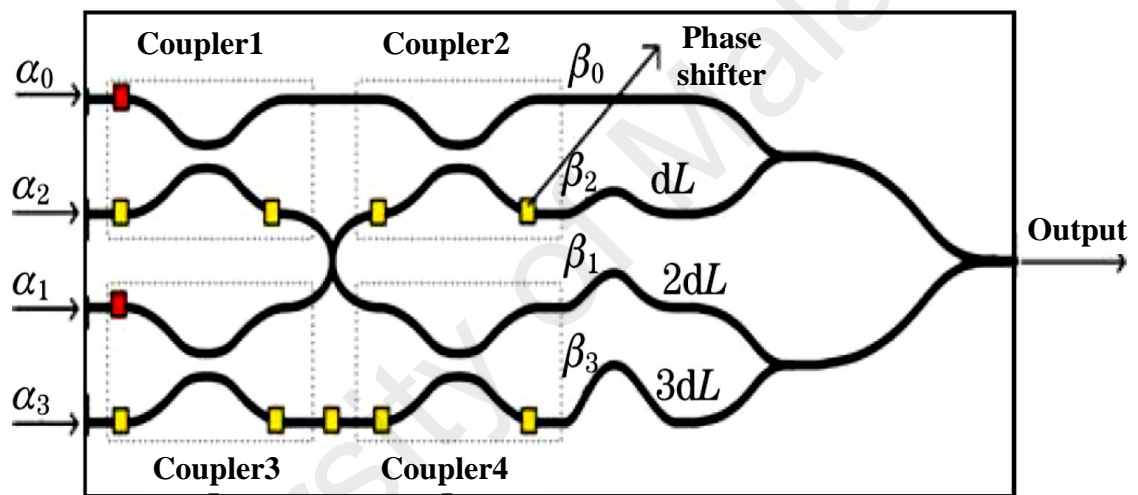


Figure 2.17: Schematic diagram of a 4×4 OIDFT (Liang et al., 2009).

Finally, it is hard to find other reported techniques that center on PAPR reduction in AO-OFDM systems. It should be mentioned that the phase pre-emphasis technique is effective in AO-OFDM systems that employing intensity modulation; while it is ineffective in AO-OFDM systems that employ high-order modulation format such as mQAM format (He et al., 2011).

2.6.2 Coherent superposition in spatially multiplexing optical signals

Coherent superposition of spatially multiplexed waves has been proposed to maximize SNR and to reduce the power of noise in the received signal. This technique is called diversity combining technique and it has first been implemented in radio communication (Winters, 1987; Winters et al., 1994). In wireless communication, the radio signal is transmitted and received by multiple antennas. The antennas are combined to maximize the SNR. In optical communication, similar technique has been used where the transmitted signal and its replicas are sent over multi fiber/core (Iida et al., 2012; Koga et al., 2013). At receiver, the received signals are coherently superimposed to maximize SNR and reduce nonlinear phase noise. The coherent superimposing of signals can be implemented in optical domain or in electrical domain. Coherent superposition has been theoretically studied to reduce the nonlinear fiber impairments based on optical coherent superposition by employing adaptive optical phase and time shifters as shown in Figure 2.18 (Shahi & Kumar, 2012). The optical phase and time shifters are adapted by electrical signal processor (ESP) for obtaining maximum power after combiner at the receiver side.

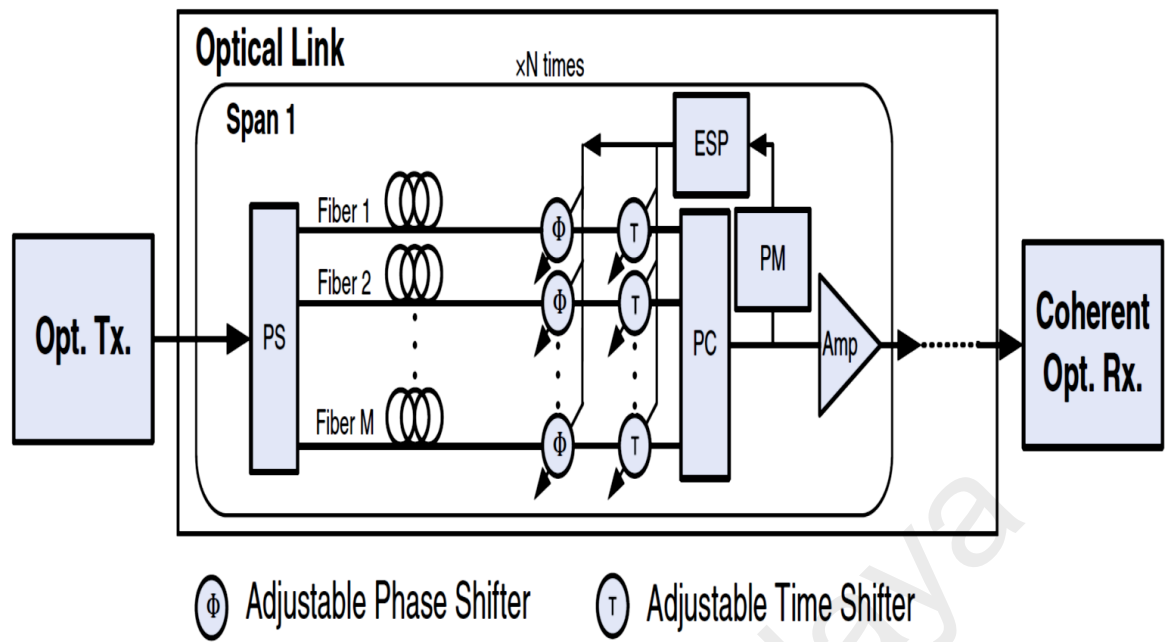


Figure 2.18: Architecture of coherent superposition of spatially multiplexed waves over multi-span multi-fiber link. M: number of fibers; PS: optical splitter; PC: optical combiner; PM: power meter (Shahi & Kumar, 2012).

The progress in digital coherent detection have enabled the digital coherent superposition (DCS) of spatially multiplexed signals at receiver (Xiang Liu et al., 2012a; Xiang Liu et al., 2012c). Indeed, to obtain best effect of proposed technique, the signal and their replicas are transmitted over multi-core fiber (MCF). Figure 2.19 shows the experimental system setup that has been used to transmit two copies of 676 Gbps 16QAM AO-OFDM over seven-core fiber (Xiang Liu et al., 2012a). The received signals have been superimposed by DCS. Figure 2.20 shows the quality of superimposed signal was improved in the presence of nonlinear phase noise, and the quality of received signal was directly proportional to the number of superimposed signals. However, the spectral efficiency is inversely proportional with the number of superimposed signals.

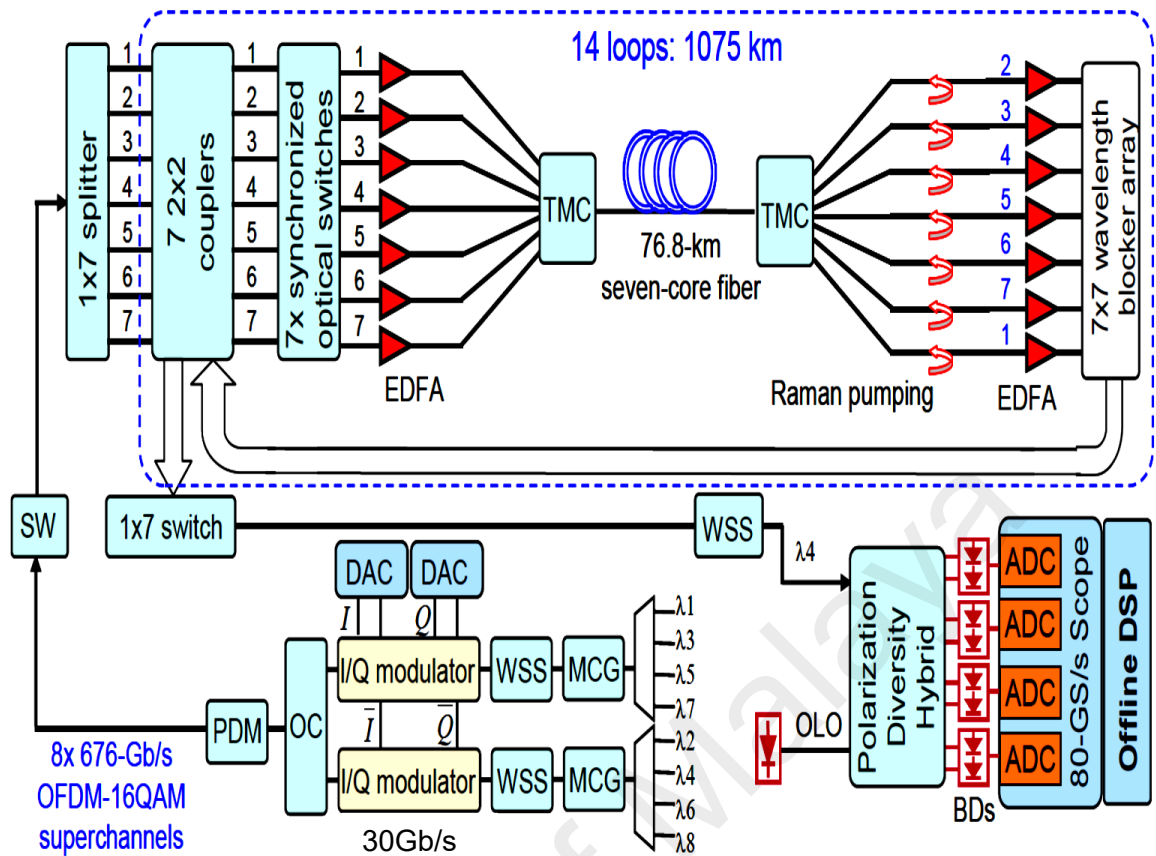


Figure 2.19: Schematic of the experimental setup. TMC: tapered multi-core coupler; OLO: optical local oscillator (Xiang Liu et al., 2012a).

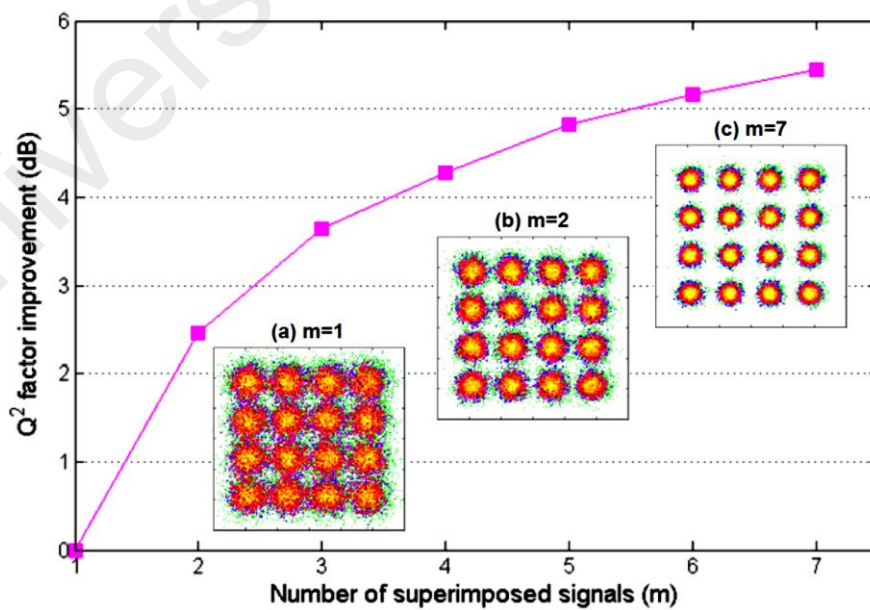


Figure 2.20: Improvement of quality factor vs. number of superimposed signals. Insets: typical recovered constellations (Xiang Liu et al., 2012a).

The nonlinear fiber impairments can induce highly correlated distortion between signal and their replicas, which decreases the benefit of the DCS in the nonlinear transmission regime (Xiang Liu et al., 2012c). In other words, the performance improvements of the system is decreased as the signal launch power increases beyond optimum power as shown in Figure 2.21 (curve with square symbol). In order to achieve the full benefit of DCS, the nonlinear distortions need to be decorrelated using some types of scrambling functions as suggested by Xiang Liu et al. (2012b). At transmitter, the constellations of signal were scrambled to eliminate the correlation between the nonlinear distortions of the superimposing signals. At receiver, the signals are coherently superimposed after unscrambling the constellation of received signals. The effective of scrambling coherent superposition (SCS) was illustrated in Figure 2.21 (curve with diamond symbol). It can be seen that the improvement in quality of the superimposed signal remains high at high signal power region and it is better than that of DCS. In addition, the recovered signal constellation after SCS is clearer than that recovered after DCS.

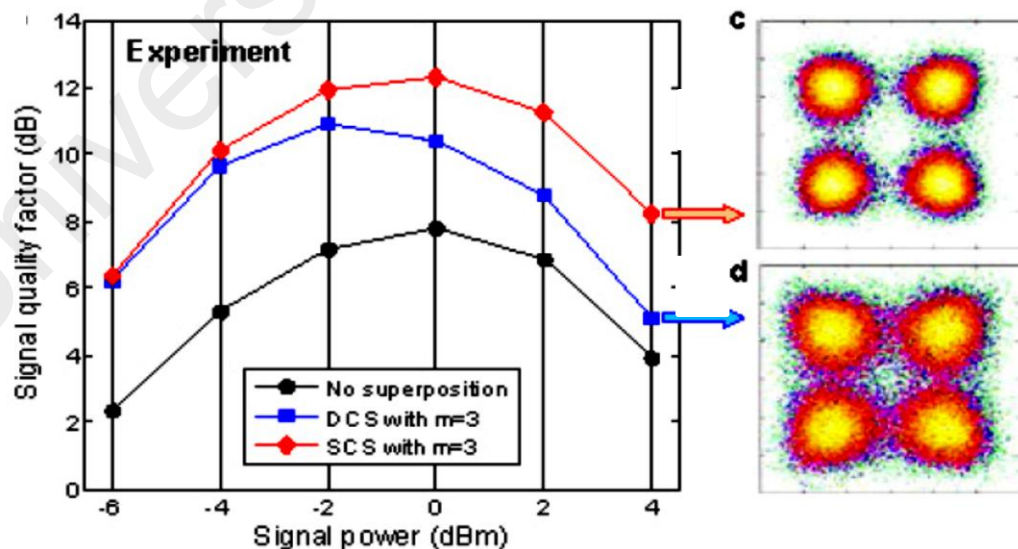


Figure 2.21: Experimentally measured signal quality versus signal launch power (Xiang Liu et al., 2012b).

2.6.3 Phase-conjugated twin waves technique

Recently, high effective technique based on coherent superposition the signal and its phase-conjugated copy has been proposed to cancel nonlinear distortion and to increase the reach transmission distance. This technique called phase-conjugated twin waves (PCTWs). In this technique, the PCTWs can be transmitted in any orthogonal dimension such as a two orthogonal polarization states (X. Liu et al., 2013), different optical wavelength (Tian et al., 2013), two different subcarrier frequencies (Le et al., 2015). The concept of the PCTWs technique is based on the nonlinear distortions that imposed on two waves are anticorrelated. In fact, when PCTWs are modulated onto a same optical carrier along two orthogonal polarization states, the nonlinear distortion can be cancelled by coherently superimposing the received PCTWs (X. Liu et al., 2013), restoring the original signal without nonlinear distortions. However, the main shortcoming of this technique is that it sacrifices half of aggregate transmission capacity.

2.6.3.1 PCTWs technique in orthogonal polarization dimension

The PCTWs technique has been experimentally implemented on two orthogonal polarization states of same optical carrier in superchannel communication system (X. Liu et al., 2013). shows the schematic of the experimental setup for implementation PCTWs technique in superchannel system. The system is able to transmit a 406.6 Gbps by utilizing eight pairs of PCTWs that modulated by quadrature phase shift keying (QPSK) modulation format over multi-span optical fiber link. Each span consisting of EDFA and 80 km of TrueWave reduced slope (TWRS) fiber with dispersion and nonlinear Kerr coefficient were 4.66 ps/nm/km and $1.79 \text{ W}^{-1}\text{km}^{-1}$, respectively. This

experiment demonstrates the effectiveness of PCTWs technique on fiber nonlinear impairments. Figure 2.23 illustrates the Q^2 -factor of the center channel versus the signal launch power after 8,000 km (100×80 km) TWRS fiber transmission. The Q^2 -factor of proposed system was increased by 5.2 dB higher than that conventional polarization division multiplexing (PDM) PDM-QPSK.

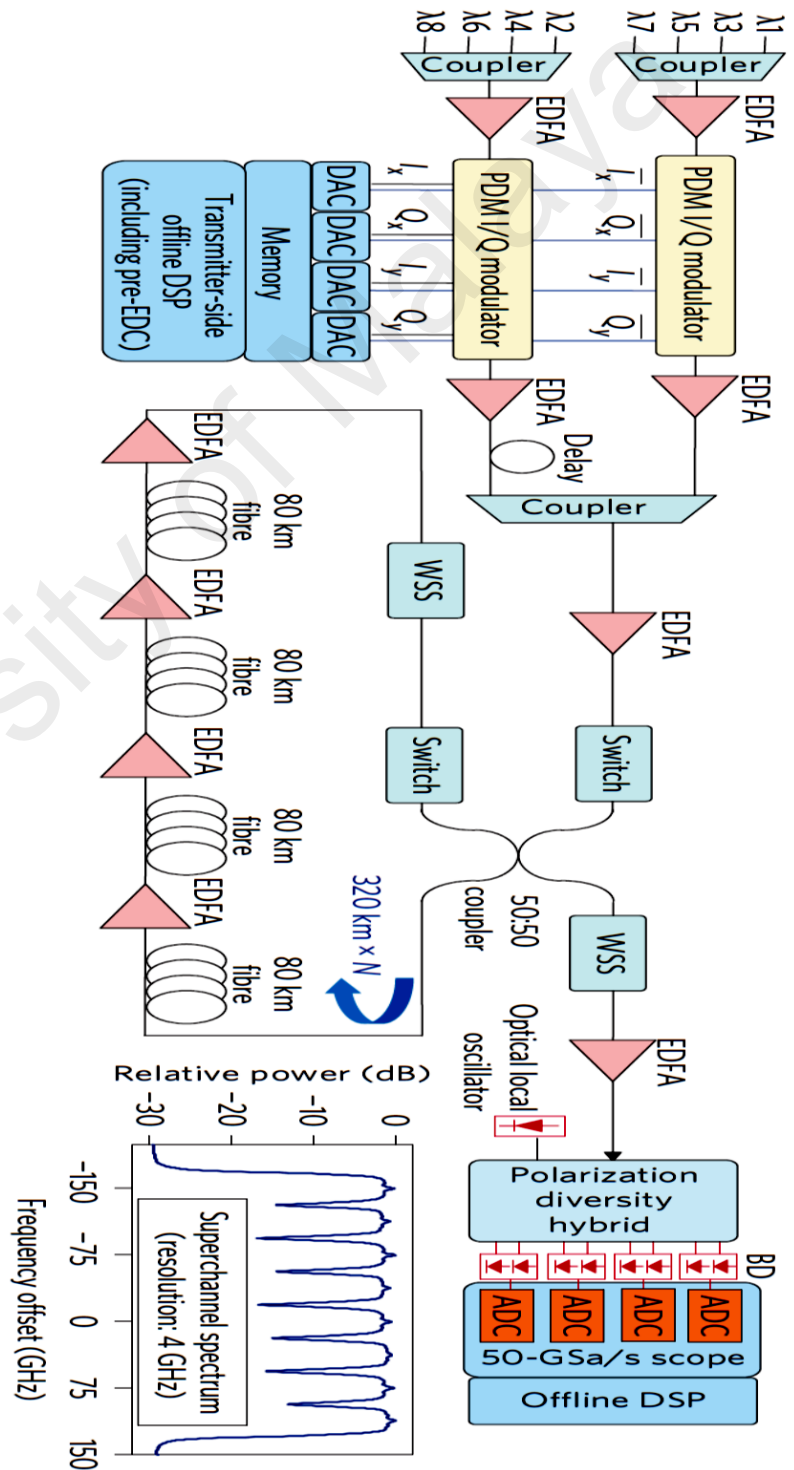


Figure 2.22: Scheme of the experimental setup for superchannel transmission with employing PCTWs technique to cancel nonlinear distortion (X. Liu et al., 2013).

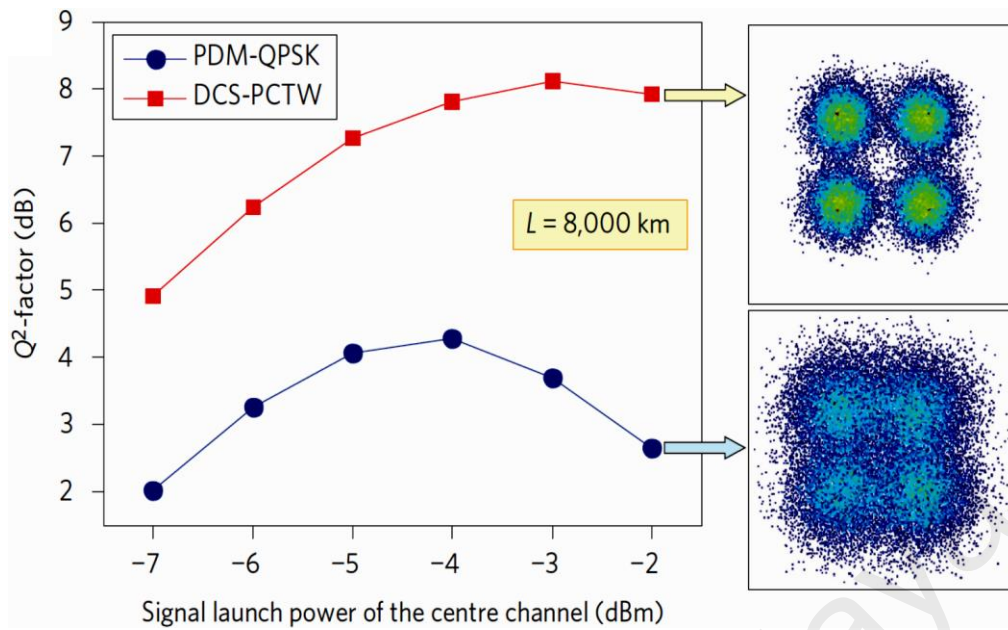


Figure 2.23: Quality factor of received signal versus launch power after 8,000 km TWRS fiber transmission, inset: recovered constellations (X. Liu et al., 2013).

2.6.3.2 PCTWs technique in two different subcarrier frequencies

The PCTWs technique has been implemented in two different subcarriers frequency where half OFDM subcarriers are transmitted as phase-conjugated of other subcarriers. This technique is named as phase-conjugated pilots (PCPs) (S. Le et al., 2014; Yi et al., 2014). In this technique, the nonlinear fiber impairments of original subcarriers can be compensated by using their corresponding PCPs. In conventional OFDM systems, the frequency spacing between adjacent subcarriers is small about tens of mega-Hertz (MHz), making the nonlinear phase noise of them at the receiver highly correlated. The nonlinear fiber impairments in OFDM systems can be effectively mitigated by using PCPs technique. However, by employing PCPs technique, the spectral efficiency of optical OFDM system is reduced to half as in the other types of PCTWs.

To enhance the spectral efficiency of the OFDM system, a portion of OFDM subcarriers are modulated as PCPs (Le et al., 2015). Indeed, it can be used one PCP to mitigate the nonlinear phase noise of other subcarriers that close to it due to high correlation of their nonlinear distortions. The PCPs technique can be easily implemented in both single polarization and PMD systems. Figure 2.24 shows the block diagram of how to implement the PCPs technique in 112 Gbps PDM coherent OFDM transmissions system. The efficiency of the PCPs technique to mitigate the nonlinear fiber impairments in the OFDM system that employs QPSK modulation format is shown in Figure 2.25. It can be observed that a full benefit of PCPs technique can be achieved when 50% of OFDM subcarriers are transmitted as PCPs. At transmission distance of 3200 km, the Q-factor of the proposed system is improved by ~ 4 dB as compared with traditional system. This result clearly indicates that the PCPs technique can effectively mitigate the nonlinear fiber impairments in conventional optical OFDM system.

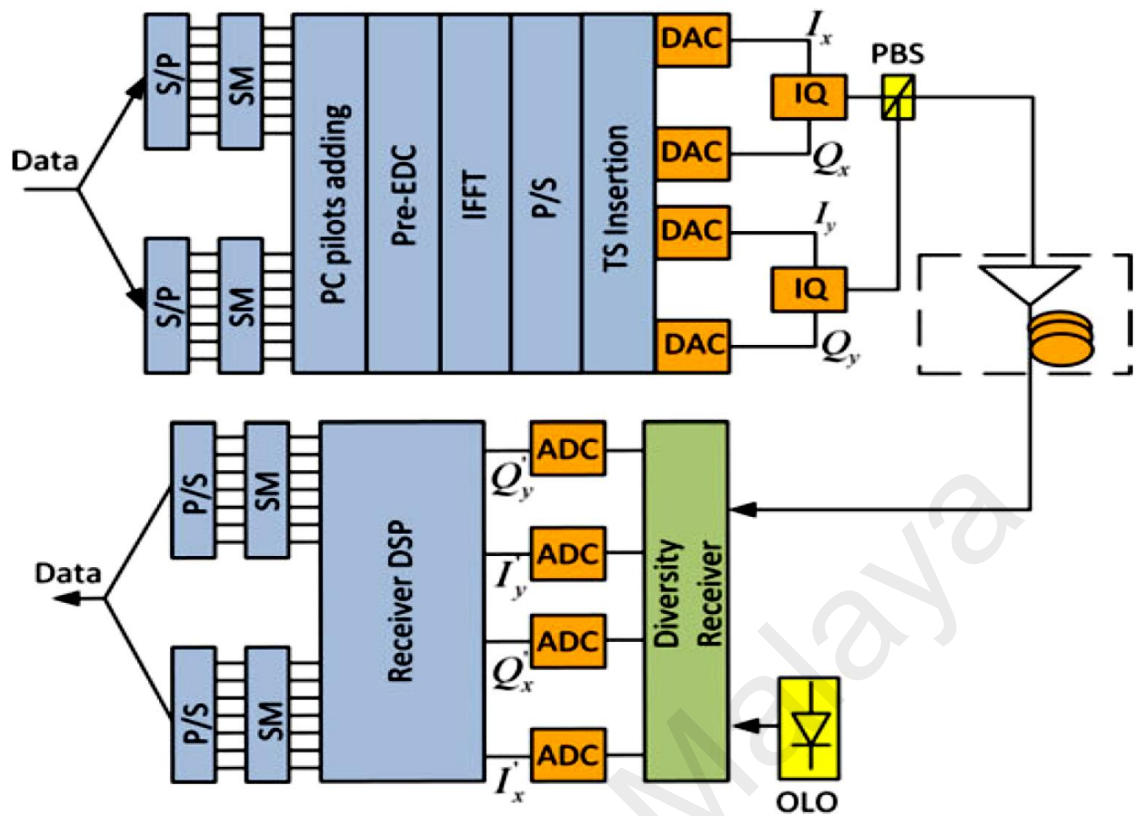


Figure 2.24: Block diagram of 112 Gbps PDM coherent OFDM transmissions with PCP technique. I/Q: I/Q modulator, PBS: polarization beam splitter (Le et al., 2015).

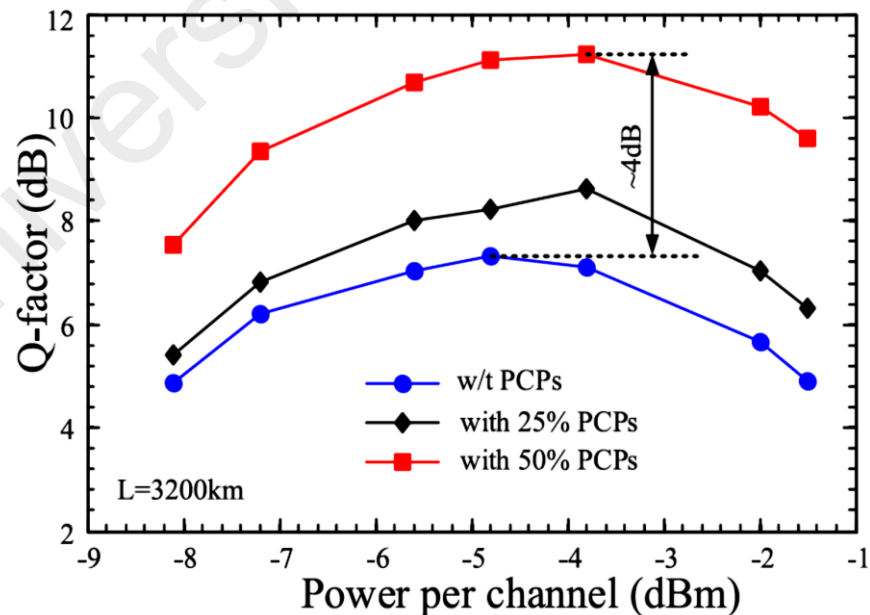


Figure 2.25: Quality factor as a function of the launch power in the system with and without PCPs for nonlinear fiber mitigation (Le et al., 2015).

CHAPTER 3

PERFORMANCE ANALYSIS OF AN ALL-OPTICAL OFDM SYSTEM IN PRESENCE OF NONLINEAR PHASE NOISE

3.1 Introduction

All-optical orthogonal frequency division multiplexing (AO-OFDM) techniques have gained a tremendous attention in recent years for optical transmission systems applications due to their intriguing ability (Hillerkuss et al., 2011; Hillerkuss et al., 2010a; Mirnia et al., 2013). For instance, they are much more resilient to dispersion when compared to conventional time division multiplexing (TDM) technique (Armstrong, 2009; Hillerkuss et al., 2011). These techniques can also convey data streams at high-data rates on a larger number of subcarriers (William Shieh et al., 2008), and are more spectral efficient when compared to wavelength division multiplexing (WDM) techniques (Armstrong, 2009; Hillerkuss et al., 2011). In conventional optical OFDM methods, both IFFT and FFT schemes are typically performed in the electronic domain, and therefore it have limited bit rates (Dixon et al., 2001; Kim et al., 2004; Ma et al., 2009). Recently, real-time electronic IFFT/FFT signal processing of 101.5 Gbps has been demonstrated for OFDM signals (Schmogrow et al., 2011). This limitation seems to be too far-fetched to reach desirable values for the generation or reception of terabit per second OFDM signals. An all-optical solution that could work beyond the state-of-art electronics speed would therefore be of immense interest (Lee et al., 2008). On the other hand, AO-OFDM techniques suffer highly from phase noise, which creates

a phase rotation term on each subcarrier, and results in interference due to the destruction of the orthogonality of subcarriers (Lin et al., 2011; Arthur James Lowery et al., 2007; Wei & Chen, 2010). In fiber-optic communication systems, the aforementioned weaknesses of OFDM might result from higher sensitivity for fiber nonlinearities, such as SPM, XPM, and FWM (Agrawal, 2013; Benlachtar et al., 2008; Arthur J Lowery et al., 2007; Zhu & Kumar, 2010). Therefore, precise calculation of induced nonlinearity, which is produced by fiber dispersion, is crucial in coping with these purported side effects of OFDM. It has been shown that optical OFDM systems are immune to chromatic dispersion (CD). At high sub-carrier peak power, the total phase noise decreases with CD effects (Zhu & Kumar, 2010).

In this chapter, an analytical model, for estimating the phase noise due to SPM, XPM, and FWM in AO-OFDM systems, is derived and developed. The developed model is then used to evaluate linear and nonlinear phase noises induced by the interaction of amplified spontaneous emission (ASE) noise with SPM, XPM, and FWM phenomena in both 4-quadrature amplitude modulation (4QAM) and 16QAM AO-OFDM transmission systems. In our model, we focus on the phase noise in single polarization. The polarization multiplexing OFDM system adds other significant interferences between the x- and y- polarized signals. With this analytical model, we are able to quantitative compare the nonlinear phase noise variation induced by SPM, XPM, and FWM due to variations in subcarrier peak power, number of subcarriers, fiber length, and channel index. In addition, the effects of CD on the total phase noise in AO-OFDM systems are studied as well. The accuracy of our analytical model is verified by quantifying the error vector magnitude (EVM) using both numerical simulation (adopting VPItransmissionMaker[®] commercial software) and the analytical model. It turned out that both EVM results are in good agreement with each other.

3.2 All-optical OFDM system architecture

In this section, we describe both transmitter and receiver architectures for the AO-OFDM system model used in this study. The schematic diagram of transmitter side of the AO-OFDM transmission system is shown in Figure 3.1 (Hillerkuss et al., 2010b; Hillerkuss et al., 2011). It consists of an optical frequency comb generator (OFCG), wavelength selected switch, optical QAM modulators, and an optical beam combiner. The OFCG part utilizes an intensity modulator and two phase modulators driven directly by a sinusoidal waveform (Dou et al., 2012). In the OFCG scheme, the flatness of OFCG is affected by the ratio of a direct current bias to half-wave voltage of the intensity modulator and the phase shifts between the sinusoidal waveforms applied to the intensity and phase modulators, as depicted in Figure 3.1. By setting appropriate values, a 29 flat top comb frequency lines, with frequency spacing of $\Delta f = 25$ GHz, can be generated. Subsequently, the wavelength selection switch splits the odd and even subcarriers. The subcarriers are individually modulated with two optical QAM modulators. As shown in Figure 3.1, an optical QAM modulation signal is generated from an IQ modulator comprising of two Mach-Zehnder modulators (MZMs) with two orthogonal components. The in-phase component of the intricate envelope modulates the optical carrier within the upper arm, while the quadrature phase component modulates the 90° stage shifted optical carrier in the lower arm. The QAM encoder is supplied by two independent branches of pseudo-random binary sequence (PRBS) signals, each has a length of $2^{11} - 1$. To preserve the orthogonality of the OFDM signals, the OFDM symbol duration is set to $T_s = 1/\Delta f$ (Hillerkuss et al., 2010a).

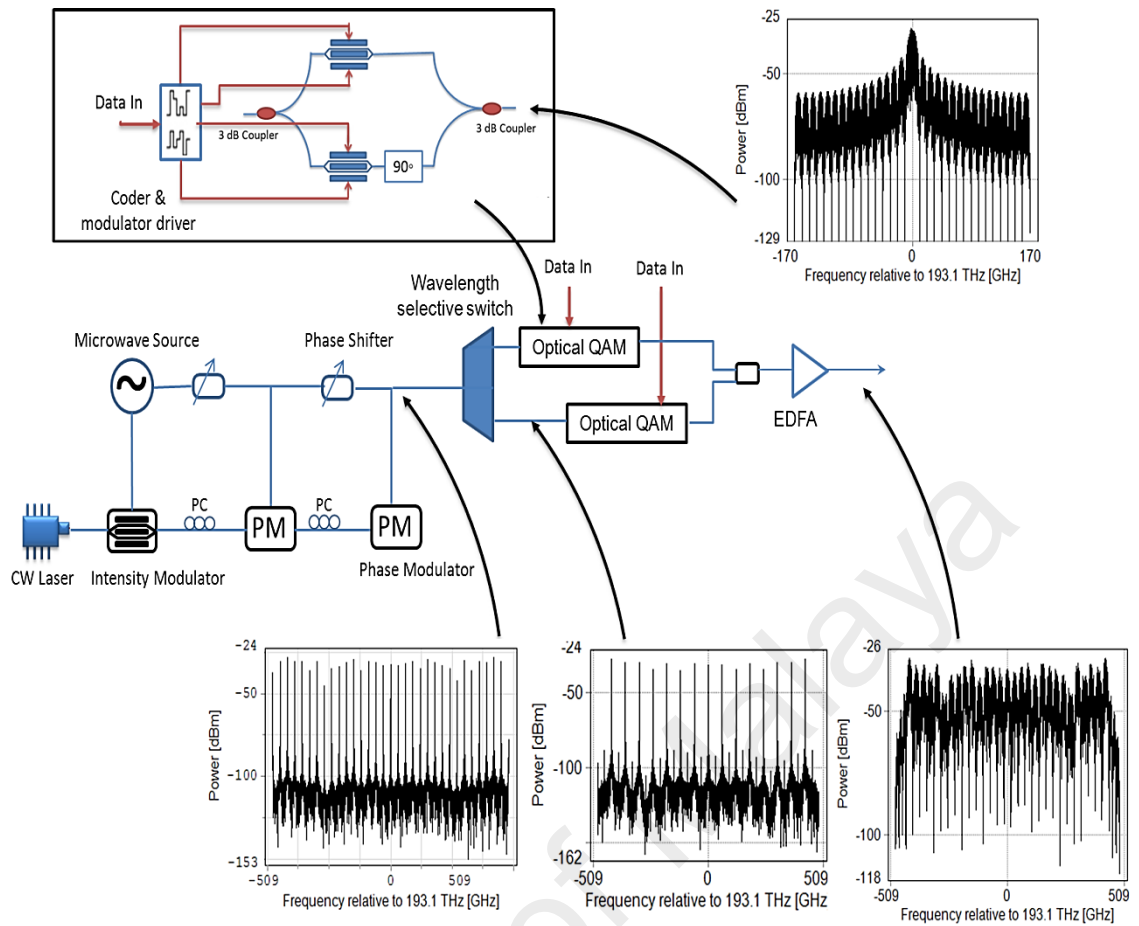


Figure 3.1: Transmitter configuration of an AO-OFDM transmission system.

The schematic diagram of an AO-OFDM receiver is shown in Figure 3.2. The received OFDM signal is processed using a low-complexity all-optical fast Fourier transform (OFFT) circuit. Our setup is composed of 4-order OFFT to perform both serial-to-parallel conversions and FFT in the optical domain using three cascaded Mach Zehnder interferometers (MZIs), with subsequent time gates and optical phase modulators. The first MZI time delay is adjusted to $T_s/2$, while the time delays of the other two subsequent parallel MZIs are set to $T_s/4$. After being processed by the OFFT, the resulting signals are sampled by electro-absorption modulators (EAMs). The output from each EAM is fed to an optical fourth-order super Gaussian band-pass filter and is

detected using a QAM demodulator. The bit error rates of the resulting signals are measured using a bit-error rate (BER) tester.

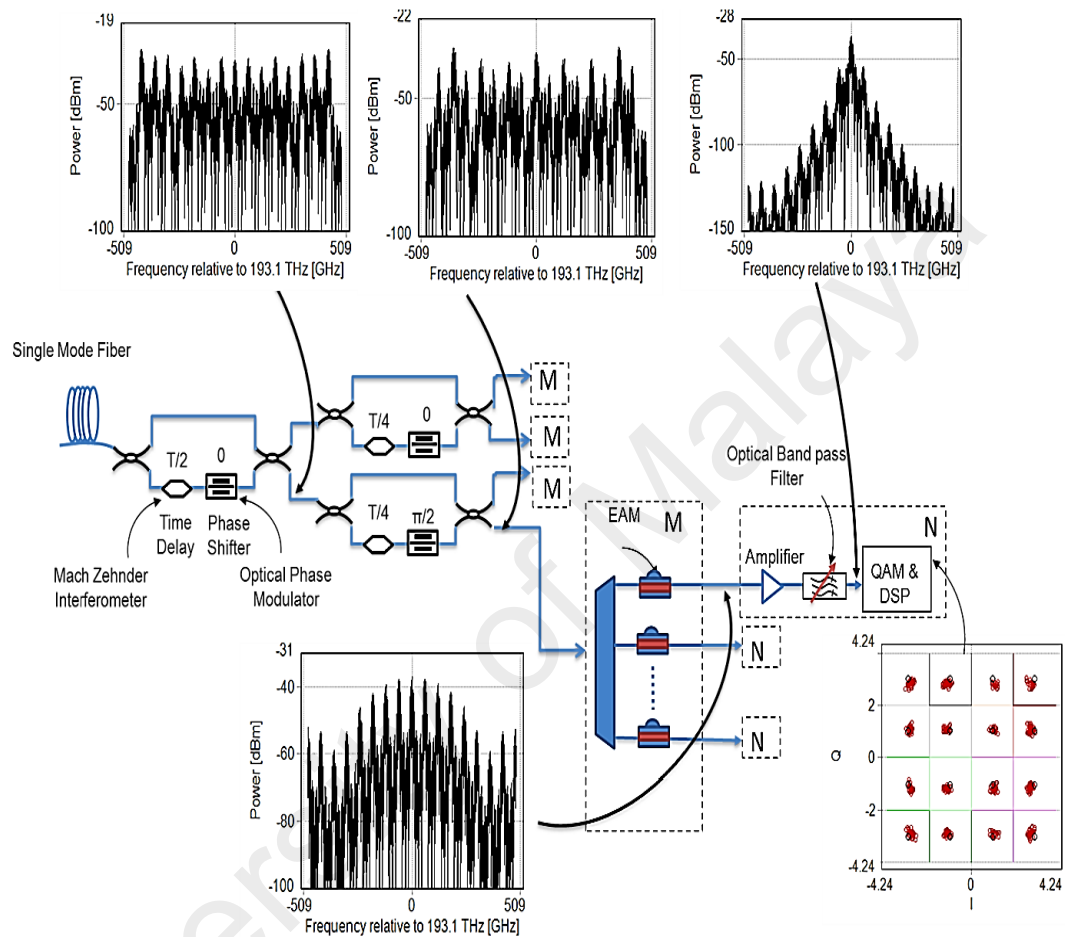


Figure 3.2: Receiver components of an AO-OFDM transmission system with OFFT scheme.

3.3 Analytical modeling of an AO-OFDM system

In this section, we provide an analytical model that describes the interaction between ASE noise and the nonlinear effects in AO-OFDM systems configured with and without dispersion. Nonlinear effects have been reported to be significant in amplified WDM transmission systems (Wu & Way, 2004). Phase degradation due to SPM, XPM, and FWM has been studied extensively for both systems with and without dispersion (Demir, 2007). It has been shown that ASE noise due to optical amplifiers adds a random nonlinear phase noise and mainly affects SPM, XPM, and FWM phenomena (Zhu & Kumar, 2010). The optical dispersion-management has significant effect on the phase noise. The residual dispersion over multi-spans fiber causes a phase array effect (X. Chen & Shieh, 2010). In our model, the dispersion compensation ratio is assumed to be one and there is no residual dispersion. We start with the following optical system model (Wu & Way, 2004):

$$u(z, t) = [u(0, t) + n(t)] \exp(j\phi), \quad (3.1)$$

where $u(0, t)$ and $u(z, t)$ are transmitted and received optical OFDM signals, respectively, z is the transmission distance, $n(t)$ is the ASE noise due to the optical amplifier, and ϕ is phase distortion in radians due to the nonlinearities and dispersion, given by:

$$\phi = \phi_{DIS} + \phi_{SPM} + \phi_{XPM} + \phi_{FWM} + \phi_{SPM}^n + \phi_{XPM}^n + \phi_{FWM}^n + \phi_{FWM}^n, \quad (3.2)$$

where ϕ_{DIS} , ϕ_{SPM} , ϕ_{XPM} , and ϕ_{FWM} denote the phase distortions due to dispersion, SPM, XPM, and FWM phenomena, respectively. ϕ_{SPM}^n , ϕ_{XPM}^n , and ϕ_{FWM}^n also denote the phase

distortions due to interaction of SPM, XPM, and FWM with ASE noise, respectively.

The optical field of the AO-OFDM signal can be written as:

$$u(z, t) = \sum_{k=-(N-1)/2}^{(N-1)/2} u_k(z, t) \exp(j\omega_k t), \quad (3.3)$$

where N represents the total number of subcarriers (assumed odd without loss of generality), $\omega_k = 2\pi k / T_s$ is the frequency offset from the reference optical carrier, $u_k(z, t)$, $k \in \{-(N-1)/2, -(N-1)/2+1, \dots, (N-1)/2\}$ is normalized slowly varying field envelope of a single QAM subcarrier. At the transmitter side, it is given by:

$$u_k(0, t) = \sqrt{\frac{P}{2}} (a_k + jb_k) \text{rect}\left(\frac{t - kT_s}{T_s}\right), \quad (3.4)$$

where P is the lowest subcarrier optical power, and

$$\text{rect}(t) = \begin{cases} 1; & \text{if } 0 \leq t < 1, \\ 0; & \text{Otherwise.} \end{cases} \quad (3.5)$$

Notice that the complex amplitude is given by $A_k = a_k + jb_k$, for any natural number k , and is dependent on the QAM constellation.

3.3.1 SPM and XPM phase noise in AO-OFDM systems

In this subsection, we derive analytical equations for nonlinear phase noise variations of both SPM and XPM phenomena in our AO-OFDM system, including the interaction of ASE noise. The first consequence of the Kerr effect is SPM, where the

optical field experiences a nonlinear phase delay that results from its own intensity. On the other hand, XPM refers to the nonlinear phase shift of an optical field induced by another field with different wavelength, direction, or state of polarization. The optical OFDM signal is commonly transmitted through multi-span optical fiber where each span is composed of an optical fiber and an optical amplifier. At the output of each amplifier, an ASE noise field is added to each subcarrier, which is appropriately modeled as an additive white Gaussian noise (AWGN) (Reichel & Zengerle, 1999). The mean noise energy per degrees of freedom (DOF) is equal to the total noise energy in overall bandwidth and time divided by the number of DOFs (Bernard, 2001; Donati & Giuliani, 1997). In our analytical model, each fiber span has the same length L and identical optical amplifier with ASE noise $n(t)$. Let us expand the noise field as a discrete Fourier transform:

$$n(t) = \sum_{k=-(N-1)/2}^{(N-1)/2} n_k(t) \exp(j\omega_k t), \quad (3.6)$$

where $n(t)$, $k \in \{-(N-1)/2, -(N-1)/2+1, \dots, (N-1)/2\}$, is the complex amplifier noise at the k th subcarrier which have noise variance of σ_k^2 . As previously explained, the AO-OFDM signal is transmitted over M fiber spans. The optical signal is periodically amplified by optical amplifiers located at end of each span, so the nonlinear phase noise is accumulated span-by-span (Ho & Kahn, 2004). In an AO-OFDM link with M optical amplifiers, the phase noise due to SPM and XPM can be expressed as:

$$\begin{aligned} \phi_{kSPM}^{n+}(ML) &= \gamma L_{eff}(L) \sum_{m=1}^M \left| u_k(0,t) + \sum_{\mu=1}^m n_{k\mu}(t) \right|^2 \\ \phi_{kXPM}^{n+}(ML) &= 2\gamma L_{eff}(L) \sum_{\substack{i=-(N-1)/2 \\ i \neq k}}^{(N-1)/2} \sum_{m=1}^M \left| u_i(0,t) + \sum_{\mu=1}^m n_{i\mu}(t) \right|^2, \end{aligned} \quad (3.7)$$

respectively, where γ is the nonlinear coefficients and $n_{k\mu}(t)$, $\mu \in \{1, 2, \dots, M\}$, is the complex amplifier noise at the μ th span and k th subcarrier. Here, $L_{eff} = (1 - e^{-\alpha L}) / \alpha$, where α is the attenuation coefficient. Expanding the right-hand sides of the last two equations, we get:

$$\begin{aligned}\phi_{kSPM}^{n+}(ML) &= \gamma L_{eff}(L) \sum_{m=1}^M \left[|u_k|^2 + 2\Re \left\{ u_k \sum_{\mu=1}^m n_{k\mu}^*(t) \right\} + \left| \sum_{\mu=1}^m n_{k\mu}(t) \right|^2 \right] \\ \phi_{kXPM}^{n+}(ML) &= 2\gamma L_{eff}(L) \sum_{\substack{i=-(N-1)/2 \\ i \neq k}}^{(N-1)/2} \sum_{m=1}^M \left[|u_i|^2 + 2\Re \left\{ u_i \sum_{\mu=1}^m n_{i\mu}^*(t) \right\} + \left| \sum_{\mu=1}^m n_{i\mu}(t) \right|^2 \right],\end{aligned}\quad (3.8)$$

respectively, where $\Re\{x\}$ and x^* denote the real part and the conjugate of complex number x , respectively. The last terms on the right-hand side of Eq. (3.8) represent the interaction of noise with itself, which have no effect on phase noise, while the first and second terms represent the interaction of the signal with itself and with ASE noise, respectively. The SPM and XPM phase noises due to interaction of the signal with itself are:

$$\begin{aligned}\phi_{kSPM}^n(ML) &= \gamma L_{eff}(L) \sum_{m=1}^M |u_k|^2 \\ \phi_{kXPM}^n(ML) &= 2\gamma L_{eff}(L) \sum_{\substack{i=-(N-1)/2 \\ i \neq k}}^{(N-1)/2} \sum_{m=1}^M |u_i|^2,\end{aligned}\quad (3.9)$$

respectively. The corresponding terms due to interaction of the signal with ASE noise are:

$$\begin{aligned}\phi_{kSPM}^n(ML) &= 2\gamma L_{eff}(L) \sum_{m=1}^M \Re \left\{ u_k \sum_{\mu=1}^m n_{k\mu}^*(t) \right\} \\ \phi_{kXPM}^n(ML) &= 4\gamma L_{eff}(L) \sum_{\substack{i=-(N-1)/2 \\ i \neq k}}^{(N-1)/2} \sum_{m=1}^M \Re \left\{ u_i \sum_{\mu=1}^m n_{i\mu}^*(t) \right\},\end{aligned}\quad (3.10)$$

respectively. For an OFDM system employing QAM modulation, $u_k \in \left\{ \sqrt{P/2A_k} \right\}$. The nonlinear phase noise variances due to interaction SPM and XPM with ASE noise can be written as:

$$\begin{aligned}\sigma_{kSPM}^2 (ML) &= \frac{M(M+1)}{2} \gamma^2 L_{eff}^2 (L) P |A_k|^2 \sigma_k^2 \\ \sigma_{kXPM}^2 (ML) &= 2M(M+1) \gamma^2 L_{eff}^2 (L) P \sum_{\substack{i=-(N-1)/2 \\ i \neq k}}^{(N-1)/2} |A_i|^2 \sigma_i^2.\end{aligned}\quad (3.11)$$

It is clear that the phase noise variance due to XPM is much higher than the phase noise variance due to SPM.

3.3.2 FWM phase noise

In this subsection, the effect of FWM on AO-OFDM is analytically demonstrated. As FWM is a phase sensitive process (the interaction depends on the relative phases of all subcarriers), its effect can efficiently accumulate over longer distances. Also, the interaction of FWM with the ASE noise inside the optical fiber is analytically presented. The interaction between FWM and random noise of optical amplifier leads to deterministic as well as stochastic impairments. By including ASE noise and FWM with the other nonlinear and dispersion effects, the optical field of signal at the end of first span can be expressed by (Lau et al., 2008):

$$\begin{aligned}u_k(L, t) &= u_k(0, t) \exp \left[j \phi_{kSPM}(L) + j \phi_{kXPM}(L) + j \phi_{kSPM}^n(L) + j \phi_{kXPM}^n(L) - j \phi_{DIS}(L) \right] \\ &\quad + n_k(t) + \delta u_k^n(L, t),\end{aligned}\quad (3.12)$$

where

$$\begin{aligned}
\phi_{DIS}(L) &= -\left(\frac{\beta_2}{2} \omega_k^2\right)L, \\
\delta u_k^n(L, t) &= j2\gamma \sum_{\substack{h=-(N-1)/2 \\ h \neq k}}^{(N-1)/2} \sum_{\substack{i=-(N-1)/2 \\ l=h+i-k \\ i \neq l}}^{(N-1)/2} L_{FWM}(L) [u_h(L, t) + n_h(t)] [u_i(L, t) + n_i(t)] [u_l^*(L, t) + n_l^*(t)], \\
L_{FWM}(L) &= \frac{1 - \exp\left[-L\left(\alpha - j\frac{\beta_2}{2}\Omega^2\right)\right]}{\alpha - j\frac{\beta_2}{2}\Omega^2}, \\
\Omega^2 &= (h^2 + i^2 - l^2 - k^2)\omega^2,
\end{aligned} \tag{3.13}$$

and β_2 is the dispersion profile. We can define $\frac{\beta_2}{2}\Omega^2 z$ as a phase mismatch between subcarriers. We can rewrite Eq. (3.12) as:

$$u_k^n(L, t) = u_k(L, t) + \Delta u_k^n(L, t), \tag{3.14}$$

The fluctuation of the optical field due to both ASE noise and its interaction with FWM for M amplifiers (M fiber spans) is determined by $\Delta u_k^n(L, t)$ and can be expressed as:

$$\Delta u_k^n(ML, t) = \sum_{m=1}^M n_{km} + j2\gamma \sum_{m=1}^M \sum_{\substack{h=-(N-1)/2 \\ h \neq k}}^{(N-1)/2} \sum_{\substack{i=-(N-1)/2 \\ l=h+i-k \\ i \neq l}}^{(N-1)/2} L_{FWM}(mL) (u_h u_i n_l^* + u_h u_l^* n_i + u_i u_l^* n_h). \tag{3.15}$$

In order to calculate the phase noise variance, the deviation of AO-OFDM field is considered. The phase noise is defined as:

$$\phi_{kFWM}^n(ML, t) \cong \frac{\Im\{\Delta u_k^n(ML, t)\}}{|u_k|}, \tag{3.16}$$

where $\Im\{x\}$ denote the imaginary part of x . By substituting the deviation of AO-OFDM field in Eq. (3.16), the phase noise variance can be expressed by:

$$\begin{aligned} \sigma_{kFWM}^2(ML, t) = & \frac{2M \sigma_k^2}{P |A_k|^2} + \frac{2\gamma^2 P}{|A_k|^2} \sum_{m=1}^M \sum_{\substack{h=-(N-1)/2 \\ h \neq k}}^{(N-1)/2} \sum_{\substack{i=-(N-1)/2 \\ i=h+i-k \\ i \neq l}}^{(N-1)/2} L_{FWM}(mL) \\ & \times \left(|A_h|^2 |A_i|^2 \sigma_i^2 + |A_h|^2 |A_l|^2 \sigma_l^2 + |A_i|^2 |A_l|^2 \sigma_h^2 \right). \end{aligned} \quad (3.17)$$

In the last equation, the first term represents the phase variance due to ASE noise of M optical amplifiers, while the second term expresses the phase noise variance due to the interaction of FWM with ASE noise. From Eq. (3.11) and Eq. (3.17), we can conclude that the phase variance due to FWM is the dominant compared to that induced by either SPM or XPM.

3.4 Results and discussions

In this section, we evaluate our analytical model numerically based on the system that described in Section 3.2. Next, the analytical results of the AO-OFDM system is demonstrated and compared with numerical simulation results.

3.4.1 Analytical results

In this subsection, the effects of phase noise on the reception of AO-OFDM system that employs 4QAM and 16QAM signals are studied. The influences of subcarrier peak power, number of sub-carriers, fiber length, and symbol rate, on the phase variation are examined as well. In our evaluations, we use a standard single mode optical fiber (SSMF) with the following parameters: dispersion coefficient of $D = 16$

ps/nm/km, attenuation coefficient of $\alpha = 0.2$ dB/km, core effective area of $A_{eff} = 80 \mu\text{m}^2$, and nonlinear refractive index of $n_2 = 2.5 \times 10^{-20} \text{ m}^2/\text{W}$. In order to compensate for the attenuation, optical amplifiers are employed at spans of spacing 55 km, each. The typical value of the noise figure is depends on the manufacture of optical amplifier. For this reason, many publications set the noise figure around 4.5 dB – 5 dB, while others fix the noise figure around 5 dB – 6 dB (L. Liu et al., 2012; Morgado et al., 2011). In the simulation, the noise figure of each optical amplifier is set to 6 dB for testing the proposed system at higher ASE noise. Furthermore, the dispersion is fully compensated by using a dispersion compensating optical fiber (DCF) at end of each span.

3.4.1.1 Phase noise variance versus subcarrier power

Figure 3.3 (a) shows the variance of total nonlinear phase noise as a function of the launch power for a 4QAM AO-OFDM system. The fiber length and the number of subcarriers are fixed at 550 km (10 spans) and 29 subcarriers, respectively. The analytical results are evaluated at two dispersion values, namely $D = 0$ ps/nm/km and $D = 16$ ps/nm/km, respectively. It is clear that the degradation due to nonlinearity is significantly compensated by CD effect, whereby, phase mismatch (that is related to dispersion) would correspond to a significant decrease in the nonlinear phase variance, cf. Eq. (3.13). The total variance of the phase noise initially decreases with the increase of launch power since the phase noise due to the interaction of ASE noise is dominant at low launch powers. However, as the launch power increases beyond -7 dBm, the variance of phase noise increases dramatically at $D = 0$ ps/nm/km, since the nonlinear phase noise due to the interaction of XPM and FWM with ASE noise becomes dominant at higher powers. As shown in Figure 3.3 (b), the interaction of FWM with ASE noise has a major contribution to phase noise in the system. This phenomenon is

because the interaction is depending on the relative phases of all subcarriers in FWM. In addition, the nonlinear phase noise due to the interaction of XPM with ASE noise increases at higher powers.

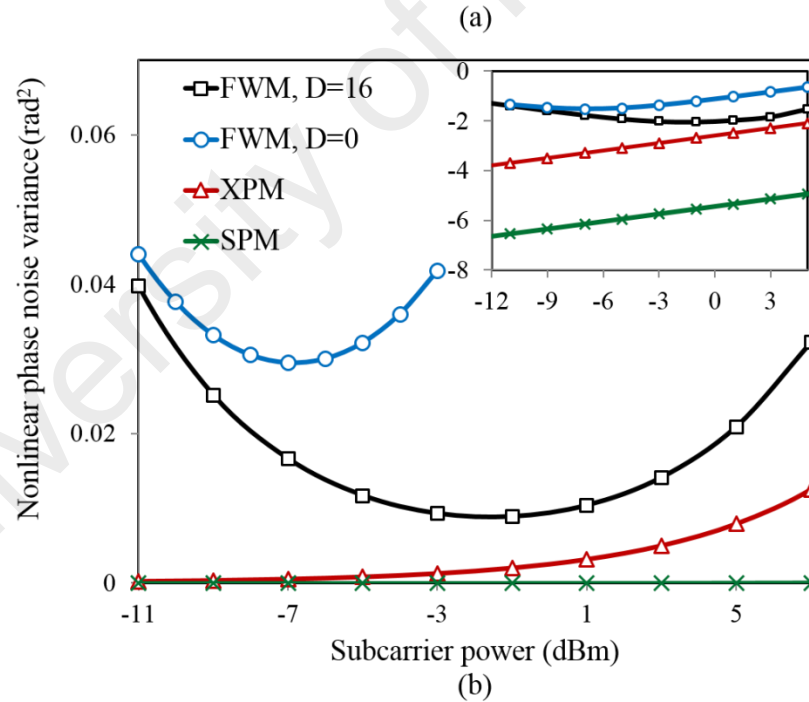
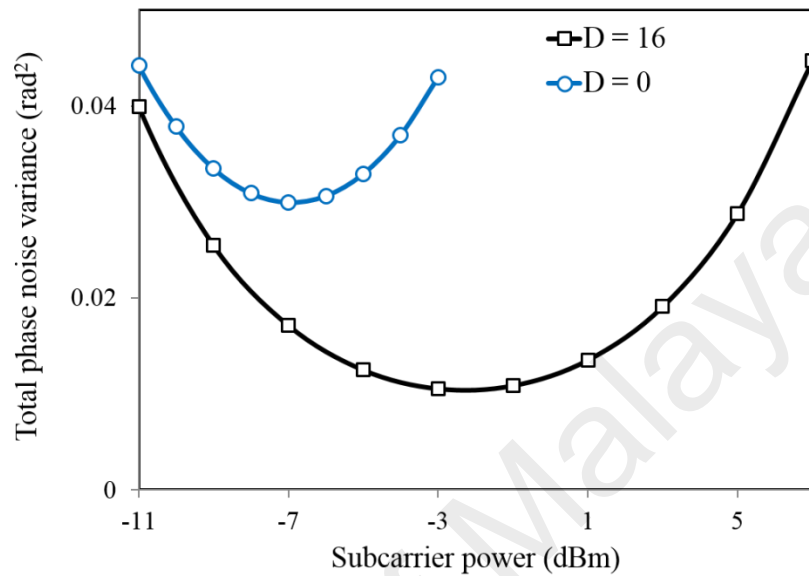


Figure 3.3: Phase noise variance versus subcarrier peak power for an AO-OFDM system employing 4QAM modulation format: (a) total phase noise variance; (b) phase noise variances due to SPM, XPM, FWM (at $D = 0$ ps/nm/km), and FWM (at $D = 16$ ps/nm/km) ; the inset is a logarithmic scale figure.

Similarly, when increasing the dispersion to $D = 16$ ps/nm/km, the variance of FWM phase noise decreases as the subcarrier power increases until the subcarrier power reaches -3 dBm, beyond which the variance of the phase noise starts to increase. That is, for 4QAM AO-OFDM system, a minimum phase noise variance of 0.0108 rad^2 is achieved at an optimum power of -3 dBm as shown in Figure 3.3 (a).

Similar observations can be obtained for a 16QAM AO-OFDM system as depicted in Figure 3.4. At fixed fiber length of 165 km (3 span), if $D = 0$ ps/nm/km and the launched power increases beyond -6 dBm, the phase noise variance would increase as shown in Figure 3.4(a) and Figure 3.4(b). By increasing the dispersion to $D = 16$ ps/nm/km, the degradation due to nonlinearity decreases and the minimum phase noise variance is obtained at a subcarrier power of -1 dBm. The optimum launch power for 16QAM is higher than for 4QAM because the 16QAM OFDM signal is transmitted over fiber length of 165 km while the transmission distance of the 4QAM OFDM system is 550 km. With longer transmission distance, the effect of phase noise on the transmitted signal become higher and the optimum power moves toward the lower power region. Further, Figure 3.4(b) shows that the nonlinear phase noise due to the interaction of FWM with ASE noise becomes dominant at higher powers.

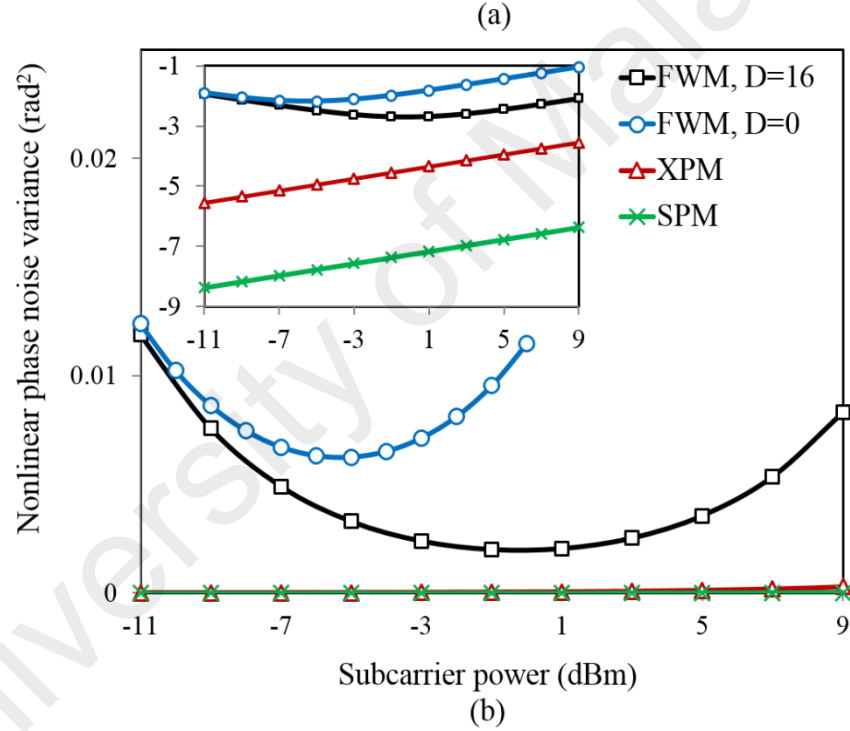
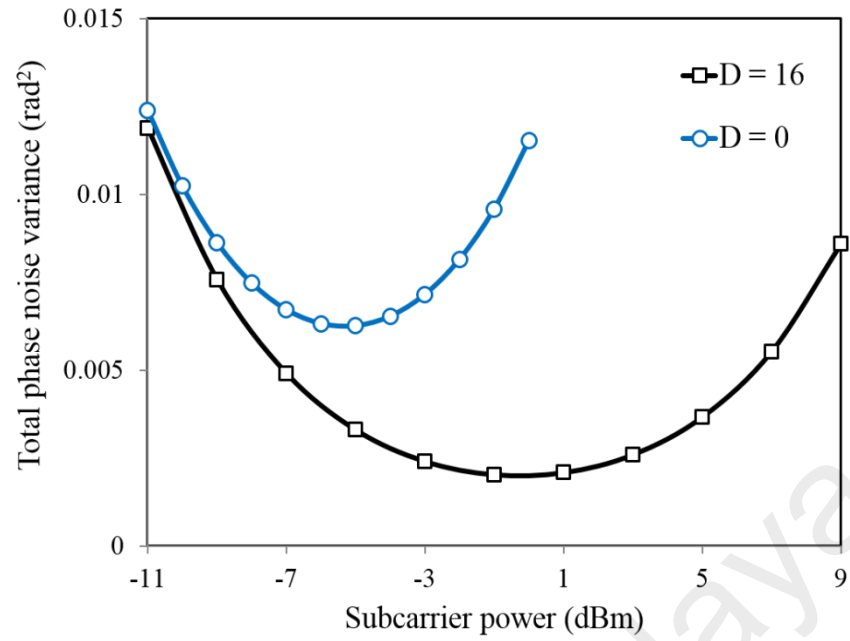
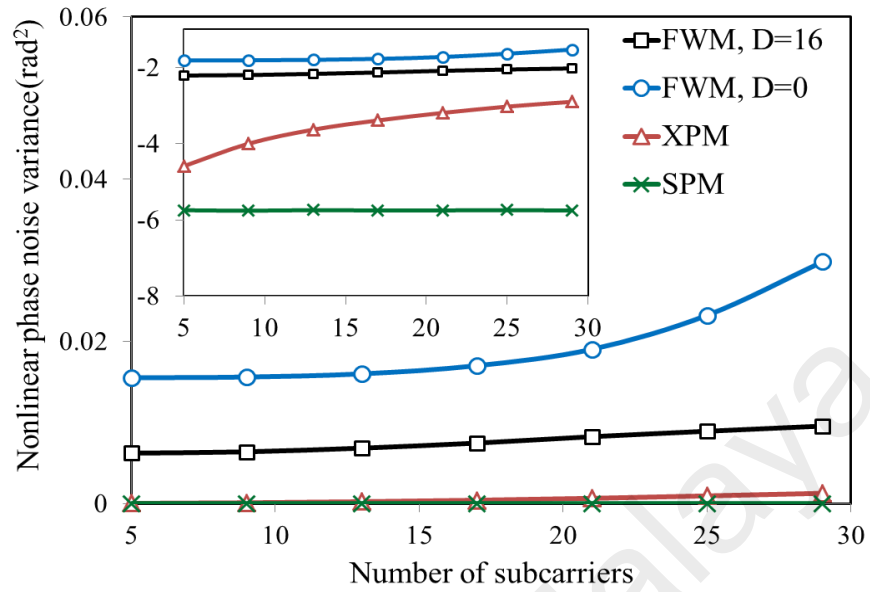


Figure 3.4: Phase noise variance versus sub-carrier peak power for an all-optical OFDM system employing 16QAM modulation format: (a) total phase noise variance; (b) phase noise variances due to SPM, XPM, and FWM; the inset is a logarithmic scale figure.

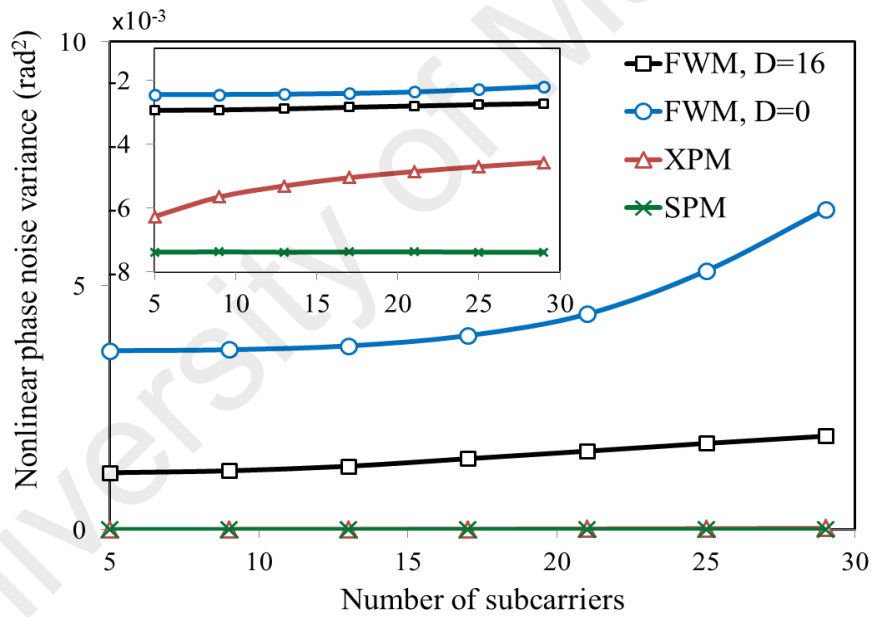
3.4.1.2 Phase noise variance versus number of subcarrier

Figure 3.5(a) and Figure 3.5(b) show the variance of phase noise due to the interaction of SPM, XPM, and FWM with ASE noise versus number of subcarriers for 4QAM and 16QAM AO-OFDM systems, respectively. For the 4QAM system, the fiber length is 550 km (10 spans) long, the noise figure of optical amplifier is 6 dB, and the sub-carrier peak power is -3 dBm. For the 16QAM system, the fiber length is 165 km (3 spans) and the sub-carrier peak power is -1 dBm. For the sake of convenience, the logarithmic values of phase variances versus the number of subcarriers are depicted in the inset of Figure 3.5.

As expected from Eq. (3.11), the SPM phase variance is robust to the number of subcarrier. On the other hand and in agreement with Eq. (3.11) and Eq. (3.17), by increasing the number of subcarriers, an increase in phase variation can be observed in both XPM and FWM respective nonlinearities. In the case of zero dispersion ($D = 0$ ps/nm/km), FWM nonlinear phenomenon is maximized where appropriate phase-matching condition is satisfied. This is due to the fact that the subcarriers of AO-OFDM systems are derived from same laser source and interact in a coherent manner. By increasing the dispersion to $D = 16$ ps/nm/km, the phase mismatch due to dispersion leads to a significant decrease of FWM phase variance.



(a)



(b)

Figure 3.5: Phase noise variance due to SPM, XPM, and FWM versus the number of subcarriers: (a) 4QAM AO-OFDM system; the inset is a logarithmic scale figure. (b) 16QAM AO-OFDM system; the inset is a logarithmic scale figure.

3.4.1.3 Phase noise variance versus transmission distance

Figure 3.6(a) and Figure 3.6(b) show the variance of the nonlinear phase noise as a function of the propagation distance for 4 and 16QAM AO-OFDM systems, respectively. The number of subcarriers is fixed at 29. The subcarrier peak power is fixed at -3 dBm for the 4QAM system and -1 dBm for the 16QAM system. During the simulation, the length of fiber span is fixed at 55 km and the number of spans is changed. As expected from Figure 3.6(a) and Figure 3.6(b), with large number of subcarriers, the nonlinear phase noise induced by FWM is significantly larger than that induced by either SPM or XPM. Moderate phase variation changes can be observed for SPM and XPM, rather than the FWM effect. This is because the overall interaction is dependent on the relative phases of all subcarriers in FWM.

To explain the effect of fiber span length on the phase noise, Figure 3.6(c) and Figure 3.6(d) compare the nonlinear phase noise variances due to SPM, XPM and FWM for span lengths of 55 km and 80 km, respectively. It can be observed that the FWM effect for 80 km fiber span is higher than its effect for 55 km, while the XPM effect for 80 km is less than its effect for 55 km. At transmission distance of 550 km, ten fiber spans with length 55 km are required, while seven fiber spans with length 80 km are required to achieve 560 km. In other words, the number of optical amplifiers is reduced from 10 to 7 amplifiers. However, for span length of 80 km, the gain of amplifiers is higher and it adds more ASE noise. The interaction of ASE noise with FWM over longer fiber produces higher phase noise because FWM effect can efficiently accumulate over longer distances and add fluctuation to the transmitted signal. On other hand, XPM effect is more affected by the number of amplifiers rather than fiber length because its effect only changes the phase of optical signal. However, the nonlinear

phase noise induced by FWM remains larger than that induced by XPM in 80 km and 55 km fiber span length.

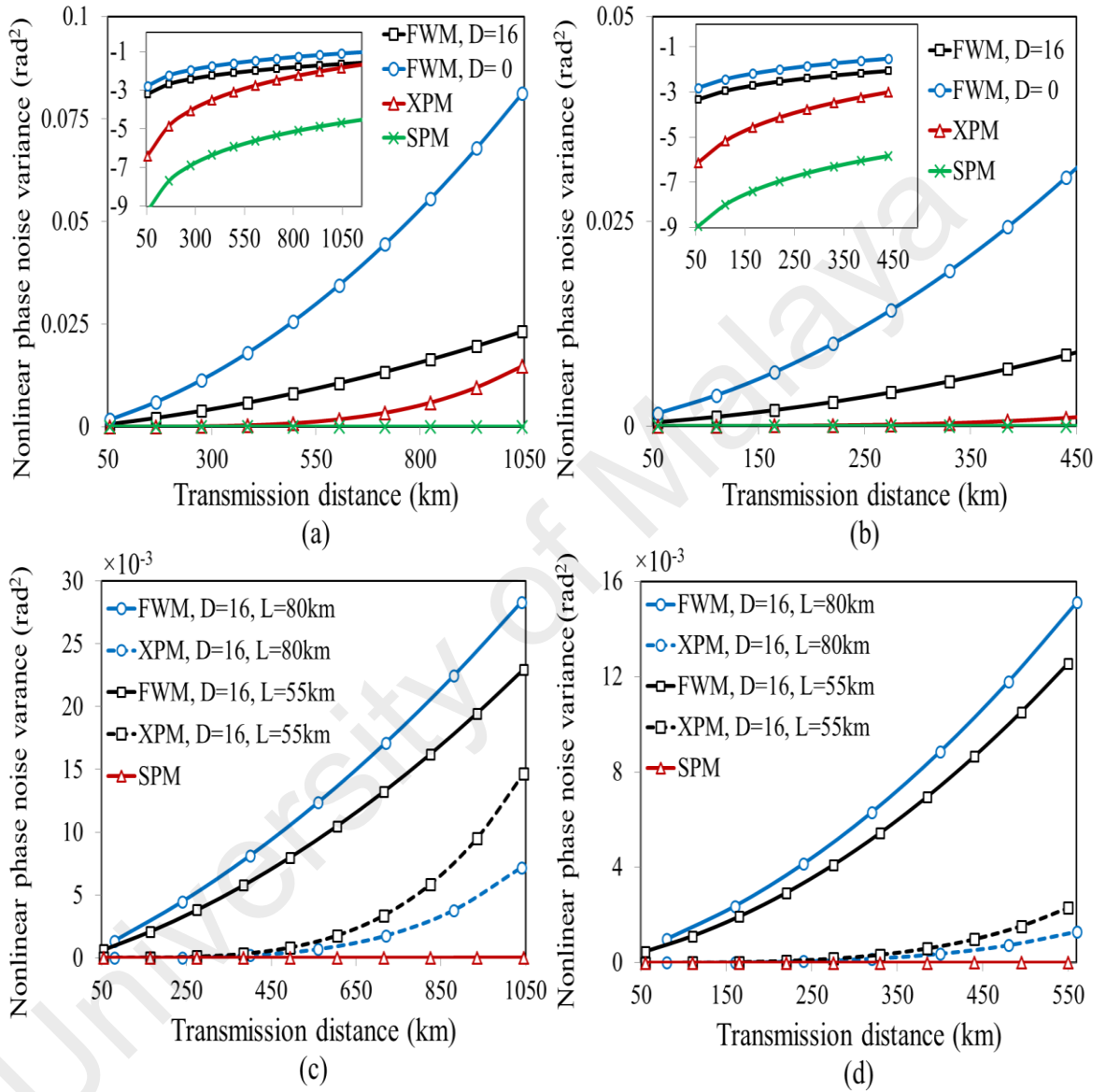


Figure 3.6: Phase noise variance due to SPM, XPM, and FWM versus transmission distance: (a) 4QAM AO-OFDM system; the inset is a logarithmic scale figure. (b) 16QAM AO-OFDM system; the inset is a logarithmic scale figure. (c) 4QAM AO-OFDM system for span lengths 55 km and 80 km. d) 16QAM AO-OFDM system for span lengths 55 km and 80 km.

3.4.1.4 Phase noise variance versus symbol rate

The impact of the symbol rate on the total phase noise variance for both 4 and 16QAM AO-OFDM systems is investigated in this subsection. In Figure 3.7, blue solid lines with hollow circle show the analytical results for a transmission fiber with $D = 0$ ps/nm/km, while black solid lines with hollow square show the analytical results with $D = 16$ ps/nm/km. It can be seen from these figures that there is minor change in the variance of the total phase noise by increasing the symbol rate for a fiber with $D = 0$ ps/nm/km. While for transmission fiber with $D = 16$ ps/nm/km, the phase variance decreases by increasing the symbol rate. This can be explained by phase mismatch definition $\beta_2 \Omega^2 z / 2$ (see Eq. (3.13)). As expected, for a fiber with $D = 0$ ps/nm/km, the effect of phase mismatch is zero. Therefore, high and constant FWM phase noise in all symbol rate ranges can be observed. On the other hand for the fiber with $D = 16$ ps/nm/km, the phase mismatch is higher than zero and its magnitude depends on the symbol rate. We observe that the magnitude of the FWM decreases when increasing the phase mismatch, which leads to low total phase noise at high symbol rate values.

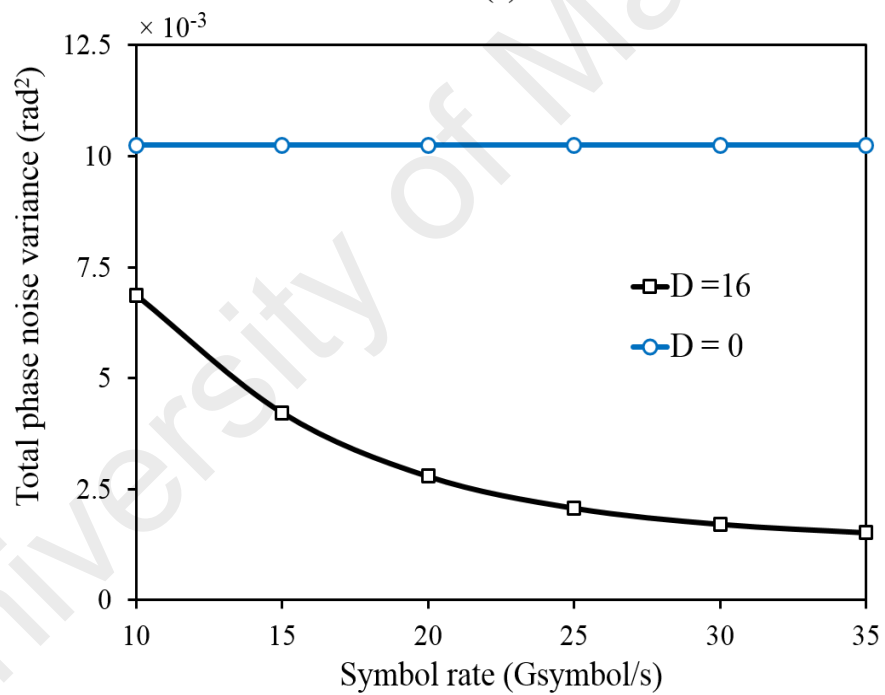
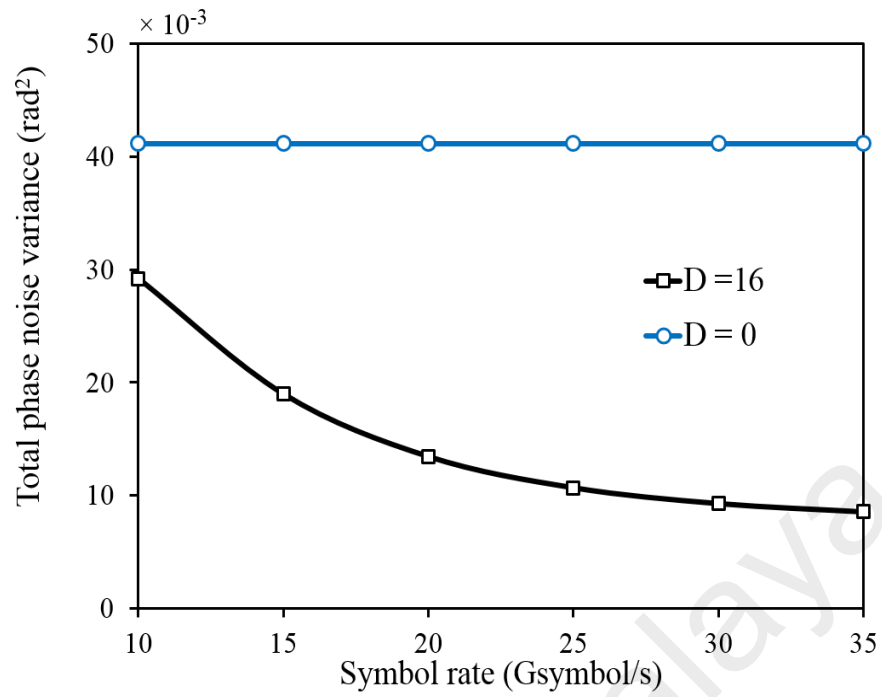


Figure 3.7: Total phase noise variance versus symbol rate: (a) 4QAM AO-OFDM system. (b) 16QAM AO-OFDM system.

3.4.1.5 Phase noise variance versus subcarrier index

In this subsection, the effects of phase noise on the center frequency are investigated. It has been shown that the power density of FWM noise is higher in the center of the OFDM band than at the edge (S. T. Le et al., 2014; Arthur J Lowery et al., 2007). In addition, the contributions of different subcarriers to the FWM noise, in general, are different. As a result, the power of the FWM noise depends strongly on the power distribution among the AO-OFDM subcarriers. Figure 3.8(a) and Figure 3.8(b) show the total nonlinear phase noise variance for each subcarrier for 4 and 16QAM AO-OFDM systems, respectively. Again, the 4QAM OFDM signal is transmitted over a distance of 550 km (10 spans), while 16QAM OFDM signal is transmitted over 165 km (3 spans). It can be seen that center subcarriers have a much larger contribution to the phase noise when compared with subcarriers at the edges for both SSMF (with $D = 0$ ps/nm/km) and zero dispersion fiber with $D = 16$ ps/nm/km.

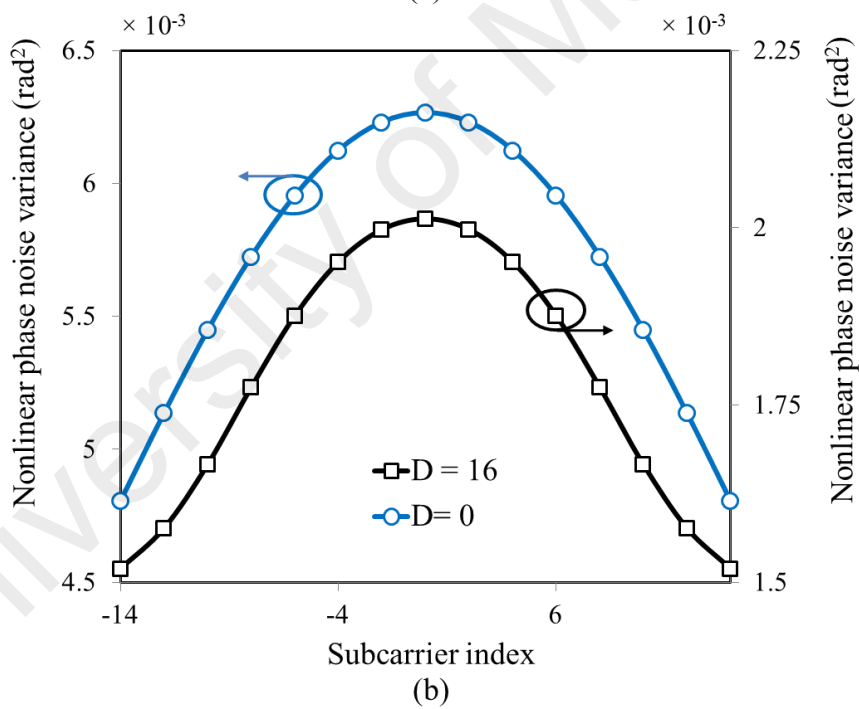
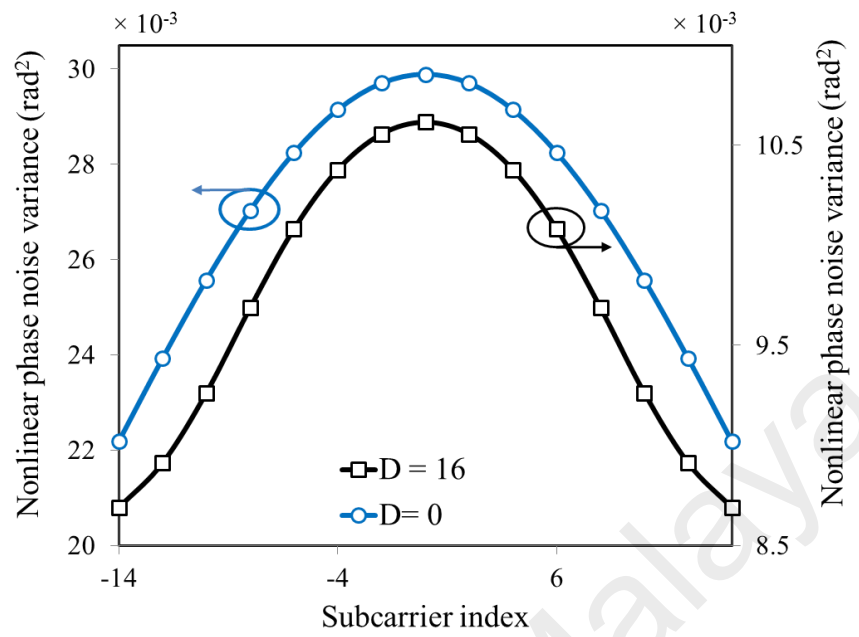


Figure 3.8: Total phase noise variance versus subcarrier index: (a) 4QAM AO-OFDM system, (b) 16QAM AO-OFDM system.

3.4.2 Comparison of simulation and analytical results

In order to verify the accuracy of our analytical results, the error vector magnitude (EVM) for both analytical and simulation results is compared in this section. Furthermore, the effects of subcarrier's power and symbol rate on EVM are analyzed and explained. To estimate the nonlinear phase noise only, we set the laser phase noise to zero in our simulation.

3.4.2.1 EVM versus subcarrier power

In Figure 3.9(a) and Figure 3.9(b), we show the impact of subcarrier power on the EVM for both 4 and 16QAM AO-OFDM systems, respectively. The transmission distances of 4 and 16QAM systems are 550 km (10 spans) and 165 km (3 spans), respectively. The number of subcarriers and symbol rate are fixed at 29 subcarriers and 25 Gsymbol/s, respectively. In comparison with the phase noise variance (cf. Figure 3.4), same trend can be observed in EVM versus subcarrier peak power of Figure 3.9. This is explained in (Georgiadis, 2004), where for QAM systems with coherent detection, one would obtain the EVM as a function of the phase noise variance (σ^2) as:

$$EVM = \sqrt{\frac{1}{SNR} + 2 - 2\exp\left(\frac{-\sigma^2}{2}\right)}, \quad (3.18)$$

where, the phase noise distribution is assumed to be Gaussian. In total agreement with the analytical results for 4QAM AO-OFDM system in the absence of dispersion, the EVM initially decreases up to 0.167 (corresponding to launch power of -7 dBm). That is, the phase noise is the dominant at low launch power due to the interaction of ASE.

However, as the launch power increases beyond -7 dBm, the EVM dramatically increases since the nonlinear phase noise due to the interaction of XPM and FWM with ASE noise becomes dominant at higher powers. At large dispersion values ($D = 16$ ps/nm/km), the EVM decreases to 0.11 when the subcarrier power reaches -3 dBm, beyond which; the magnitude of the EVM is increased. Similarly, for 16QAM AO-OFDM system with $D = 0$ ps/nm/km, the EVM increases as the launched power increases beyond -6 dBm. For normal SMF fiber ($D = 16$ ps/nm/km), the EVM increases for values of subcarrier power higher than -1 dBm. Presented analytical results show good agreement with simulation results.

University of Malaya

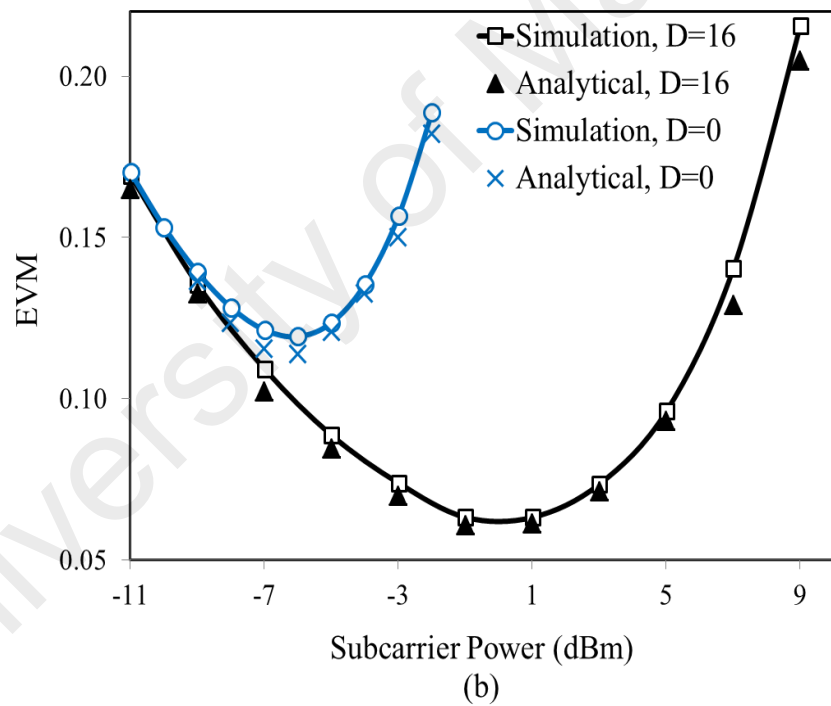
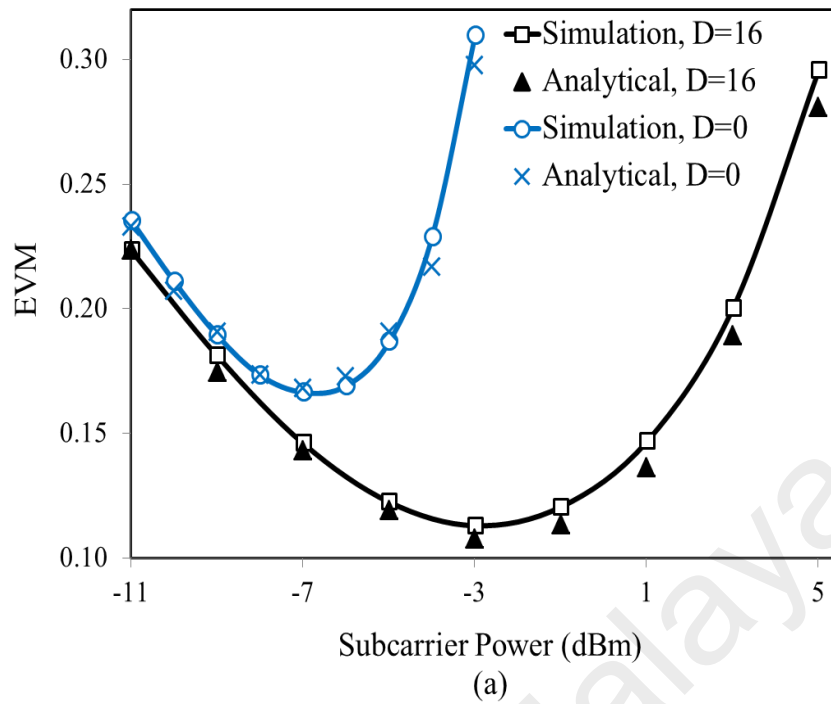


Figure 3.9: EVM versus subcarrier power: (a) 4QAM AO-OFDM system, (b) 16QAM AO-OFDM system.

3.4.2.2 EVM versus symbol rate

Finally, Figure 3.10(a) and Figure 3.10(b) show the magnitude of EVM as a function of symbol rate for 4QAM and 16QAM AO-OFDM systems respectively. In agreement with our phase noise analytical results (cf. Figure 3.7), for the fiber with $D = 16$ ps/nm/km, the EVM is decreasing with increasing the symbol rate, while the EVM approximately remains constant with increasing symbol rate for the fiber when $D = 0$ ps/nm/km. This can be explained by phase mismatch definition $\beta_2 \Omega^2 z / 2$. At $D = 0$ ps/nm/km, high and constant FWM phase noise in all symbol rate ranges are observed as the phase mismatch equals zero. On the other hand, for the fiber with $D = 16$ ps/nm/km, the phase mismatch becomes higher as the phase mismatch between subcarriers totally depends on the symbol rate.

Finally yet importance, our analytical model is valid to deal with the higher-level modulation formats such as m-array phase shift keying (mPSK) and m-array quadrature-amplitude modulation (mQAM) system over 64-level. For example, when the subcarriers are modulated by 4QAM format, the $u(0,t)$ is defined with $a_k \in \{-1,1\}$ and $b_k \in \{-1,1\}$, while the $u(0,t)$ is described with $a_k \in \{-3,-1,1,3\}$ and $b_k \in \{-3,-1,1,3\}$ for 16QAM format. In case of mPSK or mQAM system over 64-level, the a_k and b_k are defined in analytical model according to its corresponding constellation.

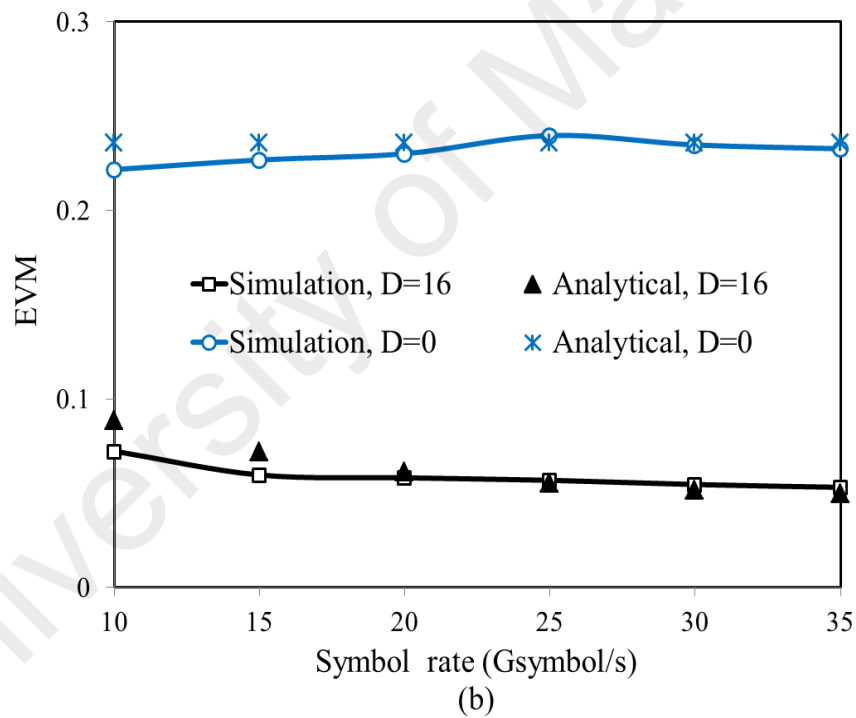
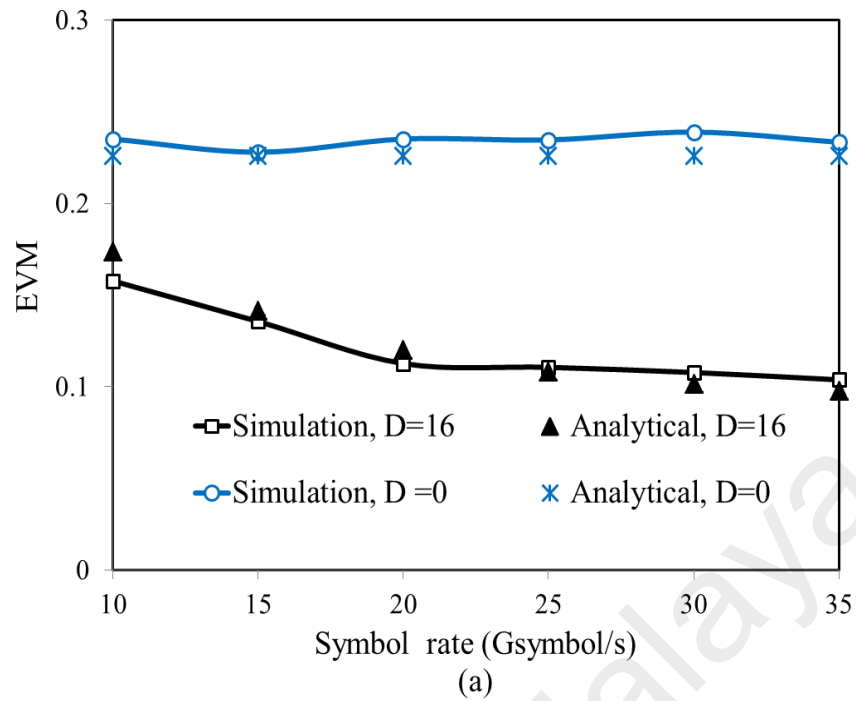


Figure 3.10: EVM versus subcarrier power: (a) 4QAM AO-OFDM system. (b) 16QAM AO-OFDM system.

3.5 Summary

The potential for higher spectral efficiency is increased interests in AO-OFDM systems. However, sensitivity of AO-OFDM system to fiber nonlinearity (leading to nonlinear phase noise) forms the main penalty. Therefore, the analytical model, for estimating the phase noise due to SPM, XPM, and FWM in AO-OFDM systems has been developed and described in this chapter. Here, new analytical equations for estimating the nonlinear phase variances due to the interaction of SPM, XPM, and FWM with ASE noise in both 4QAM and 16QAM AO-OFDM systems have been derived. The effects of the number of subcarriers, fiber length, subcarrier peak power, and dispersion on the nonlinear phase noise have then been investigated in a quantitative manner. In order to verify the results, an AO-OFDM system, that uses coupler-based inverse fast Fourier transform/fast Fourier transform without any nonlinear compensation, has been demonstrated by numerical simulation. The system has employed 29 subcarriers; each subcarrier has been modulated by a 4QAM or 16QAM format with symbol rate of 25 Gsymbol/s.

It is found that the nonlinear phase noise induced by FWM is the dominant nonlinear effect in AO-OFDM systems. This is because the interaction is dependent on the relative phases of all subcarriers in FWM, where appropriate phase-matching conditions from same laser source are satisfied at zero dispersion ($D = 0$ ps/nm/km). When increasing the dispersion ($D = 16$ ps/nm/km), the phase mismatch due to dispersion would compensate the FWM phase variation. In 4QAM AO-OFDM systems, the point of optimum performance has been achieved at -3 dBm when the SSMF is employed. This point of optimum performance increases to -1 dBm for the case of 16QAM AO-OFDM systems. In addition, the accuracy of our analytical model has been

verified by quantifying the EVM using both simulation and analytical models. It turned out that both EVM results are in good agreement with each other.

University of Malaya

CHAPTER 4

MITIGATION OF NONLINEAR FIBER IMPAIRMENTS

IN AO-OFDM SYSTEM USING RZ-mQAM

MODULATION FORMAT

4.1 Introduction

All-optical orthogonal frequency division multiplexing (AO-OFDM) systems that employ high-order modulation formats are becoming attractive because they can transmit a higher data rates as compared to the conventional optical OFDM systems (Hillerkuss et al., 2011). AO-OFDM systems combined with spectral efficient multilevel formats, such as m-array quadrature-amplitude modulation (mQAM) format represent a proven solution to target the upgrade of optical communication systems due to the ability to transmit high bit rate data with good dispersion tolerance (Huang et al., 2011; Mirnia et al., 2013). However, AO-OFDM signals show high sensitivity to phase noise due to the fiber nonlinearity and laser phase noise (J. K. Hmood et al., 2015c; Ho, 2005; Pham et al., 2011). The phase noise due to fiber nonlinearity, such as self-phase modulation (SPM), cross-phase modulation (XPM), and four-wave mixing (FWM), restricts the performance of OFDM systems (Arthur J Lowery et al., 2007; Zhu & Kumar, 2010). The conventional techniques that used for transmitting data over long distance is a multi-span fiber link where each span has one optical amplifier (Nazarathy et al., 2008). The interaction between fiber nonlinearity and random noise of optical amplifiers may lead to deterministic as well as stochastic impairments (Nakazawa et al.,

2010). In addition, the high number of subcarriers and low frequency spacing between subcarriers make both FWM and XPM as major factors for limiting the performance of optical OFDM systems (S. T. Le et al., 2014). Subcarrier power, transmission length, number of subcarriers, and number of amplifiers determine the nonlinear phase noise in optical OFDM systems (Zhu & Kumar, 2010).

In this chapter, two new approaches to mitigate fiber nonlinearity and to improve the performance of AO-OFDM system that employ mQAM format are analytically modeled and numerically demonstrated. In first approach, we proposed a new combination between return-to-zero (RZ) coding format and mQAM modulation formats for reducing the effective power of subcarriers and therefore the transmission performance of the AO-OFDM system is improved. In second approach, the minimizing time interaction between subcarriers is proposed to mitigate the nonlinear impairments in AO-OFDM systems. The time of interaction between subcarriers can be minimized by making an alternately delay between odd and even subcarriers that modulated by RZ-QAM modulation formats.

4.2 Performance improvement of AO-OFDM systems based on combining RZ coding with mQAM formats

To enhance the tolerance towards the fiber nonlinearity effects, RZ-coding format has been proposed in many single and multi-channel optical communication systems (Cheng & Conradi, 2002; Faisal & Maruta, 2010; Hayee & Willner, 1999; Tripathi et al., 2007). Moreover, the combination of RZ format with phase modulation formats, such as return-to-zero differential binary phase shift keying (RZ-DBPSK) or return-to-zero differential quadrature phase shift keying (RZ-DQPSK) modulation formats, are

reported to be more tolerant to fiber nonlinear effects in both single channel and multi-channel transmission systems (Cho et al., 2003; Gnauck et al., 2002; Wree et al., 2002). RZ-DQPSK has also been proposed as an efficient modulation scheme in the presence of SPM and dispersion (Mirnia et al., 2013). It is well-known that non-return-to-zero (NRZ) coding format is more adversely affected by nonlinearities whereas RZ format is more affected by dispersion (Hayee & Willner, 1999). Although, RZ formats is more tolerant to fiber nonlinearity effects, it is more affected by dispersion (Hayee & Willner, 1999). Thereby, dispersion-managed transmission fiber links that include a standard single mode optical fiber (SSMF) in alternating with dispersion compensating optical fiber (DCF) has been employed to minimize accumulated dispersion.

In order to increase the spectral efficiency of an optical OFDM system, a high order modulation formats is normally proposed (C. Li et al., 2014). However, optical OFDM systems that employ mQAM are greatly affected by phase noise that induced by fiber nonlinearity, causing destruction the orthogonality of subcarriers (Hoxha & Cincotti, 2013; Lin et al., 2011; Wei & Chen, 2010). The nonlinear phase noise is mainly governed by subcarrier power, transmission length, number of amplifiers and number of subcarriers (Zhu & Kumar, 2010).

In this section, we propose a new combination between RZ coding format and 4QAM and 16QAM modulation formats in AO-OFDM system for mitigating the nonlinear impairments and improving the system performance. At transmitter side, the conversion from mQAM to RZ-mQAM formats is optically realized by using a single Mach-Zehnder modulator (MZM) after mQAM modulator for each subcarrier. The MZM is driven by sinusoidal waveform. To keep the time slot for optimum gating at normal frequency, RZ-mQAM signal is converted to mQAM signal before the sampling process. This conversion is done at the receiver side by utilizing a Mach Zehnder

interferometer (MZI) with delay time equal to half symbol period. The analytical model that describes our proposed system is developed. The effectiveness of employing RZ-4QAM and RZ-16QAM formats in AO-OFDM systems is successfully demonstrated by both analytical and simulation results. The impacts of subcarrier peak power and transition distance on error vector magnitude (EVM) are also studied. Our results reveal that significant improvements on the transmission performance of the AO-OFDM system are realized by adopting RZ-4QAM and RZ-16QAM as compared with 4QAM and 16QAM AO-OFDM system.

4.2.1 Effect of employing RZ-mQAM format on phase noise

In this subsection, an analytical model of nonlinear interaction between the optical signal and the nonlinear effects in RZ-QAM AO-OFDM system is developed to describe our RZ-QAM AO-OFDM system. To explore the efficiency of our technique in mitigating the nonlinear fiber impairments, RZ-QAM OFDM system is analytically compared with traditional QAM OFDM system.

In order to generate RZ-QAM formats, an optical RZ carver is used after the QAM modulator to shape the modulated signal. Practically, RZ-mQAM signal is optically generated by employing one MZM after mQAM modulator. This MZM is driven by a sinusoidal waveform with frequency equal to the symbol rate, $f_s = 1/T_s$. Therefore, the generated RZ-QAM signal has a sinusoidal-like envelope as shown in Figure 4.1. By assuming the transfer characteristic of MZM is linear and it is biased at quadrature point, the sinusoidal-like envelope is defined as:

$$EN(t) = \frac{1 - \cos(2\pi f_s t)}{2}. \quad (4.1)$$

The RZ-QAM subcarrier can be written as:

$$\begin{aligned} u_{k_{RZ-QAM}}(0,t) &= u_k(0,t)EN(t) \\ &= \frac{\sqrt{P}}{2\sqrt{2}} A_k \left[1 - \cos\left(\frac{2\pi t}{T_s}\right) \right]. \end{aligned} \quad (4.2)$$

After combining the subcarriers, the transmitted signal can be expressed as:

$$u(0,t) = \sum_{k=-(N-1)/2}^{(N-1)/2} u_k(0,t)EN(t)\exp(j\omega_k t). \quad (4.3)$$

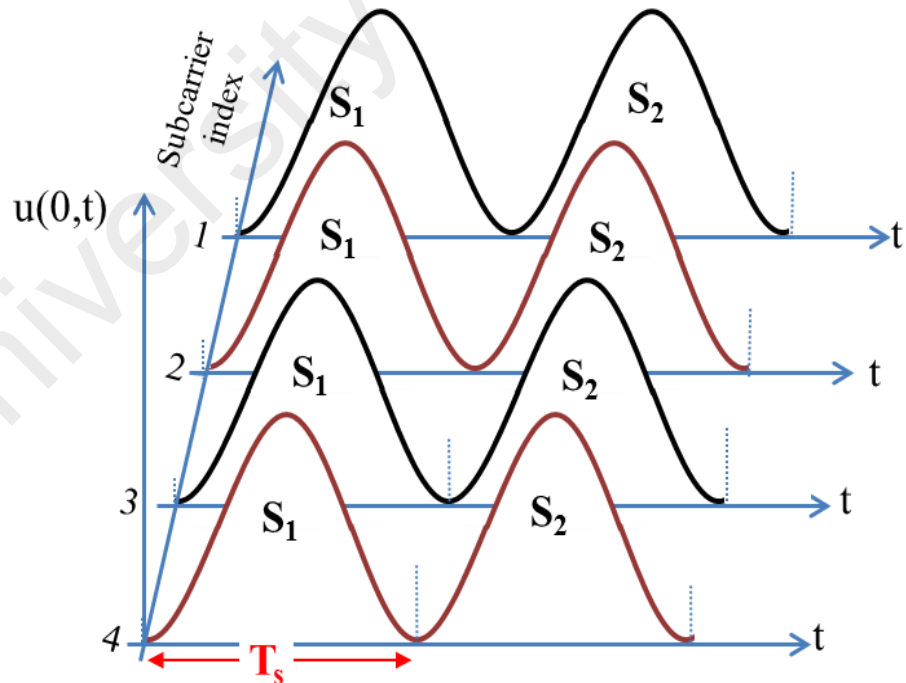


Figure 4.1: Optical fields of four subcarriers that modulated by RZ-QAM

The interaction between the OFDM subcarriers is governed by their envelope shape. The average interaction of two subcarriers can be expressed as follows. For any $k, i \in \{-(N-1)/2, -(N-1)/2+1, \dots, (N-1)/2\}$, we have;

$$\begin{aligned} \overline{u_k u_i} &= \frac{P}{8T_s} |A_k| |A_i| \int_0^{T_s} [1 - \cos(2\pi f_s t)] [1 - \cos(2\pi f_s (t))] dt \\ &= \frac{3P}{16} |A_k| |A_i|. \end{aligned} \quad (4.4)$$

It is clear that Eq. (4.4) represents the interaction of subcarriers for RZ-QAM OFDM system. On the other hand, the average interaction of two OFDM subcarriers that are modulated by traditional QAM format is given by $|u_k| |u_i| = \frac{P}{2} |A_k| |A_i|$. That is, the average interaction of RZ-QAM OFDM subcarriers is 3/8 that of QAM OFDM system.

For an OFDM system employing QAM modulation, $u_k(0, t) = \sqrt{P/2} A_k$, the XPM phase noise due to interaction of k th subcarrier with other subcarriers can be obtained by using Eq. (3.9) and written as:

$$\phi_{kXPM}(ML) = M \gamma P L_{eff}(L) \sum_{\substack{i=-(N-1)/2 \\ i \neq k}}^{(N-1)/2} |A_i|^2. \quad (4.5)$$

For the RZ-QAM OFDM system, the XPM phase noise can be modeled by substituting Eq. (4.11) in Eq. (3.9), and written as:

$$\phi_{kXPM}(ML) = \frac{3\gamma M L_{eff}(L) P}{8} \sum_{\substack{i=-(N-1)/2 \\ i \neq k}}^{(N-1)/2} |A_i|^2. \quad (4.6)$$

From Eq. (4.6), it is clear that the XPM phase noise that produced by RZ-QAM is reduced as compared to that produced in QAM OFDM system.

Another important phase noise occurs in links that include optical amplifiers. The optical amplifiers are employed to compensate the power degradation of the optical signal due to fiber attenuation. At the output of each amplifier, an amplified spontaneous emission (ASE) noise field is added to each subcarrier. The interactions of XPM and FWM with ASE noise produce random nonlinear phase noises. These phase noises may generate deterministic as well as stochastic impairments. Furthermore, the interaction of fiber Kerr nonlinearity with ASE noise cannot be compensated in receivers by digital backward propagation or other electrical compensating techniques (Zhu & Kumar, 2010). For RZ-QAM OFDM system, the phase noise variance due to interaction of XPM with ASE can be determined by substituting Eq. (4.4) in Eq. (3.10) and we get:

$$\sigma_{\phi_{XPM}}^2 (ML) = \frac{3M(M+1)}{4} \gamma^2 L_{eff} (L)^2 P \sum_{\substack{i=-(N-1)/2 \\ i \neq k}}^{(N-1)/2} |A_i|^2 \sigma_i^2. \quad (4.7)$$

The effect of employing RZ-mQAM technique is clear in reducing the nonlinear phase noise variance. By comparing between Eq. (4.7) and Eq. (3.11), the phase noise variance for RZ-mQAM system is 3/8 times the phase noise variance of mQAM OFDM system.

In order to investigate the effectiveness of RZ-mQAM technique on the phase noise variance due to interaction of ASE noise and FWM, we substitute Eq. (4.4) in Eq. (3.17). The phase noise variance for k th subcarrier in RZ-mQAM OFDM system can be expressed as:

$$\sigma_{\phi_{kFWM}}^2 (ML, \delta) = \frac{16M \sigma_k^2}{3PA_k^2} + \frac{3 \gamma^2 P}{4 A_k^2} \times \sum_{m=1}^M \sum_{\substack{h=-(N-1)/2 \\ h \neq k}}^{(N-1)/2} \sum_{\substack{i=-(N-1)/2 \\ l=h+i-k \\ i \neq l}}^{(N-1)/2} L_{FWM} \left\{ |A_h|^2 |A_i|^2 \sigma_l^2 + |A_h|^2 |A_l|^2 \sigma_i^2 + |A_i|^2 |A_l|^2 \sigma_h^2 \right\}. \quad (4.8)$$

By comparing first part of Eq. (4.8) with first part of Eq. (3.17), it is clear that the effect of ASE noise on the RZ-QAM signal is higher than its effect on the mQAM OFDM signal. This phenomenon is because RZ-QAM has lower pulse width than QAM signal. Whilst, second part of Eq. (4.8) reveals that the phase noise variance due to interaction of FWM with ASE noise is reduced as compared with second part of Eq. (3.17) that represent phase noise variance due to interaction of FWM with ASE noise in mQAM AO-OFDM system.

4.2.2 Effect of RZ-mQAM on power of FWM

The FWM effect plays a significant role to degrade the performance of AO-OFDM systems due to high number of subcarriers and low frequency spacing between them. The power of FWM noise is directly related to the power of subcarriers (Arthur J Lowery et al., 2007). Furthermore, the FWM process is phase sensitive and it is strongly dependent on the interaction time among the subcarriers. Accordingly, the shape of the modulating signal governs the power of FWM. Therefore, changing the signal envelope can be applied to suppress the impact of FWM on the performance of AO-OFDM systems.

For transmitting OFDM signal over long fiber link with many optical amplifiers, the power of FWM, P_{hil} , that produced by product three optical subcarriers with

frequencies of ω_h , ω_i , ω_l and optical powers P_h , P_i , P_l , can be expressed by (S. T. Le et al., 2014):

$$P_{hil} = \frac{D_N^2}{9} \gamma^2 L_{eff}^2 \eta P_h P_i P_l, \quad (4.9)$$

where, D_N is the degeneracy factor which equals 6 for non-degenerated (NDG) products and 3 for degenerated (DG) products and η is the FWM coefficient, which strongly depends on the relative frequency spacing between the FWM components and does not depend on the power of OFDM subcarriers (Inoue, 1992; S. T. Le et al., 2014). It is well known that the power of QAM signals are constant over symbol period, in which $P_h = P_i = P_l = P$. Eq. (4.9) can be rewritten as:

$$P_{hil(QAM)} = \frac{D_N^2}{9} \gamma^2 L_{eff}^2 P^3 \eta. \quad (4.10)$$

From Eq. (4.10), the power of FWM is proportional to the cube of power of QAM subcarrier. Therefore, the power of FWM can be efficiently reduced by decreasing the average power of QAM subcarriers. The average power of QAM subcarriers can be lowered by reshaping the QAM subcarriers using RZ carver. Thus, the average power of RZ-4QAM signal can be expressed as:

$$P_k = \frac{P}{4T_s} \int_0^{T_s} \left[1 - \cos\left(\frac{2\pi t}{T_s}\right) \right]^2 dt = \frac{3}{8} P \quad (4.11)$$

where $P_k, k \in \{h, i, l\}$ is the power of subcarrier. By substituting Eq. (4.11) in Eq. (4.9), the power of FWM can be written as:

$$P_{hil(RZ-QAM)} = \frac{3D_N^2}{512} \gamma^2 L_{eff}^2 P^3 \eta \quad (4.12)$$

By comparing Eq. (4.10) with Eq.(4.12), the power of FWM for RZ-QAM subcarriers is reduced to $(3/8)^3$ of that for QAM subcarriers.

4.2.3 AO-OFDM system setup

The setup of proposed AO-OFDM system is shown in Figure 4.2. The configuration of AO-OFDM transmitter is similar to that in Section 3.2. It uses RZ-QAM modulators instead of QAM modulators to generate RZ-QAM OFDM signal. Each subcarrier can be modulated with RZ-mQAM format by employing one RZ carver after each QAM modulator. RZ-mQAM OFDM signals is produced after combining modulated subcarriers by optical multiplexer. Then, resultant signal is launched into alternate fiber spans. Each fiber span includes SSMF, optical amplifier and DCF. The SSMF is modeled with an attenuation coefficient of 0.2 dB/km, $D = 16$ ps/nm/km, an effective area of $80 \mu\text{m}^2$, and fiber nonlinearity of $1.3 \text{ W}^{-1} \text{ km}^{-1}$. The attenuation is fully compensated by employing Erbium doped fiber amplifier (EDFAs) at spans of spacing 55 km, each. The noise figure of each optical amplifier is set to 6 dB. To maintain the data transmission ability of AO-OFDM system, the dispersion is optically compensated by DCF. In each span, the dispersion is fully compensated by the DCF with a chromatic dispersion coefficient of $D = -160$ ps/nm/km.

AO-OFDM receiver, which is explained in the Section 3.2, is modified to receive the RZ-mQAM OFDM signal by adding four MZIs before the demultiplexers as shown in Figure 4.2. These interferometers are able to convert the received RZ-mQAM signal

into mQAM signal. In AO-OFDM system, the gating is essential to complete the processing of the all-optical fast Fourier transform (OFFT). By using the RZ pulse, the time slot for optimum gating becomes shorter, making the gating more difficult. To cope with this problem, we have employed four MZIs at receiver to convert the received signal into mQAM as shown in Figure 4.2. The delay time between the arms of the MZI is set at $T_s/2$ so that each symbol can interfere with its delayed replica. This allows the RZ signal to be converted to mQAM signal at the constructive port.

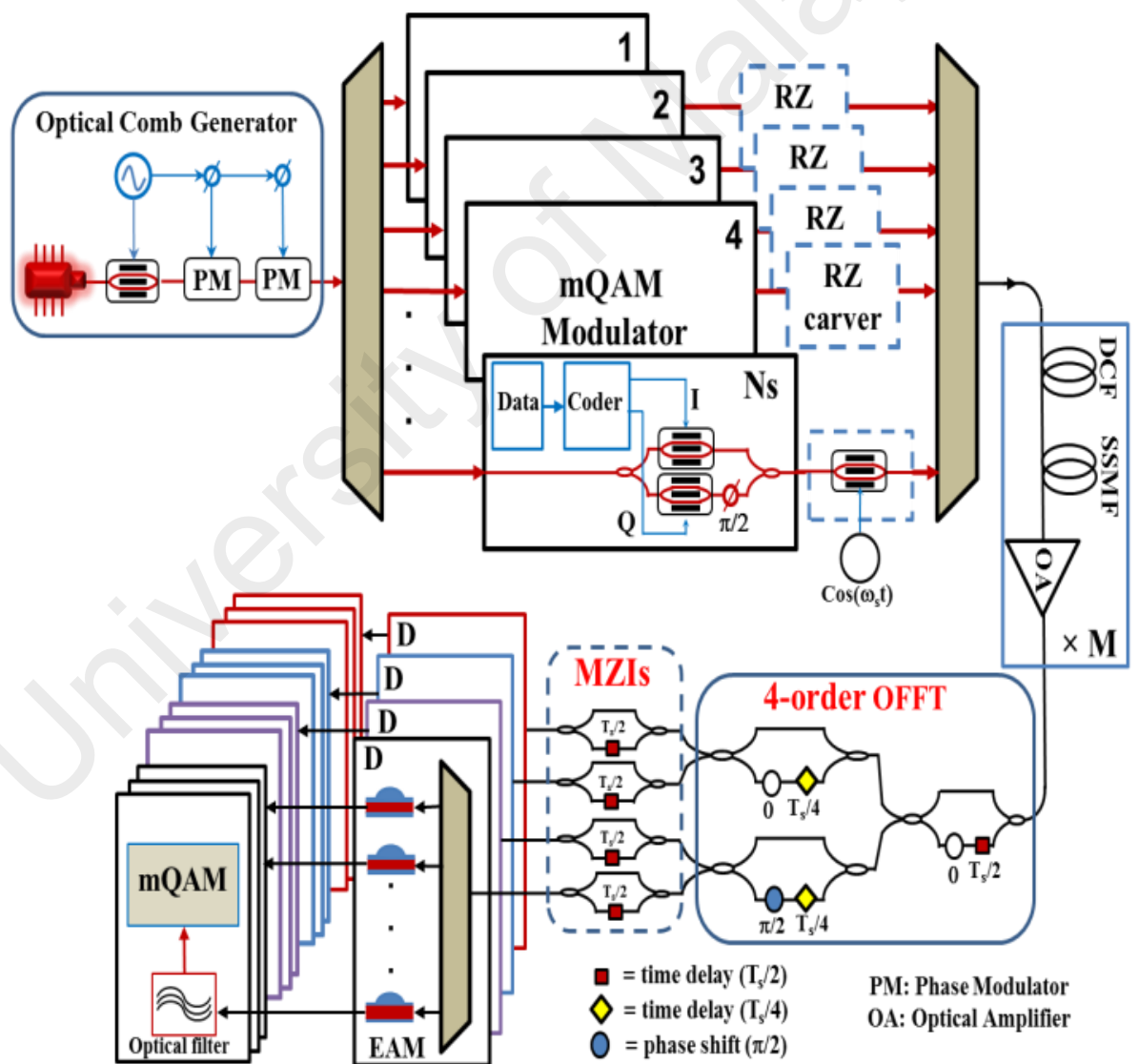


Figure 4.2: The setup of proposed system.

To explain the operation of added MZIs analytically, we assume that the transmitted signal is directly launched to the receiver (back-to-back). Then the optical envelope of single subcarrier at the constructive port can be described by the following equation:

$$\begin{aligned} u_k &= \frac{\sqrt{P}}{4\sqrt{2}} A_k \left\{ [1 - \cos(2\pi f_s t)] + [1 - \cos(2\pi f_s (t - T_s / 2))] \right\} \\ &= \frac{\sqrt{P}}{2\sqrt{2}} A_k. \end{aligned} \quad (4.13)$$

From the last equation, it is shown that this conversion keeps the time slot for optimum gating at normal frequency since the mQAM signals is recovered before sampling process.

To illustrate the conversion process by aiding the numerical simulation, the generated RZ-4QAM signal is applied to an MZI. The output of MZI is directly detected by a signal analyzer as shown in Figure 4.3. It is clear that the eye diagrams of I and Q of RZ-4QAM signal have sinusoidal shape. The eye diagrams of signal after the interferometer show that the MZI with time delay of $T_s/2$ converts the RZ-4QAM signal to 4QAM signal by interfering the signal and its delayed replica.

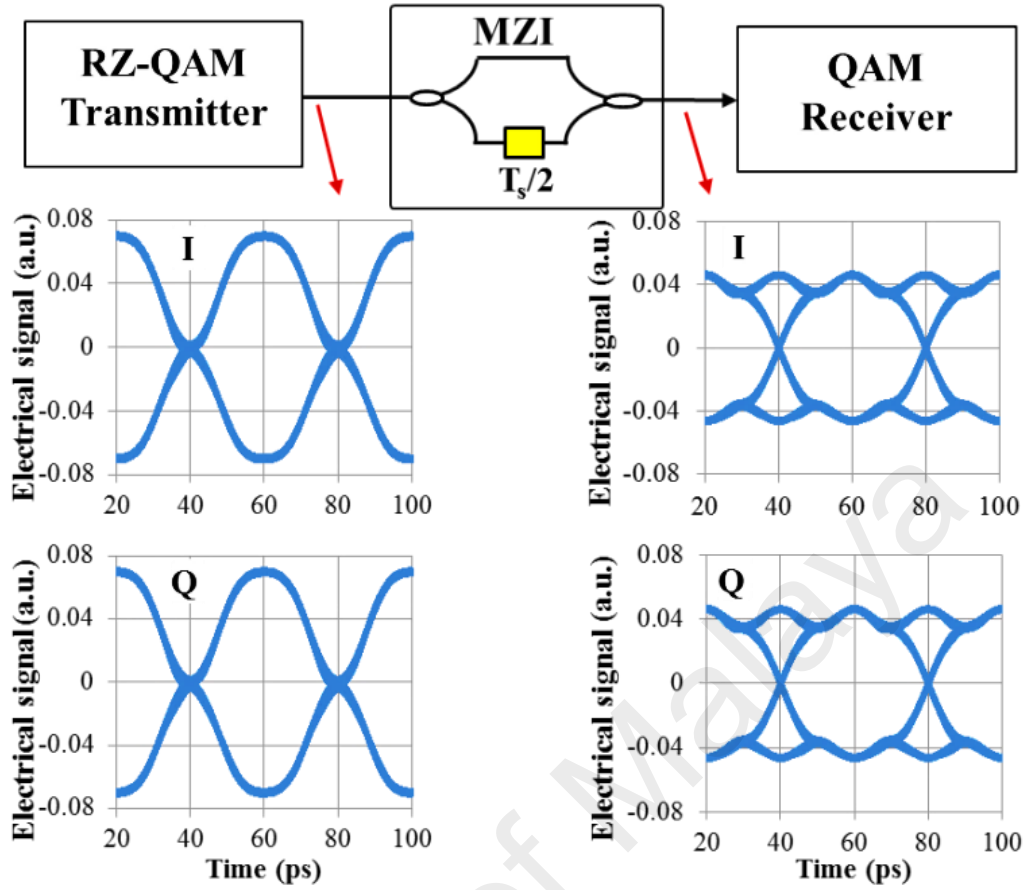


Figure 4.3: Conversion of RZ-4QAM signal to 4QAM signal by employing an MZI with delay time of $T_s/2$.

4.2.4 Results and discussion

In this subsection, we explore the efficiency of employing RZ-mQAM format for mitigating nonlinear phase noise in AO-OFDM systems. Next, the performance improvement of proposed system is demonstrated and compared with performance of the traditional QAM AO-OFDM system.

4.2.4.1 Impact of employing RZ-QAM format on phase noise

Figure 4.4 shows the influence of employing RZ-4QAM format in AO-OFDM system on the mitigation of phase noise. The results are obtained for 29 subcarriers at a transmission distance of 550 km. In Figure 4.4 (a), the phase noise variances of XPM, FWM, and ASE noise are individually plotted against power of subcarrier. At low fiber launch power, the phase noise variance is mainly produced by the ASE noise because optical signal-to-noise ratio (OSNR) is low. In general, when increasing the power of subcarrier, the phase noise variance due to the amplifier noise is decreased whereas the phase noise variances due to both XPM and FWM are increased. It can also be observed that the phase noise variances due to both FWM and XPM in RZ-4QAM AO-OFDM system are significantly reduced as compared to that of QAM OFDM system. However, the phase noise variance due to ASE noise is increased when employing RZ-QAM format because the OSNR is low for RZ pulses. For example, at a subcarrier power of 5 dBm, the phase noise variance due to FWM is reduced from 0.0275 rad^2 for QAM OFDM system to 0.006 rad^2 for RZ-QAM OFDM system. In addition, at the same power level, the phase noise variance of XPM is mitigated by ~65% when the RZ-4QAM format is adopted in AO-OFDM system. Figure 4.4 (b) shows the total phase noise variances of RZ-4QAM AO-OFDM system and traditional 4QAM AO-OFDM system versus the power of subcarrier. It can be seen that the optimum power level is increased from -3 dBm for QAM OFDM system to 1 dBm for the proposed system. That mean, the proposed system has lower phase noise variances at higher launch powers compared with that of 4QAM OFDM system. This can be explained by the average interaction between the subcarriers is lower. Furthermore, the presented simulation results show good agreement with analytical results.

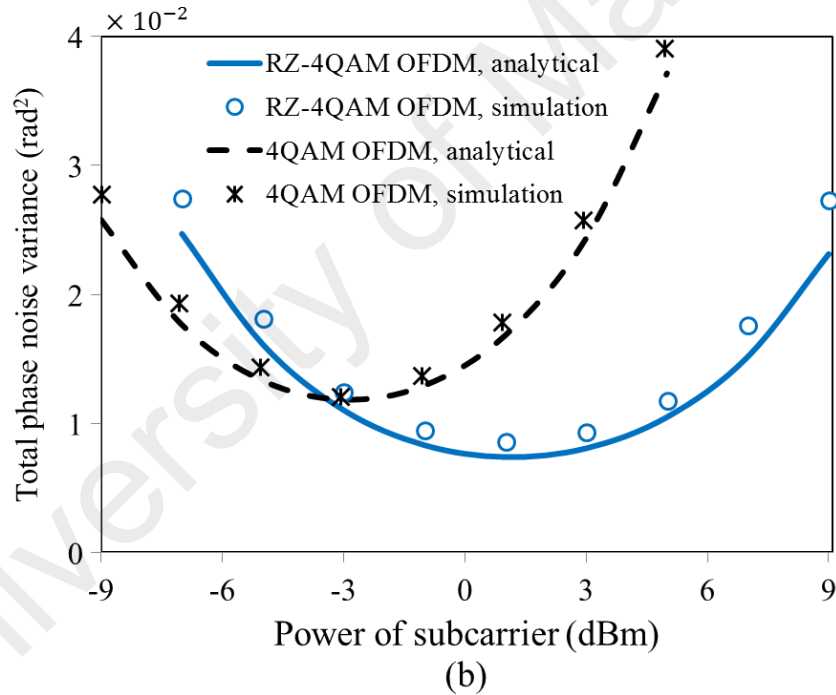
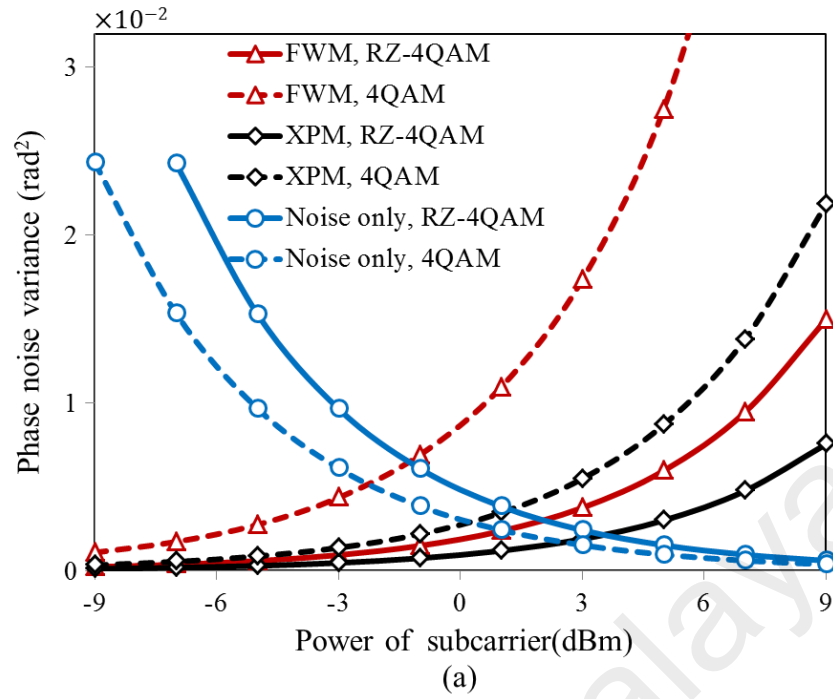


Figure 4.4: Influence of employing RZ-4QAM format on the phase noise reduction, a) details of phase noise, b) total phase noise variance.

Same observation can be seen in Figure 4.5 when the RZ-16QAM format is employed by AO-OFDM system. As expected, the phase noise variances due to XPM and FWM in proposed system are decreased as compared with traditional system.

Whilst the phase noise variance due to ASE noise is increased. Figure 4.5(b) shows the total phase noise variance at optimum power level is reduced and the optimum power level is raised to 3 dBm for RZ-16QAM AO-OFDM system.

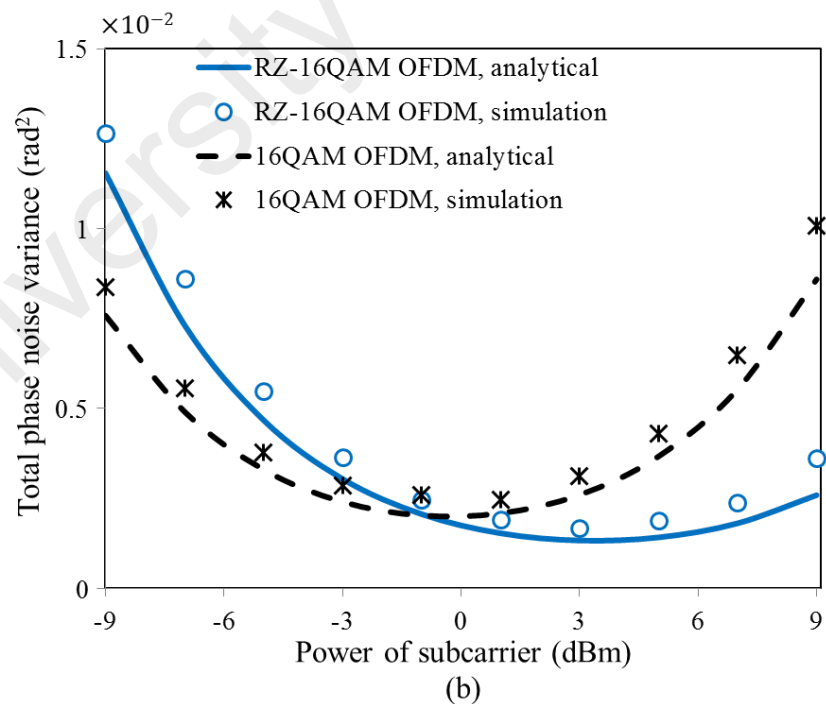
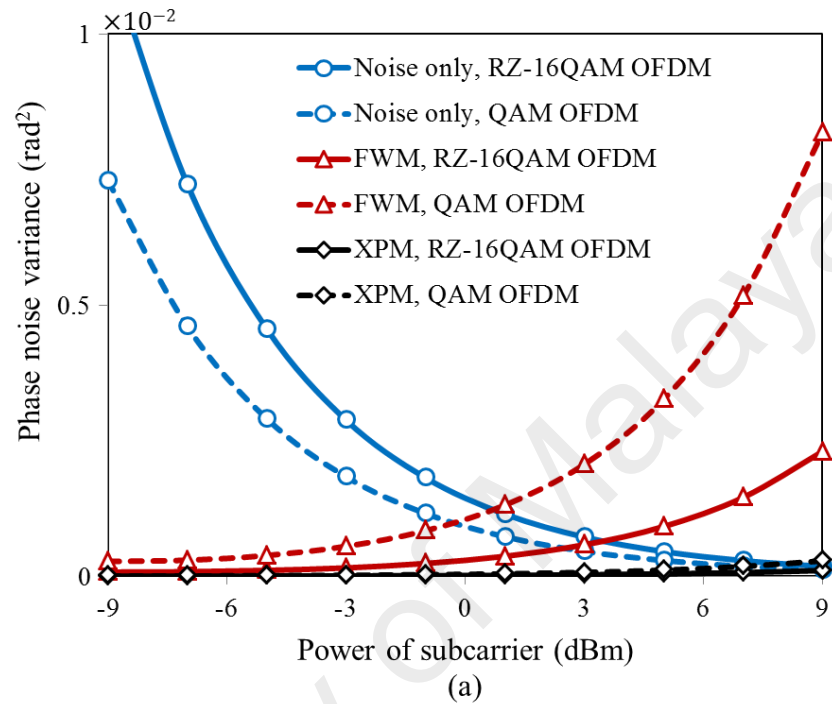


Figure 4.5: Influence of employing RZ-16QAM format on the phase noise reduction, a) details of phase noise, b) total phase noise variance.

4.2.4.2 Performance analysis of the proposed system

In this subsection, we examine the effect of employing RZ-4QAM and RZ-16QAM on the transmission performance of AO-OFDM systems. To investigate the performance improvement of proposed system, a comparison with performance of traditional QAM OFDM system is numerically demonstrated. The system setup in Figure 4.2 is numerically simulated by step-split Fourier method using VPItransmissionMaker 9.0. Each subcarrier is modulated at the symbol rate of 25 Gsymbol/s. To investigate the phase noise mitigation, EVM versus the subcarrier power and transmission distance are obtained. Furthermore, bit error rate (BER) is plotted against transmission distance and OSNR for exploring the performance of the system.

In order to show the effect of combinations RZ with 4QAM and 16QAM in AO-OFDM systems on the EVM, we first vary the subcarrier power and measure the EVM. The magnitude of EVM is mainly depends on the phase noise of SPM, XPM, and FWM. Figure 4.6(a) depicts EVM as a function of the subcarrier power for both RZ-4QAM and 4QAM AO-OFDM systems. The transmission distance and the number of subcarriers are fixed at 550 km and 29 subcarriers, respectively. Generally, EVM for RZ-4QAM and 4QAM modulation formats is initially decreased with raising the power of subcarrier since the phase noise due to the interaction of ASE noise being dominant at low powers. However, when subcarrier power increases beyond 1 dBm and -3 dBm for RZ-QAM and QAM, respectively, EVM is increased too. This is because the phase noises due to XPM and FWM and their interaction with ASE noise become dominant at higher powers. By comparing with 4QAM AO-OFDM system, RZ-4QAM AO-OFDM has lower EVM for subcarrier power greater than -3 dBm. Further, the minimum EVM is reduced from 0.127 to 0.107 by employing RZ-4QAM format instead of 4QAM format in AO-OFDM system.

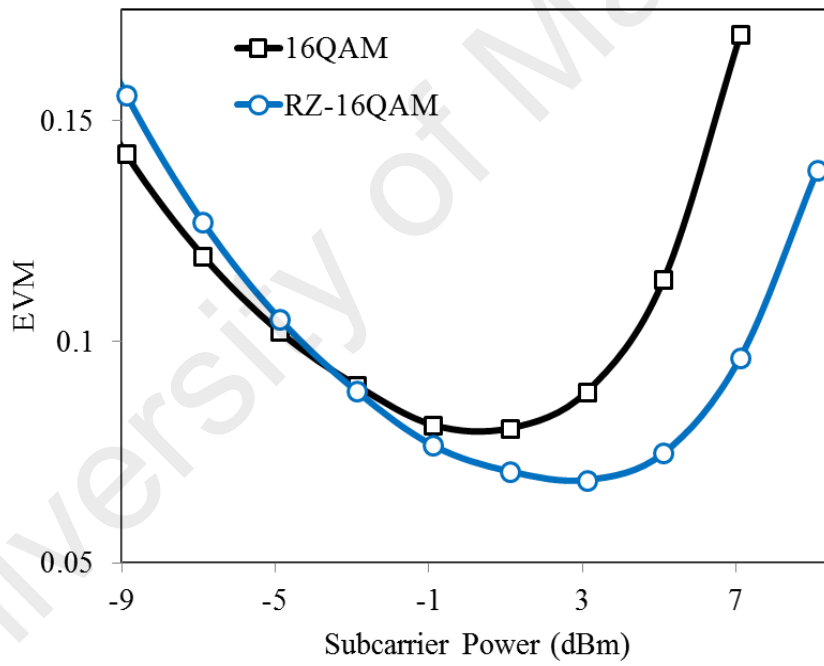
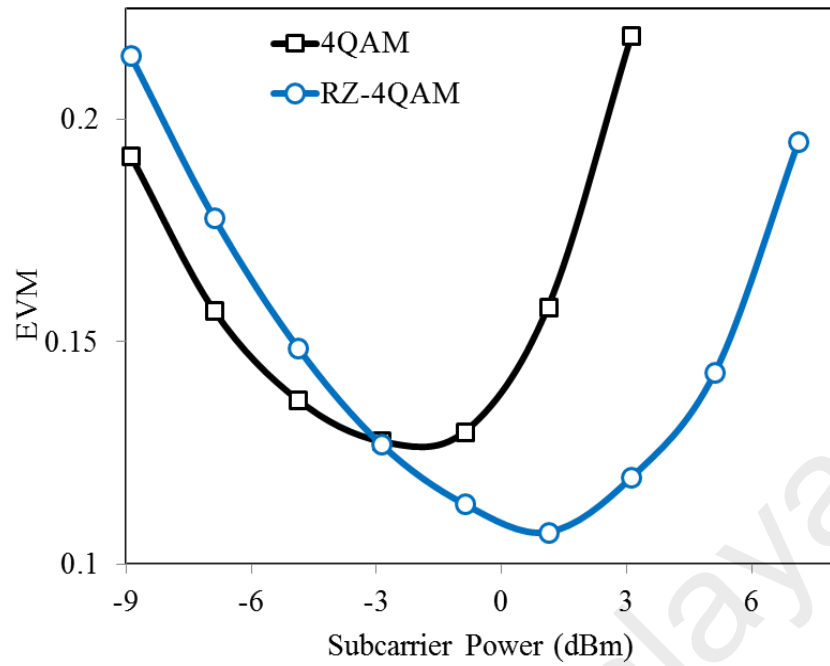
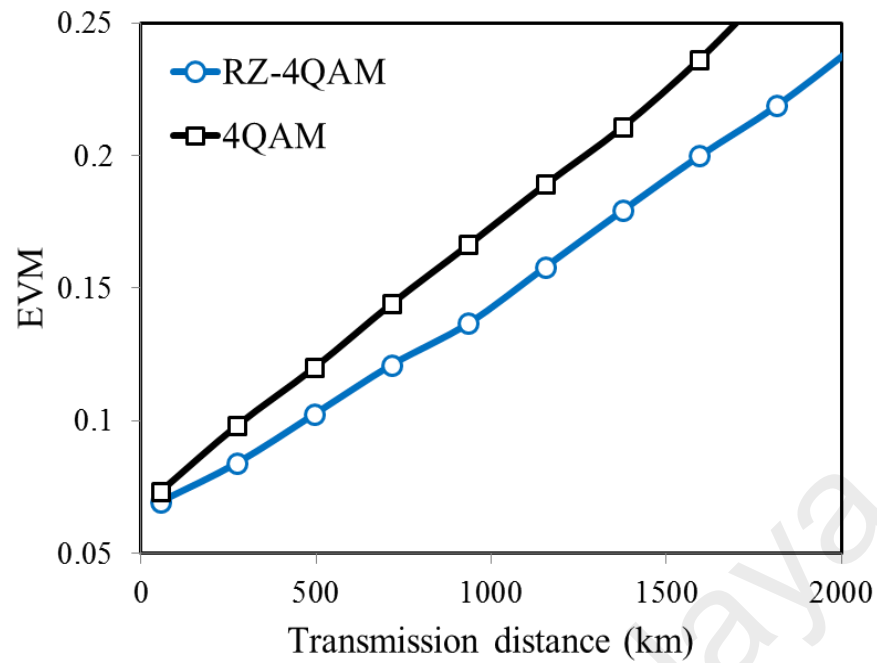


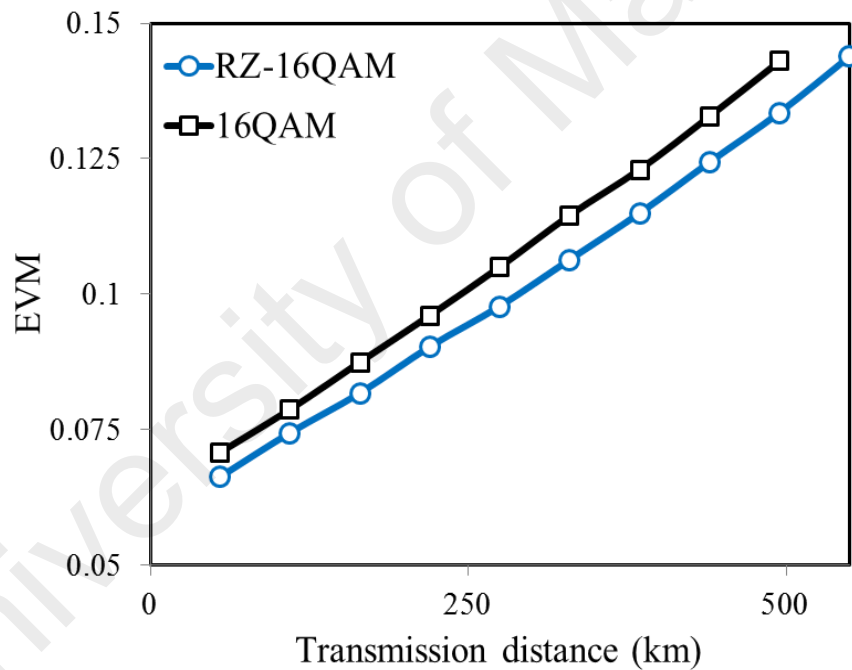
Figure 4.6: Effect of combination RZ with mQAM in AO-OFDM systems on the EVM, a) RZ-4QAM and 4QAM, b) RZ-16QAM and 16QAM.

Impact of using RZ-16QAM format on the EVM of AO-OFDM system is investigated as shown in Figure 4.6(b). EVM versus power of subcarriers of both RZ-16QAM and 16QAM AO-OFDM systems are compared to clarify the benefit of RZ-16QAM. During simulation, the transmission distance and the number of subcarriers are fixed at 165 km and 29 subcarriers, respectively. Similar to employing RZ-4QAM format, the EVM for RZ-16QAM format is lower than that for 16QAM format for power greater than -3 dBm. Moreover, the minimum EVMs are occurred at subcarrier powers of 3 dBm and -1 dBm for RZ-16QAM and 16QAM formats, respectively. This phenomenon due to the phase noise depends on average interaction among subcarriers. At a certain number of subcarriers and symbol rate, mQAM signal has lower peak power than RZ-mQAM signal, but RZ-mQAM signal has shorter interaction time than QAM signal.

Figure 4.7(a) shows EVM versus the transmission distance for RZ-4QAM and 4QAM AO-OFDM systems. At optimum powers of each modulation format, the EVMs are measured for transmission distance of 550 km (10 spans). We can see that the EVM linearly increases with increasing fiber length. Furthermore, the EVM of the proposed system is lower for all transmission distances as compared with 4QAM OFDM system. Similarly, EVM of RZ-16QAM format is less than EVM of 16QAM format as shown in Figure 4.7(b). Generally, the mitigation of phase noise is more efficient with increasing transmission distance. This phenomenon due to the effect of the dispersion becomes high on the RZ-QAM and leads to increase the mismatch phase between subcarriers. Furthermore, the average interaction between subcarriers is shorter with employing RZ-mQAM.



(a)



(b)

Figure 4.7: EVM versus transmission distance, a) RZ-4QAM and 4QAM b) RZ-16QAM and 16QAM.

Figure 4.8 (a) and Figure 4.8(b) show the constellation diagrams of the 4QAM and RZ-4QAM OFDM signals, respectively. These constellations are obtained at output of 4QAM receiver. The ideal constellation is plotted by red square. Both diagrams are

simulated for the transmission distance of 550 km and 29 subcarriers. It is shown that the RZ-4QAM signal produces a clearer constellation diagram compared to that of the conventional 4QAM one. In Figure 4.8(c) and Figure 4.8(d), we observe the similar trend for 16QAM and RZ-16QAM OFDM signals where the constellation diagram of RZ-16QAM signal is squeezed. The constellations are achieved for the same number of subcarriers and transmission distance of 165 km.

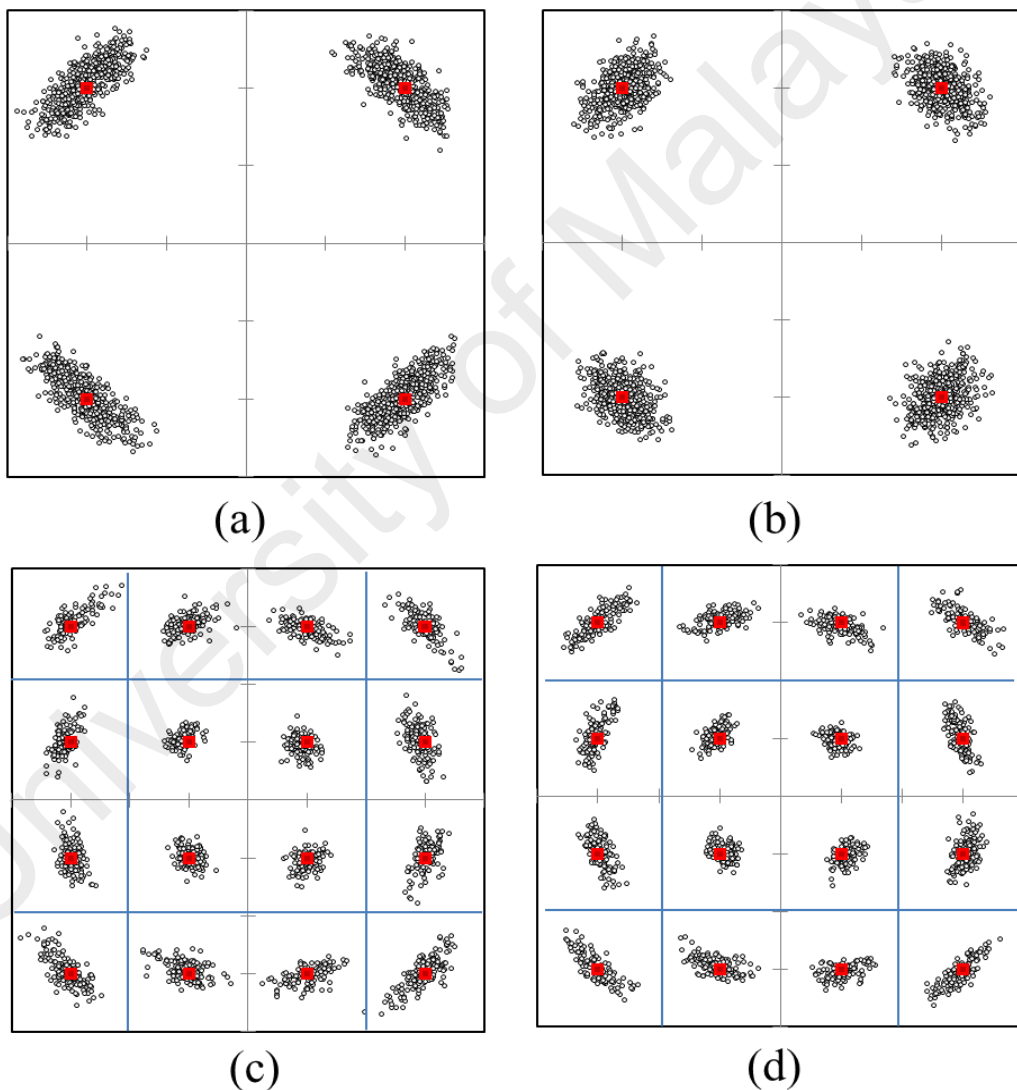
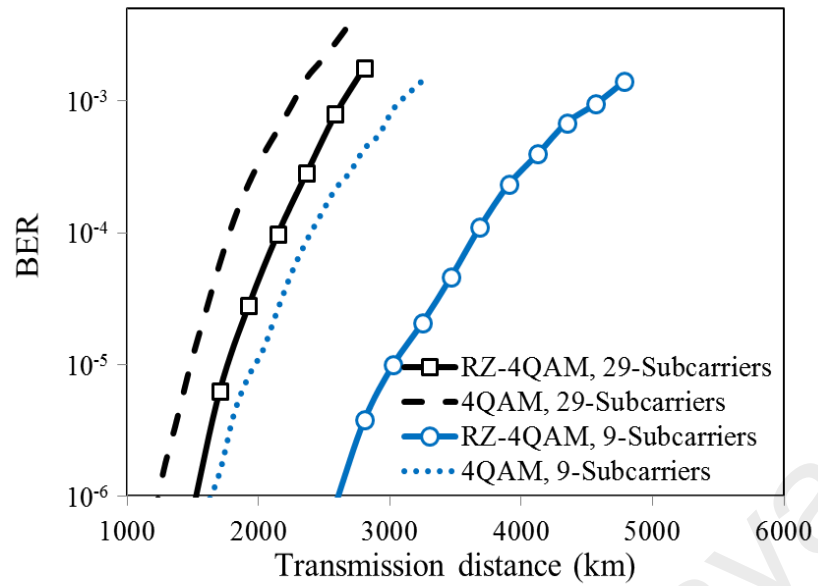


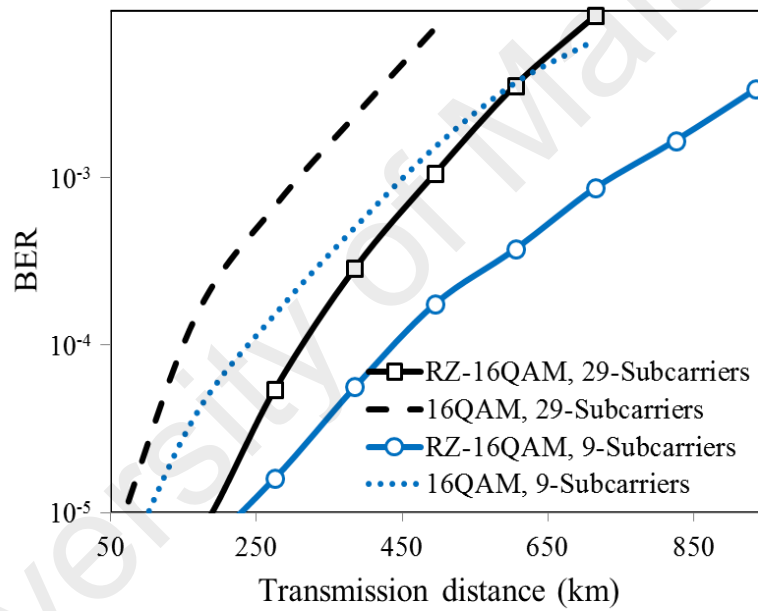
Figure 4.8: The constellation diagrams of (a) 4QAM, (b) RZ-4QAM, (c) 16QAM, (d) RZ-16QAM.

In optical OFDM transmissions, the phase noise is related to the subcarriers number since the interaction between subcarriers depends on their number such as XPM and FWM. For that reason, we numerically compared the subcarriers number dependence of AO-OFDM system performance. Figure 4.9 depicts the relation between BER and the transmission distance for 9 and 29 subcarriers. For each transmission distance, the corresponding subcarrier power that gives minimum EVM is adopted. Referring to Figure 4.9(a), the performance of AO-OFDM system that employs RZ-4QAM modulation format is superior to the performance of traditional 4QAM AO-OFDM system along transmission distance for both subcarriers numbers. In addition, the proposed system performance is highly improved with 9 subcarriers where it is able to transmit the data over 3300 km fiber length, representing a 62% increase compared to the 4QAM OFDM system.

The higher-order modulation formats such 16QAM require more OSNR to overcome the phase noise. Accordingly, the transmission distances are substantially reduced when employing 16QAM or the RZ-16QAM format in AO-OFDM signal as shown in Figure 4.9(b). As expected, at BER of 1×10^{-5} and 29 subcarriers, the transmission distance is increased from 55 km for 16QAM format to 220 km for RZ-16QAM format. Furthermore, with 9 subcarriers and at same BER, the transmission distance is expanded to 275 km, representing a 150% increase compared to the 16QAM OFDM system. However, both 16QAM and RZ-16QAM OFDM systems is limited by laser phase noise. Generally, in coherent communication systems, the laser phase noise plays significant role in the degradation of system performance (Yi et al., 2008). Therefore, BER floor is apparent in the Figure 4.9(b).



(a)



(b)

Figure 4.9: Bit rate error versus transmission distance at symbol rate of 25 Gsymbol/s, a) 4QAM and RZ-4QAM, b) 16QAM and RZ-16QAM.

Finally, the comparison between the receiver sensitivities for both RZ-mQAM and mQAM signals is carried out to explore the efficiency of proposed technique. Figure 4.10(a) illustrates BER versus OSNR for RZ-4QAM and 4QAM AO-OFDM systems for subcarriers numbers of 9 and 29. The sensitivity of RZ-4QAM and 4QAM AO-OFDM receivers is examined at a symbol rate of 25 Gsymbol/s and transmission distance of 550 km (10 spans). It can be seen that RZ-4QAM AO-OFDM system has a better BER performance for both subcarriers numbers. The required OSNR to obtain a BER of 1×10^{-5} is reduced by 1.5 dB for 9 subcarriers. The BER as a function of OSNR for RZ-16QAM and 16QAM AO-OFDM systems is shown in Figure 4.10(b). The sensitivity of RZ-16QAM and 16QAM AO-OFDM receivers is tested at a symbol rate of 25 Gsymbol/s and transmission distance of 165 km (3 spans). It can be observed that the performance of AO-OFDM system is also improved by employing the RZ-16QAM format as compared with 16QAM format.

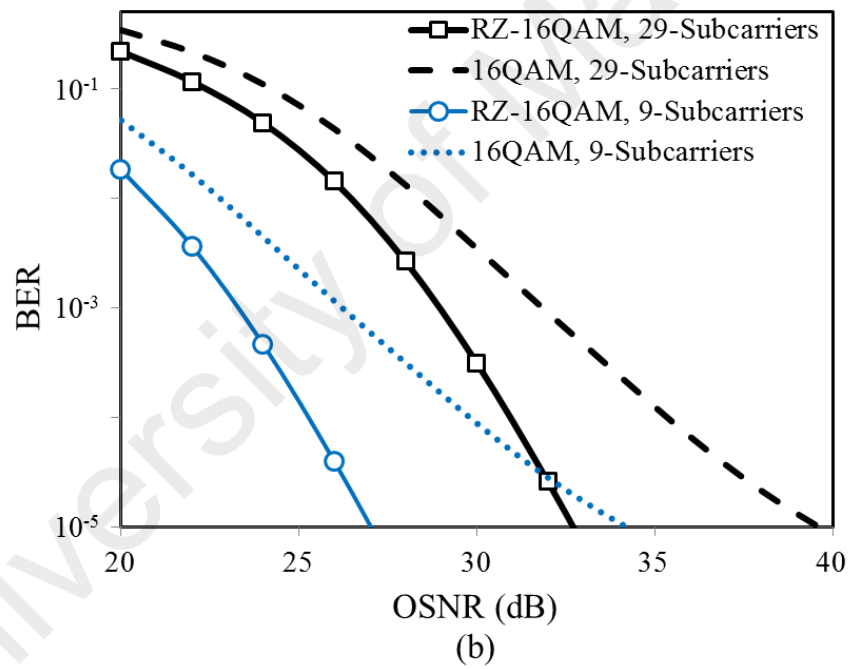
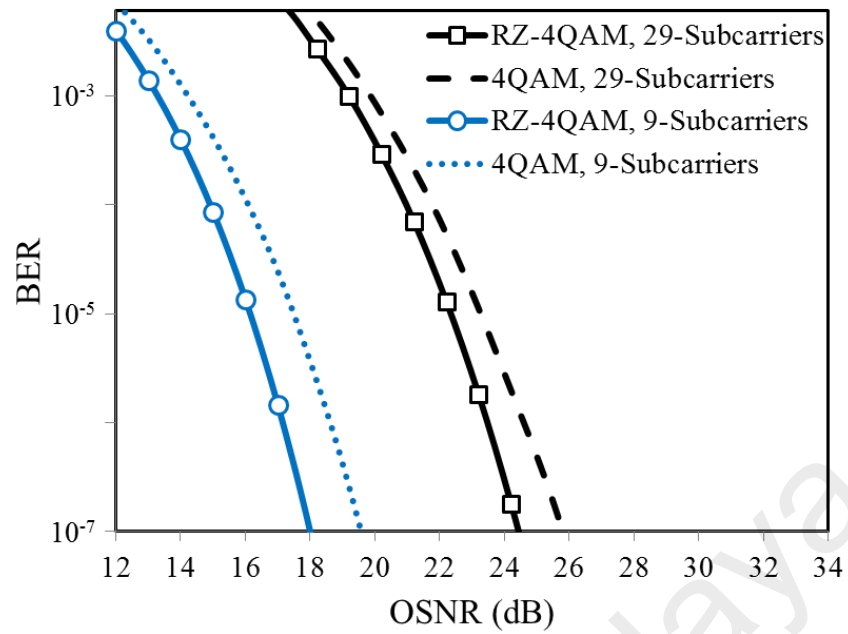


Figure 4.10: Performance comparison of AO-OFDM that employ: a) RZ-4QAM and 4QAM, b) RZ-16QAM and 16QAM.

4.3 Mitigation of phase noise in AO-OFDM systems based on minimizing interaction time between subcarriers

Various schemes have been reported to mitigate the nonlinear phase noise in multichannel systems based on reducing the interaction between subcarriers. Among them, polarization interleaving method has been employed (Tripathi et al., 2007; D van den Borne et al., 2005). However, polarization interleaving is highly sensitive to PMD and polarization dependent loss. The dispersion interleaving method has been proposed to reduce the interface between adjacent channel interference in wavelength division multiplexing (WDM) techniques (Khurgin et al., 2004). This method utilizes the residual fiber dispersion to mitigate the interference of adjacent channels. Furthermore, the interleaved OFDM has been proposed to reduce the peak-to-average power ratio (PAPR) and phase noise (Cao et al., 2014; Long et al., 2012). However, the half subcarriers are reserved and the transmission capacity of the system is reduced.

In this section, we propose a new approach for mitigating the phase noise by minimizing the interaction time between subcarriers. This is accomplished by shaping the envelopes of QAM subcarriers and making delay times among successive subcarriers. After each QAM modulator, a MZM is employed to reshape QAM signals and produce RZ-QAM signals with envelopes of cosine shapes. When optical time delayers are inserted in even subcarriers paths, the odd and even subcarriers are alternately delayed (AD) and AD RZ-QAM OFDM signals are produced. The dispersion-managed transmission fiber link is employed to minimize the effect of dispersion on AD RZ-QAM OFDM signal. To keep the time slot for optimum gating at normal frequency, RZ-QAM is converted to QAM before the sampling process by utilizing MZI with delay time equal to half the symbol period (see Section 4.2.3). Our analytical model and results reveal that the optimum delay time is equal to half the

symbol duration, where the phase noise due to both XPM and FWM are reduced to 1/4 and 1/8 of that of traditional QAM OFDM systems, respectively. It is found that the performance of the proposed system is superior to AO-OFDM systems that adopt QAM techniques.

4.3.1 Analytical model of the proposed system

In this section, we provide an analytical model that best describes our AD RZ-QAM AO-OFDM system. A comparison with traditional QAM OFDM systems is analytically presented to explore the efficiency of proposed phase noise mitigation. Generally, the nonlinear phase noise is caused by fiber Kerr nonlinearity such as SPM, XPM, and FWM (Zhu & Kumar, 2010). Moreover, the ASE noise due to optical amplifiers adds a random nonlinear phase noise that mainly affects the SPM, XPM, and FWM phenomena (S. T. Le et al., 2014). The analytical model of nonlinear interaction between the optical signal and the nonlinear effects in AD RZ-QAM AO-OFDM system is derived in this section.

In our proposed system, the subcarriers are individually modulated by RZ-QAM modulators. After that, the subcarriers that have an even index are delayed from odd subcarriers by time delay δ as shown in Figure 4.11. After combining the subcarriers, the transmitted signal can be expressed as:

$$u(0,t) = \sum_{k \in \mathcal{O}} u_k(0,t)EN(t)\exp(j\omega_k t) + \sum_{k \in \mathcal{E}} u_k(0,t-\delta)EN(t-\delta)\exp[j\omega_k(t-\delta)] \quad (4.14)$$

where, $\mathcal{O} = \{-(N-1)/2+1, -(N-1)/2+3, \dots, (N-1)/2-1\}$ and
 $\mathcal{E} = \{-(N-1)/2, -(N-1)/2+2, \dots, (N-1)/2\}$. We define the odd and even subcarriers
as:

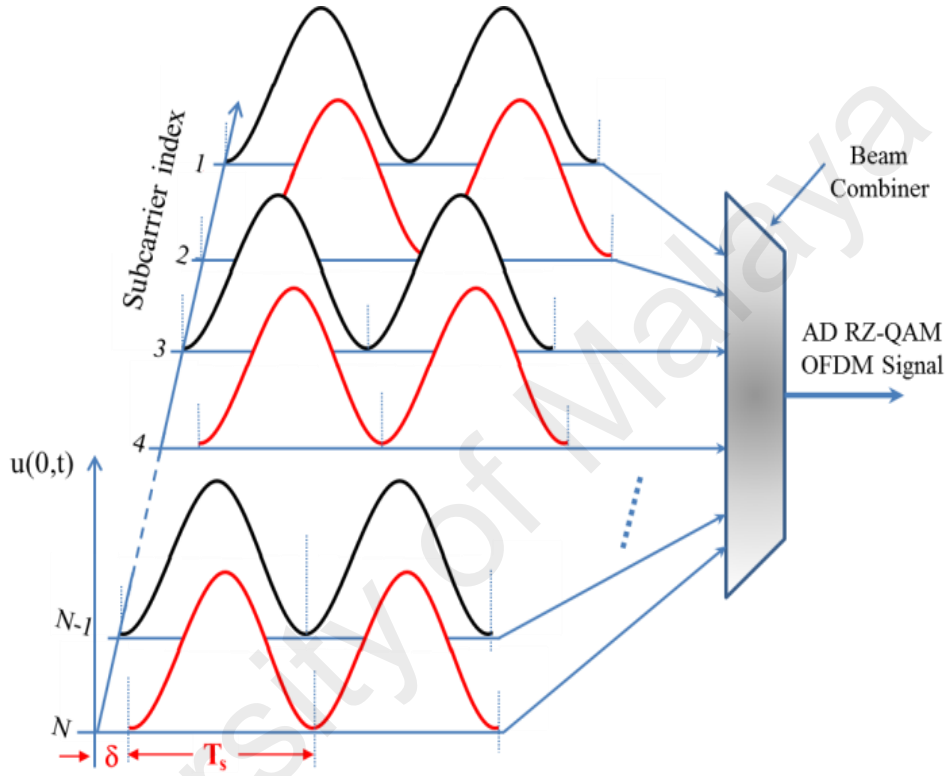


Figure 4.11: Illustration of proposed odd and even subcarriers. δ is the delay time and T_s is the symbol period.

$$\begin{aligned} u_{ok}(0,t) &= u_k(0,t)EN(t), & k \in \mathcal{O} \\ u_{ek}(0,t) &= u_k(0,t-\delta)EN(t-\delta), & k \in \mathcal{E} \end{aligned} \quad (4.15)$$

respectively. The interaction between odd and even subcarriers is governed by both their envelope shape and delay time between them. The average interaction of odd and even subcarriers can be expressed as follows. For any $k \in \mathcal{O}, i \in \mathcal{E}$, we have

$$\begin{aligned}
|u_{ok}||u_{ei}| &= \frac{P}{8T_s} |A_k||A_i| \int_0^{T_s} [1 - \cos(2\pi f_s t)][1 - \cos(2\pi f_s (t - \delta))] dt \\
&= \frac{P}{16} |A_k||A_i| [2 + \cos(2\pi f_s \delta)].
\end{aligned} \tag{4.16}$$

Similarly, the average interaction between odd and odd subcarriers or even and even subcarriers can be written as:

$$\begin{aligned}
|u_{ok}||u_{oi}| &= \frac{P}{8T_s} |A_k||A_i| \int_0^{T_s} [1 - \cos(2\pi f_s t)][1 - \cos(2\pi f_s (t)))] dt \\
&= \frac{3P}{16} |A_k||A_i|, \\
|u_{ek}||u_{ei}| &= \frac{3P}{16} |A_k||A_i|.
\end{aligned} \tag{4.17}$$

It is clear that Eq. (4.17) represents the interaction of subcarriers for RZ-QAM OFDM system. On the other hand, the average interaction of two OFDM subcarriers that are modulated by traditional QAM format is given by $|u_k||u_i| = \frac{P}{2} |A_k||A_i|$. That is, at a delay time of $\delta = T_s / 2$, the average interaction of AD RZ-QAM OFDM subcarriers is 1/8 that of QAM OFDM system

4.3.2 XPM phase noise

It is well known that XPM refers to the nonlinear phase shift of an optical field induced by another field with different wavelength, direction, or state of polarization. In long haul transmission system, the optical signal is commonly transmitted through multi-span optical fiber. Each span is constructed of a single mode optical fiber, a dispersion compensation fiber, and an optical amplifier. In an all-optical OFDM link,

the XPM phase noise is accumulated span-by-span (Ho & Kahn, 2004). For the AD RZ-QAM OFDM system, the odd subcarriers can interact with either odd or even subcarriers. By substituting Eq. (4.16) and Eq. (4.17) in Eq. (3.9), the XPM phase noise can be written as:

$$\phi_{okXPM}(ML) = \frac{3\gamma ML_{eff}(L)P}{8} \sum_{\substack{i=-(N-1)/2 \\ i \in \mathcal{O}, i \neq k}}^{(N-1)/2} |A_{oi}|^2 + (2 + \cos(2\pi f_s \delta)) \frac{\gamma ML_{eff}(L)P}{8} \sum_{\substack{i=-(N-1)/2 \\ i \in \mathcal{E}}}^{(N-1)/2} |A_{ei}|^2. \quad (4.18)$$

In Eq. (4.18), the first term represents the XPM phase noise due to odd subcarriers while the XPM phase noise due to even subcarriers is characterized in second term. From Eq. (4.18), it is clear that the XPM phase noise is substantially suppressed at $\delta = T_s/2$ compared to that produced in QAM OFDM.

A random nonlinear phase noise can be induced inside optical fiber links that include optical amplifiers. This phase noise is produced by interaction the nonlinearity with ASE noise. For our proposed system, by substituting Eq. (4.16) and Eq. (4.17) in Eq. (3.10), the phase noise variance due to interaction of XPM with ASE can be expressed as:

$$\sigma_{\phi_{okXPM}}^2(ML, \delta) = \frac{M(M+1)}{4} \gamma^2 L_{eff}(L)^2 P^2 \times \left[3 \sum_{\substack{i=-(N-1)/2 \\ i \in \mathcal{O}, i \neq k}}^{(N-1)/2} |A_{oi}|^2 \sigma_i^2 + (2 + \cos(2\pi f_s \delta)) \sum_{\substack{i=-(N-1)/2 \\ i \in \mathcal{E}}}^{(N-1)/2} |A_{ei}|^2 \sigma_i^2 \right]. \quad (4.19)$$

The effect of odd and even subcarriers is demonstrated in first and second parts of Eq. (4.19), respectively. By comparing between Eq. (4.19) and Eq. (3.11), it is clear

that, at $\delta = T_s / 2$, the minimum phase noise variance occurs and its magnitude is 1/4 times the phase noise variance for QAM subcarrier.

4.3.3 FWM phase noise

In this subsection, the influence of proposed system on the FWM and its interaction with amplifiers noises is demonstrated analytically. In fact, the FWM process is a phase sensitive process where the interaction depends on the relative phases of all subcarriers and its effect accumulates over distances. The FWM process adds a significant fluctuation to the OFDM optical signal because the frequency spacing between subcarriers is equal to the symbol rate. This fluctuation causes a high nonlinear phase noise in OFDM signal. The FWM fluctuation can be defined as:

$$\delta u_k(z, t) = j2\gamma \sum_{\substack{h=-(N-1)/2 \\ h \neq k}}^{(N-1)/2} \sum_{\substack{i=-(N-1)/2 \\ l=h+i-k \\ i \neq l}}^{(N-1)/2} L_{FWM}(z) u_h(z, t) u_i(z, t) u_l^*(z, t) \quad (4.20)$$

To investigate the reduction of FWM fluctuation by employing AD RZ-QAM OFDM technique, the FWM fluctuations for both QAM OFDM and AD RZ-QAM OFDM systems are compared. By substituting Eq. (3.4) in Eq. (4.20), the FWM fluctuation in QAM OFDM system can be written as

$$\delta u_k(z, t) = j\gamma P \sqrt{\frac{P}{2}} \sum_{\substack{h=-(N-1)/2 \\ h \neq k}}^{(N-1)/2} \sum_{\substack{i=-(N-1)/2 \\ l=h+i-k \\ i \neq l}}^{(N-1)/2} L_{FWM}(z) [A_h A_i A_l^*] \quad (4.21)$$

For the proposed system, the magnitude of the phase noise variance is governed by both the envelope shape and delay time between odd and even subcarriers. Table 4.1

shows the probability of interaction between the subcarriers. For odd subcarriers ($k \in \mathcal{O}$), the probability of interaction of an odd subcarrier with two odd subcarriers is 1/4, while the probability of its interaction with even subcarriers is 3/4. By substituting Eq. (4.16) and Eq. (4.17) in Eq. (4.20), the FWM fluctuation in proposed system is:

$$\delta u_k(z,t) = j\gamma P \sqrt{\frac{P}{2}} \left[\frac{(EN(t))^3}{4} + \frac{3EN(t)(EN(t-\delta))^2}{4} \right] \times \sum_{\substack{h=-(N-1)/2 \\ h \neq k}}^{(N-1)/2} \sum_{\substack{i=-(N-1)/2 \\ l=h+i-k \\ i \neq l}}^{(N-1)/2} L_{FWM}(z) [A_h A_i A_l^*] \quad (4.22)$$

From the last equation, the magnitude of $EN(t)(EN(t-\delta))^2$ is less than one for any $\delta > 0$. Moreover, both $EN(t)$ and $EN(t-\delta)$ vary between zero and one so its effective magnitude is less than one. Therefore, the FWM fluctuation in proposed system is less than that in conventional system.

Table 4.1: Probability of interaction between the subcarriers

$k \in$	$h \in$	$i \in$	$l \in$	$h, i, l \in$
\mathcal{O}	\mathcal{O}	\mathcal{O}	\mathcal{O}	$\mathcal{O}, \mathcal{O}, \mathcal{O}$
\mathcal{O}	\mathcal{E}	\mathcal{O}	\mathcal{E}	$\mathcal{E}, \mathcal{O}, \mathcal{E}$
\mathcal{O}	\mathcal{O}	\mathcal{E}	\mathcal{E}	$\mathcal{O}, \mathcal{E}, \mathcal{E}$
\mathcal{O}	\mathcal{E}	\mathcal{E}	\mathcal{O}	$\mathcal{E}, \mathcal{E}, \mathcal{O}$
\mathcal{E}	\mathcal{O}	\mathcal{O}	\mathcal{E}	$\mathcal{O}, \mathcal{O}, \mathcal{E}$
\mathcal{E}	\mathcal{E}	\mathcal{O}	\mathcal{O}	$\mathcal{E}, \mathcal{O}, \mathcal{O}$
\mathcal{E}	\mathcal{O}	\mathcal{E}	\mathcal{O}	$\mathcal{O}, \mathcal{E}, \mathcal{O}$
\mathcal{E}	\mathcal{E}	\mathcal{E}	\mathcal{E}	$\mathcal{E}, \mathcal{E}, \mathcal{E}$

The reduction of the FWM fluctuation directly influences the random nonlinear phase noise. It is known that the interaction of FWM fluctuation with ASE noise produces random phase noises that degrade the performance of the system (Arthur J Lowery et al., 2007; Zhu & Kumar, 2010). Moreover, the ASE noise adds a fluctuation to transmitted signal and produces an additional random phase noise. In order to explore the effect of employing the proposed approach on the phase noise variance, we analyze the first and last parts of Eq. (3.17) separately. By substituting Eq. (3.4) and Eq. (4.16) in first part of Eq. (3.17), the phase noise variance due to the ASE noise only can be written as:

$$\sigma_{\varphi_{k n(t)}}^2 (ML) = \begin{cases} \frac{2M \sigma_k^2}{PA_k^2} & \text{For QAM OFDM system} \\ \frac{16M \sigma_k^2}{3PA_k^2} & \text{For AD RZ-QAM OFDM system.} \end{cases} \quad (4.23)$$

It is obvious from Eq. (4.23) that the effect of ASE noise on the AD RZ-QAM signal is higher than its effect on the QAM OFDM signal. This phenomenon is because RZ-QAM has lower pulse width than QAM signal. By substituting Eq. (4.16) and Eq. (4.17) in the last part of Eq. (3.17) and using Table 4.1, the phase noise variance for k th subcarrier in AD RZ-QAM OFDM system can be expressed as:

$$\sigma_{\varphi_{k FWM}}^2 (ML, \delta) = \frac{\gamma^2 P}{A_k^2} \left(\frac{3}{16} + \frac{(2 + \cos(2\pi f_s \delta))^2}{16} \right) \times \sum_{m=1}^M \sum_{\substack{h=-(N-1)/2 \\ h \neq k}}^{(N-1)/2} \sum_{\substack{i=-(N-1)/2 \\ l=h+i-k \\ i \neq l}}^{(N-1)/2} L_{FWM} \left\{ |A_h|^2 |A_i|^2 \sigma_l^2 + |A_h|^2 |A_l|^2 \sigma_i^2 + |A_i|^2 |A_l|^2 \sigma_h^2 \right\}. \quad (4.24)$$

By comparing the last equation with second part of Eq. (3.17), it is clear that, at $\delta = T_s / 2$, the phase noise variance due to interaction of FWM with ASE noise is 1/8 times that for QAM OFDM system. In addition, the phase noise variance for RZ-QAM format ($\delta = 0$) is 3/8 times that for QAM OFDM system.

4.3.4 AO-OFDM system setup

In this subsection, we describe our proposed AO-OFDM system setup including the transmitter, transmission link, and receiver.

4.3.4.1 AO-OFDM transmitter

The schematic of an AO-OFDM transmitter used in this study is depicted in Figure 4.12, which is similar to the AO-OFDM transmitter setup that we used in Section 4.2.3. We add variable time delayers after RZ-QAM modulators of even subcarriers to make a delay between the odd and even subcarriers. In each RZ-QAM modulator, the QAM symbol is generated from a pseudo-random bit sequence generator. The encoder of QAM modulator is supplied by PRBS signals. To preserve the orthogonality of the OFDM signals, the OFDM symbol duration is set to 40ps ($T_s = 1 / \Delta f$). No-guard interval is used because the symbol duration is equal to inverse frequency spacing.

To generate an AD QAM-RZ OFDM signal, first, the envelope of QAM subcarriers are changed to sinusoidal-like envelope by employing RZ carver after each QAM modulator. The RZ carver is composed of a single MZM, which is driven by cosine signal with a frequency of 25 GHz. The MZM is biased at quadrature bias point.

Next, the RZ-QAM subcarriers that have even indices are delayed by a certain time to reduce the interaction time between subcarriers. Finally, the AD RZ-QAM OFDM signal is obtained by superimposing all subcarriers.

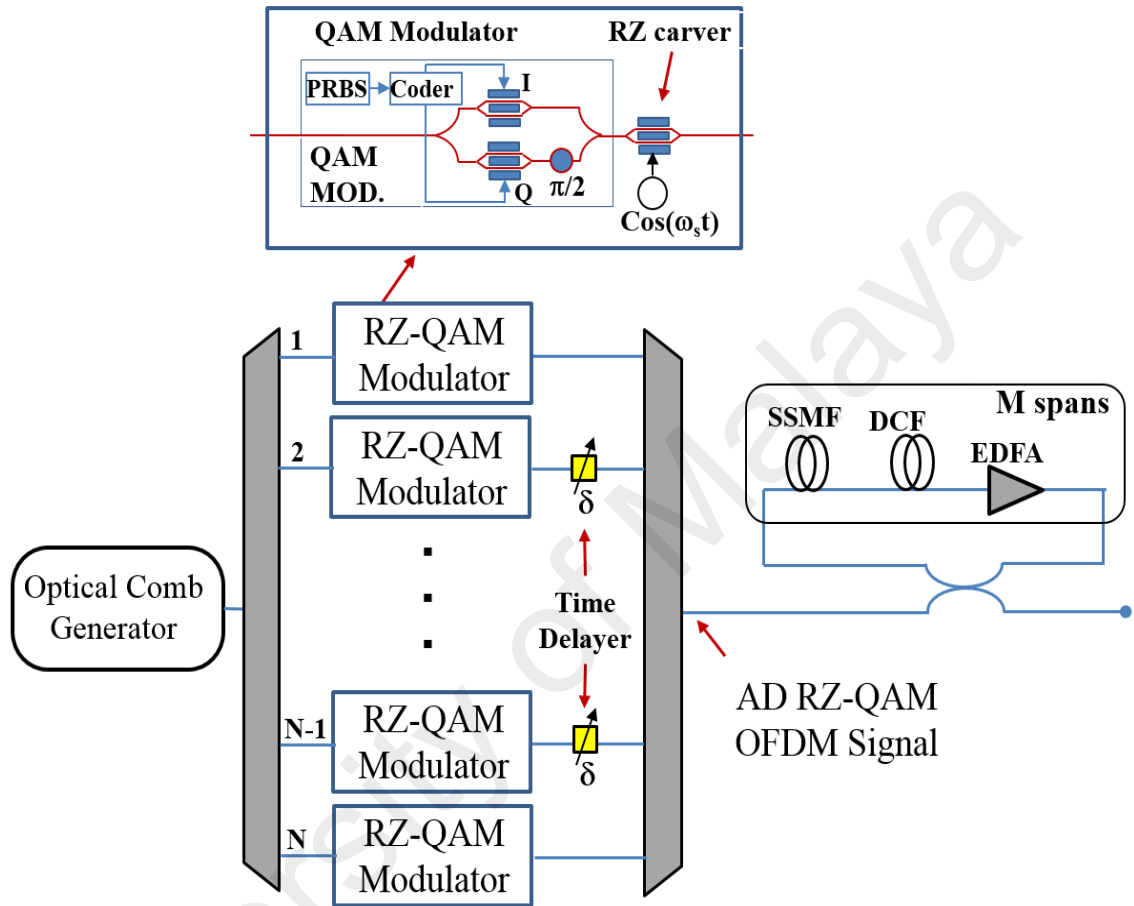


Figure 4.12: Schematic of an AD RZ-QAM OFDM transmitter.

4.3.4.2 Transmission link

The transmission link utilizes multi-spans of fiber loops. Each fiber span consists of a SSMF, a DCF, and an EDFA as shown in Figure 4.12. The SSMF is modeled with an attenuation coefficient α of 0.2 dB/km, chromatic dispersion coefficient of 16 ps/nm/km, an effective area of $80 \mu\text{m}^2$, and fiber nonlinearity γ of $1.3 \text{ W}^{-1} \text{ km}^{-1}$. A full periodic dispersion map is adopted to compensate the dispersion by utilizing a DCF

after the SSMF. The DCF has a chromatic dispersion coefficient of -160 ps/nm/km. For compensating the fibers losses, EDFAs (each has a noise figure of 6 dB) are employed at spans of 55 km spacing.

4.3.4.3 All-optical OFDM receiver

An AO-OFDM receiver comprises simple OFFT circuit (Hillerkuss et al., 2010a; Leuthold et al., 2010) and coherent QAM optical detectors as shown in Figure 4.13. The 4-order OFFT circuit is implemented according to the AO-OFDM receiver setup in Section 3.2. The AO-OFDM receiver that discussed in Section 3.2 is modified by adding one MZI with delay time of $T_s/2$ before each EAM as shown in Figure 4.13. We have employed MZI at receiver to convert the RZ-QAM signal into QAM signal. The delay time between the arms of the MZI is set at $T_s/2$ so that the received signal can interfere with its delayed replica.

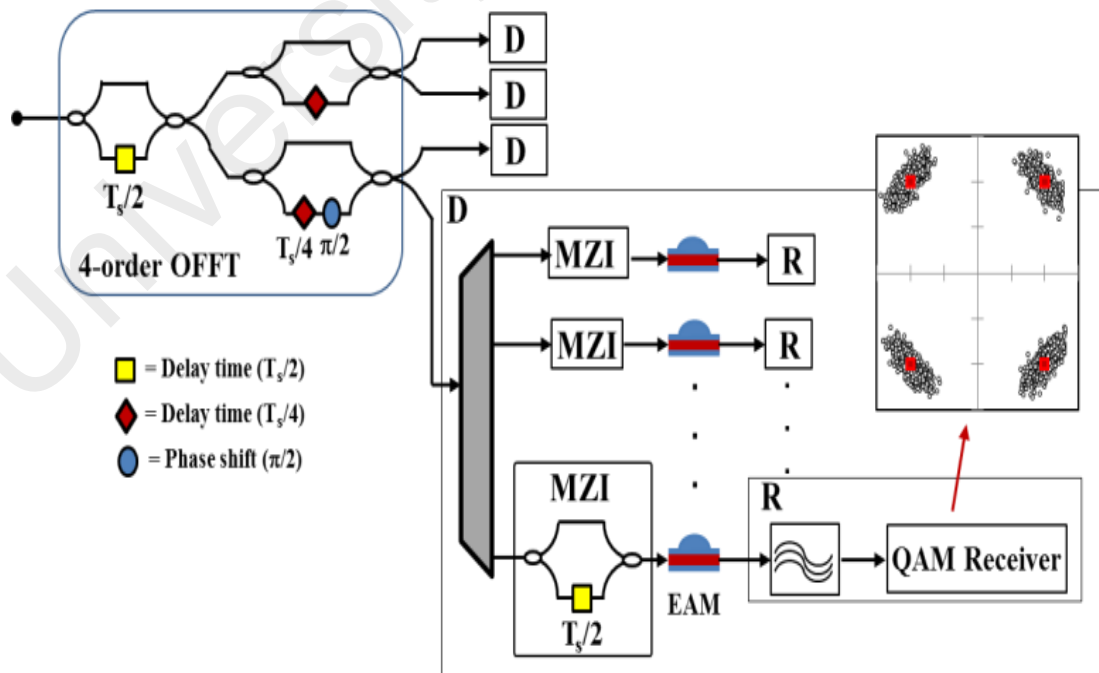


Figure 4.13: Schematic of an AD RZ-QAM OFDM receiver.

4.3.5 Results and discussion

In this section, the analytical model of the proposed system described in section 4.3.2 is carried out and compared with traditional all-optical 4QAM OFDM system. Moreover, the performance of our system is demonstrated by simulating the schematics in Figure 4.12 and Figure 4.13. The simulation is performed by VPItransmissionMaker 9.0 software. The analytical estimation results are also verified by comparing with simulation results. Both the analytical and simulation results are achieved for 29 subcarriers. Each subcarrier is modulated by a RZ-4QAM modulator at symbol rate of 25 Gsymbol/s.

4.3.5.1 Phase noise results

In order to determine the effect of the delay time on the phase noise variance due to the fiber nonlinearity, we set linewidths (LWs) of the laser source and the local oscillator to zero in both Figure 4.14 and Figure 4.15. The dependence of the nonlinear phase noise variance on the delay time δ is shown in Figure 4.14. The total phase noise variance is obtained by using both analytical modeling and simulation for a transmission distance of 550 km and subcarrier power of 3 dBm. The analytical results show that the phase noise variance (solid line) is reduced from 9.3×10^{-3} to $6.1 \times 10^{-3} \text{ rad}^2$ when the delay time δ is increased from zero to $T_s/2$. Increasing the delay time beyond $T_s/2$ would raise the phase noise variance back due to the increase in the interaction time between the subcarriers. The simulation results (squares) show similar behavior to the phase noise variance that was calculated from analytical model. The analytical and simulation results are in a good agreement.

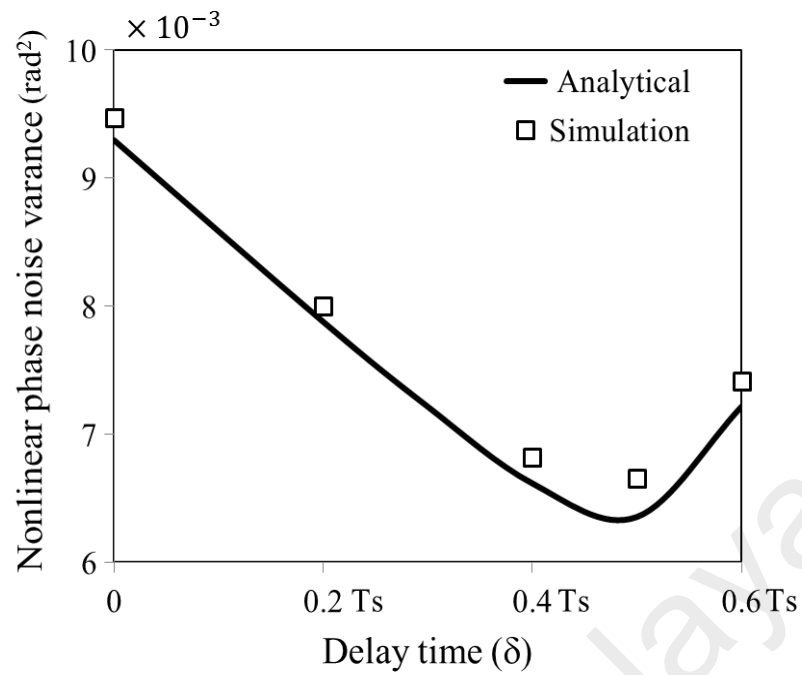


Figure 4.14: The dependence of the nonlinear phase noise variance on the delay time δ .

Figure 4.15 shows the influence of the proposed approach on the mitigation of phase noise. The results are achieved at a transmission distance of 550 km and a delay time of $T_s/2$. Figure 4.15(a) separately illustrates the phase noise variances of XPM, FWM, and ASE noise against subcarrier power. Generally, at low fiber launch power, the phase noise variance is mainly produced by the ASE noise since OSNR is low. When increasing the subcarrier power, the phase noises due to both XPM and FWM increase, whereas the phase noise due to the amplifier noise decreases. It can be seen that, when the AD RZ-4QAM AO-OFDM system is employed, the phase noise variances due to FWM and XPM are significantly reduced below that of 4QAM AO-OFDM system, while the phase noise variance due to ASE noise is increased. For example, at a subcarrier power of 5 dBm, the phase noise variance due to FWM is 0.0034 rad^2 for AD RZ-4QAM AO-OFDM system while it is 0.0275 rad^2 for 4QAM AO-OFDM system. In addition, at the same power level, the phase noise of XPM is

reduced from 0.0087 rad^2 for 4QAM AO-OFDM system to 0.00228 rad^2 for AD RZ-4QAM AO-OFDM system. The total phase noise variances of both systems versus the subcarrier power are shown in Figure 4.15(b). As expected, the total phase noise variance decreases with increasing the power until an optimum power level then it starts to increase again. The figure also indicates that the optimum power level is 3 dBm for the proposed system, while it is -3 dBm for 4QAM AO-OFDM system. Furthermore, the proposed system has lower phase noise variances at higher launch powers compared with that of 4QAM AO-OFDM system. This is because the interaction time between the subcarriers is shorter. The presented simulation results show good agreement with analytical results.

4.3.5.2 Performance of AD RZ-QAM AO-OFDM system

In this subsection, the performance of the proposed system is demonstrated by simulation and compared with traditional AO-OFDM system. All our simulation results of the optical systems are achieved by VPItransmissionMaker 9.0 simulator. In addition, all results are obtained without employing any nonlinear compensation program in receiver to investigate the mitigation efficiency of our approach.

To show the improvement in the transmission distance in the presence of fiber nonlinearities, Figure 4.16 depicts the BER versus the transmission distance for both AD RZ-4QAM AO-OFDM and 4QAM AO-OFDM systems. The results are obtained for 29 subcarriers at optimum power of each system. The LWs of the laser source and the local oscillator is set to 10^{-5} Hz . Generally, our system is able to transmit the data for longer distance, where the transmission distance for the proposed system is 2090 km at a BER of 10^{-5} , while it is only 1595 km for 4QAM AO-OFDM system.

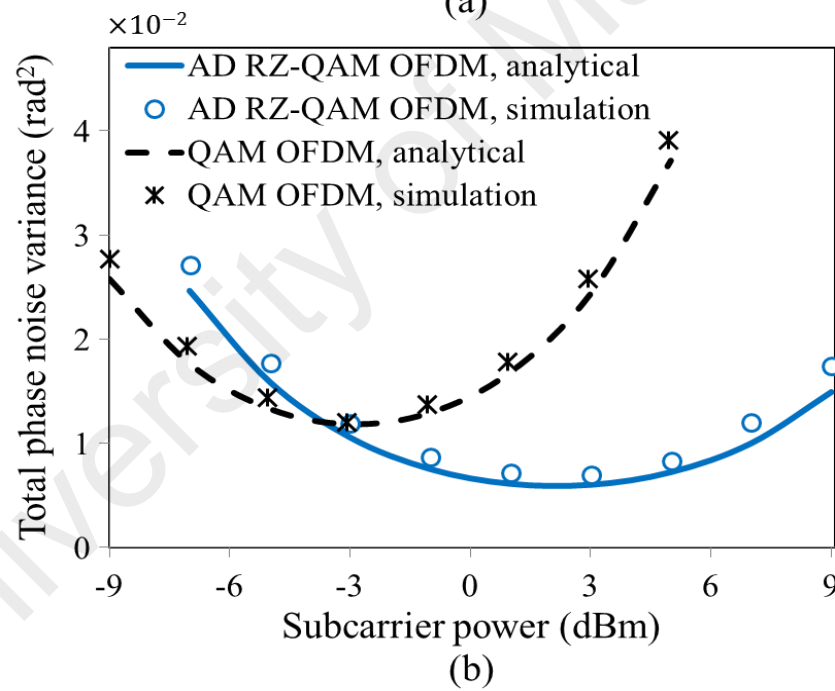
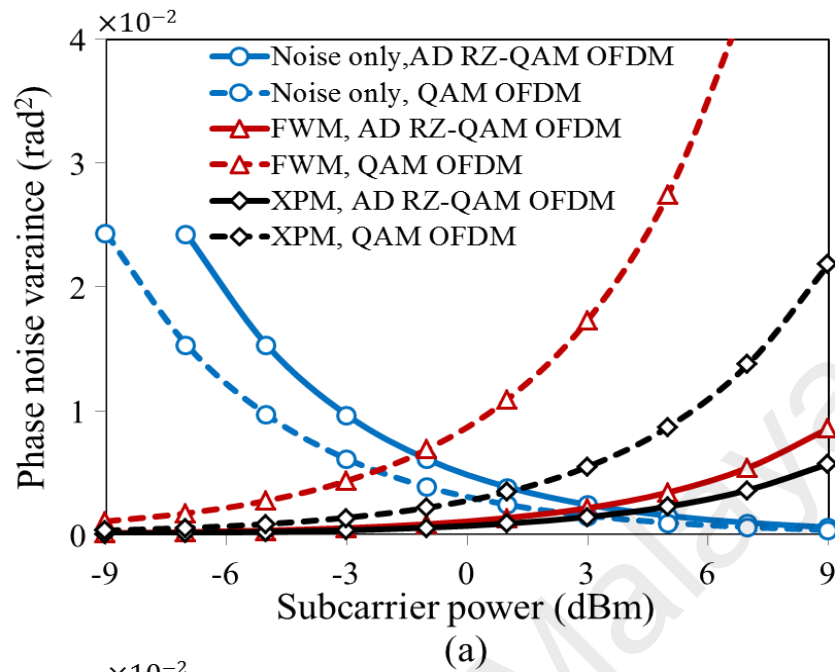


Figure 4.15: Influence of AD RZ-4QAM OFDM format on the phase noise reduction, a) details of phase noise, b) total phase noise variance.

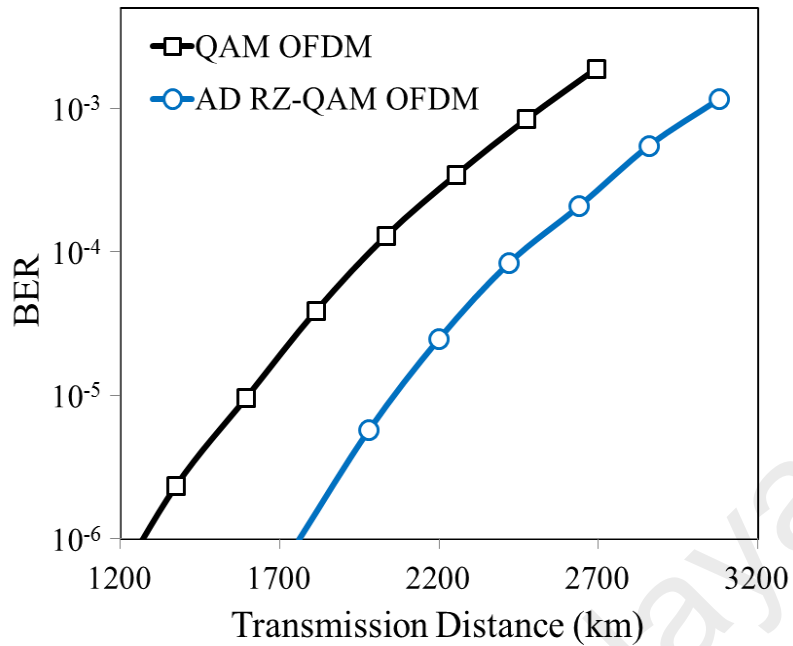


Figure 4.16: BER versus transmission distance for both AD RZ-4QAM OFDM and 4QAM OFDM systems.

Figure 4.17 shows the detected eye diagrams for both AD RZ-4QAM AO-OFDM and QAM OFDM baseband signals at transmission distances of 550 km and 1100 km. The eye diagrams represent the in-phase component (I) of detected QAM signal. The simulation results are achieved at optimum power of both systems. It is clear that the eye diagrams of the proposed system are clearer in both transmission distances. For both transmission distances, the eye heights of proposed system are larger than that of traditional 4QAM AO-OFDM system. Moreover, for proposed system, the eye slowly closes with increasing the transmission distance compared with 4QAM AO-OFDM system. This shows that the proposed system is able to mitigate the fiber nonlinearity impairments.

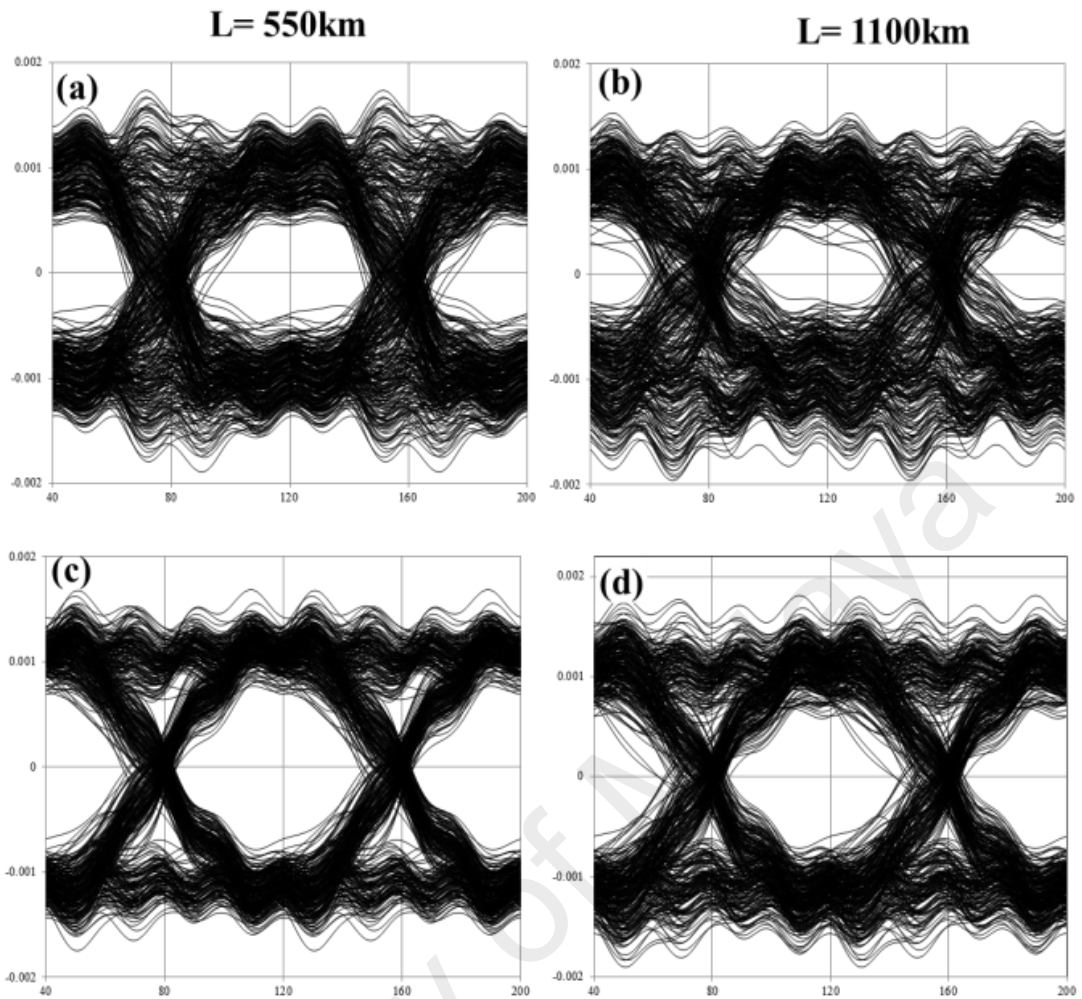


Figure 4.17: Eye diagram of in-phase component (I) of received signal at 550 km and 1100 km: (a) and (b) 4QAM AO-OFDM system, (c) and (d) AD RZ-4QAM AO-OFDM system.

Finally, the BER performances of proposed and conventional systems are depicted in Figure 4.18. The AD RZ-4QAM AO-OFDM system always exhibits a superior performance than 4QAM AO-OFDM system. For a transmission distance of 550 km, the required OSNR for proposed system at $BER=10^{-5}$ is about 22 dB, while the required OSNR for the 4QAM AO-OFDM system is about 23 dB at same BER. Furthermore, the performances of the systems are characterized for a transmission

distance of 1100 km. That is, to obtain a BER of 10^{-5} for both systems, the proposed system requires an OSNR of 1 and 1.2 dB below that required for 4QAM AO-OFDM system at transmission distances of 550 km and 1100 km, respectively.

It is worth mentioning, the proposed system is valid to deal with other higher-level modulation formats such as mPSK and mQAM formats with higher than 4-level.

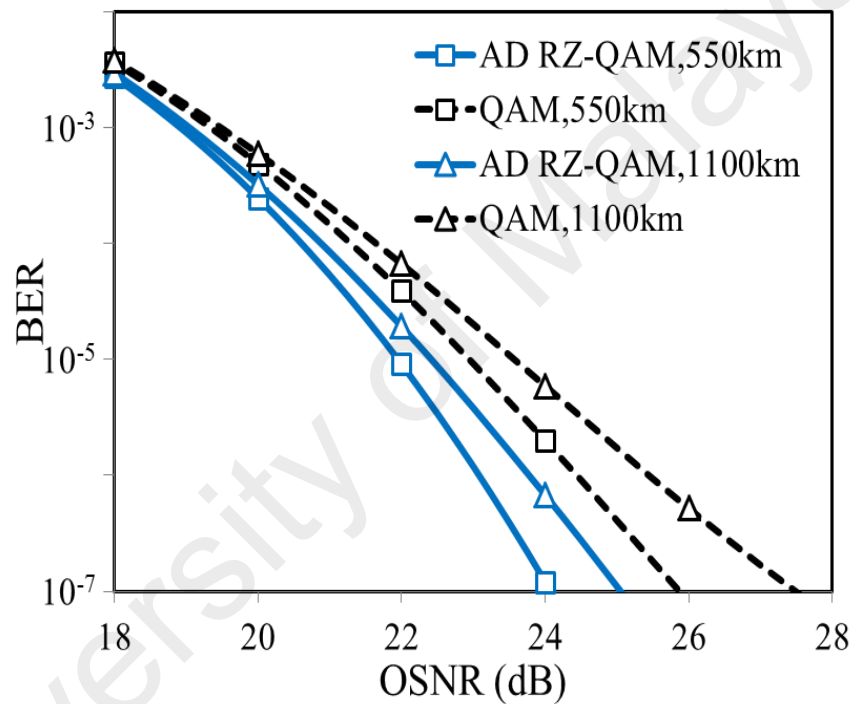


Figure 4.18: BER performances of proposed and conventional systems.

4.4 Summary

In this chapter, two new techniques have been demonstrated to mitigate the nonlinear phase noise. In first proposed technique, an efficient RZ-4QAM and RZ-16QAM modulation formats have been proposed for improving the performance of an AO-OFDM system. At transmitter side, the conversion from mQAM to RZ-mQAM

formats is optically realized by using a single MZM after mQAM modulator for each subcarrier. The MZM is driven by sinusoidal waveform. At the receiver side, the conversion from RZ-mQAM to mQAM utilizes a MZI with delay time equal to half symbol period. The performance of the proposed system have been compared to that of a conventional AO-OFDM using 4QAM and 16QAM. Our results show that the performance of the proposed system is significantly better than that of the conventional ones since the effects of fiber nonlinearities have been successfully mitigated. It is observed that the required power for getting minimum EVM increases when RZ-4QAM and RZ-16QAM formats are employed. Furthermore, the transmission distance is substantially increased when RZ-4QAM and RZ-16QAM are adopted in AO-OFDM systems, as compared to that of the conventional OFDM systems with 4QAM and 16QAM.

In second technique, mitigation of the nonlinear phase noise in AO-OFDM systems based on minimizing interaction time between subcarriers has been analytically modeled and numerically demonstrated. Minimizing the interaction time between subcarriers has been performed by shaping the envelopes of 4QAM AO-OFDM subcarriers and shifting even subcarriers with respect to odd subcarriers by half the symbol duration. The analytical results show that the phase noise variances of the proposed system, due to both XPM and FWM, are significantly reduced in the dispersion-managed fiber transmission link, when compared to that of all-optical 4QAM OFDM systems. Furthermore, at a BER of 10^{-5} , the achievable transmission distance is significantly increased from 1595 km with 4QAM AO-OFDM system to 2090 km with AD RZ-4QAM AO-OFDM system. In addition, at a transmission distance of 1100 km and 29 subcarriers, the required OSNR to obtain a BER of 10^{-5} is improved by 1.2 dB when compared to 4QAM AO-OFDM system. Simulation results have been carried out and have been shown good agreement with analytical results.

CHAPTER 5

REDUCTION OF PEAK-TO-AVERAGE POWER RATIO IN AO-OFDM SYSTEM USING ROTATED CONSTELLATION

APPROACH

5.1 Introduction

All-optical orthogonal frequency division multiplexing (AO-OFDM) system has a great potential application in high bit rate transmission systems since it eliminates the requirement of electronics signal processing (Hillerkuss et al., 2010b; Hillerkuss et al., 2011; Inuk Kang, 2012). The system also provides a better tolerance to chromatic and polarization-mode dispersions compared to other communication systems (Jansen et al., 2008; A. Lowery & Armstrong, 2006; Mirnia et al., 2013; W_ Shieh et al., 2008). As discussed in the previous chapters, the performance of the OFDM system highly suffers from phase noise which introduces phase rotation for each subcarrier and thus destroys orthogonality of subcarriers (Wei & Chen, 2010). The phase noise is mainly induced from fiber nonlinear effects such as XPM, and FWM (S. T. Le et al., 2014). This is evident when adding a number of subcarriers in the time domain for high power transmission signals (Armstrong, 2009). The combined signals induce the fiber nonlinear effects and degrades the system performance (Pechenkin & Fair, 2009; Popoola et al., 2014). Therefore, many approaches have been proposed and reported to mitigate fiber nonlinear impairment during transmission of signals in optical OFDM systems where peak-to-average power ratio (PAPR) reduction is the popular approach.

In both wireless and conventional optical OFDM systems, PAPR reduction is realized in the electrical domain. Various techniques have been developed to reduce PAPR in optical OFDM systems such as amplitude clipping and filtering (Hao et al., 2012; B. Liu et al., 2012). Although the implementation of clipping technique is simple and less complex, the clipping processes produce a distortion in the optical signal hence increasing the BER. There are also other techniques such as selected mapping (SLM) and partial transmit sequence (PTS) methods which are considered as effective for reducing PAPR in conventional optical OFDM systems (Weilin Li et al., 2009; Pechenkin & Fair, 2009). However, these methods involve a high computational complexity. Furthermore, the constant envelope of the electrical OFDM waveform has also been adopted to improve the tolerance of Mach-Zehnder modulator (MZM) nonlinearities and to relax the requirements of digital-to-analog converter (DAC) and analog-to-digital converter (ADC) (Nunes et al., 2014; Silva et al., 2012). Indeed, few investigations have been reported on the PAPR reduction techniques in AO-OFDM systems (Liang et al., 2009). They focus on the AO-OFDM systems, which employ intensity modulation rather than phase modulation. Phase pre-emphases method has been proposed to reduce PAPR in AO-OFDM systems (Shao et al., 2010).

In this chapter, we propose a simple technique to reduce PAPR based on rotated constellation in coherent AO-OFDM system. In this approach, the subcarriers are divided into odd and even subsets. Then the constellation of odd subcarriers is rotated counter clockwise while the constellation of even subcarriers is remained without rotation. The impact of the rotation angle on the PAPR is mathematically modeled. Then, the resulting PAPR reduction on the total phase noise in AO-OFDM systems is mathematically modeled and numerically investigated. The simulation results show that the proposed technique provides PAPR reduction with a better nonlinear impairment

tolerance in 4-quadrature amplitude modulation (4QAM) AO-OFDM system that employs 29 subcarriers and symbol rate of 25 Gsymbol/s.

5.2 PAPR reduction principle

In this section, a new approach to mitigate fiber nonlinear impairment by reducing PAPR is analytically explained. First, the subcarriers are divided into odd and even subsets. Then, at QAM modulators, the original constellation of odd subcarriers is rotated with an angle of θ (counter clockwise) while the constellation of even subcarriers is determined by the standard 4QAM constellation as shown in Figure 5.1. This approach is suitable for both conventional optical OFDM and AO-OFDM systems where the constellation is realized in electrical domain. The output of the AO-OFDM transmitter is given by:

$$u(t) = \sum_{\substack{k=-(N-1)/2 \\ k \in \mathcal{O}}}^{(N-1)/2} u_k(t) \exp(j\theta) \exp(j\omega_k t) + \sum_{\substack{k=-(N-1)/2 \\ k \in \mathcal{E}}}^{(N-1)/2} u_k(t) \exp(j\omega_k t), \quad (5.1)$$

where θ , $0 \leq \theta \leq \pi/4$ is the angle of rotation. By substituting Eq. (3.4) in Eq. (5.1), the optical field the OFDM signal can be expressed as:

$$\begin{aligned} u(t) = & \sqrt{\frac{P}{2}} \exp(j\theta) \sum_{\substack{k=-(N-1)/2 \\ k \in \mathcal{O}}}^{(N-1)/2} A_k \operatorname{rect}\left(\frac{t - kT_s}{T_s}\right) \exp(j\omega_k t) \\ & + \sqrt{\frac{P}{2}} \sum_{\substack{k=-(N-1)/2 \\ k \in \mathcal{E}}}^{(N-1)/2} A_k \operatorname{rect}\left(\frac{t - kT_s}{T_s}\right) \exp(j\omega_k t). \end{aligned} \quad (5.2)$$

The maximum optical field is obtained when all subcarriers are coherently combined. In other words, all subcarriers are modulated with same QAM symbol, making the summations of magnitudes of odd and even subcarriers equal to half summation of magnitude of all subcarriers and the angle between them is equal to the rotating angle. The magnitude of optical field of OFDM signal can be written as:

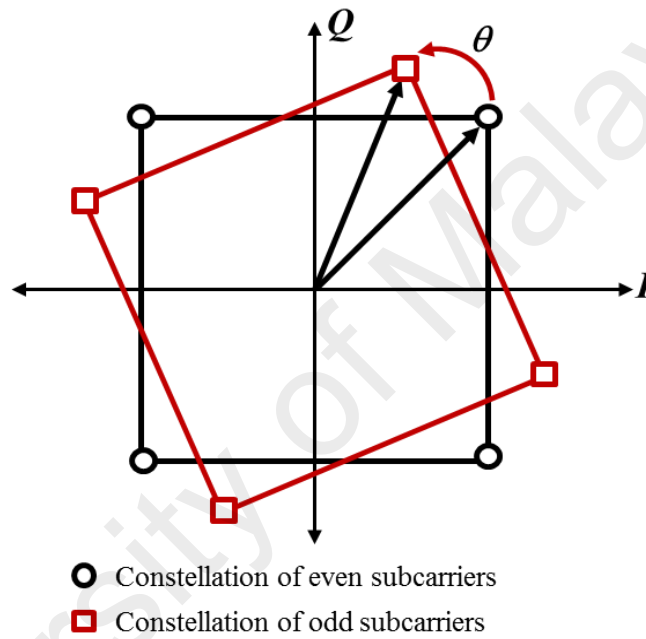


Figure 5.1: Rotated 4QAM constellation.

$$|u(t)| = \sqrt{\frac{P}{2}} \left[\frac{1 + \exp(j\theta)}{2} \right] \sum_{k=-(N-1)/2}^{(N-1)/2} |A_k| \quad (5.3)$$

By doing some algebra, the magnitude of optical field can be expressed as:

$$\begin{aligned}
|u(t)| &= \sqrt{\frac{P}{2}} \left| \cos\left(\frac{\theta}{2}\right) \exp\left(j\frac{\theta}{2}\right) \right| \sum_{k=-(N-1)/2}^{(N-1)/2} |A_k| \\
&= \sum_{k=-(N-1)/2}^{(N-1)/2} \sqrt{\frac{P}{2}} \cos\left(\frac{\theta}{2}\right) |A_k|.
\end{aligned} \tag{5.4}$$

From Eq. (5.4), it can be considered that the magnitude of optical field of k th subcarrier equal to:

$$|u_k(t, \theta)| = \sqrt{\frac{P}{2}} \cos\left(\frac{\theta}{2}\right) |A_k|. \tag{5.5}$$

The PAPR of the signal, $u(t)$, is defined as the ratio of the peak of instantaneous power to the average power (B. Liu et al., 2012), and is given as:

$$PAPR = \frac{\max(|u(t)|^2)}{E[(u(t))^2]}, \tag{5.6}$$

where $E[\bullet]$ is the expectation operator. For 4QAM constellation, the $|A_k| = \sqrt{2}$ because $a_k = b_k = 1$. The magnitude of optical field and the power of k th subcarrier after rotating the constellation can be expressed as:

$$\begin{aligned}
|u_k(t, \theta)| &= \sqrt{P} \cos\left(\frac{\theta}{2}\right), \\
|u_k(t, \theta)|^2 &= P \cos^2\left(\frac{\theta}{2}\right),
\end{aligned} \tag{5.7}$$

respectively. The maximum power is occurred when powers of N subcarriers are coherently added and it equals to:

$$\begin{aligned}\max(|u(t)|^2) &= \sum_{k=-(N-1)/2}^{(N-1)/2} P \cos^2\left(\frac{\theta}{2}\right) \\ &= PN \cos^2\left(\frac{\theta}{2}\right),\end{aligned}\tag{5.8}$$

The average power can be expressed as:

$$E[(u(t))^2] = \sqrt{N} \frac{P}{\sqrt{2}}.\tag{5.9}$$

By substituting Eq. (5.8) and Eq. (5.9) in Eq. (5.6), the PAPR becomes:

$$PAPR(\theta) = \sqrt{2N} \cos^2\left(\frac{\theta}{2}\right).\tag{5.10}$$

From Eq. (5.10), the relation between the PAPRs for the system with and without employing rotation constellation technique is factor $\cos^2\left(\frac{\theta}{2}\right)$. Therefore, the cumulative distribution function (CDF) of ($PAPR < x$) for proposed system can be written as:

$$\begin{aligned}CDF &= \int_0^x \frac{y}{\cos^2\left(\frac{\theta}{2}\right) \sigma^2} \exp\left(\frac{-y^2}{2\sigma^2 \cos^4\left(\frac{\theta}{2}\right)}\right) dy \\ &= 1 - \exp\left(\frac{-x^2}{2\sigma^2 \cos^4\left(\frac{\theta}{2}\right)}\right).\end{aligned}\tag{5.11}$$

For large N OFDM symbols, the PAPR is considered as a random variable where its distribution is given by:

$$P(PAPR \leq x) = \left(1 - \exp\left(\frac{-x^2}{2\sigma^2 \cos^4\left(\frac{\theta}{2}\right)} \right) \right)^N. \quad (5.12)$$

The complementary cumulative distribution function (CCDF) describes PAPR statistics. It shows the probability of an OFDM signal exceeding a given PAPR, and it can be written as:

$$CCDF = 1 - \left(1 - \exp\left(\frac{-x^2}{2\sigma^2 \cos^4\left(\frac{\theta}{2}\right)} \right) \right)^N. \quad (5.13)$$

5.3 Effect of rotated constellation method on fiber nonlinearity

In this section, the effect of rotated constellation of odd subcarriers on the fiber nonlinearity impairments is described. The intensity of the optical signal is one of the main factors that affect the phase noise caused by XPM and FWM. By reducing the high peaks of the OFDM signal, the nonlinear distortion should decrease.

5.3.1 XPM Phase Noise

It is well known that XPM refers to the nonlinear phase shift of an optical field induced by another field with different wavelength, direction, or state of polarization. In long haul transmission system, the optical signal is commonly transmitted through multi-span optical fiber. Each span is constructed of a standard single mode optical fiber (SSMF), a dispersion compensating optical fiber (DCF), and an optical amplifier. Normally, an optical amplifier is used to compensate power loss due to the fiber attenuation in each span. However, these amplifiers add a random noise to the transmitted signal where a field of amplified spontaneous emission (ASE) noise is added to each of the subcarriers. The nonlinear phase noise due to XPM in the presence ASE noise is accumulated span-by-span, and it can be expressed as:

$$\begin{aligned} \phi_{kXPM}^{+n}(ML, t, \theta) = \gamma L_{eff}(L) & \left[\sum_{\substack{i=-(N-1)/2 \\ i \neq k, k \in \mathcal{O}}}^{(N-1)/2} \sum_{m=1}^M \left| u_i(t) \exp(j\theta) + \sum_{\mu=1}^m n_{i\mu}(t) \right|^2 \right. \\ & \left. + \sum_{\substack{i=-(N-1)/2 \\ i \neq k, k \in \mathcal{E}}}^{(N-1)/2} \sum_{m=1}^M \left| u_i(t) + \sum_{\mu=1}^m n_{i\mu}(t) \right|^2 \right]. \end{aligned} \quad (5.14)$$

By substituting Eq. (5.5) in Eq. (5.14) and by doing same steps in Section 3.3.1, the phase noise variance can be written as:

$$\sigma_{\phi_{kXPM}^{+n}}^2(ML, \theta) = 2M(M+1)\gamma^2 L_{eff}^2 P \cos^2\left(\frac{\theta}{2}\right) \sum_{\substack{i=-(N-1)/2 \\ i \neq k}}^{(N-1)/2} |A_i|^2 \sigma_i^2. \quad (5.15)$$

From the last equation, it is clear that the angle of rotation θ governs the variance of phase noise due to interaction of XPM with ASE noise.

5.3.2 FWM phase noise

The FWM process is a phase sensitive process where the interaction depends on the relative phases of all subcarriers and its effect can efficiently accumulate over longer distances. The FWM process adds a fluctuation to the optical field that causes a phase noise. For the proposed approach, the magnitude of the phase noise variance is governed by the angle between odd and even constellations. By substituting Eq. (5.5) in Eq. (3.15), the phase noise variance for the proposed system can be expressed as:

$$\sigma_{\varphi_{k(n(t)+FWM)}}^2(ML, t) = \frac{2M \sigma_k^2}{P |A_k|^2} + \frac{2\gamma^2 P}{|A_k|^2} \cos^4\left(\frac{\theta}{2}\right) \quad (5.16)$$

$$\times \sum_{m=1}^M \sum_{\substack{h=-(N-1)/2 \\ h \neq k}}^{(N-1)/2} \sum_{\substack{i=-(N-1)/2 \\ l=h+i-k \\ i \neq l}}^{(N-1)/2} L_{FWM} \left\{ |A_h|^2 |A_i|^2 \sigma_l^2 + |A_h|^2 |A_l|^2 \sigma_i^2 + |A_i|^2 |A_l|^2 \sigma_h^2 \right\}.$$

From last equation, the phase noise variance due to interaction of FWM with ASE noise can be controlled by adjusting the angle of rotation.

5.4 All-optical OFDM system setup

The schematic diagram of AO-OFDM system setup used in this study is shown in Figure 5.2. The system includes three subsystems: transmission, transmission link, and reception. The transmission subsystem is similar to that described in Section 3.2 of Chapter 3. The optical frequency comb generator (OFCG) utilizes two IMs and one time delay to generate 29 subcarriers with constant frequency spacing (J. K. Hmood et al., 2015a). Subsequently, the generated subcarriers are split into odd and even subcarriers. The odd subcarriers are modulated according to rotated QAM constellation, while standard QAM constellation is used to modulate the even subcarriers. The odd and even

subcarriers are directly superimposed upon modulating by using beam combiner to generate OFDM signal.

The transmission link comprises multi-span fiber loops. Each span consists of 55 km SSMF, DCF and an Erbium doped fiber amplifier (EDFA) as shown in Figure 5.2. The SSMF is modeled with an attenuation coefficient α of 0.2 dB/km, chromatic dispersion coefficient of 16 ps/nm/km, an effective area of $80 \mu\text{m}^2$, and fiber nonlinearity γ of $1.3 \text{ W}^{-1} \text{ km}^{-1}$. The DCF fully compensates the chromatic dispersion (CD) of SSMF with chromatic dispersion coefficient of -160 ps/nm/km. The EDFAs with a noise figure of 6 dB are employed to compensate the fiber loss and control the launching power into the SSMF and DCF.

The AO-OFDM receiver is completely similar to the AO-OFDM receiver that described in Section 3.2. It comprises simple all-optical fast Fourier transform (OFFT) circuit (Hillerkuss et al., 2010b) and coherent QAM optical detectors.

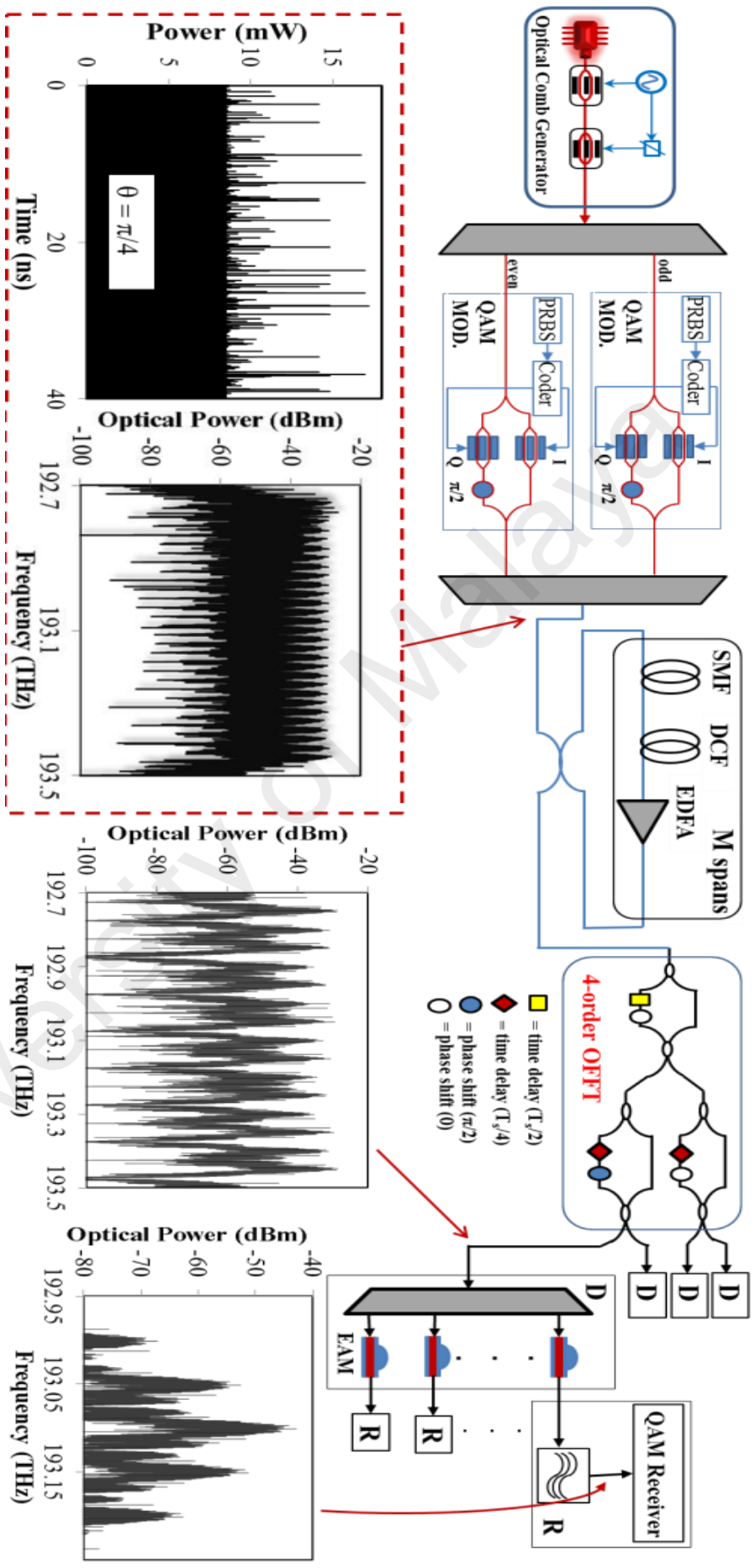


Figure 5.2: All-optical OFDM system setup

5.5 Results and discussion

In order to investigate the validity of our approach, model analysis is carried out and the finding is compared with the result of numerical simulation generated by VPItransmissionMaker 9.0. The analytical and simulation results are obtained for 29 subcarriers. Each subcarrier is modulated with 4QAM constellation at a symbol rate of 25 Gsymbol/s and transmitted through multi-span fiber with a total length of 1100 km.

5.5.1 Transmitter side

Figure 5.3 depicts the impact of rotation angle on the PAPR. The results are achieved for subcarriers number of $N=29$, 4QAM mapping and subcarrier power of -3 dBm. The comparison of CCDF performances for the proposed approach at $\theta = \pi/6$ rad and $\theta = \pi/4$ rad against the original system (without using any PAPR reduction method) is shown in Figure 5.3(a). It is shown that for the original OFDM ($\theta=0$), 1 in every 10^3 OFDM frames has its PAPR greater than 8.9 dB. Using the rotated constellation technique, at $\theta = \pi/4$ rad, 1 in every 10^3 OFDM frames has its PAPR exceeding 8.1 dB. The PAPR is improved by more than 0.8 dB for $\text{CCDF} = 1 \times 10^{-3}$ over the conventional system. The PAPR for various rotation angles is shown in Figure 5.3(b). It is clear that the PAPR is reduced with increasing the rotation angle from 0 to $\pi/4$ rad. However, when the rotation angle is increased beyond the $\pi/4$, the PAPR is also increased because the constellation of odd subcarriers approaches to the constellation of even subcarriers in next quarter as shown in inset of Figure 5.3(b). Therefore, the PAPR (θ) is considered a periodic function and the optimum angle is $\pi/4$. The analytical result (dashed line) indicates that the PAPR drops from 8.8 dB to 8.1 dB when the rotation angle increases from zero to $\pi/4$ rad. The simulation result

(solid line) exhibits similar behavior and there exist a good agreement between the analytical and simulation results.

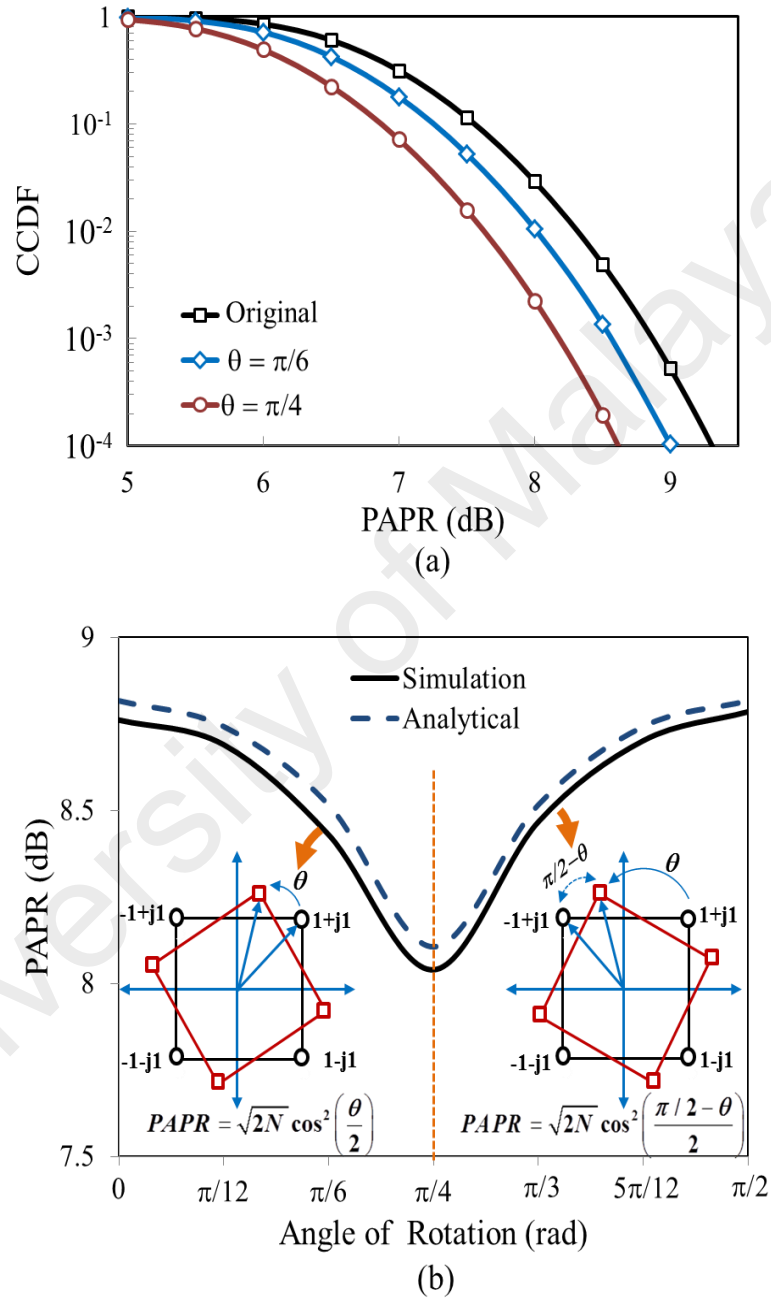


Figure 5.3: The impact of rotation angle on the PAPR, a) complementary cumulative distribution function (CCDF) versus PAPR, b) the PAPR for various rotation angles.

Figure 5.4 shows the optical waveforms of AO-OFDM signals for various rotation angles. The results are obtained for 4QAM mapping with different rotation angles but at the same power of subcarriers ($P = -3$ dBm). It can be observed from Figure 5.4(a) that the original system ($\theta=0$) generates an optical OFDM signal with a maximum peak of 20.4 mW. By increasing the rotation angle θ to $\pi/4$ rad, the maximum peaks of the transmitted optical OFDM signal are obtained at 17.2 mW as shown in Figure 5.4(b). This indicates that the increment of the rotation angle decreases the signal peaks significantly. This phenomenon results from combining the odd and even subcarriers with different rotated angles. In agreement with Eq. (5.8), a higher rotation angle leads to reduction in peak power of the generated OFDM signal.

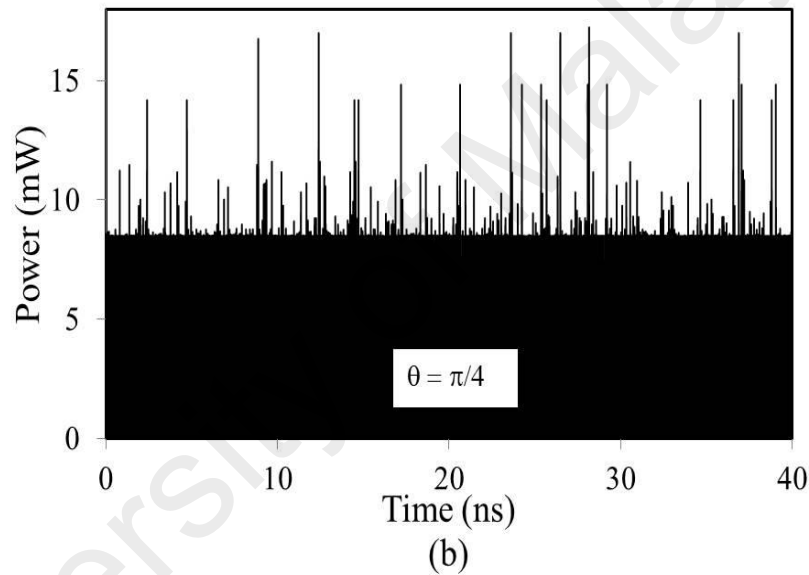
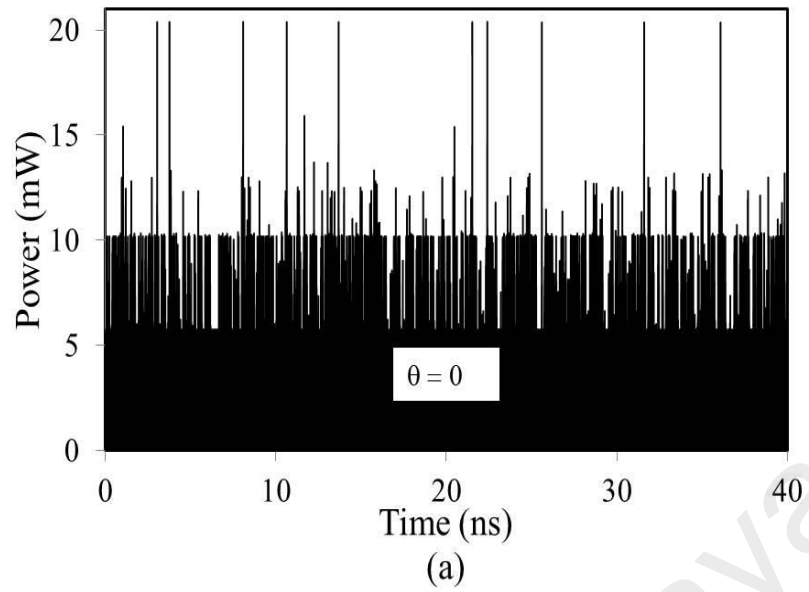


Figure 5.4: Effect of rotation angle on the optical waveforms of AO-OFDM signals.

5.5.2 Receiver side

To show the mitigation results of the fiber nonlinear impairments, Figure 5.5 depicts the nonlinear phase noise variance against the power of subcarrier for the proposed system at rotation angles of $\theta = \pi/4$ rad and the original OFDM system. The results are quantified using both simulation and the analytical model for 29 subcarriers

and transmission distance of 1100 km. It is found that the phase noise variance is successfully reduced when the angle of rotation is set to $\theta = \pi/4$ rad. At low signal power, the phase noise variances of both systems are slightly different. This is because the performance of the system is governed by the optical amplifier noises at low signal power. However, with higher signal power, the difference between the phase noise variances is become clearer. This is because the proposed system reduces the PAPR and mitigates the fiber nonlinear impairments without any additional distortion. In addition, it can be noted that the presented analytical results show good agreement with the simulation results.

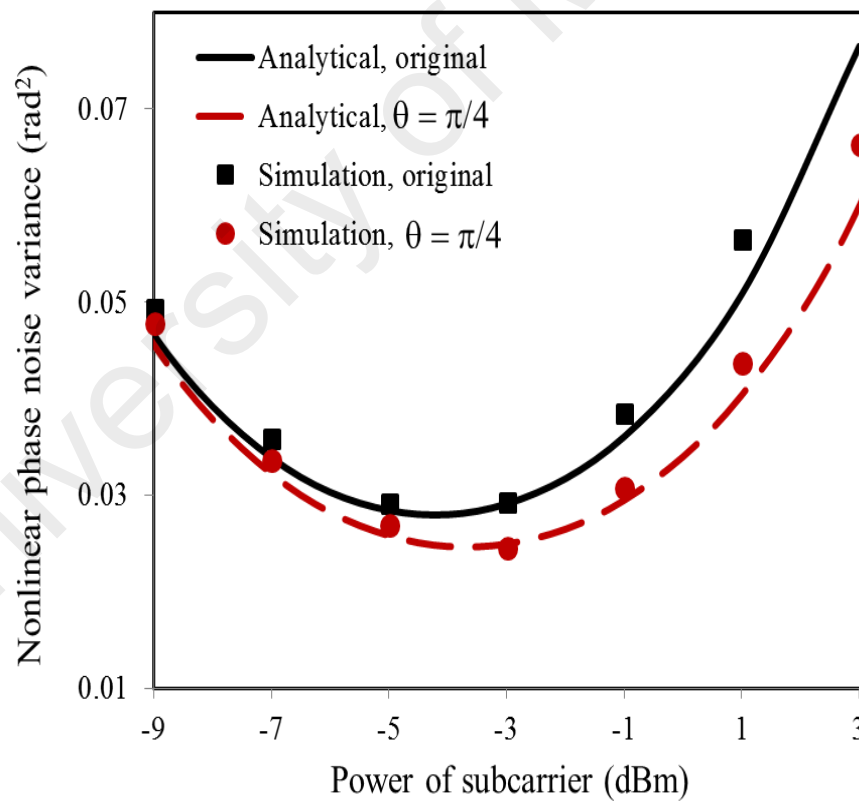


Figure 5.5: Influence of rotated constellation on the fiber nonlinearities impairments

Figure 5.6(a) shows the influence of the angle of rotation on both optical signal-to-noise ratio (OSNR) and bit error rate (BER) performance in the AO-OFDM system that employs 4QAM. Referring to Eq. (5.15) and Eq. (5.16), both XPM and FWM are reduced with increasing the rotation angle because the power of the OFDM symbol is reduced with employing proposed approach. Clearly, the BER reduces as the angle of the rotation increases. The highest BER occurs at $\theta = 0$ rad, whereas the minimum BER occurs at $\theta = \pi/4$ rad. Furthermore, the OSNR is raised with increasing the angle of rotation. It is improved by ~ 2.3 dB at rotation angle of $\theta = \pi/4$ rad and transmission distance of 1100 km. This indicates that the performance of the system improves with the increment of the rotation angle due to mitigation of fiber nonlinearity impairments. Insets of Figure 5.6(a) depict the received constellations for $\theta = 0, \pi/6$ and $\pi/4$ rad. Figure 5.6(b) illustrates BER versus OSNR for the both proposed and original OFDM system. The rotation angle is set to $\theta = \pi/4$ rad. The receiver sensitivity is obtained at a symbol rate of 25 Gsymbol/s and transmission distance of 1100 km. At $\theta = \pi/4$ rad, the AO-OFDM system acquires the best BER performance where the required OSNR to obtain a $\text{BER} = 1 \times 10^{-7}$ is reduced by 0.5 dB.

Finally yet importantly, we can confirm that the rotated constellation approach is a simple and viable method for reducing PAPR value, mitigating phase noise, and improving performance of OFDM systems. Furthermore, to implement this approach, only simple computations or components are required. In addition, the proposed system is valid to deal with higher-level modulation formats such as 16QAM format. However, the proposed system is more efficient with employing 4QAM format because the rotation angle becomes bigger, leading to higher PAPR reduction.

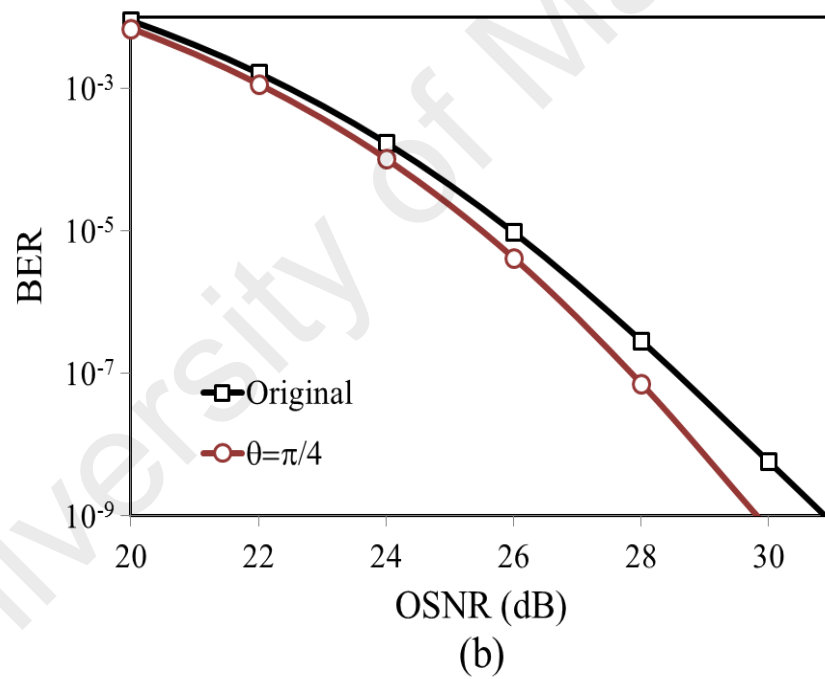
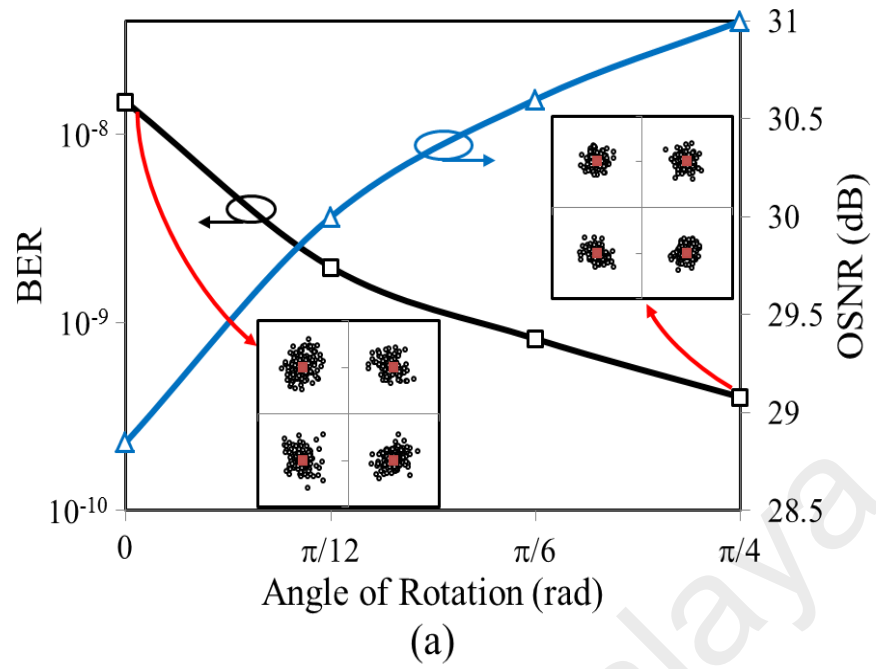


Figure 5.6: Influence of the angle of rotation on the BER performance of the AO-OFDM system.

5.6 Summary

In this chapter, a new approach for reducing PAPR and mitigating the nonlinear fiber impairments based on modulated half subcarriers in AO-OFDM systems with rotated QAM constellation has been presented. To reduce the PAPR, the odd subcarriers have been modulated with rotated QAM constellation, while the even subcarriers have been modulated with standard QAM constellation. The impact of the rotation angle on the PAPR has been analytically modeled and numerically demonstrated. The effect of PAPR reduction on the system performance has been investigated by simulating the AO-OFDM system, which uses optical coupler-based IFFT/ FFT. The AO-OFDM system has been numerically demonstrated with 29 subcarriers. Each subcarrier has been modulated by a QAM modulator at a symbol rate of 25 Gsymbol/s. The results reveal that the performance of the system is dependent on the angle difference between constellations of the odd and even subcarriers and best performance can be obtained at rotation angle of $\pi/4$ rad. The proposed technique can improve the PAPR by 0.8 dB at $\text{CCDF} = 1 \times 10^{-3}$ and can reduce the phase noise variance due to fiber nonlinearity, too. In addition, the optical OSNR of the proposed system can be improved in comparison with the original AO-OFDM system without PAPR reduction where, at transmission distance of 1100 km and rotation angle of $\pi/4$ rad, the OSNR is improved by ~ 2.3 dB.

CHAPTER 6

EFFECTIVENESS OF PHASE-CONJUGATED TWIN WAVES ON FIBER NONLINEARITY IN SPATIALLY MULTIPLEXED AO-OFDM SYSTEM

6.1 Introduction

All-optical orthogonal frequency division multiplexing (AO-OFDM) systems have intriguing ability to transmit higher data rate. They employ a multi-level modulation format to enhance the spectral efficiency as discussed in the previous chapters and many literatures (Hillerkuss et al., 2011; X. Liu et al., 2011b). However, the achievable transmission distance is limited due to the distortion effect caused by fiber nonlinearity and amplified spontaneous emission (ASE) noise from the optical amplifiers. Specifically, AO-OFDM system with a high-order modulation format is sensitive to nonlinear phase noises induced by self-phase modulation (SPM), cross-phase modulation (XPM), and four-wave mixing (FWM) effects. The interaction of fiber nonlinearity with ASE noise may cause a random nonlinear phase noise, which is difficult to compensate.

Several compensation techniques have been proposed and demonstrated to mitigate fiber nonlinearity impairments. For instance, digital-back-propagation (DBP) technique was proposed to eliminate nonlinear distortion by inverting the distorted signal at the receiver digitally (Ip & Kahn, 2008; Rafique & Ellis, 2011). However,

DBP requires solving the inverse nonlinear Schrödinger equation for the channel and is computationally expensive. The optical based compensation techniques were also proposed to suppress the nonlinear phase noises in the optical domain to reduce the processing time. The optical diversity transmission based on the coherent superposition of light waves have also been reported in recent years to mitigate fiber nonlinearity (Shahi & Kumar, 2012). In this technique, an optical signal and its replicas are simultaneously transmitted through multi-core/fiber and they are coherently superimposed at the reception. Furthermore, in order to achieve the full benefit of coherent superposition, the nonlinear distortions need to be decorrelated using some types of scrambling functions (Xiang Liu et al., 2012b). The performance of the system was improved in the presence of nonlinear phase noise, where a SNR was observed to be directly proportional to the number of superimposed signals. However, the spectral efficiency decreased by a factor equal to the number of cores. A mid-link optical phase conjugation (OPC) has also been proposed to cancel the nonlinear distortion (L. Li et al., 2011; Morshed et al., 2013; Pechenkin & Fair, 2010). However, the effectiveness of nonlinearity cancellation of OPC is governed by symmetry conditions where the OPC is inserted at the middle point of the link. This condition can significantly reduce the flexibility in an optical network.

Another interesting method called phase-conjugated twin waves (PCTWs) was also proposed to cancel the nonlinear distortion (X. Liu et al., 2013; Tian et al., 2013) by transmitting a signal and its phase-conjugated copy on the two signaling dimensions. The nonlinear distortion cancellation can be achieved by coherently superimposing two waves. The effectiveness of the PCTWs technique was demonstrated by transmitting PCTWs on orthogonal polarization (X. Liu et al., 2013). Moreover, the PCTWs technique was investigated on different wavelengths (Tian et al., 2013). However, by using PCTWs technique, the system sacrifices half of the spectral efficiency. In order to

increase the spectral efficiency, a phase-conjugated pilots (PCPs) technique has been proposed to cancel the fiber nonlinearity by transmitting a portion of the OFDM subcarriers as phase-conjugates of other subcarriers (Le et al., 2015).

In this chapter, we investigate and demonstrate a PCTWs technique to mitigate fiber nonlinear impairments and to suppress the nonlinear phase noise in spatially multiplexed AO-OFDM. In this technique, the m-array quadrature-amplitude modulation (mQAM) AO-OFDM signal and its phase-conjugated copy are transmitted through two identical fiber links. At the receiver, the two signals are coherently superimposed to cancel the correlated distortion and to enhance the signal to noise ratio. AO-OFDM signal and its phase-conjugated copy are optically generated by using OIFFT/OFFT circuits. The generated signal includes 29 subcarriers where each subcarrier is modulated by a 4QAM or 16QAM format at a symbol rate of 25 Gsymbol/s. To show the effectiveness of proposed technique, a spatially multiplexed AO-OFDM system is demonstrated by numerical simulation. A numerical results show that the proposed scheme improves nonlinearity tolerance and enhances achievable transmission distance.

6.2 Basic principle of PCTWs technique

The simplified diagram of a spatially multiplexed transmission link based on PCTWs technique, where the twin-conjugated waves are transmitted over two identical fiber links, is shown in Figure 6.1. We assume the two fiber links are identical (they have the same lengths, fiber parameters, and optical amplifiers), which lead to anticorrelated nonlinear distortions on the two waves. Therefore, it is possible for the nonlinear distortions of two waves to cancel each other out when they are coherently

combined. However, in reality, two fibers will never be identical, leading to reduce the efficiency of the PCTWs technique. The nonlinear distortions of the signal and its phase-conjugated copy are not exactly equal but they almost equal when two fibers have same length. In fact, to achieve the full benefit of proposed technique and to minimize the cost of implantation, two signals should be transmitted over a multi-core fiber (MCF) link with integrating optical amplifiers. In long haul transmission links, the distortion can be divided into linear and nonlinear distortion. The linear distortion is mainly caused by dispersion while the nonlinear distortion is induced by fiber nonlinearity and its interaction with ASE noises (Ip & Kahn, 2008). The proposed technique is able to cancel the nonlinear distortion due to fiber nonlinearity by assuming the distortion of the signal is anticorrelated with distortion of its phase-conjugated copy. Unfortunately, nonlinear distortions due to ASE noise and its interaction with fiber nonlinearity cannot be suppressed because of their random nature.

At the receiver site, the PCTWs are coherently superimposed to produce a new signal with lower nonlinear distortion. At the end of the transmission link, the optical field of the signals can be expressed as:

$$\begin{aligned} u_1(z,t) &= u(0,t) + \delta u_1, \\ u_2(z,t) &= u^*(0,t) + \delta u_2, \end{aligned} \tag{6.1}$$

where $u_1(z,t)$ and $u_2(z,t)$ are the optical field of the signals that propagate through two fiber links, respectively, z is the transmission distance, $u(0,t)$ and $u^*(0,t)$ are the optical fields of transmitted signal and its phase-conjugated copy. Here δu_1 and δu_2 represent the distortions of $u_1(z,t)$ and $u_2(z,t)$ signals, respectively. The distortions of

δu_1 and δu_2 are caused by fiber nonlinearity and noise of optical amplifiers and thus they can be expressed as:

$$\begin{aligned}\delta u_1 &= \delta u_{1NL} + \delta u_{1RNL}, \\ \delta u_2 &= \delta u_{2NL} + \delta u_{2RNL},\end{aligned}\tag{6.2}$$

where δu_{1NL} and δu_{2NL} are distortions due to fiber nonlinearity while δu_{1RNL} and δu_{2RNL} are distortions due to ASE noise and its interaction with fiber nonlinearity. After coherent superposition of PCTWs and averaging the received signal, the optical field of received signal becomes;

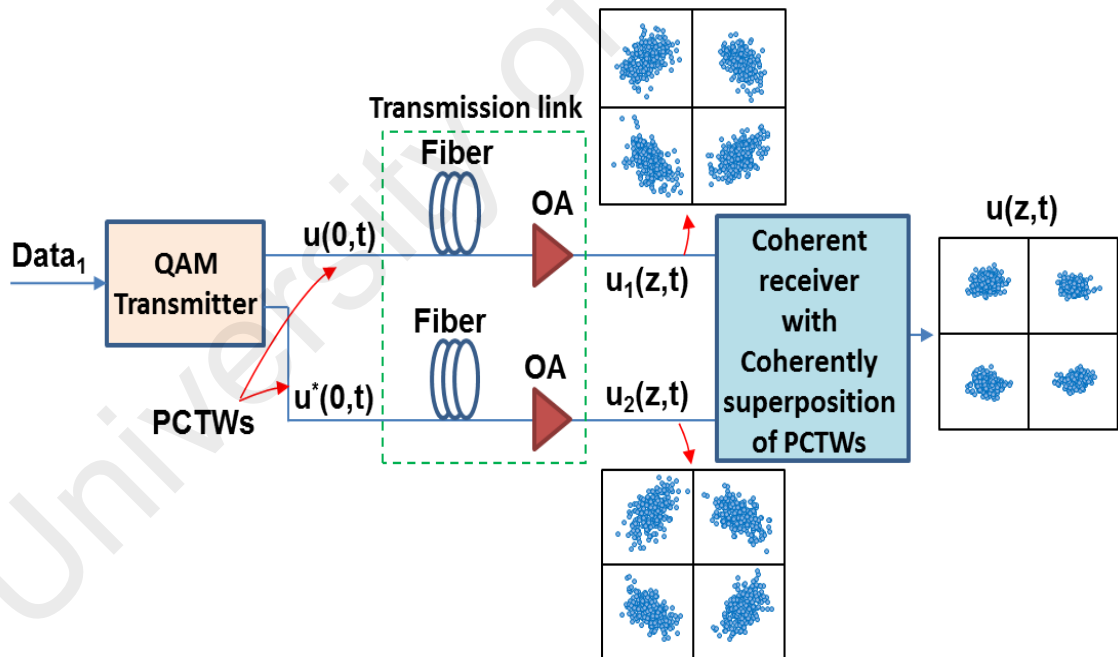


Figure 6.1: Illustration of the spatially multiplexed transmission link based on PCTWs technique.

$$u(z,t) = \frac{u_1(z,t) + u_2^*(z,t)}{2}. \quad (6.3)$$

By substituting Eq. (6.1) and Eq. (6.2) into Eq. (6.3), the received signal can be written as:

$$u(z,t) = u(0,t) + \frac{\delta u_{1NL} + (\delta u_{2NL})^* + \delta u_{1RNL} + (\delta u_{2RNL})^*}{2} \quad (6.4)$$

In the proposed system, both waves are modulated by the same optical carrier before they are launched to propagate over two identical fiber links, which uses the similar fiber parameters and optical amplifiers. This leads to anticorrelation between nonlinear distortions of two waves, $\delta u_{1NL} = -(\delta u_{2NL})^*$ (X. Liu et al., 2014). Therefore, it is possible for the nonlinear distortions of two waves to cancel each other out when they are coherently combined (X. Liu et al., 2014; X. Liu et al., 2013). However, the random nonlinear distortion of the received signal, which is induced by ASE noise and its interaction with fiber nonlinearity, is included in the random distortions term $[\delta u_{1RNL} + (\delta u_{2RNL})^*]/2$ and it can produce a random nonlinear phase noise ϕ_{RNL} in the received signal. The random nonlinear phase noise of the received signal can be calculated by taking the mean of participated phase noises and can be expressed as:

$$\phi_{RNL} = \frac{\phi_{1RNL} + \phi_{2RNL}}{2}, \quad (6.5)$$

where ϕ_{1RNL} and ϕ_{2RNL} are the random nonlinear phase noises due to distortions δu_{1RNL} and δu_{2RNL} , respectively. The phase noise variance of received signal $\sigma_{\phi_{RNL}}^2$ can be written as:

$$\sigma_{\phi_{RNL}}^2 = \frac{\sigma_{\phi_{1RNL}}^2 + \sigma_{\phi_{2RNL}}^2}{4} \approx \frac{\sigma_{\phi_{1RNL}}^2}{2}, \quad (6.6)$$

where $\sigma_{\phi_{1RNL}}^2$ and $\sigma_{\phi_{2RNL}}^2$ are the variances of random nonlinear phase noise of signal and its phase-conjugated copy, respectively.

6.3 Spatially multiplexed AO-OFDM system setup

Figure 6.2 shows the schematic of the spatially multiplexed AO-OFDM transmission system using two fiber links. The system is composed of an AO-OFDM transmitter, two multi-span fiber links, and AO-OFDM receiver. The AO-OFDM transmitter consists of an optical frequency comb generator (OFCG), wavelength selected switch, optical QAM modulators, and an optical beam combiner. The OFCG generates 29 subcarriers with frequency spacing of 25 GHz from a single laser source. Subsequently, the generated subcarriers are split and applied to optical QAM modulators. In each modulator, the QAM symbol and its phase-conjugated copy are generated from a PRBS generator. The modulated subcarriers of PCTWs are combined in time domain using two optical beam combiners to generate QAM AO-OFDM signal and its phase-conjugated copy. Then, the generated signals are transmitted through multi-span fiber links.

The transmission link utilizes two identical multi-span fiber links. Each fiber span consists of a standard single mode optical fiber (SSMF), a dispersion compensating optical fiber (DCF), and an Erbium doped fiber amplifier (EDFA) as shown in Figure 6.2. The SSMF is modeled with an attenuation coefficient of 0.2 dB/km, a dispersion coefficient of 16 ps/nm/km, an effective area of 80 μm^2 , and a fiber

nonlinearity coefficient of 1.3 W/km. A full periodic dispersion map is adopted to compensate the dispersion by utilizing a DCF. The DCF has a dispersion coefficient of -160 ps/(nm²km). For compensating the fibers losses, EDFAs (each has a noise figure of 6 dB) are employed at spans of 55 km spacing. The optical amplifiers must be kept close enough and their power gain is not much high for limiting the effect of ASE noise on the system performance.

An AO-OFDM receiver comprises two OFFT circuits (Hillerkuss et al., 2010a) and coherent QAM optical detectors as shown in Figure 6.2. The 4-order OFFT circuit is implemented in similar to that described in Section 3.2. Then, the output signals of OFFT are filtered by an optical band-pass filter before demodulating by coherent QAM optical detector. The resulted signals from demodulator are coherently superimposed to cancel the nonlinear distortion of received signal.

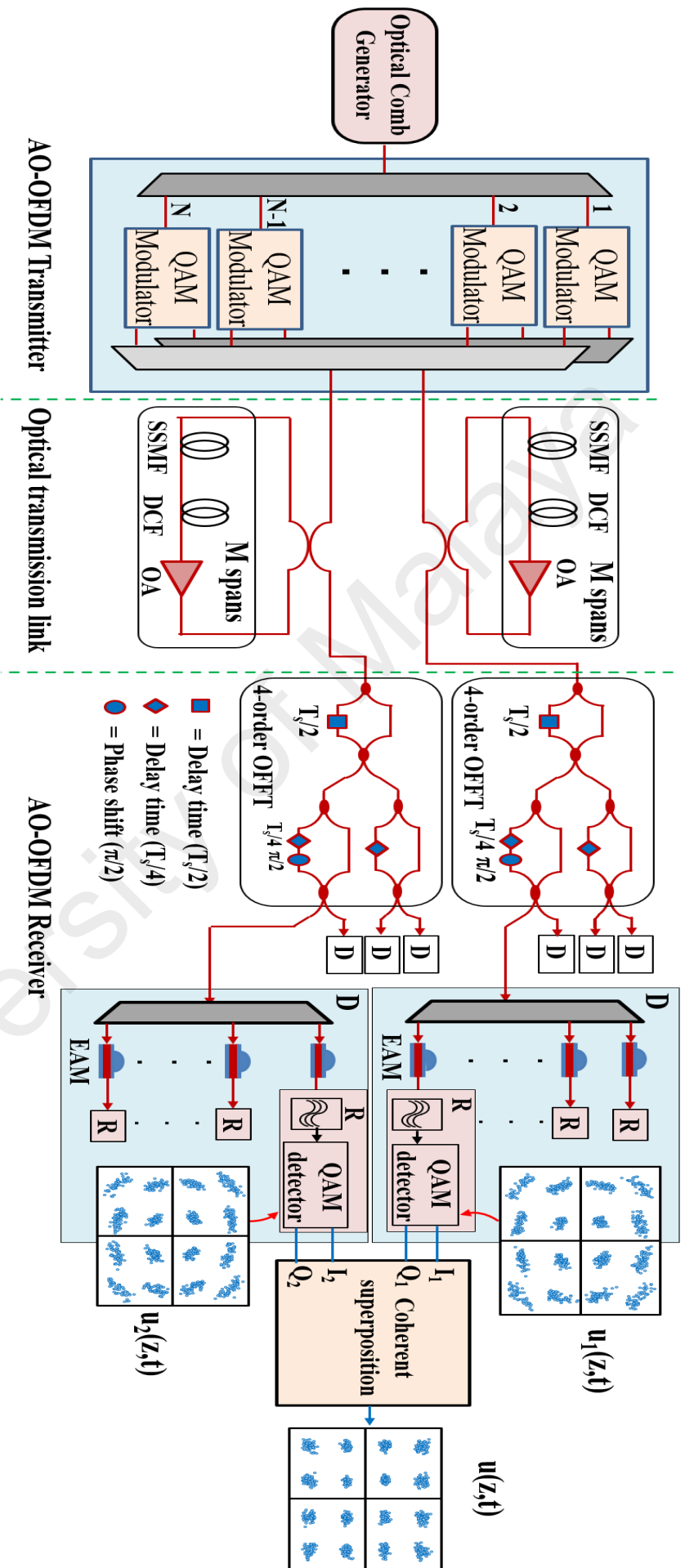


Figure 6.2: Schematic of a spatially multiplexed AO-OFDM system based on PCTW technique.

6.4 Results and discussions

The performance of spatially multiplexed AO-OFDM system is investigated and demonstrated by a simulation according to the schematic diagram shown in Figure 6.2. The numerical simulation is performed by VPItransmissionMaker 9.0 software. Each of the AO-OFDM signal and its phase-conjugated copy consist of 29 subcarriers. The proposed system is simulated with 4QAM and 16QAM at a symbol rate of 25 Gsymbol/s. To quantify the effectiveness of the proposed scheme, the obtained results are compared with those of original AO-OFDM system (without PCTWs technique).

The effectiveness of fiber nonlinearity cancellation is explained by plotting error vector magnitudes (EVMs) of the proposed and original AO-OFDM systems versus launched power as shown in Figure 6.3. The transmission distances are set to 550 km (10 spans) and 165 km (3 spans) for 4QAM and 16QAM format, respectively. It can be observed that the EVM of proposed scheme is lower than that for original system over entire subcarrier power range. In other words, the phase noise at low signal power is mostly resulted by ASE noise of optical amplifiers but our approach able to mitigate it. This is because the proposed system can reduce the random phase noise. Similarly, at high signal power, the random nonlinear phase noise is mitigated. When the power of subcarrier is increased from -1 dBm to 3 dBm, the EVM is increased by 0.091 for original system and by 0.0545 with using PCTWs technique. Moreover, the EVMs of proposed system for both 4QAM and 16QAM are reduced by ~29% as compared with original system.

To explore the improvement of our technique, the SNR of the proposed and original spatially multiplexed AO-OFDM systems is plotted against the power of subcarrier as depicted in Figure 6.4. The transmission distances are set at 550 km (10 spans) and 165 km (3 spans) for 4QAM and 16QAM format, respectively. It is

observed that the SNR of proposed scheme is higher than that of the original system. For both 4QAM and 16 QAM AO-OFDM systems, the proposed technique can improve SNR by ~ 3.5 dB and ~ 2.5 dB, respectively, due to cancelling the nonlinear distortion and reducing the random nonlinear phase noise.

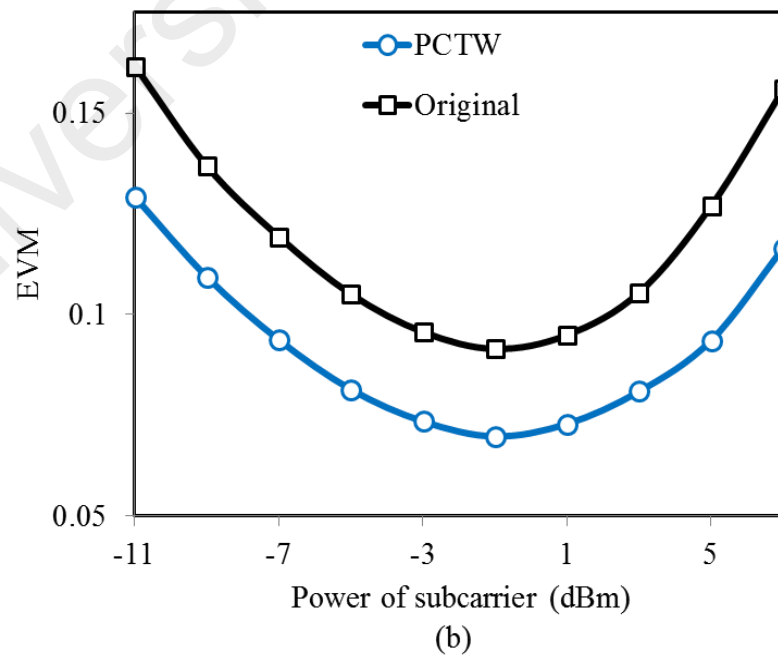
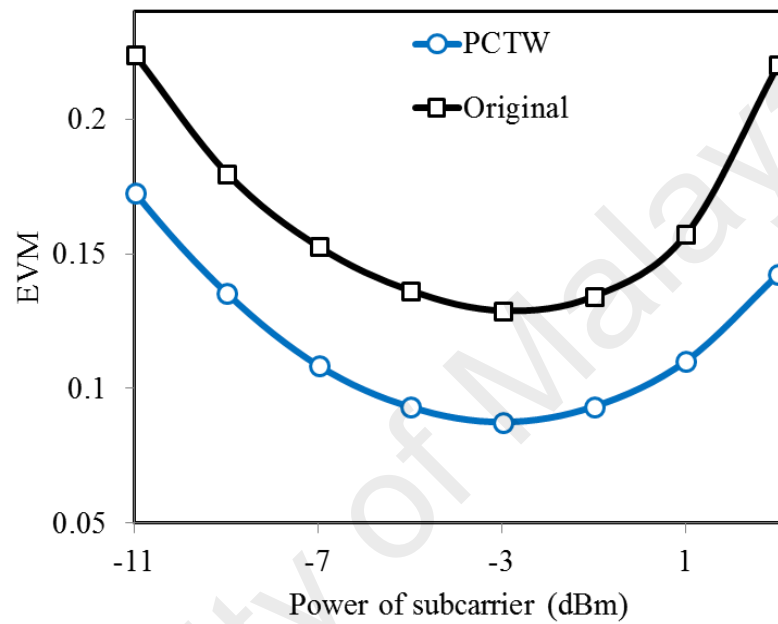


Figure 6.3: EVM versus power of subcarrier in AO-OFDM system with and without PCTW, a) 4QAM AO-OFDM system, b) 16QAM AO-OFDM system.

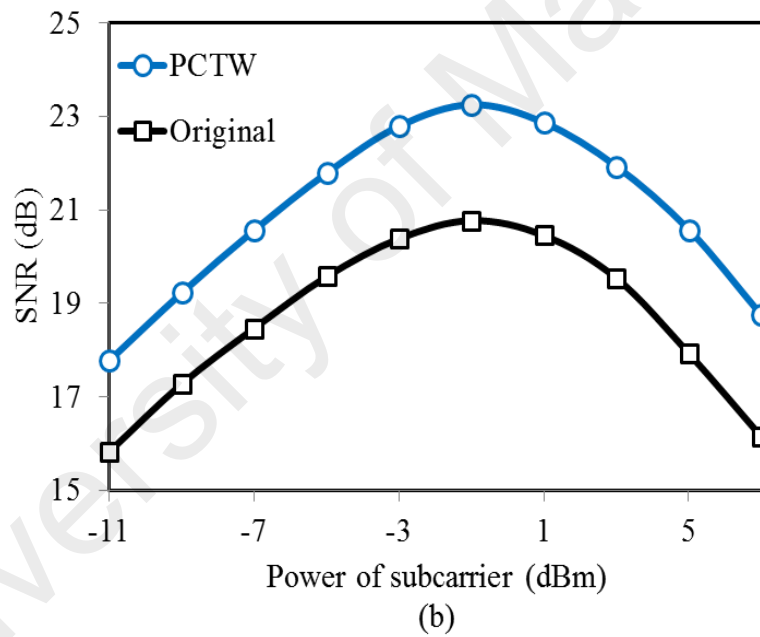
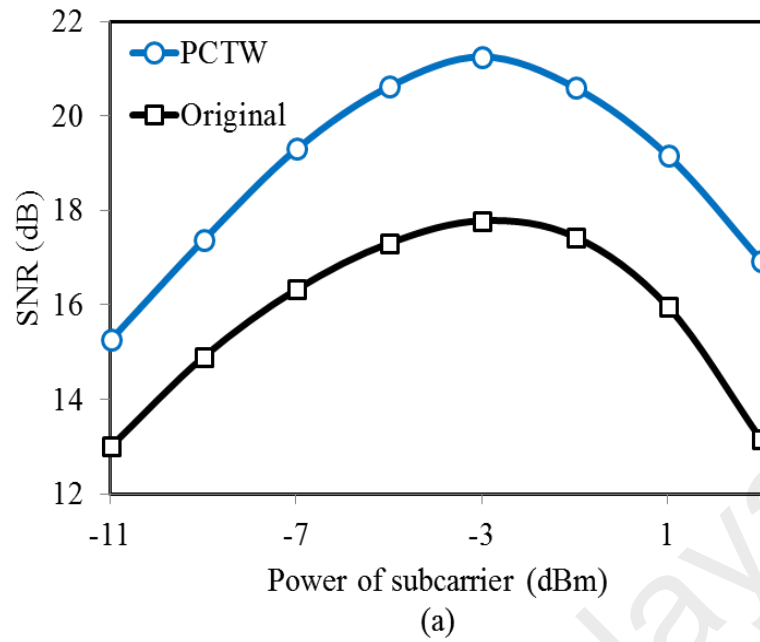


Figure 6.4: SNR versus power of subcarrier in AO-OFDM system with and without PCTW, a) 4QAM AO-OFDM system, b) 16QAM AO-OFDM system.

Due to fiber nonlinearity mitigation, a longer transmission distance can be achieved by employing PCTWs technique for both 4QAM and 16QAM formats as shown in Figure 6.5. At a BER of 3.8×10^{-3} , the transmission distance of the proposed

system that employs 4QAM is increased by ~45% as compared to the system without PCTWs technique. In addition, at a BER of 3.8×10^{-3} , the achievable transmission distance for 16QAM format increases from 330 km for original system to 495 km for the system with PCTWs technique.

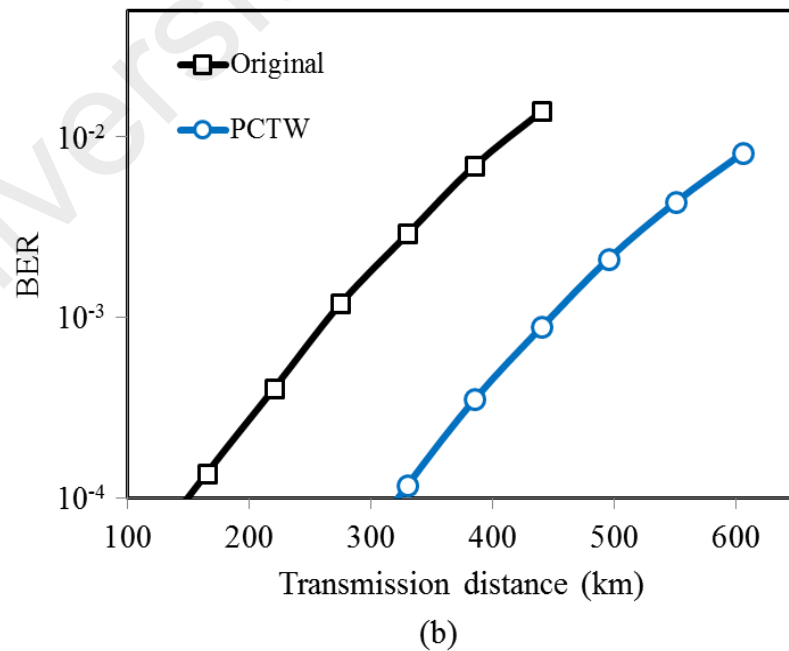
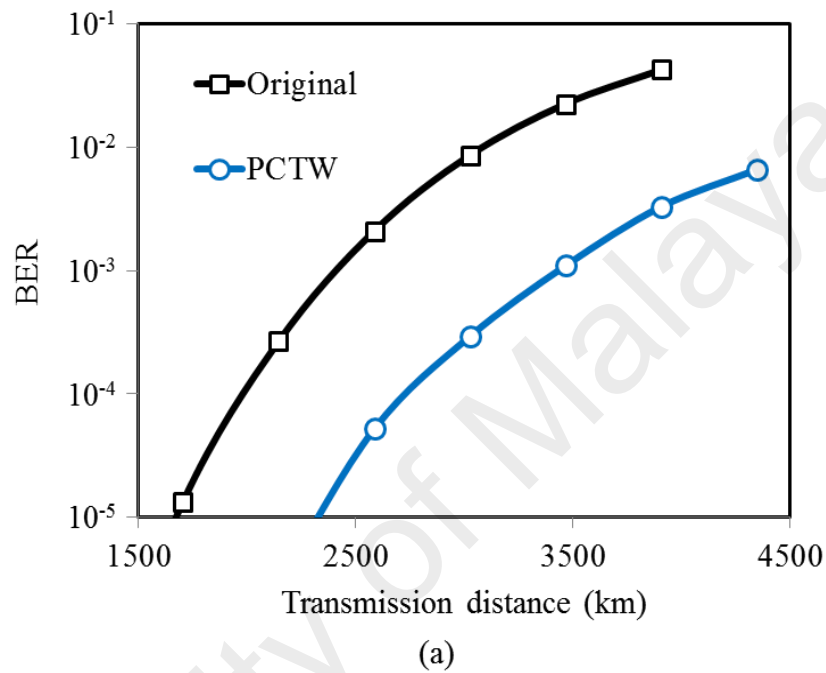


Figure 6.5: Bit rate error versus transmission distance in AO-OFDM system with and without PCTW, a) 4QAM AO-OFDM system, b) 16QAM AO-OFDM system.

Figure 6.6 shows the constellation diagrams of received signals with and without employing PCTWs technique. The results are obtained for 29 subcarriers and transmission distances of 1100 km and 275 km for 4QAM and 16QAM formats, respectively. The power of the subcarrier is set to the optimum value where it is equal to -3 dBm for 4QAM format and -1 dBm for 16QAM format. It can be observed that the constellation become easily discernable when the PCTWs technique is employed because the constellations become more squeezed around the ideal constellation (red squares). Thanks to the PCTWs technique, we successfully cancel the nonlinear phase noise and reduce the random nonlinear phase noise in AO-OFDM system that employ 4QAM and 16QAM formats.

Finally, BER performance of both proposed and original systems are depicted in Figure 6.7. The spatially multiplexed AO-OFDM system that employs PCTWs technique always exhibits a superior BER performance than original system. For proposed system that employ 4QAM modulation, the required optical signal-to-noise ratio (OSNR) to obtain BER of 3.8×10^{-3} , at transmission distance of 1100 km, is reduced by 4.5 dB as compared with original system. Furthermore, the required OSNR to obtain BER of 3.8×10^{-3} , for proposed system that employ 16QAM modulation, is 4 dB below that required for conventional system. Based on the results in Figure 6.5, Figure 6.6 and Figure 6.7, we can conclude that the transmission performance of proposed system is substantially improved.

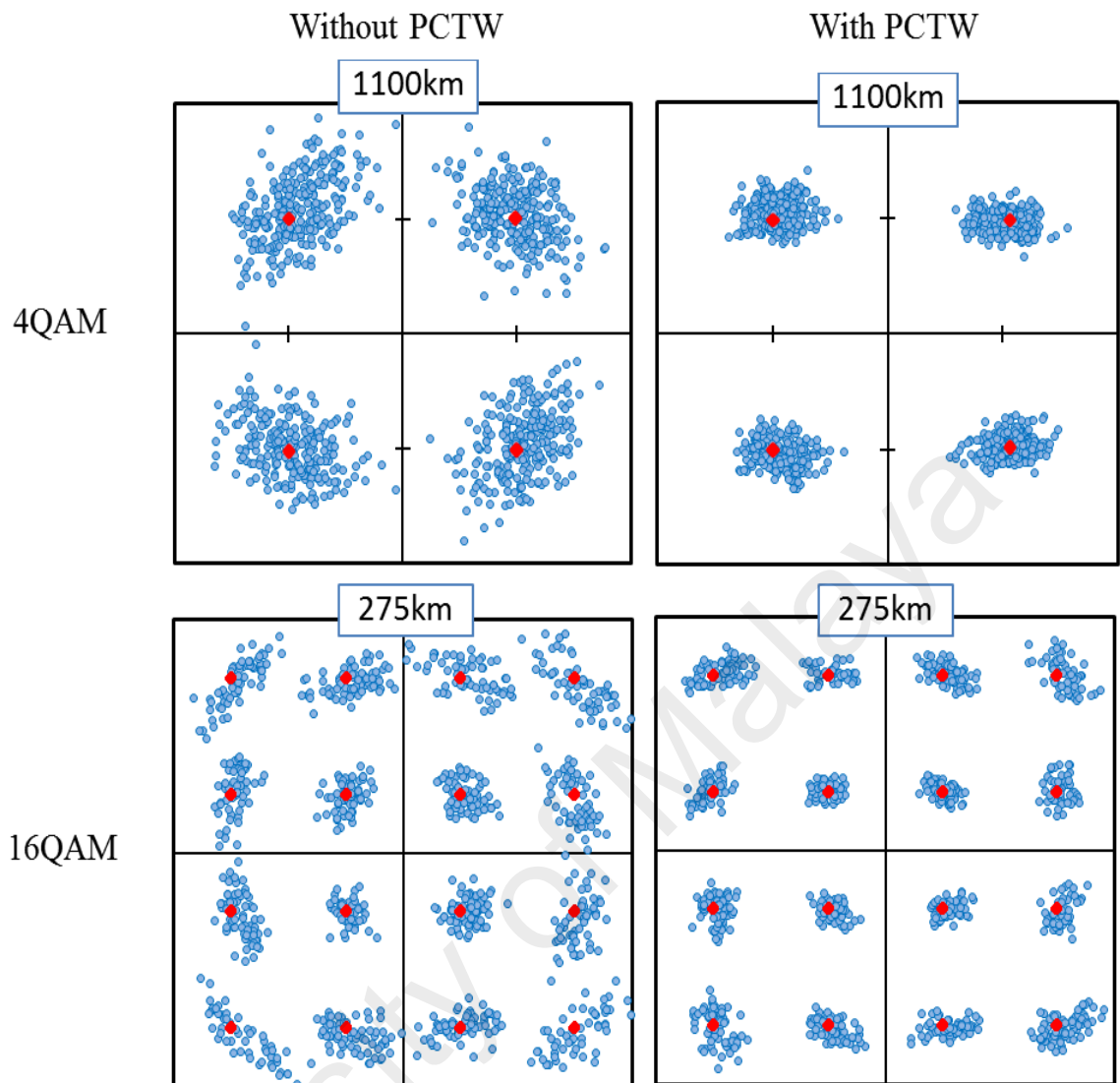
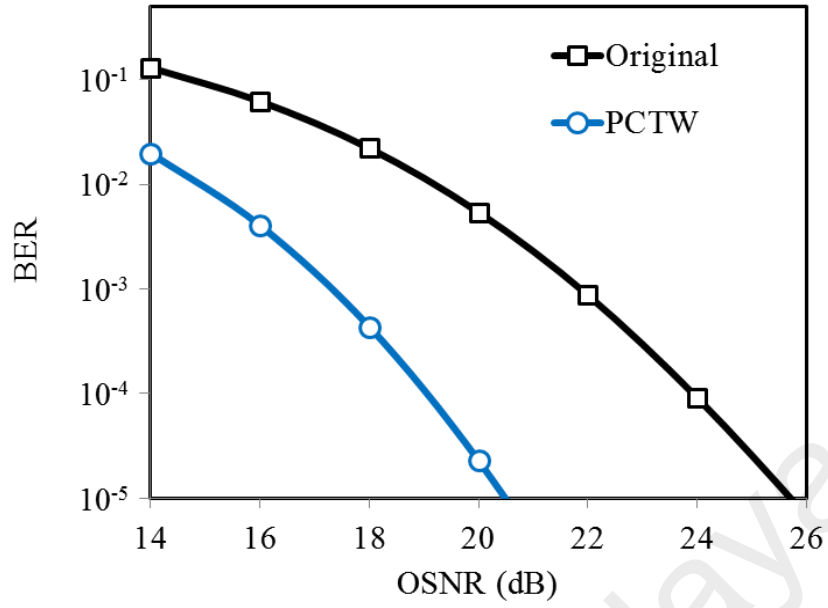
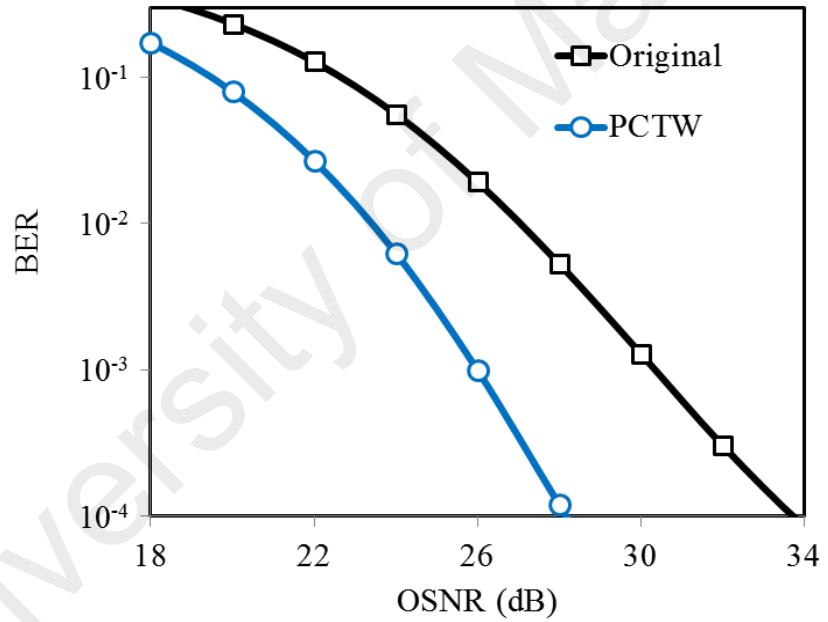


Figure 6.6: Constellation diagrams of the AO-OFDM signal with and without PCTWs technique for 4QAM and 16QAM formats.



(a)



(b)

Figure 6.7: BER performance for spatially multiplexed AO-OFDM, a) 4QAM, b) 16QAM.

6.5 Summary

We have demonstrated a new technique to suppress nonlinear phase noise in spatially multiplexed AO-OFDM systems based on PCTWs technique. In this technique, AO-OFDM signal and its phase-conjugated copy have been directly transmitted through two identical fiber links. At the receiver, the two signals have been coherently superimposed to cancel the phase noise and to enhance signal-to-noise ratio. To show the effectiveness of proposed technique, a spatially multiplexed AO-OFDM system has been demonstrated by numerical simulation. AO-OFDM signal and its phase-conjugated copy have been optically generated by using coupler-based all-optical inverse fast Fourier transform / fast Fourier transform (OIFFT/OFFT). The generated signal includes 29 subcarriers where each subcarrier has been modulated by a QAM format at a symbol rate of 25 Gsymbol/s. The results reveal that the performance of the proposed system has been substantially improved where SNR has been increased by ~3.5 dB as compared with original system. In addition, the transmission performance of the system has been improved, where the transmission distance of the proposed system that employs 4QAM is increased by ~45% as compared to that of the system without PCTWs.

CHAPTER 7

CONCLUSIONS AND FUTURE WORKS

7.1 Conclusions

This thesis has presented the comprehensive analysis of all-optical orthogonal frequency division multiplexing (AO-OFDM) system performance in presence of nonlinear phase noises. Here, four techniques have been theoretically studied to mitigate the nonlinear fiber impairments in an AO-OFDM system. In this work, the performance of m-array quadrature amplitude modulation (mQAM) AO-OFDM systems has been investigated by using the analytical modeling as well as simulation in the presence of various impairments. These impairments are phase noise of laser sources, fiber attenuation, chromatic dispersion, nonlinear fiber impairments and amplified spontaneous emission (ASE) noise. The performance of AO-OFDM system has been investigated by demonstrating and comparing analytical results based on the newly developed model and simulation results using VPItransmissionMaker software. The proposed AO-OFDM system uses coupler-based optical inverse fast Fourier transform/fast Fourier transform (OIFFT/OFFT) without any digital nonlinear compensation. The system employs 29 subcarriers; each subcarrier has been modulated by a 4QAM or 16QAM format with symbol rate of 25 Gsymbol/s. The analytical and simulation results have enabled us to estimate the optimum performance and the factors that limit the transmission distance.

At first, a new analytical model has been developed in Chapter 3 to estimate the phase noise due to the nonlinear fiber impairments and their interaction with ASE noise

in AO-OFDM systems that employ high-order modulation formats. By using this analytical model, the influences of the launched power, number of subcarriers, transmission distance, and dispersion on the nonlinear fiber impairments in AO-OFDM system have been quantitatively explored. It is found that the nonlinear phase noise induced by FWM effect in a transmission fiber is the dominant nonlinear effect in AO-OFDM systems, especially when the system is operating at near zero dispersion wavelengths. This is attributed to photon-photon interaction among all subcarriers, where appropriate phase-matching conditions are easily satisfied at near zero dispersion ($D = 0$ ps/nm/km) wavelength especially when these subcarriers are generated from the same laser source. It is found that the optimum performance with minimum phase noise has been achieved at input signal powers of -3 dBm and -1 dBm for 4QAM and 16QAM AO-OFDM systems, respectively using a transmission fiber with $D = 16$ ps/nm/km. To validate our analytical model, the analytical results have been compared with simulation results. It has been clarified that the simulation results show a good agreement with the analytical results.

The following chapters proposed various new techniques for mitigating the effect of nonlinear fiber impairments. Two techniques have been proposed in Chapter 4. In first technique, mitigation of nonlinear fiber impairments has been demonstrated based on reducing the effective power of the subcarriers by reshaping their envelopes. Therefore, each subcarrier has been modulated by return-to-zero mQAM (RZ-mQAM) format. To keep the processing speed of OIFFT, the subcarriers have optically been modulated at transmitter in which each subcarrier has first been modulated by mQAM format and then directly shaped by RZ carver. At the receiver side, the conversion from RZ-mQAM to mQAM has been done by using a Mach-Zehnder interferometer (MZI) with delay time equal to half symbol period. The analytical model has been developed to estimate the nonlinear fiber impairments in proposed system. The nonlinear phase

noise variances of proposed system have been compared with that evaluated in Chapter 3 for investigating the efficiency of proposed technique. Although, the phase noise variance due to ASE noise has been increased, the analytical results have shown a good reduction in phase noise variances due to XPM and FWM. The performance of the proposed system has also been examined by VPItransmissionMaker software for RZ-4QAM and RZ-16QAM formats and compared with original AO-OFDM system that uses 4QAM and 16QAM formats. The simulation results reveal that the performance of the proposed system is better than that of the conventional system with original m-QAM format due to the reduction of its nonlinear phase noise. The minimum error vector magnitude (EVM) has been obtained at higher launched input power when RZ-4QAM and RZ-16QAM formats are employed. In addition, the transmission distance has been substantially increased when RZ-4QAM and RZ-16QAM are adopted in AO-OFDM systems, as compared to that of the conventional OFDM systems with 4QAM and 16QAM formats. This is attributed to the proposed system is able to transmit higher power at certain nonlinear phase noise.

In second technique, the nonlinear fiber impairments have been optically mitigated by minimizing interaction time among AO-OFDM subcarriers. To minimize the interaction time, the subcarriers have first been modulated by RZ-mQAM format and then even subcarriers have been delayed in time with respect to odd subcarriers. Therefore, the odd and even subcarriers have been alternately delayed (AD) and AD RZ-QAM OFDM signals can be produced. The analytical model that describes the proposed system has been developed to calculate the optimum delay time and the resulted variance of nonlinear phase noise. It has been found that the optimum performance with minimum phase noise has been obtained at delay time equal to half the symbol duration. At optimum delay time, the total nonlinear phase noise variance of the proposed system can be reduced by 34% for subcarrier input power of 3 dBm and

transmission distance of 550 km. Furthermore, the simulation results reveal that the performance of AD RZ-QAM OFDM system is superior to that of QAM OFDM system. At a bit error rate (BER) of 10^{-5} , the achievable transmission distance can be extended from 1595 km with 4QAM OFDM system to 2090 km with AD RZ-4QAM OFDM system.

In Chapter 5, the nonlinear fiber impairments have been mitigated by reducing peak-to-average power ratio (PAPR) of QAM OFDM system based on modulating half subcarriers with rotated QAM constellation. In this system, the odd subcarriers have been modulated with rotated QAM constellation, while the even subcarriers have been modulated with standard QAM constellation. The analytical model has been developed for describing the proposed system and estimating the complementary cumulative distribution function (CCDF) of $(PAPR < x)$, the optimum rotation angle and the variance of nonlinear phase noise. The effectiveness of rotation constellation technique on PAPR has been numerically investigated. The analytical results indicate that the optimum performance can be obtained at rotation angle of $\pi/4$, where, at $CCDF = 1 \times 10^{-3}$, the PAPR can be reduced by more than 0.8 dB as compared with conventional AO-OFDM system. The maximum peaks can be also lowered by ~15% at rotation angle of $\pi/4$. In addition, the performance of the AO-OFDM system has been improved since the nonlinear fiber impairments can be mitigated. The simulation results show that, at transmission distance of 1100 km and rotation angle of $\pi/4$, the required optical signal-to-noise ratio (OSNR) can be improved by ~2.3 dB as compared with AO-OFDM system without PAPR reduction.

In Chapter 6, the nonlinear fiber impairments in AO-OFDM system have been optically mitigated based on phase-conjugated twin waves (PCTWs) technique. Here, AO-OFDM signal and its phase-conjugated copy have been directly transmitted through

two identical fiber links. That means the AO-OFDM signal and its phase-conjugated copy have been transmitted over two orthogonal spatial paths. At the receiver, the PCTWs have been coherently superimposed to cancel the phase noise and to enhance signal-to-noise ratio (SNR). The performance of proposed system has been demonstrated by numerical simulation. The results reveal that the performance of the system has been substantially improved due to cancelling the nonlinear distortion and reducing the random nonlinear phase noise. For both 4QAM and 16QAM AO-OFDM systems, the proposed technique can improve SNR by ~ 3.5 dB and ~ 2.5 dB, respectively. In addition, with employing 4QAM formats, the achievable transmission distance of the proposed system can be extended by $\sim 45\%$ as compared to that of the system without PCTWs.

In summary, the performance of mQAM AO-OFDM system has been comprehensively analyzed in presence of nonlinear phase noises. Four techniques have been proposed for mitigating the nonlinear fiber impairments in mQAM AO-OFDM system. Each technique has been analytically modeled and numerically demonstrated.

7.2 Future works

In this section, a brief discussion on future research works is given with some suggestions.

1. In this thesis, the analytical models have been developed to describe the AO-OFDM system in single polarization. The polarization multiplexing OFDM system adds other significant interferences between the x- and y- polarized signals such as the cross-polarization modulation (XPoIM). In future work, the

analytical models can be developed to investigate the nonlinear fiber impairments in polarization multiplexing AO-OFDM system.

2. This thesis theoretically investigates various optical techniques to mitigate the nonlinear fiber impairments in 4QAM and 16QAM AO-OFDM system. The future research efforts can be made on investigating these techniques experimentally.
3. One of the ideas for future work is the performance investigation of AO-OFDM system with employing a higher order of modulation format such as m-array phase shift keying (mPSK) and mQAM formats over 64-level can be obtained using the model.
4. The modulation and detection of mQAM AO-OFDM signal require the use of laser sources. The linewidth of laser sources degrades the performance of the system specifically with employing high order modulation formats. Reducing the linewidth of lasers is essential to reduce the phase noise in future mQAM AO-OFDM systems.
5. The nonlinear fiber impairments are effectively mitigated by the PCTWs technique. For future work, the implementation of PCTWs technique in AO-OFDM system by utilizing two orthogonal time slots would be desirable.

REFERENCES

- Abdalla, A., Ferreira, R., Shahpari, A., Reis, J. D., Lima, M., & Teixeira, A. (2014). Improved nonlinear tolerance in ultra-dense WDM OFDM systems. *Optics Communications*, 326, 88-93.
- Agrawal, G. P. (2007). *Nonlinear fiber optics*: Academic press.
- Agrawal, G. P. (2012). *Fiber-optic communication systems* (Vol. 222): John Wiley & Sons.
- Agrawal, G. P. (2013). *Nonlinear fiber optics*: Academic press.
- Ahmed, J., Siyal, M. Y., Adeel, F., & Hussain, A. (2013). *Optical Signal Processing by Silicon Photonics*: Springer.
- Al-Mamun, S., & Islam, M. (2011). *Effect of Chromatic Dispersion on four-wave mixing in optical WDM transmission System*. Paper presented at the Industrial and Information Systems (ICIIS), 2011 6th IEEE International Conference on.
- Armstrong, J. (2009). OFDM for optical communications. *Journal of Lightwave Technology*, 27(3), 189-204.
- Benlachtar, Y., Gavioli, G., Mikhailov, V., & Killey, R. I. (2008). Experimental investigation of SPM in long-haul direct-detection OFDM systems. *Optics express*, 16(20), 15477-15482.
- Bernard, S. (2001). *Digital communications fundamentals and applications*. Prentice Hall, Inc.
- Bhandare, S., Sandel, D., Milivojevic, B., Hidayat, A., Fauzi, A. A., Zhang, H., . . . Noé, R. (2005). 5.94-Tb/s 1.49-b/s/Hz ($40 \times 2 \times 2 \times 40$ Gb/s) RZ-DQPSK polarization-division multiplex C-band transmission over 324 km. *IEEE Photonics Technology Letters*, 17(4), 914-916.
- Cao, Z., van den Boom, H., Tangdiongga, E., & Koonen, T. (2014). Interleaved and partial transmission interleaved optical coherent orthogonal frequency division multiplexing. *Optics letters*, 39(7), 2179-2182.
- Chandrasekhar, S., Liu, X., Zhu, B., & Peckham, D. (2009). Transmission of a 1.2-Tb/s 24-carrier no-guard-interval coherent OFDM superchannel over 7200-km of ultra-large-area fiber. *ECOC 2009*.

- Chang, R. W. (1966). Synthesis of Band-Limited Orthogonal Signals for Multichannel Data Transmission. *Bell System Technical Journal*, 45(10), 1775-1796.
- Chen, X., Al Amin, A., Li, A., & Shieh, W. (2013). Multicarrier Optical Transmission. *Optical Fiber Telecommunications Volume VIB: Systems and Networks*, 337.
- Chen, X., & Shieh, W. (2010). Closed-form expressions for nonlinear transmission performance of densely spaced coherent optical OFDM systems. *Optics express*, 18(18), 19039-19054.
- Chen, Y., Adhikari, S., Hanik, N., & Jansen, S. L. (2012). *Pilot-aided sampling frequency offset compensation for coherent optical OFDM*. Paper presented at the Optical Fiber Communication Conference.
- Cheng, K., & Conradi, J. (2002). Reduction of pulse-to-pulse interaction using alternative RZ formats in 40-Gb/s systems. *Photonics Technology Letters, IEEE*, 14(1), 98-100.
- Cho, P. S., Grigoryan, V. S., Godin, Y. A., Salamon, A., & Achiam, Y. (2003). Transmission of 25-Gb/s RZ-DQPSK signals with 25-GHz channel spacing over 1000 km of SMF-28 fiber. *Photonics Technology Letters, IEEE*, 15(3), 473-475.
- Demir, A. (2007). Nonlinear phase noise in optical-fiber-communication systems. *Journal of Lightwave Technology*, 25(8), 2002-2032.
- Dixon, B. J., Pollard, R. D., & Iezekiel, S. (2001). Orthogonal frequency-division multiplexing in wireless communication systems with multimode fiber feeds. *Microwave Theory and Techniques, IEEE Transactions on*, 49(8), 1404-1409.
- Djordjevic, I. B., & Vasic, B. (2006). Orthogonal frequency division multiplexing for high-speed optical transmission. *Optics express*, 14(9), 3767-3775.
- Donati, S., & Giuliani, G. (1997). Noise in an optical amplifier: Formulation of a new semiclassical model. *Quantum Electronics, IEEE Journal of*, 33(9), 1481-1488.
- Dou, Y., Zhang, H., & Yao, M. (2012). Generation of flat optical-frequency comb using cascaded intensity and phase modulators. *Photonics Technology Letters, IEEE*, 24(9), 727-729.
- Ellis, A. D., & Gunning, F. C. G. (2005). Spectral density enhancement using coherent WDM. *Photonics Technology Letters, IEEE*, 17(2), 504-506.

- Faisal, M., & Maruta, A. (2010). Cross-phase modulation induced phase fluctuations in optical RZ pulse propagating in dispersion compensated WDM transmission systems. *Optics Communications*, 283(9), 1899-1904.
- Georgiadis, A. (2004). Gain, phase imbalance, and phase noise effects on error vector magnitude. *Vehicular Technology, IEEE Transactions on*, 53(2), 443-449.
- Gnauck, A., Raybon, G., Chandrasekhar, S., Leuthold, J., Doerr, C., Stulz, L., . . . Hunsche, S. (2002). 2.5 Tb/s (64x42.7 Gb/s) transmission over 40x100 km NZDSF using RZ-DPSK format and all-Raman-amplified spans. Paper presented at the Optical Fiber Communication Conference.
- Goebel, B., Fesl, B., Coelho, L. D., & Hanik, N. (2008). *On the effect of FWM in coherent optical OFDM systems*. Paper presented at the Optical Fiber Communication Conference.
- Guan, P., Kong, D., Meldgaard Røge, K., Mulvad, H. C. H., Galili, M., & Oxenløwe, L. K. (2014). *Real-time all-optical OFDM transmission system based on time-domain optical fourier transformation*. Paper presented at the Optical Fiber Communication Conference.
- Hao, Y., Li, Y., Wang, R., & Huang, W. (2012). Fiber nonlinearity mitigation by PAPR reduction in coherent optical OFDM systems via biased clipping OFDM. *Chinese Optics Letters*, 10(1), 010701.
- Hayee, M., Cardakli, M., Sahin, A., & Willner, A. (2001). Doubling of bandwidth utilization using two orthogonal polarizations and power unbalancing in a polarization-division-multiplexing scheme. *Photonics Technology Letters, IEEE*, 13(8), 881-883.
- Hayee, M., & Willner, A. (1999). NRZ versus RZ in 10-40-Gb/s dispersion-managed WDM transmission systems. *Photonics Technology Letters, IEEE*, 11(8), 991-993.
- He, Z., Li, W., Tao, Z., ng Shao, J., Liang, X., Deng, Z., & Huang, D. (2011). *PAPR reduction in all-optical OFDM systems based on phase pre-emphasis*. Paper presented at the Journal of Physics: Conference Series.
- Hillerkuss, D., Marculescu, A., Li, J., Teschke, M., Sigurdsson, G., Worms, K., . . . Leuthold, J. (2010a). *Novel optical fast Fourier transform scheme enabling real-time OFDM processing at 392 Gbit/s and beyond*. Paper presented at the Optical Fiber Communication Conference.

- Hillerkuss, D., Schellinger, T., Schmogrow, R., Winter, M., Vallaitis, T., Bonk, R., . . . Meyer, J. (2010b). *Single Source Optical OFDM Transmitter and Optical FFT Receiver Demonstrated at Line Rates of 5.4 and 10.8 Tbit/s*. Paper presented at the Optical Fiber Communication Conference.
- Hillerkuss, D., Schmogrow, R., Schellinger, T., Jordan, M., Winter, M., Huber, G., . . . Frey, F. (2011). 26 Tbit s⁻¹ line-rate super-channel transmission utilizing all-optical fast Fourier transform processing. *Nature Photonics*, 5(6), 364-371.
- Hillerkuss, D., Winter, M., Teschke, M., Marculescu, A., Li, J., Sigurdsson, G., . . . Freude, W. (2010a). Simple all-optical FFT scheme enabling Tbit/s real-time signal processing. *Optics express*, 18(9), 9324-9340.
- Hillerkuss, D., Winter, M., Teschke, M., Marculescu, A., Li, J., Sigurdsson, G., . . . Leuthold, J. (2010b). *Low-complexity optical FFT scheme enabling Tbit/s all-optical OFDM communication*. Paper presented at the Photonic Networks, 2010 ITG Symposium on.
- Hmood, J., Noordin, K., Ahmad, H., & Harun, S. (2015). Performance Improvement of All-optical OFDM Systems based on Combining RZ coding with m-array QAM. *JOURNAL OF OPTOELECTRONICS AND ADVANCED MATERIALS*, 17(1-2), 33-38.
- Hmood, J. K., Emami, S. D., Noordin, K. A., Ahmad, H., Harun, S. W., & Shalaby, H. M. (2015a). Optical frequency comb generation based on chirping of Mach-Zehnder Modulators. *Optics Communications*, 344, 139-146.
- Hmood, J. K., Harun, S. W., Emami, S. D., Khodaei, A., Noordin, K. A., Ahmad, H., & Shalaby, H. M. (2015b). Performance analysis of an all-optical OFDM system in presence of non-linear phase noise. *Optics express*, 23(4), 3886-3900.
- Hmood, J. K., Noordin, K. A., Arof, H., & Harun, S. W. (2015c). Peak-to-average power ratio reduction in all-optical orthogonal frequency division multiplexing system using rotated constellation approach. *Optical Fiber Technology*, 25, 88-93.
- Hmood, J. K., Noordin, K. A., & Harun, S. W. (2016). Effectiveness of phase-conjugated twin waves on fiber nonlinearity in spatially multiplexed all-optical OFDM system. *Optical Fiber Technology*, 30, 147-152.
- Hmood, J. K., Noordin, K. A., Harun, S. W., & Shalaby, H. M. (2015d). Mitigation of phase noise in all-optical OFDM systems based on minimizing interaction time between subcarriers. *Optics Communications*, 355, 313-320.

- Ho, K.-P. (2005). *Phase-modulated optical communication systems*: Springer Science & Business Media.
- Ho, K.-P., & Kahn, J. M. (2004). Electronic compensation technique to mitigate nonlinear phase noise. *Lightwave Technology, Journal of*, 22(3), 779-783.
- Hoxha, J., & Cincotti, G. (2013). *Performance limits of all-optical OFDM systems*. Paper presented at the Transparent Optical Networks (ICTON), 2013 15th International Conference on.
- Huang, Y.-K., Ip, E., Wang, Z., Huang, M.-F., Shao, Y., & Wang, T. (2011). Transmission of spectral efficient super-channels using all-optical OFDM and digital coherent receiver technologies. *Lightwave Technology, Journal of*, 29(24), 3838-3844.
- Iida, T., Mizutori, A., & Koga, M. (2012). *Optical diversity transmission and maximum ratio combine in multi-core fiber to mitigate fiber non-linear distortion*. Paper presented at the 2012 17th Opto-Electronics and Communications Conference.
- Inoue, K. (1992). Phase-mismatching characteristic of four-wave mixing in fiber lines with multistage optical amplifiers. *Optics letters*, 17(11), 801-803.
- Ip, E., & Kahn, J. M. (2008). Compensation of dispersion and nonlinear impairments using digital backpropagation. *Lightwave Technology, Journal of*, 26(20), 3416-3425.
- Jacobsen, G., Bertilsson, K., & Xiaopin, Z. (1998). WDM transmission system performance: Influence of non-Gaussian detected ASE noise and periodic DEMUX characteristic. *Lightwave Technology, Journal of*, 16(10), 1804-1812.
- Jansen, S. L., Morita, I., Schenk, T. C., & Tanaka, H. (2008). Long-haul transmission of 16×52.5 Gbits/s polarization-division-multiplexed OFDM enabled by MIMO processing. *Journal of Optical Networking*, 7(2), 173-182.
- Jayapalasingam, A., & Alias, M. Y. (2012). *Peak-to-average power ratio reduction of OFDM signals using IIR filters*. Paper presented at the Telecommunication Technologies (ISTT), 2012 International Symposium on.
- Kang, I. (2012). *All-optical OFDM transmission using photonic integrated optical DFT devices*. Paper presented at the Opto-Electronics and Communications Conference (OECC), 2012 17th.

- Kang, I., Chadrachar, S., Rasras, M., Liu, X., Cappuzzo, M., Gomez, L., . . . Jaques, J. (2011). Long-haul transmission of 35-Gb/s all-optical OFDM signal without using tunable dispersion compensation and time gating. *Optics express*, 19(26), B811-B816.
- Khurgin, J. B., Xu, S., & Boroditsky, M. (2004). Reducing adjacent channel interference in RZ WDM systems via dispersion interleaving. *Photonics Technology Letters, IEEE*, 16(3), 915-917.
- Kikuchi, K. (2011). Analyses of wavelength-and polarization-division multiplexed transmission characteristics of optical quadrature-amplitude-modulation signals. *Optics express*, 19(19), 17985-17995.
- Kim, A., Joo, Y. H., & Kim, Y. (2004). 60 GHz wireless communication systems with radio-over-fiber links for indoor wireless LANs. *Consumer Electronics, IEEE Transactions on*, 50(2), 517-520.
- Koga, M., Mizutori, A., & Iida, T. (2013). Optical diversity transmission and maximum-ratio combined receiver in multi-core fiber to mitigate fiber non-linear phenomenon. *IEICE Communications Express*, 2(2), 67-73.
- Kumar, S. (2011). *Impact of Nonlinearities on Fiber Optic Communications* (Vol. 7): Springer Science & Business Media.
- Kumar, S., & Yang, D. (2008). Optical implementation of orthogonal frequency-division multiplexing using time lenses. *Optics letters*, 33(17), 2002-2004.
- Kumar, S., & Yang, D. (2009). *Application of time lenses for high speed fiber-optic communication systems*. Paper presented at the Computers and Devices for Communication, 2009. CODEC 2009. 4th International Conference on.
- Lau, A. P. T., Rabbani, S., & Kahn, J. M. (2008). On the statistics of intrachannel four-wave mixing in phase-modulated optical communication systems. *Journal of Lightwave Technology*, 26(14), 2128-2135.
- Le Khoa, D., Tu, N. T., Thu, N. T. H., & Phuong, N. H. (2012). *Scrambling algorithms for peak-to-average power ratio reduction in long haul coherent optical OFDM systems*. Paper presented at the Signal Processing and Information Technology (ISSPIT), 2012 IEEE International Symposium on.
- Le, S., McCarthy, M., Mac Suibhne, N., Ellis, A., & Turitsyn, S. (2014). *Phase-conjugated pilots for fibre nonlinearity compensation in CO-OFDM transmission*. Paper presented at the Optical Communication (ECOC), 2014 European Conference on.

- Le, S. T., Blow, K., & Turitsyn, S. (2014). Power pre-emphasis for suppression of FWM in coherent optical OFDM transmission. *Optics express*, 22(6), 7238-7248.
- Le, S. T., McCarthy, M. E., Suibhne, N. M., Ellis, A. D., & Turitsyn, S. K. (2015). Phase-Conjugated Pilots for Fibre Nonlinearity Compensation in CO-OFDM Transmission. *Journal of Lightwave Technology*, 33(7), 1308-1314.
- Lee, K., Thai, C. T., & Rhee, J.-K. K. (2008). All optical discrete Fourier transform processor for 100 Gbps OFDM transmission. *Optics express*, 16(6), 4023-4028.
- Leuthold, J., Hillerkuss, D., Winter, M., Li, J., Worms, K., Koos, C., . . . Narkiss, N. (2010). *Terabit/s FFT Processing—Optics Can do it on-the-Fly*. Paper presented at the Transparent Optical Networks (ICTON), 2010 12th International Conference on.
- Li, C., Luo, M., Xiao, X., Li, J., He, Z., Yang, Q., . . . Yu, S. (2014). 63-Tb/s (368×183.3-Gb/s) C-and L-band all-Raman transmission over 160-km SSMF using PDM-OFDM-16QAM modulation. *Chinese Optics Letters*, 12(4), 040601.
- Li, L., Qiao, Y., & Ji, Y. (2011). Optimized optical phase conjugation configuration for fiber nonlinearity compensation in CO-OFDM systems. *Chinese Optics Letters*, 9(6), 060604.
- Li, W., Liang, X., Ma, W., Zhou, T., Huang, B., & Liu, D. (2010). A planar waveguide optical discrete Fourier transformer design for 160Gb/s all-optical OFDM systems. *Optical Fiber Technology*, 16(1), 5-11.
- Li, W., Qiao, Y., Han, Q., & Zhang, H. (2009). A PMD-supported 100-Gb/s optical frequency-domain IM-DD transmission system. *Chinese Optics Letters*, 7(8), 679-682.
- Li, W., Yu, S., Qiu, W., Zhang, J., Lu, Y., & Gu, W. (2009). FWM mitigation based on serial correlation reduction by partial transmit sequence in coherent optical OFDM systems. *Optics Communications*, 282(18), 3676-3679.
- Li, X., Zhang, F., Chen, Z., & Xu, A. (2007). Suppression of XPM and XPM-induced nonlinear phase noise for RZ-DPSK signals in 40 Gbit/s WDM transmission systems with optimum dispersion mapping. *Optics express*, 15(26), 18247-18252.
- Li, Y., Li, W., Yang, K., Qiao, Y., Mei, J., & Zhang, H. (2010). Experimental implementation of an all-optical OFDM system based on time lenses. *Chinese Optics Letters*, 8(3), 275-277.

- Li, Y., Li, W., Ye, F., Wang, C., Liu, D., Huang, B., & Yang, K. (2011). Experimental implementation of an all-optical OFDM system based on time lens. *Optics Communications*, 284(16), 3983-3989.
- Liang, X., Li, W., Ma, W., & Wang, K. (2009). A simple peak-to-average power ratio reduction scheme for all optical orthogonal frequency division multiplexing systems with intensity modulation and direct detection. *Optics express*, 17(18), 15614-15622.
- Lim, S.-J., & Rhee, J.-K. K. (2011). System tolerance of all-optical sampling OFDM using AWG discrete Fourier transform. *Optics express*, 19(14), 13590-13597.
- Lin, C.-T., Wei, C.-C., & Chao, M.-I. (2011). Phase noise suppression of optical OFDM signals in 60-GHz RoF transmission system. *Optics express*, 19(11), 10423-10428.
- Liu, B., Xin, X., Zhang, L., & Yu, J. (2012). 277.6-Gb/s LDPC-coded CO-OFDM transmission system with low PAPR based on subcarrier pre-filtering technology. *Optics Communications*, 285(24), 5397-5400.
- Liu, H., Zhang, X., & Chen, K. (2006). Comparison of polarization-mode dispersion tolerances in polarization-multiplexing systems with different modulation formats. *Optics Communications*, 259(2), 640-644.
- Liu, L., Li, L., Huang, Y., Cui, K., Xiong, Q., Hauske, F. N., . . . Cai, Y. (2012). Intrachannel nonlinearity compensation by inverse Volterra series transfer function. *Lightwave Technology, Journal of*, 30(3), 310-316.
- Liu, X., Chandrasekhar, S., Chen, X., Winzer, P., Pan, Y., Taunay, T., . . . Fini, J. (2011a). 1.12-Tb/s 32-QAM-OFDM superchannel with 8.6-b/s/Hz intrachannel spectral efficiency and space-division multiplexed transmission with 60-b/s/Hz aggregate spectral efficiency. *Optics express*, 19(26), B958-B964.
- Liu, X., Chandrasekhar, S., Chen, X., Winzer, P., Pan, Y., Zhu, B., . . . Fini, J. M. (2011b). 1.12-Tb/s 32-QAM-OFDM superchannel with 8.6-b/s/Hz intrachannel spectral efficiency and space-division multiplexing with 60-b/s/Hz aggregate spectral efficiency. Paper presented at the European Conference and Exposition on Optical Communications.
- Liu, X., Chandrasekhar, S., Gnauck, A. H., Winzer, P., Randel, S., Corteselli, S., . . . Fishteyn, M. (2012a). *Digital coherent superposition for performance improvement of spatially multiplexed 676-Gb/s OFDM-16QAM superchannels*. Paper presented at the European Conference and Exhibition on Optical Communication.

- Liu, X., Chandrasekhar, S., Winzer, P., Chraplyvy, A., Tkach, R., Zhu, B., . . . DiGiovanni, D. (2012b). Scrambled coherent superposition for enhanced optical fiber communication in the nonlinear transmission regime. *Optics express*, 20(17), 19088-19095.
- Liu, X., Chandrasekhar, S., Winzer, P., Chraplyvy, A., Zhu, B., Taunay, T., & Fishteyn, M. (2012c). *Performance improvement of space-division multiplexed 128-Gb/s PDM-QPSK signals by constructive superposition in a single-input-multiple-output configuration*. Paper presented at the Optical Fiber Communication Conference.
- Liu, X., Chandrasekhar, S., Winzer, P. J., Tkach, R., & Chraplyvy, A. (2014). Fiber-nonlinearity-tolerant superchannel transmission via nonlinear noise squeezing and generalized phase-conjugated twin waves. *Lightwave Technology, Journal of*, 32(4), 766-775.
- Liu, X., Chraplyvy, A., Winzer, P., Tkach, R., & Chandrasekhar, S. (2013). Phase-conjugated twin waves for communication beyond the Kerr nonlinearity limit. *Nature Photonics*, 7(7), 560-568.
- Liu, X., Ciaramella, E., Wada, N., & Chi, N. (2011c). *Optical Transmission Systems, Subsystems, and Technologies IX*. Paper presented at the Society of Photo-Optical Instrumentation Engineers (SPIE) Conference Series.
- Liu, X., Zhan, L., Luo, S., Gu, Z., Liu, J., Wang, Y., & Shen, Q. (2012). Multiwavelength erbium-doped fiber laser based on a nonlinear amplifying loop mirror assisted by un-pumped EDF. *Optics express*, 20(7), 7088-7094.
- Long, W., Zhang, J., Wang, D., Han, J., Chen, S., Han, A. M., . . . Zhu, W. (2012). Mitigation of the interference between odd and even terms in optical fast OFDM scheme based on interleaved multiplexing. *Photonics Technology Letters, IEEE*, 24(13), 1160-1162.
- Lowery, A., & Armstrong, J. (2006). Orthogonal-frequency-division multiplexing for dispersion compensation of long-haul optical systems. *Optics express*, 14(6), 2079-2084.
- Lowery, A. J., & Armstrong, J. (2005). 10Gbit/s multimode fiber link using power-efficient orthogonal-frequency-division multiplexing. *Optics Express*, 13(25), 10003-10009.
- Lowery, A. J., & Du, L. (2011). All-optical OFDM transmitter design using AWGRs and low-bandwidth modulators. *Optics express*, 19(17), 15696-15704.

- Lowery, A. J., Du, L. B., & Armstrong, J. (2007). Performance of optical OFDM in ultralong-haul WDM lightwave systems. *Journal of Lightwave Technology*, 25(1), 131-138.
- Lowery, A. J., Wang, S., & Premaratne, M. (2007). Calculation of power limit due to fiber nonlinearity in optical OFDM systems. *Optics express*, 15(20), 13282-13287.
- Ma, Y., Yang, Q., Tang, Y., Chen, S., & Shieh, W. (2009). 1-Tb/s single-channel coherent optical OFDM transmission over 600-km SSMF fiber with subwavelength bandwidth access. *Optics express*, 17(11), 9421-9427.
- Mirnia, S. E., Zarei, A., Emami, S. D., Harun, S. W., Arof, H., Ahmad, H., & Shalaby, H. M. (2013). Proposal and Performance Evaluation of an Efficient RZ-DQPSK Modulation Scheme in All-Optical OFDM Transmission Systems. *Journal of Optical Communications and Networking*, 5(9), 932-944.
- Morgado, J. A., Fonseca, D., & Cartaxo, A. V. (2011). Experimental study of coexistence of multi-band OFDM-UWB and OFDM-baseband signals in long-reach PONs using directly modulated lasers. *Optics express*, 19(23), 23601-23612.
- Morshed, M. M., Du, L. B., & Lowery, A. J. (2013). Mid-span spectral inversion for coherent optical OFDM systems: Fundamental limits to performance. *Lightwave Technology, Journal of*, 31(1), 58-66.
- Nakazawa, M., Hirooka, T., Yoshida, M., & Kasai, K. (2013). Extremely Higher-Order Modulation Formats. *Optical Fiber Telecommunications VIB, I. Kaminow*, 297-336.
- Nakazawa, M., Kikuchi, K., & Miyazaki, T. (2010). *High Spectral Density Optical Communication Technologies* (Vol. 6): Springer Science & Business Media.
- Nazarathy, M., Khurgin, J., Weidenfeld, R., Meiman, Y., Cho, P., Noe, R., . . . Karagodsky, V. (2008). Phased-array cancellation of nonlinear FWM in coherent OFDM dispersive multi-span links. *Optics Express*, 16(20), 15777-15810.
- Nunes, R. B., Rocha, H. R. d. O., Segatto, M. E., & Silva, J. A. (2014). Experimental validation of a constant-envelope OFDM system for optical direct-detection. *Optical Fiber Technology*, 20(3), 303-307.
- Okamoto, K. (2010). *Fundamentals of optical waveguides*: Academic press.

- Omiya, T., Yoshida, M., & Nakazawa, M. (2013). 400 Gbit/s 256 QAM-OFDM transmission over 720 km with a 14 bit/s/Hz spectral efficiency by using high-resolution FDE. *Optics express*, 21(3), 2632-2641.
- Pan, Q., & Green, R. J. (1996). Bit-error-rate performance of lightwave hybrid AM/OFDM systems with comparison with AM/QAM systems in the presence of clipping impulse noise. *Photonics Technology Letters, IEEE*, 8(2), 278-280.
- Pechenkin, V., & Fair, I. J. (2009). Correlation between peak-to-average power ratio and four-wave mixing in optical OFDM systems. *Journal of Optical Communications and Networking*, 1(7), 636-644.
- Pechenkin, V., & Fair, I. J. (2010). Analysis of four-wave mixing suppression in fiber-optic OFDM transmission systems with an optical phase conjugation module. *Journal of Optical Communications and Networking*, 2(9), 701-710.
- Pham, D. T., Hong, M.-K., Joo, J.-M., Nam, E.-S., & Han, S.-K. (2011). Laser phase noise and OFDM symbol duration effects on the performance of direct-detection based optical OFDM access network. *Optical Fiber Technology*, 17(3), 252-257.
- Popoola, W. O., Ghassemlooy, Z., & Stewart, B. G. (2014). Pilot-Assisted PAPR Reduction Technique for Optical OFDM Communication Systems. *Journal of lightwave technology*, 32(7), 1374-1382.
- Rafique, D., & Ellis, A. D. (2011). Impact of signal-ASE four-wave mixing on the effectiveness of digital back-propagation in 112 Gb/s PM-QPSK systems. *Optics express*, 19(4), 3449-3454.
- Reichel, S., & Zengerle, R. (1999). Effects of nonlinear dispersion in EDFA's on optical communication systems. *Journal of Lightwave Technology*, 17(7), 1152.
- Sano, A., Masuda, H., Yoshida, E., Kobayashi, T., Yamada, E., Miyamoto, Y., . . . Hagimoto, K. (2007). 30 x 100-Gb/s all-optical OFDM transmission over 1300 km SMF with 10 ROADM nodes. *ECOC 2007*.
- Sano, A., Yamada, E., Masuda, H., Yamazaki, E., Kobayashi, T., Yoshida, E., . . . Takatori, Y. (2009). No-guard-interval coherent optical OFDM for 100-Gb/s long-haul WDM transmission. *Journal of Lightwave Technology*, 27(16), 3705-3713.
- Schmogrow, R., Winter, M., Nebendahl, B., Hillerkuss, D., Meyer, J., Dreschmann, M., . . . Freude, W. (2011). 101.5 Gbit/s real-time OFDM transmitter with 16QAM modulated subcarriers. Paper presented at the Optical Fiber Communication Conference.

- Seimetz, M. (2009). *High-order modulation for optical fiber transmission* (Vol. 143): Springer.
- Shahi, S. N., & Kumar, S. (2012). Reduction of nonlinear impairments in fiber transmission system using fiber and/or transmitter diversity. *Optics Communications*, 285(16), 3553-3558.
- Shang, L., Wen, A., Lin, G., & Gao, Y. (2014). A flat and broadband optical frequency comb with tunable bandwidth and frequency spacing. *Optics Communications*, 331, 262-266.
- Shao, J., Li, W., & Liang, X. (2010). Phase pre-emphasis for PAPR reduction in optical OFDM systems based on ODFM or time lens. *Chinese Optics Letters*, 8(9), 875-880.
- Shieh, W., Bao, H., & Tang, Y. (2008). Coherent optical OFDM: theory and design. *Optics Express*, 16(2), 841-859.
- Shieh, W., & Djordjevic, I. (2009). *OFDM for optical communications*: Academic Press.
- Shieh, W., Yang, Q., & Ma, Y. (2008). 107 Gb/s coherent optical OFDM transmission over 1000-km SSMF fiber using orthogonal band multiplexing. *Optics express*, 16(9), 6378-6386.
- Shieh, W., Yi, X., & Tang, Y. (2007). Transmission experiment of multi-gigabit coherent optical OFDM systems over 1000 km SSMF fibre. *Electronics letters*, 43(3), 183-185.
- Shimizu, S., Cincotti, G., & Wada, N. (2012). Demonstration and performance investigation of all-optical OFDM systems based on arrayed waveguide gratings. *Optics express*, 20(26), B525-B534.
- Silva, J. A., Cartaxo, A. V., & Segatto, M. E. (2012). A PAPR reduction technique based on a constant envelope OFDM approach for fiber nonlinearity mitigation in optical direct-detection systems. *Optical Communications and Networking, IEEE/OSA Journal of*, 4(4), 296-303.
- Tian, Y., Huang, Y.-K., Zhang, S., Prucnal, P. R., & Wang, T. (2013). Demonstration of digital phase-sensitive boosting to extend signal reach for long-haul WDM systems using optical phase-conjugated copy. *Optics express*, 21(4), 5099-5106.

- Tripathi, R., Gangwar, R., & Singh, N. (2007). Reduction of crosstalk in wavelength division multiplexed fiber optic communication systems. *Progress In Electromagnetics Research*, 77, 367-378.
- van den Borne, D., Jansen, S., Calabrò, S., Hecker-Denschlag, N., Khoe, G., & de Waardt, H. (2005). Reduction of nonlinear penalties through polarization interleaving in 2 x 10 Gb/s polarization-multiplexed transmission. *IEEE photonics technology letters*, 17(6), 1337-1339.
- van den Borne, D., Jansen, S., Gottwald, E., Krummrich, P., Khoe, G., & De Waardt, H. (2007). 1.6-b/s/Hz spectrally efficient transmission over 1700 km of SSMF using 40x 85.6-Gb/s POLMUX-RZ-DQPSK. *Journal of Lightwave Technology*, 25(1), 222-232.
- Wang, W., Zhuge, Q., Morsy-Osman, M., Gao, Y., Xu, X., Chagnon, M., . . . Li, R. (2014). Decision-aided sampling frequency offset compensation for reduced-guard-interval coherent optical OFDM systems. *Optics express*, 22(22), 27553-27564.
- Wang, Z., Kravtsov, K. S., Huang, Y.-K., & Prucnal, P. R. (2011). Optical FFT/IFFT circuit realization using arrayed waveguide gratings and the applications in all-optical OFDM system. *Optics express*, 19(5), 4501-4512.
- Wei, C. C., & Chen, J. J. (2010). Study on dispersion-induced phase noise in an optical OFDM radio-over-fiber system at 60-GHz band. *Optics express*, 18(20), 20774-20785.
- Weinstein, S., & Ebert, P. (1971). Data transmission by frequency-division multiplexing using the discrete Fourier transform. *Communication Technology, IEEE Transactions on*, 19(5), 628-634.
- Winters, J. H. (1987). On the capacity of radio communication systems with diversity in a Rayleigh fading environment. *Selected Areas in Communications, IEEE Journal on*, 5(5), 871-878.
- Winters, J. H., Salz, J., & Gitlin, R. D. (1994). The impact of antenna diversity on the capacity of wireless communication systems. *Communications, IEEE Transactions on*, 42(234), 1740-1751.
- Wree, C., Hecker-Denschlag, N., Gottwald, E., Krummrich, P., Leibrich, J., Schmidt, E.-D., . . . Rosenkranz, W. (2003). High spectral efficiency 1.6-b/s/Hz transmission (8 x 40 Gb/s with a 25-GHz grid) over 200-km SSMF using RZ-DQPSK and polarization multiplexing. *IEEE Photonics Technology Letters*, 15(9), 1303-1305.

- Wree, C., Leibrich, J., & Rosenkranz, W. (2002). RZ-DQPSK format with high spectral efficiency and high robustness towards fiber nonlinearities. *Proc. ECOC2002, Paper*, 9(6).
- Wu, M., & Way, W. I. (2004). Fiber nonlinearity limitations in ultra-dense WDM systems. *Journal of Lightwave Technology*, 22(6), 1483.
- Xiao, Y., Chen, M., Li, F., Tang, J., Liu, Y., & Chen, L. (2015). PAPR reduction based on chaos combined with SLM technique in optical OFDM IM/DD system. *Optical Fiber Technology*, 21, 81-86.
- Xie, C. (2009). WDM coherent PDM-QPSK systems with and without inline optical dispersion compensation. *Optics express*, 17(6), 4815-4823.
- Yang, D., & Kumar, S. (2009). Realization of optical OFDM using time lenses and its comparison with optical OFDM using FFT. *Optics express*, 17(20), 17214-17226.
- Yao, S., Fu, S., Li, J., Tang, M., Shum, P., & Liu, D. (2013). Phase noise tolerant inter-carrier-interference cancellation for WDM superchannels with sub-Nyquist channel spacing. *Optics Express*, 21(18), 21569-21578.
- Yi, X., Sharma, D., Zhang, J., Chen, X., Yang, Q., & Qiu, K. (2014). *Enhanced phase noise tolerance of coherent optical OFDM using digital coherent superposition*. Paper presented at the Optical Fibre Technology, 2014 OptoElectronics and Communication Conference and Australian Conference on.
- Yi, X., Shieh, W., & Ma, Y. (2008). Phase noise effects on high spectral efficiency coherent optical OFDM transmission. *Journal of Lightwave Technology*, 26(10), 1309-1316.
- Yonenaga, K., Sano, A., Yamazaki, E., Inuzuka, F., Miyamoto, Y., Takada, A., & Yamada, T. (2008). *100 Gbit/s All-Optical OFDM Transmission Using 4x25 Gbit/s Optical Duobinary Signals with Phase-Controlled Optical Sub-Carriers*. Paper presented at the Optical Fiber Communication Conference.
- Zhu, X., & Kumar, S. (2010). Nonlinear phase noise in coherent optical OFDM transmission systems. *Optics express*, 18(7), 7347-7360.

LIST OF PUBLICATIONS

1. **Hmood, Jassim K.**, Harun, S. W., Emami, S. D., Khodaei, A., Noordin, K. A., Ahmad, H., & Shalaby, H. M. (2015). Performance analysis of an all-optical OFDM system in presence of non-linear phase noise. *Optics express*, 23(4), 3886-3900.
2. **Hmood, Jassim K.**, Noordin, K. A., Ahmad, H., & Harun, S. W. (2015). Performance Improvement of All-optical OFDM Systems based on Combining RZ coding with m-array QAM. *Journal of Optoelectronics and Advanced Materials*, 17(1-2), 33-38.
3. **Hmood, Jassim K.**, Noordin, K. A., Harun, S. W., & Shalaby, H. M. (2015). Mitigation of phase noise in all-optical OFDM systems based on minimizing interaction time between subcarriers. *Optics Communications*, 355, 313-320.
4. **Hmood, Jassim K.**, Noordin, K. A., Arof, H., & Harun, S. W. (2015). Peak-to-average power ratio reduction in all-optical orthogonal frequency division multiplexing system using rotated constellation approach. *Optical Fiber Technology*, 25, 88-93.
5. **Hmood, Jassim K.**, Noordin, K. A., & Harun, S. W. (2016). Effectiveness of phase-conjugated twin waves on fiber nonlinearity in spatially multiplexed all-optical OFDM system. *Optical Fiber Technology*, 30, 147-152.